Preclinical testing of potential therapeutics for Amyotrophic Lateral Sclerosis

Hannah Marlene Jostock Kaneb

Imperial College London, Department of Medicine

Thesis submitted for a PhD in Clinical Medicine Research

(Neuroscience and Mental Health)

Abstract

Amyotrophic Lateral Sclerosis (ALS) is a fatal neurological disorder caused by the selective degeneration of upper and lower motor neurons, for which there are currently no effective treatments. 10% of ALS cases are familial, of which 15-20% are caused by mutations in the copper/zinc superoxide dismutase gene (SOD1). The primary triggers for motor neuron degeneration in ALS are unknown, but research in patients and SOD1 models has revealed several mechanisms which may contribute. These include: oxidative stress, mitochondrial abnormalities, inflammation and protein aggregation. This study focused on the pre-clinical testing of two-potential therapeutics for ALS in the $SOD1^{G93A}$ murine model of the disease; metformin, an anti type II diabetes drug which has been shown to have anti-inflammatory and anti-oxidant properties and the ability to bring about mitochondrial biogenesis, and trehalose, a chemical chaperone and enhancer of autophagy, which has been shown to reduce protein misfolding and aggregation. We performed an initial study in which oral metformin administration from 35 days increased the survival of functional motor units in the hindlimbs of male and female $SOD1^{G93A}$ mice at 100 days. Consequently we performed a dose-response survival study in $SOD1^{G93A}$ mice with longitudinal monitoring of weight and neurological score. Surprisingly, metformin had no effect in males and brought about a dose-dependent negative effect on the onset of neurological symptoms and on disease progression in females. We hypothesise this negative effect may have resulted from a metformin-induced reduction in oestrogen production. Oral trehalose administration was tested using the same survival study format. Although trehalose treatment brought about a dose-dependent delay in weight-loss in males, it had no effect on the onset or progression of neurological symptoms or on

survival in male or female mice. We conclude that neither metformin nor trehalose represent strong candidates for clinical trial in ALS patients when administered orally.

Table of Contents

Abstract 2

List of Figures 16

List of Tables 19

Declaration of originality 21

List of abbreviations 22

Acknowledgements 24

1. Introduction 25

1.1 Amyotrophic Lateral Sclerosis (ALS) 25

1.2 Genetics of ALS 26

1.2.1 Familial ALS caused by mutations in copper/zinc superoxide dismutase 1 27

1.3 Commonly used murine models of SOD1-related ALS pathology 29

1.3.1 $SOD1^{G93A}$ mice 30

1.3.1.1 The effect of transgene copy number on pathology in $SOD1^{G93A}$ mice 30

1.3.1.2 The timeline of pathology in high copy $SOD1^{G93A}$ mice 31

1.3.2 $SOD1^{G37R}$ mice 35

1.3.3 $SOD1^{G85R}$ mice 35

1.4 Toxic processes that may contribute to motor neuron degeneration in ALS 38

1.4.1 Inflammation and the non-cell autonomous nature of ALS 40

1.4.1.1 Functions of microglia, astrocytes in the CNS 40

1.4.1.2 Glial activation in ALS 42
1.4.1.3 Mechanisms by which reactive microglia may contribute to ALS pathology .. 44
1.4.1.4 Mechanisms by which reactive astrocytes may contribute to ALS pathology . 46
1.4.1.6 Schwann cells in ALS 48
1.4.1.6 Oligodendrocytes and $NG2^{+}$ cells in ALS 49
1.4.2 Protein misfolding and aggregation in ALS 50
1.4.2.1 Misfolding and aggregation of SOD1 in familial ALS 50
1.4.2.1.1 Induction of endoplasmic reticulum stress 51
1.4.2.1.2 Impairment of axonal transport 54
1.4.2.1.3 Cellular degradation pathways for misfolded/aggregated mutant SOD1 ... 56
1.4.2.1.4 Toxicity associated with secretion of misfolded mutant SOD1 by motor neurons 58
1.4.2.1.4 Does SOD1 misfold and aggregate in ALS patients whose pathology is not caused by mutations in SOD1? 59
1.4.2.2 TDP-43 and FUS aggregation in ALS and relationship between ALS and Frontotemporal Dementia (FTD) 61
1.4.3 Mitochondrial abnormalities in ALS 66
1.4.3.1 Direct effects of mutant SOD1 on mitochondria 66
1.4.3.2 Oxidative stress and defective oxidative phosphorylation in ALS patients and models 68
1.4.3.3 Impaired calcium buffering 70
1.4.3.4 Altered mitochondrial morphology and distribution 70

1.4.3.5 Mitochondrial apoptosis in ALS 72
1.4.3.6 Hypermetabolism in ALS 73
1.4.4 ALS genetics 75
1.4.4.1 An update on mutations identified in familial and sporadic ALS 75
1.4.4.2 Convergent and divergent pathways in familial and sporadic ALS 80
1.5 Development of therapeutics for ALS 83
1.5.1 Therapeutics previously tested in mutant SOD1 murine models of ALS. 83
1.5.2 The disparity between preclinical and clinical results for potential ALS therapeutics. 85
1.5.3 Therapeutic strategies currently under investigation in the ALS clinic 87
1.5.3.1 Anti-glutamatergic strategies 88
1.5.3.2 Targeting protein misfolding and accumulation 88
1.5.3.3 Knockdown of mutant SOD1 proteins 89
1.5.3.4 Improving/maintaining mitochondrial function 90
1.5.3.5 Administration of growth factors. 91
1.5.3.6 Targeting the muscles of ALS patients 93
1.6 Specific aims of this thesis 93
1.6.1 Metformin 95
1.6.2 Trehalose 98
2. Materials and Methods 101
2.1 Materials 101

2.1.1 Reagents....101
2.1.2 Kits....103
2.1.3 Antibodies....103
2.1.3.1 Primary antibodies....103
2.1.3.2 Secondary antibodies....103
2.1.4 Equipment....104
2.2 Methods....104
2.2.1 Solutions....104
2.2.1.1 Genotyping....104
2.2.1.1.1 10x Stock of Ear Homogenisation Buffer....104
2.2.1.1.2 6X Stock of DNA gel loading buffer (10ml)....105
2.2.1.1.3 5X Stock of TBE Buffer (1 litre)....106
2.2.1.2 Immunohistochemistry....106
2.2.1.2.1 4% paraformaldehyde (PFA) (1 litre)....106
2.2.1.2.2 Gelatin solution for embedding spinal cords (1 litre)....106
2.2.1.2.3 Nissl Stain (500ml)....107
2.2.2 Animals....107
2.2.2.1 SOD1 ^{G93A} mouse breeding and maintenance....107
2.2.2.2 Genotyping of SOD1^{G93A} transgenic mice....108
2.2.2.3 Assessment of potential variations in copy number in SOD1^{G93A} transgenic mice....110

2.2.2.3.1 Quantitative PCR for assessment of potential variations in copy number-background 110

2.2.2.3.2 Quantitative –PCR protocol for assessment of potential variations in copy number in SOD1^{G93A} mice 111

2.2.3 SOD1^{G93A} mouse treatment protocols 114

2.2.3.1 Metformin electrophysiology study 114

2.2.3.2 Metformin dose-response survival study 115

2.2.3.2.1 Experimental groups 115

2.2.3.2.2 Metformin treatment regime 115

2.2.3.3 Metformin blood collection study 116

2.2.3.4 Trehalose dose-response survival study 116

2.2.3.4.1 Experimental groups 116

2.2.3.4.2 Trehalose treatments 117

2.2.3.5 Trehalose spinal cord histology experiment 118

2.2.4 In vivo electrophysiology 119

2.2.4.1 Surgical preparation for in vivo electrophysiology 119

2.2.4.2 Measurement of TA and EDL maximum and specific forces 119

2.2.4.3 Measurement of motor unit number 120

2.2.4.4 Fatigue test 121

2.2.4.5 Tissue collection following in vivo electrophysiology 122

2.2.4.6 Statistical analyses for metformin in vivo electrophysiology experiments 122

2.2.5 Dose-response survival studies in SOD1^{G93A} mice 123

2.2.5.1 Cage conditions, food and water 123

2.2.5.2 Analysis of disease onset, progression and survival 124

2.2.5.2.1 Neurological Score 124

2.2.5.2.2 Body Weight 125

2.2.5.2.3 Survival 125

2.2.5.3 Graphical representation of data and statistical analyses 125

2.2.6 Mouse spinal cord extraction and preparation for cryosectioning 127

2.2.7 Histological analysis of trehalose-treated SOD1^{G93A} mouse spinal cords 128

2.2.7.1 Cryosectioning and immunostaining for trehalose survival study 128

2.2.7.2 Quantification of USOD positive motor neurons and surviving motor neurons in the sciatic motor pool of trehalose-treated mice 129

2.2.8 17β-oestradiol radioimmunoassay (RIA) 130

2.2.8.1 Radioimmunoassay principles 131

2.2.8.2 Chemicals and reagents 132

2.2.8.3 Assay protocol 133

3.1 Metformin electrophysiology study 135

3.1 Introduction 135

3.2 Methods and n-numbers 137

3.3 Results 139

3.3.1 Assessment of potential variations in copy number 139

3.3.2 The effect of metformin treatment on the weights of SOD1^{G93A} and WT mice between 55 and 99 days of age. 143
3.3.3 Functional motor unit measurements 148
3.3.3.1 SOD1^{G93A} EDL muscles have significantly fewer motor units than their WT counterparts at 100 days. 148
3.3.3.2 Metformin treatment brought about a significant preservation of motor units in SOD1^{G93A} male EDL muscles and SOD1^{G93A} female TA muscles. 151
3.3.3.3 Metformin treatment did not affect motor unit number in WT mice. 155
3.3.4 Maximal force and specific force measurements 157
3.3.4.1 The TA and EDL muscles of SOD1^{G93A} mice are significantly weaker than those of WT mice at 100 days. 157
3.3.4.2 Metformin treatment did not increase the maximal or specific forces of SOD1^{G93A} - TA and EDL muscles. 162
3.3.4.3 Metformin treatment significantly increased the maximal and specific forces of WT female EDL but not TA muscles and had no effect on WT male muscles. 165
3.3.5 Muscle fatigability measurements 168
3.3.5.1 SOD1 EDL muscles are significantly more resistant to fatigue than WT EDL muscles at 100 days of age. 168
3.3.5.2 Metformin treatment brought about a significant increase in the resistance to fatigue of male SOD1^{G93A} EDL muscles. 171
3.3.5.3 Metformin treatment did not significantly increase the resistance to fatigue of WT EDL muscles at 100 days of age, despite a trend towards this effect. 173

3.4 Discussion 175

3.4.1 Conclusions drawn from control data 175

3.4.2 The effect of metformin treatment on disease severity in SOD1G93A mice at 100 days of age. 182

4. Metformin dose-response survival study 187

4.1 Introduction 187

4.2 Results 194

4.2.1 Assessment of potential variations in transgene copy number 194

4.2.2Metformin treatment had no effect on disease onset, progression or survival in male mice. 197

4.2.2.1 N-numbers, weight balancing and non-ALS deaths in male mice 197

4.2.2.2 Effect of metformin on body weight, disease onset and disease progression in male $SOD1^{G93A}$ mice. 197

4.2.2.3 Effect of metformin on the definitive onset of neurological disease and the change in neurological score over time in male $SOD1^{G93A}$ mice. 201

4.2.2.4 Effect of metformin on survival in male mice 201

4.2.3 Metformin treatment negatively affected disease onset and progression in female mice in a dose-dependent fashion. 203

4.2.3.1 N-numbers, weight balancing and non-ALS deaths in female mice 203

4.2.3.2 Effect of metformin on body weight, disease onset and disease progression in female $SOD1^{G93A}$ mice. 203

4.2.3.3 Effect of metformin on the definitive onset of neurological disease and the change in neurological score over time in female SOD1^{G93A} mice. 207
4.2.3.4 Effect of metformin on survival in female mice 207
4.2.4 Effect of metformin on survival in female mice 209
4.4 Discussion 215
5. Trehalose Survival Study 221
5.1 Introduction 221
5.2 Results 227
5.2.1 Copy number variations 227
5.2.2 Trehalose treatment had no effect on the onset of neurological symptoms, disease progression or survival in male mice but brought about a dose-dependent delay in weight loss. 227
5.2.2.1 N-numbers, weight balancing and non-ALS deaths in male mice 227
5.2.2.2 Effect of trehalose on body weight, disease onset and disease progression in male SOD1^{G93A} mice. 227
5.2.2.3 Effect of trehalose on the definitive onset of neurological disease and the change in neurological score over time in male SOD1^{G93A} mice. 231
5.2.2.4 Effect of trehalose on survival in male mice 231
5.2.3 Trehalose treatment had no effect on disease onset, progression or survival in female mice 233
5.2.3.1 N-numbers, weight balancing and non-ALS deaths in female mice 233

5.2.3.2 Effect of trehalose on body weight, disease onset and disease progression in female SOD1^{G93A} mice. 234

5.2.3.3 Effect of trehalose on the definitive onset of neurological disease and the change in neurological score over time in female SOD1^{G93A} mice. 237

5.2.3.4 Effect of trehalose on survival in female mice 237

5.2.4 Trehalose treatment did not reduce the amount of misfolded/aggregated SOD1 in the spinal cords of male or female SOD1^{G93A} mice.....239

(A and B) representative ChAT (brown)/ Nissl (blue)-stained sections from the ventral horns (lumbar region, L4) of (A) a 75 day old WT mouse and (B) a 75 day old SOD1G93A mouse. ChAT staining within motor neurons of WT mice (A) was found to be present throughout the cytoplasm and nicely overlaid with Nissl whereas ChAT staining within the motor neurons of 75 day old SOD1G93A mice (B) was less uniform and often punctuate in nature (solid arrows). Scale bar in (A) applies to both (A) and (B) and represents 100µm. (C and D) graphs showing the mean numbers of ChAT/Nissl positive motor neurons counted in equivalent sections L3-L5 in control and 5% trehalose-treated male SOD1G93A mice (C) and in control and 5% trehalose-treated female SOD1G93A mice (D). Error bars in (C) and (D) represent standard error of the mean (SEM). n=3 SOD1G93A males, n=4 SOD1G93A females, n=4 trehalose-treated SOD1G93A males and n=5 trehalose- treated SOD1G93A females. No significant differences were seen between control and trehalose-treated SOD1G93A males or between control and trehalose-treated SOD1G93A females by Mann-Whitney test (Table 16). The threshold for significance was set at $P<0.05$. Note: clearly degenerating motor neurons showing vacuolation and faint Nissl/ChAT staining (broken arrow in B) were included in motor neuron counts as these were often the motor neurons in which USOD staining was observed. 244

5.3 Discussion 245

6. Future directions 256

6.1 Continuation of work performed in this thesis 256

6.1.1 Experiments to establish potential reasons for the lack of benefit of oral metformin treatment in SOD1^{G93A} mice 259

6.1.2 Further experiments to establish potential reasons for the lack of benefit of oral trehalose treatment in SOD1^{G93A} mice 263

6.1.2.1 Re-counting USOD positive motor neurons in SOD1^{G93A} spinal cords using a system accounting for USOD distribution and intensity within motor neurons 263

6.1.2.2 Investigating the autophagy system in the motor neurons of SOD1^{G93A} mice 265

6.1.2.3 Investigating the levels of trehalose in the spinal cords of trehalose treated and control SOD1^{G93A} mice. 267

6.2 Future perspectives for the development of effective therapeutics for ALS 273

6.4 Overall conclusions 285

7. Appendices 286

7.1 Appendix 1: Summary of therapies tested to date in mutant SOD1-based murine models of ALS 286

7.2 Appendix 2. Optimising survival studies in SOD1^{G93A} mice 303

7.2.1 The requirement to address animal husbandry and welfare issues when performing survival studies in SOD1^{G93A} mice. 303

7.2.2 Minimising fighting between male mice 304

7.2.3 Employing the ALSTDI neurological scoring system 308

7.2.3.1 Establishing the difference between a score of 0 and a score of 1 308

7.2.3.2 Determining the existence of toe curling in SOD1^{G93A} mice non-invasively. 312

7.2.3.3 Determining the humane end stage of SOD1^{G93A} mice in conditions that are relevant to the home cage environment. 313

7.2.4 Changing bedding and enrichment conditions to accommodate advancing pathology in SOD1^{G93A} mice.....313

7.2.5 The correct time to introduce long sipper tubes and a mashed diet in survival studies in SOD1^{G93A} mice.....317

7.2.6 Eye problems in SOD1^{G93A} mice at late symptomatic time points. 320

7.2.7 Separating SOD1^{G93A} mice at late symptomatic time points from healthier cage mates to prevent over grooming and hindlimb mutilation. 323

7.2.7 The importance of twice daily checks in survival studies in SOD1^{G93A} mice at late symptomatic time points.....324

7.2.8 Optimising the humane end point used for SOD1^{G93A} mice in survival studies. ..325

7.2.9 Optimal husbandry for survival studies in SOD1^{G93A} mice 327

7.3 Appendix 3. Potential method for assessing the ability of orally administered trehalose to reach the CNS. 329

List of Figures

Figure 1: Time course of clinical and neuropathological events in high copy number transgenic SOD1^{G93A} mice (adapted from Turner and Talbot 2008, Figure 2). 33

Figure 2: Proposed mechanisms of toxicity in SOD1-mediated ALS (Adapted from Ilieva et al., 2009, Figure 1).....39

Figure 3: Comparison of the weights of WT and SOD1^{G93A} mice between 55 and 99 days of age. 145

Figure 4: The effect of metformin treatment on the weight of SOD1^{G93A} mice between 55 and 99 days of age. 146

Figure 5: The effect of metformin treatment on the weight of WT mice between 55 and 99 days of age. 147

Figure 6: Typical traces recorded for motor unit assessment protocol in WT and SOD1^{G93A} male EDL muscles at 100 days of age. 149

Figure 7: Comparison of the number of functional motor units in the EDL muscles of SOD1^{G93A} mice and WT mice at 100 days. 150

Figure 8: Typical traces recorded for motor unit assessment protocol in WT and metformin treated and untreated SOD1^{G93A} male EDL muscles at 100 days of age. 152

Figure 9: Comparison of the number of functional motor units in the EDL muscles of metformin treated and untreated SOD1^{G93A} mice at 100 days.....153

Figure 10: Comparison of the number of functional motor units in the TA muscles of metformin treated and untreated SOD1^{G93A} mice at 100 days.....154

Figure 11: Comparison of the number of functional motor units in the EDL muscles of metformin-treated and untreated WT mice at 100 days.....156

Figure 12: Comparison of the maximal forces of the right TA and EDL muscles of (A) male and (B) female, WT and SOD1^{G93A} mice at 100 days of age. 159
Figure 13: Comparison of the specific forces of the right TA and EDL muscles of WT and SOD1^{G93A} mice at 100 days of age. 160
Figure 14: Comparison of the maximal forces of the right TA and EDL muscles of (A) male and (B) female metformin-treated and control SOD1^{G93A} mice at 100 days of age. 163
Figure 15: Comparison of the specific forces of the right TA and EDL muscles of metformin-treated and untreated SOD1^{G93A} mice at 100 days of age. 164
Figure 16: Comparison of the maximal forces of the right TA and EDL muscles of (A) male and (B) female metformin-treated and untreated WT mice at 100 days of age. 166
Figure 17: Comparison of the specific forces of the right TA and EDL muscles of metformin-treated and untreated WT mice at 100 days of age. 167
Figure 18: Typical fatigue traces for the EDL muscles of SOD1^{G93A} mice and WT mice at 100 days. 169
Figure 19: Comparison of the fatigue index of the right EDL muscles of SOD1^{G93A} mice and WT mice at 100 days. 170
Figure 20: Comparison of the fatigue index of the right EDL muscles of metformin-treated and untreated SOD1^{G93A} mice at 100 days. 172
Figure 21: Comparison of the fatigue index of the right EDL muscles of metformin-treated and untreated WT mice at 100 days. 174
Figure 22: Effect of metformin on body weight, disease onset and disease progression in male SOD1^{G93A} mice. 199
Figure 23: Effect of metformin on neurological score, neurological disease onset and survival in male SOD1^{G93A} mice. 202

Figure 24: Effect of metformin on body weight, disease onset and disease progression in female SOD1^{G93A} mice. 205

Figure 25: Effect of metformin on neurological score, neurological disease onset and survival in female SOD1^{G93A} mice. 208

Figure 26: Comparison of the definitive onset of symptomatic neurological disease and survival in control and metformin-treated female mice and male control mice. 211

Figure 27: Comparison serum 17β-estradiol levels in control and metformin-treated (A) SOD1^{G93A} and (B) WT female mice at 70 days. 214

List of Tables

Table 1: Pathological timecourse of SOD1^{G85R} transgenic mice, a model of ALS 37

Table 2: Summary of genes/loci in which ALS-causing mutations have been identified to date 79

Table 3: Sample preparation for 17β-oestradiol radioimmunoassay (RIA) 134

Table 4: Summary of the n-numbers used in metformin electrophysiology study.....138

Table 5: Summary of Δ CT values obtained for SOD1^{G93A} mice in metformin electrophysiology study 141

Table 6 A & B: Summary of results obtained for electrophysiological analysis of (A) control and (B) metformin-treated SOD1^{G93A} TA and EDL muscles at 100 days of age.....142

Table 7: Summary of the mean maximum and specific force values measured for metformin-treated and control WT and SOD1^{G93A} (SOD1) TA and EDL muscles, via in vivo electrophysiology. 161

Table 8: Conversion of animal doses to Human Equivalent Doses (HED) based on Body Surface Area (BSA) 191

Table 9: Summary of the survival times and Δ CT values of mice for which copy number variation assessments were performed in our metformin survival study.....196

Table 10: Kaplan Meier time to event analyses for male SOD1^{G93A} mice $^{1, 2, 3}$ 200

Table 11: Kaplan Meier time to event analyses for female SOD1^{G93A} mice$^{1, 2, 3}$ 206

Table 12: Summary of median time to reach score 2,2 and median survival for all female groups and the male control group.....212

Table 13: Summary of statistical analyses performed to compare the time taken for mice to reach a score of 2 in both hindlimbs and the time taken for mice to reach the humane end stage of the inability to right within 30s of being placed on a side between all groups. 213
Table 14: Kaplan Meier time to event analyses for male SOD1G93A mice[1, 2, 3] 230
Table 15: Kaplan Meier time to event analyses for female SOD1^{G93A} mice[1, 2, 3] 236
Table 16: Summary of mean numbers (+/- SEM) and statistical analyses of USOD and ChAT positive motor neurons in equivalent levels of the sciatic motor pool in control and trehalose treated SOD1^{G93A} mice. 242

Declaration of originality

All experiments described in this thesis were performed by me with the exception of the 17β-oestradiol assay, which was performed in collaboration with Dr Zhangrui Cheng at the Royal Veterinary Collage, as is referenced in the relevant sections of the document.

List of abbreviations

ACC: Acetyl-CoA carboxylase

AMPA: alpha-amino-3-hydroxy-5-methyl-4-isoxazolepropionic acid

ALS: Amyotrophic Lateral Sclerosis

AMPK: AMP-activated Protein Kinase

BBB: Blood Brain Barrier

BSA: Body Surface Area

BSU: Biological Sciences Unit

CSF: Cerebrospinal fluid

EDL: Extensor Digitorum Longis

DPN: Deep Peroneal Nerve

F: Female

FDA: Food and Drug Administration

FI: Fatigue Index

FTD: Frontotemporal Dementia

FTLD: Frontotemporal Lobar Degeneration

FUS: Fused in sarcoma

FUS/TLS*:* fused in sarcoma/translocated in liposarcoma

IFNγ: interferon γ

IGF1: insulin-like growth factor 1

IL1β: interleukin 1β

IL2: Interleukin 2

IL4: Interleukin 4

IL10: Interleukin 10

M: Male

mIL2: mouse IL2

mSOD1: mutant human SOD1

MUs: Motor Units

NO: nitric oxide

PBS: Phosphate Buffered Saline

PCOS: Polycystic ovary syndrome

RIA: Radioimmunoassay

RNAi: RNA interference

RO: Reverse Osmosis

RVC: Royal Veterinary College

ShRNA: Short hairpin RNA

SOD1: Cu/Zn Superoxide Dismutase 1

TA: Tibialis Anterior

TDP-43: TAR-DNA binding protein-43

TNFα: tumour necrosis factor α

WT: Wild Type

Acknowledgements

I would like to thank my primary supervisor Professor Dominic Wells for all his support, advice and help during my PhD and for allowing me the freedom to develop my own ideas and develop as a researcher, whilst always being there to give guidance when needed. I would also like to thank my second supervisor, Professor Jackie de Belleroche for giving me great advice and mentoring throughout the course of this PhD and my wonderful family and husband for always encouraging me, inspiring me and being there for me. Additionally I would like to thank Dr Paul Sharp for introducing me to the field of ALS research, for teaching me *in vivo* electrophysiology and for all his advice, Dr Sue Brown for her support and guidance, Nazanin Rahmani-Kondori for her many hours of help whilst performing my survival studies, Douglas Lopes for giving me an invaluable introduction to *in vivo* work, Dr Sophia Muses, Rebecca Terry and Charlotte Whitmore for all their support and help, all staff in the Comparative Biomedical Services unit at the Hammersmith Hospital and the Biological Services Unit at the Royal Veterinary College for their hard work, advice and continued monitoring of animal health and welfare during this PhD, Dr Avi Chakrabartty for generously donating us the USOD antibody, Dr Zhangrui Cheng for kindly carrying out a 17β-oestradiol assay for us, the Medical Research Council and L'Association française contre les myopathies for funding my research and all members of the Wells and Brown groups past and present for their help and support and for making our work environment so welcoming and inspiring.

1. Introduction

1.1 Amyotrophic Lateral Sclerosis (ALS)

Amyotrophic lateral sclerosis (ALS) is a fatal and progressive, late onset neurodegenerative disorder that was first described in 1869 by the French neurologist Jean-Martin Charcot (Charcot and Joffory, 1869). ALS is characterised by the combined degeneration of corticospinal upper motor neurons that reside in the precentral gyrus and lower motor neurons that reside in the ventral horn of the spinal cord and in the brain stem (Rowland and Shneider, 2001). Clinical signs associated with the loss of upper motor neurons include stiffness (spasticity) and abnormally active reflexes, whereas those associated with the loss of lower motor neurons include muscle weakness and atrophy as well as fasciculations (involuntary muscle contractions arising from the spontaneous discharge of skeletal muscle fibers within a muscle fascicle) (Körner et al., 2011). Although the 'classical form' of ALS is characterised by both upper and lower motor neuron degeneration, clinical subtypes with solely lower motor neuron degeneration (also called ''progressive muscular atrophy'') or solely upper motor neuron degeneration (or ''primary lateral sclerosis'') can occur. Whether or not these clinical subtypes can be described as ALS is still a matter of debate (Gordon et al., 2006, Kim et al., 2009)

Upper and lower motor symptoms in ALS patients usually begin in a focal and asymmetric fashion, spreading through contiguous anatomical segments as the disease progresses (Ravits et al., 2007). Approximately two thirds of patients with typical ALS show spinal disease onset with symptoms related to focal muscle weakness in the upper or lower limbs. The remaining third of patients display a bulbar-onset involving the muscles of the face, mouth

and throat and often present with speech difficulties (dysarthria) (Körner et al., 2011, Wijesekera and Leigh, 2009). A subset of approximately 5% of patients present with respiratory weakness without significant limb or bulbar symptoms (Wijesekera and Leigh, 2009). Regardless of the site of onset, ALS patients display a progressive paralysis that leads to death, usually through respiratory failure within 2–3 years for bulbar onset cases and 3–5 years for spinal onset ALS cases (Wijesekera and Leigh, 2009).

Although ALS affects people worldwide, an exact incidence of this disease is not yet known (Cronin et al., 2007). However, population-based studies have established that the incidence of ALS in Europe is fairly uniform at approximately 2.7 per 100 000 person-years among those over 18 years of age, with a male to female ratio of 1.3:1 (Logroscino et al., 2010). These studies also revealed the overall population-based lifetime risk of ALS in Europe to be 1:400 for women and 1:350 for men and the peak age at onset to be 58–63 years for sporadic disease and 47–52 years for familial disease (Logroscino et al., 2010).

1.2 Genetics of ALS

In approximately 90% of cases, ALS manifests as a sporadic disorder with no clear inheritance, the remaining ~10 % of cases are familial and usually display autosomal dominant inheritance. Mutations in a number of genes have been discovered as causative for ALS, with a particular explosion of discoveries in recent years. These genes are discussed in more detail in section 1.4.4.1.

1.2.1 Familial ALS caused by mutations in copper/zinc superoxide dismutase 1

The first gene identified to be involved in typical familial ALS was the *SOD1* gene, which encodes copper/zinc superoxide dismutase 1 (Rosen et al., 1993a). SOD1 is a 32 kDa homodimeric enzyme composed of two monomeric eight-stranded beta barrels, each with a binding site for one copper ion and one zinc ion (Rakhit and Chakrabartty, 2006). It is a ubiquitously expressed enzyme whose normal function is to catalytically convert highly reactive superoxide (oxygen with an additional electron) to either hydrogen peroxide or oxygen. In excess of 130 mutations, which account for 12-23% of familial ALS, have now been reported in the *SOD1* gene (Millecamps et al., 2010) and these mutations have been found to encompass all coding regions of the gene (Turner and Talbot, 2008).

The discovery of SOD1 mutations in familial ALS lead to the generation of various lines of transgenic mice expressing mutant SOD1 mini genes (Gurney, 1994). These mini-genes are usually composed of 12-15kb human genomic fragments encoding SOD1 driven by the endogenous promoter and regulatory sequences (Turner and Talbot, 2008). Critically, despite the existence of considereable heterogeneity in transgene copy number, steady-state transcript and protein levels and dismutase activities in these models, all have been observed to exhibit fatal symptoms that are indicative of ALS, albeit with difference disease latencies and progression rates (Turner and Talbot, 2008). Furthermore, the fact that these murine models show ALS-like symptoms, despite having their full complement of endogenous WT murine SOD1 has revealed that mutations in SOD1 are likely to cause ALS through a gain of function mechanism.

The gain of function hypothesis for ALS-causing mutations in SOD1 was initially supported by reports that SOD1 homozygote knockout mice were viable and appeared to develop without obvious motor abnormalities (Reaume et al., 1996). However, investigation of these mice at later time points has revealed that they develop a chronic age-related peripheral axonopathy that leads to significant locomotor deficits (Flood et al., 1999). Furthermore, motor unit estimation in these mice has revealed that by two months of age, they have a reduced number of functional motor axons, after which the estimated number of functional motor units continues to decline at a slow but significant rate throughout their lifespan (Shefner et al., 1999). These changes occur in the absence of any changes in motor neuron cell body number (Flood et al., 1999, Shefner et al., 1999). This has lead to the suggestion that SOD1 is not required for normal motor neuron survival, but is necessary for the maintenance of normal neuromuscular junctions and healthy axons by hindlimb motor neurons (Flood et al., 1999). Consequently, although the occurrence of pathology in murine models expressing their full complement of WT murine SOD1 as well as a mutant human SOD1 transgene, indicates that that mutant SOD1 proteins gain additional toxic properties, a loss of function element to pathology cannot be completely excluded from the pathogenic mechanism of all SOD1 mutants in ALS patients.

Investigation of transgenic mice overexpressing human $SOD1^{WT}$ has revealed that they show mild vacuolar pathology and axonal loss in their spinal cords at late time points (Dal Canto and Gurney, 1995, Jaarsma, 2006). Furthermore these mice have been shown to experience impaired regeneration after peripheral nerve injury (Kotulska et al., 2006). Considering the pathology observed in both SOD1 knockout mice and these pathological features in $SOD1^{WT}$ mice, it appears that intermediary thresholds of SOD1 expression are important for long-term

maintenance of motor neurons and their axonal and synaptic connections. It is also important to note that native SOD1 has been shown to be capable of bringing about several other cellular effects in addition to the conversion of superoxide to hydrogen peroxide or oxygen. These include: catalyzing hydroxyl radical production from hydrogen peroxide (Yim et al., 1990), catalyzing nitration by peroxynitrite (Beckman et al., 1993), copper buffering (Culotta et al., 1995), maintenance of the activity of the phosphatase calcineurin (Wang et al., 1996), zinc homeostasis (Wei et al., 2001), thiol oxidation (Winterbourn et al., 2002) and finally, modulation of inflammation (Marikovsky et al., 2003). It is thus possible that the pathological effects of knocking out, overexpressing or mutating SOD are derived at least in part from modulation of the ability of SOD1 to carry out one or more of these additional processes.

1.3 Commonly used murine models of SOD1-related ALS pathology

The majority of research carried out on ALS pathophysiology to date has been performed in rodent models bearing mutations in SOD1. Although at least 15 different SOD1-based rodent models have been generated (Turner and Talbot, 2008), the most commonly used are $SOD1^{G93A}$ (Gurney, 1994), followed by $SOD1^{G37R}$ (Wong et al., 1995) and $SOD1^{G85R}$ (Bruijn et al., 1997) rodents. The mutant SOD1 proteins produced in these models are either abundantly expressed, stable and dismutase active ($SOD1^{G93A}$ and $SOD1^{G37R}$) or expressed at low levels and unstable with limited dismutase activity ($SOD1^{G85R}$) in the CNS.

1.3.1 SOD1^{G93A} mice

1.3.1.1 The effect of transgene copy number on pathology in SOD1^{G93A} mice

The first published SOD1^{G93A} mouse line, designated G1, was produced by Gurney and colleagues and had 18 predicted transgene copies (Gurney, 1994). This line has subsequently produced two further lines of SOD1^{G93A} mice through intra-locus recombination events during meiosis that resulted in copy number changes (Gurney, 1997, Alexander et al., 2004).

1. The high copy number or G1H line (25 predicted copies), designated B6SJL-TgN(SOD1-G93A)1Gur, which is now commercially available at the Jackson Laboratory (Chiu et al., 1995)
2. A low copy number line (8 predicted copies), designated B6SJL-TgN(SOD1-G93A)1Gur^{dl} (Gurney, 1997, Acevedo-Arozena et al., 2011).

The high copy number line is the most commonly used G93A line in ALS research and will be referred to as SOD1^{G93A} for the remainder of this thesis, whereas the less frequently used low copy line will be referred to as SOD1$^{G93A\ G1L}$. Comparison of these models shows that transgene copy number strongly influences the clinical phenotype experienced by mutant SOD1 mice (Alexander et al., 2004). Specifically, SOD1$^{G93A\ G1L}$ mice display a substantially delayed disease onset and increased survival time compared to the high copy SOD1^{G93A} line. It is therefore essential that any mice possessing transgene copy numbers that are different to the rest of their cohort are excluded from experimental analyses as this could introduce error into results. (Scott et al., 2008).

1.3.1.2 The timeline of pathology in high copy SOD1^{G93A} mice

The key pathological features of SOD1^{G93A} mice are summarized in **Figure 1.** SOD1^{G93A} mice are considered to be pre-symptomatic until ~90 days of age (3 months) when fine tremors and weakness can be seen in their hindlimbs. Weakness and paresis in the hindlimbs then progressively worsens until ~120 days (4 months) when mice usually develop rigid hindlimb paralysis. In order to prevent excessive suffering following the onset of paralysis, artificial end points are used when investigating lifespan in SOD1^{G93A} mice. The most commonly used end point is the inability of mice to right themselves within 30s of being placed on a side (Scott et al., 2008). Pathologically, evidence of the denervation of hindlimb muscles has been observed as early as 25 days of age in SOD1^{G93A} mice (Gould et al., 2006), and is fully underway by 45 days of age when 40% of endplates have been observed to be denervated in these animals (Fischer et al., 2004). This is closely followed by a progressive accumulation of misfolded and aggregated SOD1 in the cytoplasm of motor neurons as well mitochondrial vacuolation within these cells and the occurrence of increased astrogliosis in the spinal cord (Gould et al., 2006). A severe loss of motor axons from the ventral root occurs between approximately 47 and 80 days of age and loss of α-motor neuron cell bodies from the lumbar spinal cord occurs after day 80. A 50% drop-out of lower motor neurons is evident at 100 days (Fischer et al., 2004). This retrograde sequence of neurodegeneration, starting at the neuromuscular junction and progressing through the axon to the motor neuron cell body, has lead to the hypothesis that ALS may be a distal axonopathy with motor neurons degenerating via a 'dying back' mechanism (Fischer et al., 2004). In direct support of this, complete rescue of motor neurons from mutant SOD1-mediated death, by deletion of the pro-apoptotic factor Bax in SOD1^{G93A} mice, failed to prevent neuromuscular denervation and ALS-like pathology (Gould et al., 2006). This supports the idea that clinical symptoms in

the SOD1^{G93A} model of ALS largely result from damage to the distal motor axon rather than from activation of the cell death pathway (Gould et al., 2006). Furthermore, autopsy of a single 58-year old ALS patient who died unexpectedly through non-ALS related causes after having shown symptoms for a 6-month period, demonstrated denervation and reinnervation changes in muscle but normal appearing motor neurons in the spinal cord. Although a far greater sample size would be required to draw firm conclusions on this, these observations are in support of the distal axonopathy hypothesis for ALS patients.

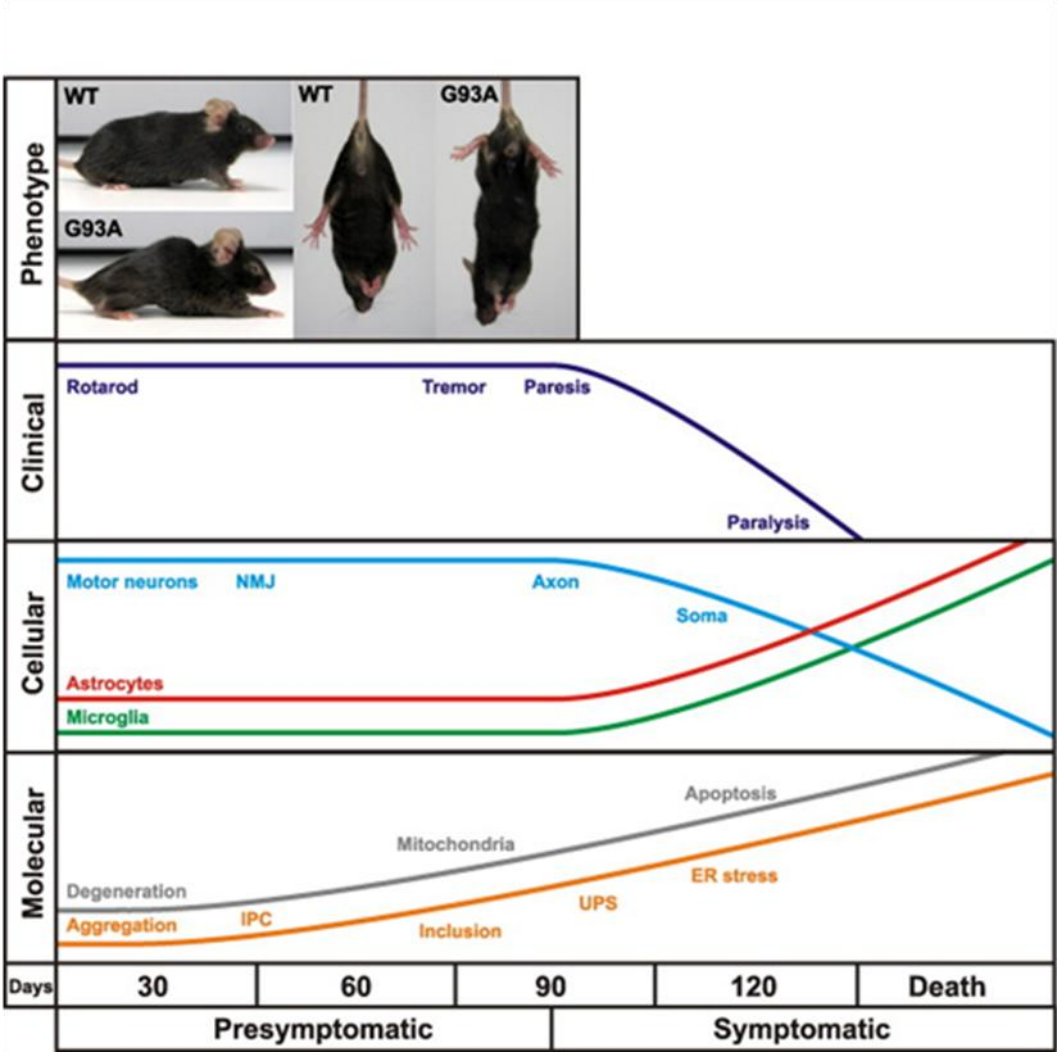


Figure 1: Time course of clinical and neuropathological events in high copy number transgenic SOD1^{G93A} mice (adapted from Turner and Talbot 2008, Figure 2).

SOD1^{G93A} mice develop hindlimb tremor, weakness and locomotor deficits at approximately 90 days of age (symptom onset) which is preceded by distal synaptic and axonal degeneration. This progresses into fatal paralysis by approximately 120 days of age, concomitant with spinal motor neuron loss. Microglia and astrocytes become progressively activated following disease onset. Pathology in SOD1^{G93A} mice is accompanied by a sequence of mutant SOD1 aggregation in motor neurons, beginning with the formation of insoluble protein complexes (IPC) and eventually leading to the formation of inclusion bodies that are modified by the ubiquitin-proteasome system (UPS) and are thought to lead to ER stress. Mitochondrial dysfunction in motor neurons and astrocytes is observed early on in the disease course and may lead to damage in motor neuron axons and eventual motor neuron death through induction of apoptosis.

Interestingly, electrophysiological recording of hindlimb muscle and motor unit isometric forces throughout the lifespan of SOD^{G93A} mice, combined with histological analyses within these muscles, has revealed that the neuromuscular junctions and axons of large motor neurons innervating large motor units in fast twitch muscles, are the first to degenerate in these animals. The neuromuscular junctions and axons of smaller motor neurons innervating small motor units in slow twitch muscles are more resistant to mutant SOD1-mediated toxicity and survive until the latter stages of the disease (Hegedus et al., 2007). This results in the muscles of $SOD1^{G93A}$ mice adopting a progressively slower phenotype and has indicated that the size of motor neurons, their axons, and their motor unit size are important determinants of motor neuron susceptibility in ALS (Hegedus et al., 2007, Hegedus et al., 2008). This idea was first highlighted by the work of Fisher and colleagues who observed that the longest and largest motor neuron axonal fibers with the highest metabolic demand seemed to be the most susceptible to dying back in $SOD1^{G93A}$ mice (Fischer et al., 2004).

It is also important to note that pathology in $SOD1^{G93A}$ mice is not limited to lower motor neurons. Indeed experiments performed by Zang and colleagues involving the insertion of the retrograde tracer Fluorogold into the T12 segment of the spinal cord and subsequent counting of the number of labeled neurons in the sensorimotor cortex and brainstem of 60, 90 and 110 day-old $SOD1^{G93A}$ mice, revealed a small loss of corticospinal and bulbospinal projections at 60 days of age (Zang and Cheema, 2002). This increased to a loss of 53% of corticospinal, 41% of bulbospinal and 43% of rubrospinal motor neurons by 110 days of age. In light of these observations, they suggested that the $SOD1^{G93A}$ mouse develops a pathology that resembles the late stages of human motor neuron disease where both lower motor neurons and descending cortical and bulbar motor neurons are affected (Zang and Cheema, 2002).

1.3.2 SOD1^{G37R} mice

Despite confirmation in vitro that SOD1 enzymes carrying the G37R mutation retain full specific dismutase activity (Borchelt et al., 1994), transgenic mice expressing high levels of this mutant protein (in addition to their endogenous murine SOD1) develop classic ALS-like pathology. Specifically, these mice appear normal during their first few months of life but begin show overt ALS-like symptoms including fine axial tremor, asymmetric weakness of limbs, poor grooming, rough coat and muscle wasting (particularly along the flanks) between 4 and 6 months of age (120-180 days of age) and eventually develop hindlimb paralysis (Wong et al., 1995). Motor neuron loss occurs in the ventral horns of the lumbar, thoracic and cervical spinal cords of these animals as well as in the brainstem and activated microglia and astrocytes can be seen in the spinal cord. Interestingly, these mice, like high copy SOD1^{G93A} mice, show vacuolation of mitochondria within motor neurons (Wong et al., 1995).

1.3.3 SOD1^{G85R} mice

Transgenic SOD1^{G85R} mice are characterised by a late-onset (at 8-10 months of age) and aggressive disease with a short duration (mice are usually completely paralysed within 2 weeks of showing initial signs of hindlimb weakness and atrophy) (Bruijn, 1997). Interestingly, these mice develop disease at mutant protein levels that are lower (20-90%) than endogenous murine SOD1 and the mutant SOD1 protein expressed has negligible dismutase activity (Bruijn et al., 1997, Ratovitski et al., 1999). The timecourse of ALS-like pathology in SOD1^{G85R} mice is summarised in **Table 1.** These mice show SOD1 positive inclusions in both neurons and glia that increase with disease progression and additionally show a concomitant decrease in the glial glutamate transporter (GLT-1) (see below). Unlike SOD1^{G93A} mice and SOD1^{G37R} mice, these mice do not show vacuolation of mitochondria

within motor neurons. Although this remains to be determined, the fact that $SOD1^{G85R}$ mice differ clinically (later onset plus rapid progression) and pathologically (presence of astroglial inclusions and absence of vacuoles) from $SOD1^{G93A}$ and $SOD1^{G37R}$ mice, could be explained by differences 1) in the toxic properties of the mutants, such as preferential, conformation-dependent use of peroxide, peroxynitrite, or other abnormal substrates and 2) the susceptibility of different cell types (i.e. neurons and glia) to each mutant's toxic effects.

Table 1: Pathological timecourse of SOD1^{G85R} transgenic mice, a model of ALS

Astroglial							
Astrocytosis	-	-	-	-	+	+	+++
SOD1-immunoreactive inclusions	-	-	-	+	-	++	+++
Ubiquitin-immunoreactive inclusions	-	-	-	+	-	++	+++
Neuronal							
Neuronal loss	-	-	-	-	-	-	++
Axonal degeneration	-	-	-	-	+	++	+++
SOD1 and ubiquitin-immunoreactive inclusions	-	-	-	-	-	+	++
SOD1-immunoreactive perikaryal aggregates	-	-	-	+	+	+	+
Ubiquitin-immunoreactve perikaryal aggregates	-	-	-	+	+	+	+
Clinical phenotype	-	-	-	-	-	disease onset	end stage
Age in months	2	3.5	5.5	6	6.5	7.5	8

Table adapted from Bruijn et al. (Bruijn et al., 1997). Spinal cords of SOD1^{G85R} animals at various ages were examined for severity of ventral root degeneration and astrogliosis as well as neuronal or glial inclusions. These parameters were assessed and graded as follows: +, mild degree or infrequent occurrence; ++, moderate density or moderate occurrence; and +++, marked degree and frequent.

1.4 Toxic processes that may contribute to motor neuron degeneration in ALS

Although the primary triggers/mechanisms for motor neuron degeneration in ALS remain elusive, research in patients and mutant SOD1 based models has revealed several processes that may contribute to pathology. The most commonly discussed of these mechanisms include: inflammation and toxic glial activation, oxidative stress, excitotoxicity, mitochondrial abnormalities, protein aggregation, axonal transport defects and ER stress (Ilieva et al., 2009, Cozzolino et al., 2008a, Wijesekera and Leigh, 2009), many of which are closely interrelated and will be discussed below. These mechanisms and their interactions are summarized in **Figure 2.**

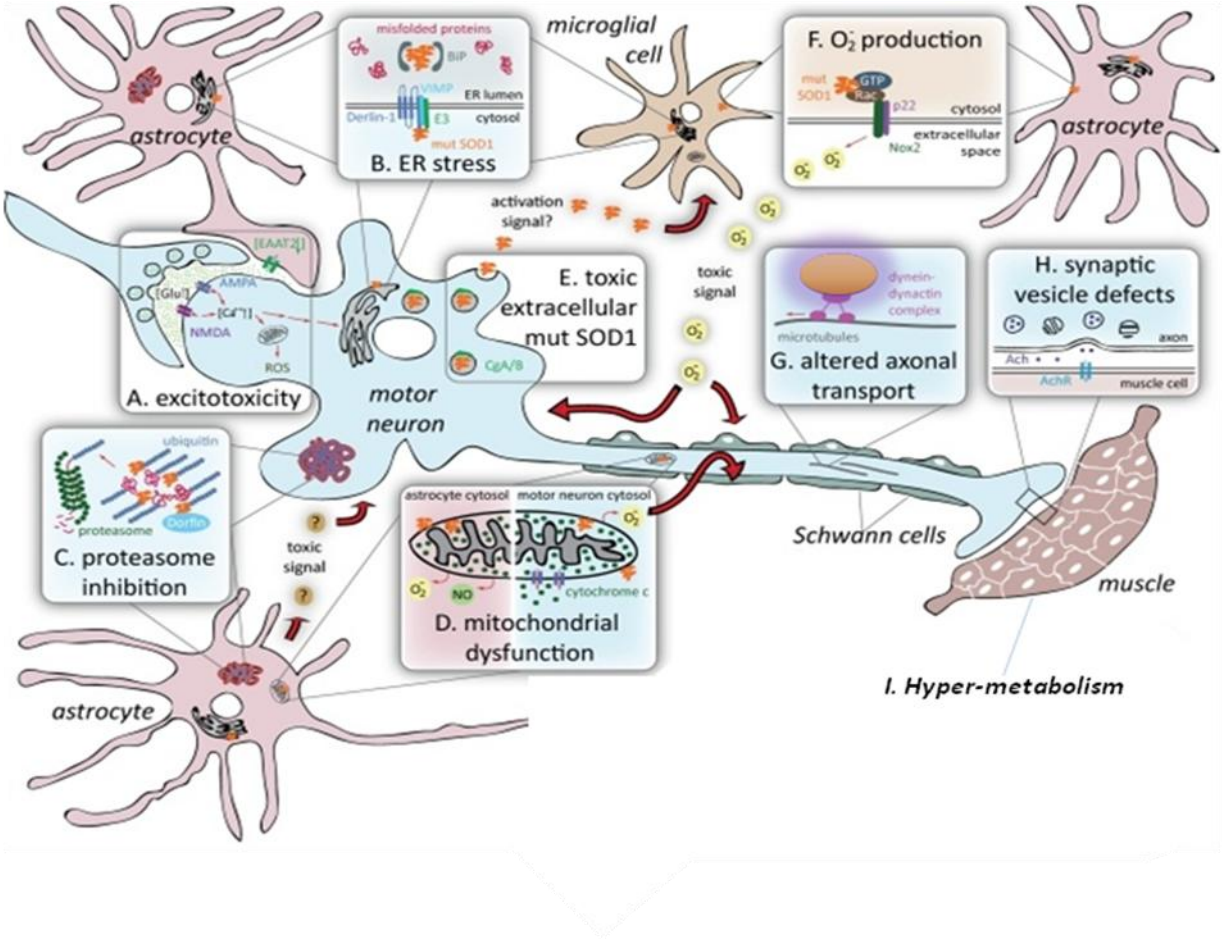


Figure 2: Proposed mechanisms of toxicity in SOD1-mediated ALS (Adapted from Ilieva et al., 2009, Figure 1)

(A) Excitotoxicity involves the hyperactivation of motor neurons and can result from failure to rapidly remove the neurotransmitter glutamate from synapses. This may occur in ALS due to a deficiency in the glutamate transporter EAAT2 in neighboring astrocytes. (B) ER stress may be induced by abnormal interactions of mutant SOD1 with ER proteins. (C) Proteasome inhibition due to "overload" of the proteasome degradation pathway with ubiquitinated misfolded protein aggregates may damage astrocytes and motor neurons. (D) Mitochondrial dysfunction mediated by mutant SOD1 deposition on the mitochondrial membrane (or other mechanisms) may provoke the release of toxic molecules from mitochondria in both motor neurons and astrocytes (E) Toxic extracellular mutant SOD1 secreted from motor neurons after interaction with components of neurosecretory vesicles may contribute to toxic microglial activation. (F) Superoxide production by microglia or astrocytes may damage neighboring motor neurons. (G) Altered axonal transport may confer toxicity to motor neurons (H) Synaptic vesicle defects such as stalling and loss from distal synapses in vulnerable motor neurons is an early event in ALS and may contribute to pathology. (I) muscles in ALS patients and murine SOD1 show a hyper-metabolic rate, which may also contribute to pathology.

1.4.1 Inflammation and the non-cell autonomous nature of ALS

1.4.1.1 Functions of microglia, astrocytes in the CNS

Microglia are derived from the hematopoetic cell lineage and are the resident macrophages of the nervous system. They are distributed throughout the CNS and continuously monitor the extracellular environment with mobile arborizations of cell processes (Hanisch and Kettenmann, 2007). Microglia are the first line of defense against infection or injury to the nervous system. In response to CNS insults, these cells change their morphology from a ramified to more amoeboid form and migrate towards the site of damage in order to clear it. Although microglia are always active through their surveying of the environment, this shift in morphology and mobilisation to defend the CNS is generally referred to as microglial activation (Hanisch and Kettenmann, 2007). The responses of activated microglia to CNS insults van be varied, however microglial activation is often associated with the secretion of proinflammatory molecules such as tumor necrosis factor (TNF) α, interferon γ (IFNγ), and interleukin 1β (IL1β) and the upregulation of oxidant molecules such as nitric oxide (NO) and $O_2^{\cdot-}$, which can protect against invading organisms. This pro-inflammatory action serves to clear hazards and repair any damage and resolves again when anti-inflammatory molecular networks outweigh proinflammatory molecular networks. In addition to contributing to the proinflammatory phase of CNS-defense, microglia can also contribute to the resolution and regulation of inflammation through secretion of trophic and anti-inflammatory factors such as insulin-like growth factor 1 (IGF1), interleukin 4 (IL4), and interleukin 10 (IL10) (Singh et al., 2011). The behavior of microglia in terms of their proinflammatory and anti-inflammatory actions has been shown to be influenced by the surrounding astrocytes and inflammatory T-cell subsets within their environment. Indeed it is increasingly becoming clear that microglia can adopt a deleterious (so-called M1 microglia) or a neuroprotective/

benign (so-called M2 microglia) phenotype, depending on their intrinsic properties, interaction with the cellular microenvironment, and presence of pathogenic factors. (Hanisch and Kettenmann, 2007, Henkel et al., 2009, Tiemessen et al., 2007, Kigerl et al., 2009). Maintenance of an appropriate balance between M1 and M2 microglia is therefore important to prevent excessive inflammation and microglia-induced damage in the CNS (Kigerl et al., 2009).

Astrocytes are ectodermal cells that outnumber neuronal cells by over five-fold and have many important trophic functions in the CNS. These functions include but are not limited to: regulation of blood flow, homeostasis of extracellular fluid, ions and neurotransmitters, energy provision and regulation of synapse function and synaptic remodeling (Sofroniew and Vinters, 2010). In addition to these normal functions, astrocytes have been shown to respond to various CNS insults such as infection, trauma, ischemia and neurodegenerative disease by a process that has been termed reactive astrogliosis. Reactive astrogliosis involves changes in the molecular expression and morphology of astrocytes and in severe cases this leads to scar formation (Sofroniew, 2009). Although the functions and effects of reactive astrocytes remain to be fully elucidated, transgenic deletion studies have shown that
reactive astrocytes can exert a number of protective functions in response to CNS insults, including blood brain barrier (BBB) repair, neural protection and restricting the spread of inflammatory cells, and infection. (Sofroniew, 2009, Sofroniew and Vinters, 2010). However, disruption or loss of these functions or gain of novel functions during reactive astrogliosis has the potential to contribute to neuronal dysfunction and pathology (Hamby and Sofroniew, 2010).

1.4.1.2 Glial activation in ALS

Although, the degeneration of motor neurons and their axons is the ultimate cause of death in ALS patients and models (Gould et al., 2006), histological assessment of the spinal cords of both ALS patients and rodent modes have revealed that motor neurons are not the only cells within which disease-related changes can be observed. Indeed, many studies have documented the activation of microglia and astrocytes, and the appearance of lymphocytes in post-mortem spinal cord tissues of patients (Kawamata et al., 1992, Engelhardt et al., 1993, Nagy et al., 1994, Schiffer et al., 1996, Kushner et al., 1991) and transgenic mutant SOD1 models (Hall et al., 1998, Alexianu et al., 2001). Furthermore, work using positron emission tomography has provided direct evidence of widespread microglial activation in the brains of living ALS patients (Turner et al., 2004b) These observations lead to the hypothesis that ALS is a non-cell autonomous process, involving toxic events in motor neurons as well as in their neighboring non-neuronal cells. The first evidence for this was derived from analysis of chimeric mice, in which a protective effect of wild-type non-neuronal cells surrounding mutant SOD1 expressing motor neurons was observed (Clement et al., 2003). Subsequent analyses involving cell type specific Cre-mediated excision of the mutant SOD1 gene in transgenic mice, have shown that reducing mutant SOD1 expression in motor neurons delays disease onset (Boillee et al., 2006), whereas reducing mutant SOD1 expression in a similar fashion in either microglia (Boillee et al., 2006) or astrocytes (Yamanaka et al., 2008) delays disease progression. These studies suggest that the convergence of damage within a number of cell types is involved in the degeneration of motor neurons in ALS (Ilieva et al., 2009).

Interestingly, the contribution of microglia to motor-neuron degeneration appears to be influenced by infiltrating T-cells (Appel et al., 2010). In $SOD1^{G93A}$ mice, T-cells are not

initially observed in the central nervous system (CNS), but readily infiltrate the spinal cord as the disease progresses, in a manner that is concomitant with microglial activation (Chiu et al., 2008, Beers et al., 2008). Unfortunately however, there is some debate surrounding the nature of this T-cell increase, with one study reporting an increase in both $CD4^+$ (helper T-cells) and $CD8^+$ (cytotoxic) T-cells early in the disease (Chiu et al., 2008) and another detecting $CD8^+$ cells only at the end stage of the disease (Beers et al., 2008). In order to elucidate the role of these infiltrating T-cells in the disease course, experiments were performed in which $SOD1^{G93A}$ mice were depleted of T-cells, either by crossing them to $RAG2^{-/-}$ knockout mice (which also resulted in the deletion of B cells) or to $CD4^{-/-}$ knockout mice (which allowed the selective deletion of $CD4^+$ T-cells). In both instances disease progression was significantly accelerated, whilst disease onset remained the same (Beers et al., 2008). Furthermore, this accelerated disease progression was accompanied by altered microglial morphology, increased mRNA levels for glial-derived proinflammatory cytokines and NOX2, and decreased levels of trophic factors and glial glutamate transporters (Beers et al., 2008). As the results observed were very similar when all T- and B-cells were depleted and when only CD4+ T-cells were depleted, this suggested to the authors that the absence of $CD4^+$ T-cells may have been largely responsible for the changes seen in $RAG2^{-/-}$ mice. They therefore hypothesized that $CD4^+$ T-cells provide supportive neuroprotection for motor neurons by modulating the trophic/cytotoxic balance of microglia in the spinal cord (Beers et al., 2008). This hypothesis was supported by experiments in which transplantation of bone marrow from either mutant SOD1 or WT murine donors attenuated the acceleration in disease progression and microglial changes associated with $CD4^+$ T-cell depletion. Furthermore, in subsequent experiments involving the adoptive transfer of activated $CD4^+$ T-regulatory cells (T-cells involved in suppressing the activation of the immune system) or T-effector cells (activated T-

cells that fight infection) from WT-donor mice into the spinal cords of normal SOD1^{G93A} mice, both types of T-cell were shown to increase survival (Banerjee et al., 2008).

1.4.1.3 Mechanisms by which reactive microglia may contribute to ALS pathology

In order to gain further insight into the mechanisms by which microglia may contribute to motor neuron degeneration in ALS, various *in vitro* experiments have been performed involving the co-culture of primary motor neurons with WT or mutant SOD1-expressing microglia (Xiao et al., 2007, Zhao et al., 2004). Xiao et al., for example showed that following activation with lipopolysaccharide, microglia derived from SOD1^{G93A} mice released more nitric oxide, more superoxide, and less insulin-like growth factor-1 than microglia from WT mice. Furthermore in microglia/motor neuron co-cultures, SOD1^{G93A} microglia brought about increased motor neuron death compared to WT microglia. Motor neuron survival in the presence of SOD1^{G93A} glia was inversely correlated with nitrate and nitrite concentrations, suggesting an important role of nitric oxide and therefore oxidative stress in microglia-induced motor neuron injury (Lundberg et al., 2008). Indeed in previous studies Zhao and colleagues showed that microglial-induced motor neuron injury, could be prevented by a microglial iNOS inhibitor (Zhao et al., 2004).

In addition to producing increased levels of NO, mutant SOD1^{G93A}-expressing glia have been observed to produce more superoxide **(Figure 2F)**. This is thought to occur at least partially, through a stronger association of mutant SOD1 than SOD1^{WT} with Rac1, a small GTPase that controls the activation of NADPH oxidase (a multiprotein membrane-associated complex whose catalytic subunit is Nox2). In phagocytic cells such as microglia, Nox2 normally functions to produce highly toxic extracellular superoxide in order to eradicate bacteria and

other pathogens. Under reducing conditions $SOD1^{WT}$ is thought to bind to Rac-GTP and to stabilize Rac activation by inhibiting intrinsic GTP hydrolysis. The resultant increased Rac-GTP levels are thought to lead to activation of Nox2 and therefore increased production of $O_2^{\bullet-}$. The $O_2^{\bullet-}$ generated by the Nox2 complex is then thought to be converted to H_2O_2 by SOD1. As the local concentration of H_2O_2 rises, oxidation of Rac has been observed to lead to the dissociation of SOD1. In the absence of bound SOD1, Rac-GTP, hydrolysis to Rac-GDP occurs more quickly, leading to inactivation of the Nox2 complex (Harraz et al., 2008). Through this mechanism, SOD1 is thought to sense the local concentration of ROS at sites of Rac/Nox2 complex activation and to control the activity of the complex accordingly. Interestingly however, Harraz and colleagues have shown that in certain ALS-causing SOD1 mutants, redox-dependent dissociation of SOD1 from Rac1 is impaired, leading to sustained activation of Rac1-GTP and therefore higher levels of superoxide production **(Figure 2F)** (Harraz et al., 2008). In support of toxicity resulting from increased association of mutant SOD1 proteins with Rac1, glial cell toxicity associated with expression of SOD1 mutants in culture was shown by Harraz and colleagues to be significantly attenuated by treatment with the Nox inhibitor apocynin. Furthermore, treatment of $SOD1^{G93A}$ mice with apocynin also significantly increased their survival (Harraz et al., 2008).

In addition to these studies documenting increased production of free radicals by mutant SOD1-expressing microglia, various studies have documented aberrant expression of a number of proinflammatory cytokines, including IL1β and TNFα by these cells (Weydt et al., 2004, Meissner et al., 2010). In accordance with this, many types of pro-inflammatory mediators have been shown to be increased in ALS patients (Cereda et al., 2008, Kuhle et al., 2009) and in SOD1-based models (Hensley et al., 2002, Yoshihara et al., 2002). It thus seems

likely that microglia contribute to disease progression in ALS through bringing about increased oxidative stress and damage through aberrant expression of pro-inflammatory cytokines and chemokines.

1.4.1.4 Mechanisms by which reactive astrocytes may contribute to ALS pathology

One of the major protective functions of astrocytes in the CNS is to keep extracellular glutamate levels low. This is necessary for the prevention of the excitotoxicity that can result from glutamate-induced excessive neuronal firing and thus increased cellular calcium influx. Riluzole, the only drug to date that has shown any protection against disease progression in ALS patients (Bensimon et al., 1994, Lacomblez et al., 1996), is thought to bring about its beneficial effect through its anti-excitotoxic properties (Doble, 1996). It is therefore thought that excitotoxicity may play a significant role in ALS pathology (Van Den Bosch et al., 2006). Astrocytes clear excess glutamate neurotransmitter from neuronal synaptic clefts using the EAAT2 (GLT1 in mice) transporter in their plasma membrane. Interestingly, in support of a role for astrocyte-mediated excitotoxicity in ALS, Rothstein and collaborators have extensively published results indicating that astrocytic clearance of glutamate is impaired in both sporadic and familial cases of ALS and in SOD1-based rodent models, due to a loss of the EAAT2/GLT1 transporter in the astrocytic processes that surround the synapses of motor neurons **(Figure 2A)** (Rothstein et al., 1995, Bruijn, 1997, Howland et al., 2002, Yang et al., 2009). Furthermore, they have reported that this specific loss of the EAAT2 transporter is likely due to aberrant mRNA splicing. Specifically, they analyzed EAAT2 mRNA in frozen postmortem tissue in 30 ALS patients and 48 non-ALS controls by reverse transcriptase polymerase chain reaction (RT-PCR) and S1 nuclease protection assays and identified a number of transcript variants in ALS patients that were not present in controls. These

included transcripts retaining part of intron 7 (20 of 30 cases) and transcripts skipping exon 9 (11 of 30 cases) (Lin et al., 1998). When performing experiments to investigate how these transcript variants may contribute to ALS pathology, they identified that the intron 7–retaining transcript inhibited the expression of wildtype EAAT2 protein in Cos7 cells, which suggested that the presence of these transcripts in ALS patients may contribute to the observed reductions in EAAT2 levels (Lin et al., 1998). However it must be noted that the levels of wildtype EAAT2 mRNA were not changed in these experiments, which is surprising. Additionally, several other groups were unable to identify ALS-specific EAAT2 transcripts and instead identified the presence of EAAT2 splice variants retaining intron 7 and as well as those skipping exon 9 in the CNS of normal controls as well as ALS in cases (Meyer et al., 1999, Flowers et al., 2001). In the case of Flowers and colleagues, these investigations were made with a more robust technique (TaqMan real-time reverse transcriptase polymerase chain reaction assay rather than RT-PCR and S1 nuclease protection assays) and their results therefore shed serious doubt on the importance of intron 7–retaining and exon 9 excluding EAAT2 transcripts in ALS. An alternative explanation for the observed decreases in the expression of the EAAT2 transporter in ALS patients is therefore required. .

In support of a role for astrocyte-mediated excitotoxicity in ALS pathogenesis, in co-culture experiments, normal astrocytes have been shown to induce the upregulation of the glutamate receptor subunit GluR2 in motor neurons. This GluR2 subunit produces glutamate receptors that are impermeable to calcium and therefore protects neurons from excitotoxic damage. However, mutant SOD1 expression in astrocytes has been shown to abrogate their ability to induce GluR2 expression in neighboring motor neurons, thus leaving these motor neurons more vulnerable to excitotoxicity (Van Damme et al., 2007).

In addition to a potential astrocyte mediated excitotoxic effect in ALS, experiments with $SOD1^{G93A}$ expressing astrocytes have revealed several other mechanisms by which these cells may contribute to ALS pathogenesis. For example, astrocytes derived from $SOD1^{G93A}$ rodents have been shown to release more pro inflammatory cytokines (including TNFα, IL1β and IFNγ) (Hensley et al., 2006) and NO than WT astrocytes (Vargas et al., 2006) suggesting that they may contribute to oxidative stress and inflammation in ALS patients and models. Furthermore experiments in which primary astrocytes derived from $SOD1^{G93A}$ mice were co-cultured with motor neurons derived from either WT or $SOD1^{G93A}$ mice have revealed that $SOD1^{G93A}$ astrocytes can bring about negative changes in mitochondrial function in both WT and mutant neurons. These changes include both a reduction in the mitochondrial redox state and a decrease in the mitochondrial membrane potential (Bilsland et al., 2008). This represents another mechanism by which astrocytes may cause damage to motor neurons in ALS.

1.4.1.6 Schwann cells in ALS

Schwann cells are myelin generating cells that are closely associated with the full length of the axons of lower motor neurons **(Figure 2)** and are known to participate in axonal development and regeneration. Interestingly, selective excision of dismutase-active $SOD1^{G37R}$ from a substantial proportion of Schwann cells (70%) in $SOD1^{G37R}$ mice has been shown to bring about a significant acceleration of disease progression in these animals (Lobsiger et al., 2009). In light of observations that dismutase inactive mutants uniformly generate more rapidly progressing disease in mice than dismutase active mutants (Lobsiger et al., 2009), Lobsinger and colleagues proposed that dismutase activity in within Schwann cells

surrounding lower motor neurons may normally act to protect these motor neurons from ROS induced damage in $SOD1^{G37R}$ mice (Lobsiger et al., 2009). However, experiments to investigate this hypothesis (potentially by elevating dismutase activity selectively within Schwann cells in $SOD1^{G37R}$ mice) are yet to be performed and therefore the role of Schwann cells in ALS pathogenesis requires further elucidation.

1.4.1.6 Oligodendrocytes and $NG2^+$ cells in ALS

The mammalian CNS contains a ubiquitous population of glial progenitors referred to as $NG2^+$ cells that have the ability to develop into oligodendrocytes (and potentially other glial and neuronal cell types (Guo et al., 2009)) and undergo dramatic changes in response to injury and demyelination. Kang and colleagues recently set out to examine how $NG2^+$ cells in the spinal cord respond to pathology in $SOD1^{G93A}$ mice. In order to do this they administered BrdU to these mice for 2 days prior to analysis at 75 (presymptomatic), 90 (symptomatic), or ~120 (end stage) days of age (Kang et al., 2010). Interestingly, the number of $BrdU^+$ $NG2^+$ cells in the spinal cord in $SOD1^{G93A}$ mice was observed to increase 4-fold in the lumbar spinal cord by symptom onset and 20-fold by end stage, indicating that $NG2^+$ cells contribute to the extensive gliosis observed in $SOD1^{G93A}$ mice (Kang et al., 2010). Kang and colleagues also identified that these $NG2^+$ cells underwent accelerated differentiation into oligodendrocytes and remained committed to the oligodendrocyte lineage rather than differentiating into other cell types such as astrocytes (Kang et al., 2010). Interestingly, in follow up studies (which are yet to be published but have been presented verbally at several meetings, including the André-Delambre Symposium on ALS, held 24-25 September 2010 in Québec City, Canada and the Muscular Dystrophy Association National Scientific Conference, held 13-16 March in Las Vegas, Nevada), Kang and colleagues have discovered

that oligodendrocytes in mutant SOD1 mice are malformed and readily degenerate. Furthermore, they have observed that selective deletion of mutant SOD1 in oligodendrocytes in a mutant SOD1 mouse model, extends the survival of these animals for a longer period than observed following the deletion of mutant SOD1 in any other cell type to date (ALS-Forum, 2011). It will therefore be interesting to study these results further when they are published and to observe the results of future studies investigating the role of $NG2^{+}$ cells in ALS pathology.

1.4.2 Protein misfolding and aggregation in ALS

1.4.2.1 Misfolding and aggregation of SOD1 in familial ALS

A common feature of ALS-causing mutant SOD1 proteins is their propensity to misfold and aggregate (Wang et al., 2008b, Shaw et al., 2008, Wang et al., 2002a). Although this remains a matter of debate, several lines of evidence suggest that mutant SOD1 aggregates or intermediates in the aggregation process may be toxic to motor neurons. Wang et al., have for example demonstrated that the aggregation propensity and stability of different mutant forms of SOD1 in a cohort of familial ALS patients, could together account for 69% of the variability in patient survival time (Wang et al., 2008b) and Lindberg and colleagues have also reported similar results (Lindberg et al., 2005). Furthermore, strong correlations between disease progression and the levels of insoluble mutant SOD1 species present in affected neuromuscular tissues have been observed in various murine SOD1-based models (Johnston et al., 2000, Wang et al., 2002a, Wang et al., 2005, Turner et al., 2003c). Several mechanisms have been proposed by which misfolded and/or aggregated species of mutant SOD1 in motor

neurons may contribute to ALS pathology, a number of these will be discussed below (or in subsequent sections).

1.4.2.1.1 Induction of endoplasmic reticulum stress

Endoplasmic reticulum (ER) stress signaling, otherwise known as the unfolded protein response (UPR), is triggered by an increased load of misfolded proteins in the organelle (Schroder and Kaufman, 2005). The aim of the UPR is to bring about a decrease in the folding demand and an increase in the folding capacity of the ER in order to maintain homeostasis within the organelle. In order to decrease the folding demand, transcription of genes encoding secretory proteins and translation are downregulated and the clearance of slowly folding or misfolded proteins through the ER-associated degradation (ERAD) pathway is increased. To increase the folding capacity of this organelle, the synthesis of ER resident molecular chaperones and foldases is increased and the ER increases in size to permit dilution of the increased unfolded protein load (Schroder and Kaufman, 2005) Although the UPR is usually a short term homeostatic mechanism and is necessary for cell survival, prolonged induction of the UPR leads to the triggering of apoptosis and can be damaging (Atkin et al., 2006) .

Several pathways by which mutant SOD1 may induce/perturb ER stress- signaling have been identified. Firstly, Kikuchi and colleagues have identified that in $SOD1^{G93A}$ mice, mutant SOD1 accumulates inside the ER, where it forms insoluble high molecular weight complexes and interacts with the ER chaperone, immunoglobulin-binding protein (BiP) **(Figure 2B)** This accumulation increases with disease progression and occurs specifically in affected spinal cord tissues (Kikuchi et al., 2006). In normal conditions, BiP binds to the luminal

domains of ER stress transducers such as the kinase and endonuclease IRE1, the basic leucine-zipper transcription factor ATF6, and the PERK kinase, in order to keep them in an inactive state (Schroder and Kaufman, 2005). However, as unfolded proteins accumulate in the ER lumen, BiP dissociates from these ER stress sensors, which brings about their activation. Interestingly, Kikuchi and colleagues found an age dependent activation of ATF6 specifically in degenerating areas, such as the spinal cord, but not in unaffected areas, such as cerebellum, in transgenic $SOD1^{G93A}$ mice. This suggested to them that during the course of pathology in these animals, BiP is titrated from the luminal domain of ATF6 and potentially other ER stress tansducers, by the ER accumulation of mutant $SOD1^{G93A}$, thus bringing about a progressive induction of ER stress.

The second mechanism by which misfolded SOD1 is thought to induce ER stress is through inhibition of the ERAD pathway. The first critical step of the ERAD pathway is the retrograde transport of misfolded proteins out of the ER lumen into the cytosol, where they become ubiquitinated and subsequently degraded by the proteasome. Interestingly, a number of SOD1 mutants (including $SOD1^{G93A}$ and $SOD1^{G85R}$) but not WT SOD1 have been shown to interact with Derlin-1, a transmembrane ER protein that is critical for the transport of misfolded proteins from the ER to the cytosol **(Figure 2B)** (Nishitoh et al., 2008). Nishitoh and colleagues have shown that this interaction brings about inhibition of ERAD and also that it is involved in the induction of ER stress by mutant SOD1 (Nishitoh et al., 2008). In the same body of work Nishitoh and colleagues showed that mutant SOD1-induced ER stress in NSC-34 cells (a motor neuron-like cell line), activated the apoptosis signal-regulating kinase 1 (ASK1)-dependent cell death pathway. Furthermore, they showed that perturbation of binding between mutant SOD1 and Derlin-1 by a Derlin-1-derived oligopeptide in spinal cord

cultures derived from E12.5 mouse embryos (infected with lentiviral vectors containing mutant SOD1), suppressed mutant SOD1-induced ER stress, ASK1 activation, and motor neuron death. This lead them to cross ASK1 knockout mice with $SOD1^{G93A}$ mice, which resulted in an extension of the life span of these animals but no change in disease onset (Nishitoh et al., 2008). These findings suggest that while ER stress-induced ASK1 activation may not be the primary trigger for ALS pathology, it may be involved in disease progression in familial ALS.

Interestingly, elegant work by Saxena and colleagues has lent further weight to the hypothesis that ER stress may accelerate disease progression in ALS. They have shown in three separate lines of SOD1 mice (G93A high and low copy and G85R) that fast fatigable motor neurons, which are known to be more vulnerable to ALS pathology than fast fatigue-resistant and slow motor neurons (Hegedus et al., 2007), are selectively prone to ER stress and show gradually upregulated ER stress markers (including elevated BiP signaling and upregulation of the UPR marker phosphorylated eukaryotic initiation factor 2α (P_i-eIF2α)), from as early as birth onwards (Saxena et al., 2009). Interestingly, they have also shown that while all motor neuron types show an accumulation of ubiquitin in these mice, it is only the vulnerable fast fatigable motor neurons in which this leads to a marked UPR response until very late in the disease when the more resistant motor neurons show evidence of UPR induction prior to degenerating. This suggests that increased susceptibility to ER stress plays a contributory role to the increased vulnerability of fast fatigable motor neurons in ALS. This is supported by additional experiments performed by Saxena and colleagues in which they showed that the specific ER stress-protective agent salubrinal, could attenuate axon pathology and

denervation and extend survival in $SOD1^{G93A}$ mice, while not affecting motoneuron ubiquitin signals (Saxena et al., 2009).

It is also interesting to speculate that the association of mutant SOD1 with the ER, could impede the synthesis of a number of important proteins, such as the glutamate transporter EAAT2 **(Figure 2A)**, whose proper synthesis and maturation requires passage through this organelle. If these proteins are important for motor neuron health (or the health of other non-neuronal cells), then disruption of their synthesis could further contribute to pathology.

1.4.2.1.2 Impairment of axonal transport

Motor neurons are highly differentiated and polarised neuronal cells with extremely long axonal processes. Consequently, efficient axonal transport is essential to permit the distribution of proteins, lipids, mRNAs and organelles (mitochondria, membranous organelles, synaptic vesicle precursors, ribosomes etc.) to the cellular locations where they are required. These cargoes are actively transported downstream to the synaptic terminus (anterograde transport) or upstream to the soma (retrograde transport) in a finely regulated manor, along a framework of cytoskeletal filaments (microtubules, intermediate filaments and actin) (Sau et al., 2011). SOD1 mutants have been revealed to slow both anterograde (Williamson and Cleveland, 1999) and retrograde (Murakami et al., 2001, Bilsland et al., 2010) axonal transport in mutant SOD1 murine models, long before disease onset **(Figure 2G)**. Furthermore, axonal disorganization characterized by neurofilament misaccumulation is a common feature of both sporadic (Wong et al., 2000) and familial (Hirano et al., 1984a, Rouleau et al., 1996) forms of ALS. This has lead to the suggestion that defective axonal transport may contribute to motor neuron degeneration in ALS. Interestingly, it has been

determined that in the axons of the motor neurons that are most vulnerable to degeneration in ALS (those innervating fast fatigable muscle fibers), an early sign of vulnerability is synaptic vesicle stalling and depletion from distal synapses **(Figure 2H)** (Pun et al., 2006). Considering the importance of axonal transport in the delivery of synaptic vesicle precursors to the synapse (Sinadinos and Mudher, 2011), it seems likely that axonal transport defects are at least partially responsible for these phenomena and possibly also the vulnerability of these motor neurons to degeneration.

Cytoplasmic dynein and its essential cofactor dynactin drive retrograde axonal transport (Holzbaur, 2004) and also mediate neurofilament transport and synaptic stability in motor neurons **(Figure 2G)** (Holzbaur, 2004). The hypothesis that the disruptions in retrograde transport seen in mutant SOD1 models may play a substantial role in motor neuron degeneration is supported by the observation that a mutation in dynactin results in a slowly progressive, autosomal dominant form of lower motor neuron disease in humans (Puls et al., 2003). Furthermore, inhibition of dyenin-mediated axonal transport by postnatal overexpression of the motor protein dynamitin, has also been shown to bring about a late-onset progressive motor neuron degenerative disease in mice (LaMonte et al., 2002). Additionally Loa (legs at odd angles) and Cra1 (Cramping 1) mice that are heterozygous for mutations in the dynein cytoplasmic heavy chain 1gene have been shown by some to undergo progressive α- motor neuron degeneration and locomotor defects (Hafezparast et al., 2003) and others to develop a proprioceptive sensory neuropathy (Ilieva et al., 2008, Chen et al., 2007). Regardless of whether α-motor neuron degeneration or sensory proprioceptive neuron degeneration are more prominent in these models, the fact that disruption of axonal transport through dynein heavy chain mutation, can cause the degeneration of these two highly polar

cell types, further supports the notion that the axonal transport defects seen in mutant SOD1 mice are likely to contribute to motor neuron degeneration.

With respect to the role of misfolded/aggregated SOD1 in bringing about axonal transport defects in mutant SOD1 mice, dynein has been shown to colocalise with SOD1 aggregates in both $SOD1^{G93A}$ mice and in rat embryonic motor neurons infected with HSV expressing mutant SOD1 (Ligon et al., 2005) and also to co-immunoprecipitate mutant SOD1, but not wild-type SOD1 in $SOD1^{G93A}$ and $SOD1^{G85R}$ mice (Zhang et al., 2007a). This has lead to the suggestion that SOD1 may disrupt axonal transport through inhibiting dynein/dynactin function (Ligon et al., 2005). However, it must be stressed that when these co-immunoprecipitation experiments were carefully reproduced in $SOD1^{G93A}$ mice by El-Kadi and colleagues, a direct interaction between mutant SOD1 and dynein could not be detected (El-Kadi et al., 2010). Further work is therefore required to elucidate how mutant SOD1 brings about the disruption of axonal transport.

1.4.2.1.3 Cellular degradation pathways for misfolded/aggregated mutant SOD1

Cytoplasmic proteins are mainly degraded by two pathways, the ubiquitin-26 S proteasome pathway (Goldberg, 2003) and macroautophagy (Ravikumar et al., 2010). The 26S proteasome is a 2.5-MDa molecular machine built from approximately 50 different subunits, which catalyzes protein degradation and functions to rid the cell of proteins that are non-functional, misfolded or potentially harmful. It consists of a barrel-shaped proteolytic core complex (the 20S proteasome), capped at one or both ends by 19S regulatory complexes, which are responsible for substrate recognition and transport into the core particle (Goldberg, 2003). Macroautophagy (hitherto referred to as autophagy) is a cellular process that involves

the formation of double membrane-bound structures called autophagosomes around portions of cytoplasm and associated organelles. These autophagosomes then fuse with lysosomes, in order to permit degradation of their contents (Yang and Klionsky, 2010). Autophagy plays a critical role in intracellular organelle homeostasis and is also employed in conditions of starvation to maintain cellular nutrient levels (Yang and Klionsky, 2010). Furthermore, autophagy has been shown to play an essential role in the removal of toxic/aggregated proteins and damaged organelles such as mitochondria that may cause toxicity to cells under conditions of stress (Metcalf et al.).

In vitro studies have shown that mutant SOD1 proteins are turned over more rapidly than wild-type SOD1 proteins (Hoffman et al., 1996) and furthermore that they can be degraded by the proteasome (Hoffman et al., 1996, Urushitani et al., 2002) as well as by autophagy (Kabuta et al., 2006) . However, in investigating mutant SOD1 degradation by these pathways further, it has been discovered that the proteasome is altered in composition (Edor et al., 2008) and its activity decreased (Kabashi et al., 2004, Cheroni et al., 2009) in the spinal cords of mutant SOD1 mice at symptomatic time points (and in some studies prior to symptom onset (Kabashi et al., 2004)). Additionally, sustained expression of mutant SOD1 in Neuro2A cells (a neuronal cell line) has been shown to reduce proteasome activity (Urushitani et al., 2002). These results suggest that mutant SOD1 proteins are damaging to the proteasome in motor neurons and that in damaging the proteasome they may lead to their own buildup within the cell **(Figure 2C)**. Furthermore it has been suggested that the buildup of mutant SOD1 proteins in the cell as a result of proteasomal inhibition, may lead to the sequestering of essential cellular components within mutant SOD1 aggregates, thus causing further damage to motor neurons (Bruijn et al., 1998).

As mentioned, mutant SOD1 proteins (A4V, G85R, and G93A) have been shown to be degraded by autophagy *in vitro* (Kabuta et al., 2006), thus suggesting that autophagy may be another mechanism by which mutant SOD1 species are cleared from cells *in vivo*. In support of this, markers of autophagy have been shown to be greatly increased in the spinal cords of $SOD1^{G93A}$ mice compared to wild-type (WT) mice (Morimoto et al., 2007, Li et al., 2008). However it must be noted that autophagic pathways are increasingly becoming implicated in neurodegenerative disease pathophysiology (Boland et al., 2008, Cheung and Ip, 2011) and therefore further work is required to identify whether the massive induction of autophagy observed in mutant SOD1 mice is protective or damaging to motor neurons.

1.4.2.1.4 Toxicity associated with secretion of misfolded mutant SOD1 by motor neurons

Chromogranin-A and chromogranin-B are soluble, acidic glycophosphoproteins and are major constituents of secretory large dense-core vesicles (LDCV) in neurons and endocrine cells. LDCVs store neuropeptides and hormones and undergo regulated exocytosis in response to appropriate cellular stimulation (Taupenot et al., 2003). Interestingly, both chromogranin A and B have been shown to interact with and mediate the secretion of mutant SOD1 proteins (both $SOD1^{G93A}$ and $SOD1^{G85R}$) from neurons and astrocytes (Urushitani et al., 2006). Moreover, Zhao and colleagues have recently shown that extracellular mutant human $SOD1^{G93A}$ or $SOD1^{G85R}$ induce the morphological and functional activation of primary microglia from WT mice, increasing their release of pro-inflammatory cytokines and free radicals **(Figure 2E)**. Furthermore, exposure of co-cultures of primary WT microglia and motor neurons to extracellular mutant SOD1 species, leads to motor neuron degeneration, by a mechanism that is dependent on the presence of microglia (Zhao et al., 2010). By contrast,

exposure of these co-cultures to extracellular WT human SOD1 species does not bring about significant microglial activation or motor neuron degeneration. Zhao and colleagues continued to identify that in this *in vitro* system at least, the activating effects of extracellular mutant SOD1 species on microglia are likely to be transduced through a CD14-TLR (toll-like receptor) dependent pathway. Since CD14 is a pattern recognition receptor, Zhao and colleagues suggest that the reason why the toxic activation of microglia specifically occurs with mutant SOD1 species over WT ones, may be that the CD14 receptor has much greater recognition for misfolded forms of the protein than correctly folded WT forms (Zhao et al., 2010). In support of a direct contribution of extracellular misfolded SOD1 species to disease pathology in ALS, overexpression of chromogranin A has been shown to bring about acceleration of the onset of motor impairment and increased numbers of activated microglia as well as misfolded SOD1 species in the spinal cords of $SOD1^{G85R}$ mice (Ezzi et al., 2010).

1.4.2.1.4 Does SOD1 misfold and aggregate in ALS patients whose pathology is not caused by mutations in SOD1?

Protein misfolding and aggregation is not just limited to cases of ALS-resulting from mutations in SOD1. Indeed the formation of inclusion bodies consisting of aggregated and unbiquitinated proteins has long been recognised as a hallmark of pathology in the spinal cords of both sporadic and familial forms of ALS (Migheli et al., 1990, LEIGH et al., 1991). This raises the question of whether misfolding and/or aggregation of SOD1 can be seen in ALS patients that do not bear mutations in this gene. This question has recently been addressed by two independent groups with contrasting results. Using a mouse monoclonal antibody (C4F4) that recognizes mutant $SOD1^{G93A}$ (and to a lesser extent $SOD1^{G37R}$) but not WT SOD1(Urushitani et al., 2007), Bosco and colleagues recently discovered that oxidized

WT SOD1 and mutant SOD1 share a conformational epitope that is not present in normal WT SOD1 (Bosco et al., 2010b). This prompted them to incubate spinal cord sections from a number of sporadic ALS patients with the C4F4 antibody to look for evidence of misfolded WT species that could have been generated as a result of oxidative stress. Interestingly, in 4 out of the 9 human sporadic ALS cases investigated, motor neurons in the lumbosacral spinal cord were markedly C4F6 immunoreactive, suggesting that an aberrantly folded WT SOD1 species were present. These observations prompted Bosco and colleagues to compare the effects mutant SOD1 and oxidised WT SOD1 proteins in an ALS-relevant biological assay. Specifically, the effects of these proteins on anteretrograde and retrograde axonal transport were analysed in a vesicle motility assay in isolated squid axoplasm. These assays revealed that oxidized WT SOD1 and misfolded WT SOD1 immunopurified from sporadic ALS tissues were both capable of inhibiting kinesin-based fast axonal transport in a similar fashion to mutant SOD1(Bosco et al., 2010b). These results suggest a potential toxic role for aberrantly folded WT SOD1 in some sporadic cases of ALS.

Kerman and Colleagues have also developed conformation specific antibodies against misfolded SOD1 species: the USOD antibody, targeted against SOD1 residues 42-48, that specifically recognises SOD1 in which the beta barrel is unfolded and the SEDI antibody that recognises the SOD1 dimer interface (Kerman et al., 2010, Rakhit et al., 2007). They recently showed that these antibodies labeled the same inclusions in serial spinal cord sections from two familial SOD1 ALS cases, suggesting that in this type of ALS, SOD1 molecules present in inclusions adopt misfolded conformations that expose the most buried core of the molecule (Kerman et al., 2010). However, in contrast to the results of Bosco et al., Kerman and colleagues could not detect any misfolded SOD1 in 10 sporadic ALS cases by either

immunohistochemistry or immunoprecipitation using their USOD and SEDI antibodies (Kerman et al., 2010). These results lead them to conclude that there is no detectable accumulation of misfolded SOD1 in motor neurons in sporadic ALS.

The contrast in the results of Bosco and colleagues and Kerman and colleagues could be explained in various ways. Firstly, both groups used a small sample size of sporadic ALS patients and considering that less than half showed C4F4 staining in the Bosco study, it is possible that by chance the patient samples used in the Kerman study were all ones that would not have shown staining with the C4F4 antibody either. Secondly, it is possible that the antibodies used in the two studies recognise different forms of misfolded SOD1. For example, the aberrant conformation adopted by oxidised WT SOD1 may not be so extreme that it brings about exposure of the dimer interface or unfolding of the beta barrel and therefore it may not be recognised by the SEDI and USOD antibodies. Finally, it is possible that the tissue preparation/ immunohistochemistry techniques used by the two groups were slightly different, thus yielding different results. Whether or not a proportion of WT SOD1 is misfolded in sporadic and familial forms of ALS without mutations in *SOD1*, recent work has shed much light on what the major protein components of ubiquitinated inclusions in these cases are. These discoveries will be discussed below.

1.4.2.2 TDP-43 and FUS aggregation in ALS and relationship between ALS and Frontotemporal Dementia (FTD)

Frontotemporal Dementia (FTD) is the most frequent cause or presenile dementia in humans and is a clinically, genetically and pathologically heterogeneous syndrome. Clinical

phenotypes encompassed by FTD include: behavioral variant FTD, semantic dementia and progressive non-fluent aphasia. Although Frontotemporal Lobar Degeneration (FTLD) is responsible for all these phenotypes, the microscopic features associated with this degeneration vary (McKhann et al., 2001). Until recently, FTLD subtypes were classified as those involving an abnormal accumulation of tau (FTLD-tau) and those associated with tau-negative, ubiquitin-positive inclusions FTLD-U (McKhann et al., 2001). Interestingly, in the early 2000's it began to become clear that a subset of ALS patients develop cognitive defects associated with neuronal degeneration in the frontotemporal lobe and furthermore that this neuropathology closely resembled FTLD-U. This lead to the hypothesis that ALS and FTD with FTLD-U might be related conditions (Lomen-Hoerth et al., 2002, Murphy et al., 2007, Mackenzie and Feldman, 2005). This hypothesis was confirmed in 2006 when the DNA/RNA binding protein TDP-43 was identified as the pathological protein in most SOD1-negative ALS cases (ALS-TDP) (Neumann et al., 2006b, Mackenzie et al., 2007) as well as in the majority of cases of FTLD-U (Neumann et al., 2006b, Arai et al., 2006a) (renamed as FTLD-TDP) (Mackenzie et al., 2010a). It is also interesting to note that while mutations in the TDP-43 gene (*TARDBP*) are not required for the occurrence of TDP-43 aggregates in ALS patients, *TARDBP* mutations that are causative for ALS have subsequently been found and are thought to account for 5–10% of classic familial ALS cases as well as some sporadic cases(Kabashi et al., 2008b). The discovery of these mutations in the RNA-binding protein, TDP-43 lead to the investigation of potential mutations in functionally related genes in a region of chromosome 16 that had previously been linked to some familial forms of ALS. These investigations resulted in the discovery of ALS-causing mutations in another RNA-binding protein, FUS (fused in sarcoma), and the identification of this protein as the pathological protein in TDP-43-negative, SOD1-negative ALS cases (ALS-FUS)

(Kwiatkowski et al., 2009, Vance et al., 2009). Furthermore, FUS was subsequently identified as the pathological protein in most of the remaining tau-negative,TDP-43-negative FTLD subtypes (renamed as FTLDFUS) (Mackenzie et al., 2010a). This lead to the now widely accepted notion that ALS AND FTD are a clinico-pathologically related spectrum of diseases and also to the intriguing possibility that defects in RNA metabolism may be involved in the pathogenesis of ALS and FTD (Mackenzie et al., 2010b, Bäumer et al., 2010). The possible involvement of RNA metabolism/processing in ALS is further supported by that fact mutations in *ANG* , which encodes, angiogenin, (another protein with RNA-processing abilities (Bäumer et al., 2010, Crabtree et al., 2007)) have also been found in both familial and sporadic ALS patients (Greenway et al., 2006)

Following the discovery of *TARDBP* mutations and TDP-43 inclusions in ALS patients, much work has been performed to create animal models of TDP-43-related ALS pathology. Indeed it has been shown that overexpression of TDP-43 (wild-type or disease mutant) in worms (Ash et al., 2010, Liachko et al., 2010), flies (Li et al., 2010, Miguel et al., 2011), zebrafish (Kabashi et al., 2010), mice (Wils et al., 2010, Xu et al., 2010) and rats (Zhou et al., 2010) is toxic in a dose-dependent manner, and can bring about neurodegeneration. However, as with aggregation of mutant SOD1 in familial ALS, it is not clear whether aggregation of TDP-43 contributes to its observed toxicity in patients and models. Additionally, TDP-43 inclusions are only observed in a subset of invertebrate and fish models (Li et al., 2010, Liachko et al., 2010), despite the existence of clear TDP-43-mediated toxicity in all models (Ash et al., 2010, Miguel et al., 2011, Li et al., 2010, Liachko et al., 2010). Furthermore, TDP-43 inclusions only appear to be a minor component of pathology in rodent models. It is still possible however that smaller, soluble oligomers of TDP-43 are toxic in models lacking

TDP-43 inclusions, or that cells containing TDP-43 inclusions have already degenerated in these models and therefore cannot be seen (Baloh, 2011). Clearly, as with SOD1, further work is required to establish whether aggregation of TDP-43 contributes to its observed toxicity.

As mutations in *FUS* (also known as *FUS/TLS* (fused in sarcoma/translocated in liposarcoma)) were discovered later than mutations in *TARDBP*, fewer FUS/TLS animal models have been reported (Da Cruz and Cleveland, 2011). However, Huang and colleagues recently reported the production of transgenic rats expressing human wild-type or an ALS-linked mutant form of FUS/TLS (R521C) in a conditional fashion. In these studies, expression of the mutant protein at levels at three to six times above that of the endogenous protein in the CNS led to degeneration of motor axons, loss of cortical and hippocampal neurons, increased denervation of neuromuscular junctions and paralysis within 30–70 days of transgene induction. Although ubiquitinated cytoplasmic aggregates were seen at the time of neuronal degeneration in these animals, these aggregates surprisingly didn't co-localise with FUS/TLS (Huang et al., 2011). Expression of WT FUS/TLS at similar levels to those in the mutant FUS/TLS mice produced a less severe pathology involving a mild loss of neurons in the cortex and hippocampus accompanied by the formation of some FUS/TLS-negative ubiquitinated aggregates at one year of age. This suggests that overexpression of mutant FUS/TLS in the CNS is more toxic than overexpression of the wild-type protein in rats. In addition to these rat models, two recent studies have identified that overexpression of WT FUS/TLS in yeast is toxic and brings about the formation of FUS/TLS containing cytoplasmic aggregates (Sun et al., 2011, Ju et al., 2011). Interestingly, in one of these studies Ju and colleagues identified five yeast DNA/RNA binding proteins, encoded by the yeast

genes *ECM32*, *NAM8*, *SBP1*, *SKO1* and *VHR1*, that could ameliorate the toxicity of human FUS/TLS without changing its expression level, cytoplasmic translocation, or inclusion formation. This could either suggest that inclusion formation seen was not essential to the FUS/TLS-mediated toxicity or potentially, that the inclusions sequestered other critical DNA/RNA binding proteins and therefore prevented them from carrying out their normal cellular functions. In addition to these studies in yeast, two further recent studies have shown that overexpression of WT or mutant forms of FUS/TLS in *Drosophila* brings about neuronal defects motor impairments in these animals (Chen et al., 2011, Lanson et al., 2011). Although Chen and colleagues did not discuss whether or not overexpression of WT or mutant FUS/TLS in their *Drosophila* brought about the formation of ubiquitinated aggregates, Lanson and colleagues saw ubiquitinated aggregates in some FUS/TLS mutants (but not all and not with WT FUS/TLS), however they did not describe whether these aggregates contained FUS/TLS. As with the transgenic FUS/TLS rats described above, overexpression of mutant forms of FUS/TLS in *Drosphila* in these studies brought about more severe defects than overexpression of the WT protein. Finally, in contrast to results in rats, yeast and *Drosophila*, overexpression of wild-type and ALS-linked mutants of FUS/TLS in zebrafish has so far failed to cause significant alterations in morphology or motor axon outgrowth (unlike with TDP-43) (Bosco et al., 2010a). Considering the results of these early studies and the variation in the results seen in different models, further work is required to establish how perturbations in FUS/TLS can bring about toxicity to motor neurons and whether aggregation of this protein is associated with its toxicity. However at this stage, as with SOD1 and TDP-43, it cannot be ruled out that FUS/TLS aggregation at least partially contributes to its toxicity in ALS patients.

1.4.3 Mitochondrial abnormalities in ALS

Mitochondria are critically important organelles in aerobic cells, carrying out many vital functions including ATP production via oxidative phosphorylation, maintenance of calcium homeostasis, calcium signaling and the regulation of intrinsic apoptosis (Shi et al., 2010). Mitochondria are highly motile organelles and in motor neurons, they use tracks of microtubules to distribute themselves evenly along axons and to travel quickly to areas of metabolic demand. In healthy cells, mitochondria form interconnected branched networks throughout the cytoplasm, via the dynamic processes of fission and fusion (Diaz and Moraes, 2008). This network allows them to provide support to all parts of the cell and is critical to their function (Cho et al., 2010). Disturbed mitochondrial ultrastructure in motor neurons (and muscles (Afifi et al., 1966)) in both sporadic (Hirano et al., 1984b, Sasaki and Iwata, 1996, Sasaki and Iwata, 2007) and familial (Hirano et al., 1984c) ALS patients first implicated mitochondria in ALS pathogenesis. Evidence for the disruption of several mitochondrial functions has subsequently been identified in various ALS models (Shi et al., 2010, Duffy et al., 2011) and will be discussed below.

1.4.3.1 Direct effects of mutant SOD1 on mitochondria

A proportion of misfolded SOD1 has been shown to be localized to the intermembrane space (IMS) between the inner (IMM) and outer (OMM) mitochondrial membranes in $SOD1^{G93A}$ mice. In support of a toxic role for $SOD1^{G93A}$ accumulation in this location, Cozzolino and colleagues have shown that expression of $SOD1^{G93A}$ (but not $SOD1^{WT}$) proteins specifically targeted to the IMS in mitochondria in NSC-34 cells (a motor-neuron like cell line), leads to rounding and fragmentation of the mitochondria as well as a reduction in mitochondrial metabolism , increased caspase-3 activation and cell death (Cozzolino et al., 2009).

Furthermore mutant $SOD1^{G93A}$ accumulation in the IMS has been shown to bring about a surprising and paradoxical increase the production of mitochondrial ROS through a mechanism that is thought to involve the promotion of cytochrome *c*-catalyzed peroxidation **(Figure 2D)** (Goldsteins et al., 2008). As mentioned above, mitochondria in the motor neurons of dismutase active $SOD1^{G93A}$ (Gurney et al., 1994) and $SOD1^{G37R}$ (Wong et al., 1995) (but not dismutase inactive $SOD1^{G85R}$) mice become vacuolated due to expansion of the IMS. In line with a toxic accumulation of mutant SOD1 in the IMS, these vacuoles were found to contain mutant SOD1 in proteinaceous aggregates in both murine models (Wong et al., 1995, Jaarsma et al., 2001, Higgins et al., 2003).

In addition to these cases where an IMS location for mutant SOD1 is seen, Vande Velde and colleagues have shown that in a large number of mutant SOD1 models (both dismutase active and inactive), misfolded mutant SOD1 is deposited onto the cytoplasmic face of the OMM **(Figure 2D)**. Furthermore ,this association is restricted to the spinal cord, indicating the existence of a specific microenvironment conducive to mutant SOD1 misfolding and mitochondrial association in the spinal cords of these animals (Vande Velde et al., 2008). Although this is yet to be determined for all SOD1-related ALS models, Vande Velde and colleagues have subsequently shown that within the spinal cords of $SOD1^{G37R}$ and $SOD1^{G85R}$ mice, the axonal mitochondria of motor neurons are primary targets for misfolded SOD1. (Vande Velde et al., 2011). Interestingly, it has also recently been shown that mutant SOD1 proteins directly interact with the voltage-dependent anion channel (VDAC1) in the OMM in spinal cord tissues derived from transgenic rats expressing dismutase active $SOD1^{G93A}$ or dismutase inactive $SOD1^{H46R}$ (Israelson et al., 2010). Furthermore, direct binding of mutant SOD1 to VDAC1 has been shown to inhibit conductance of individual channels when

reconstituted in a lipid bilayer (Israelson et al., 2010). VDAC1 is a primary contributor to ATP/ADP flux across the OMM and is also important for the import/export of Ca^{2+} and other cations (Shoshan-Barmatz et al., 2010) and it therefore seems likely that a mutant SOD1 mediated impairment in the conductance of this channel would negatively affect mitochondrial function and potentially motor neuron survival. In support of this, Israelson and colleagues have shown that reducing VDAC1 activity in $SOD1^{G37R}$ mice by crossing them to mice heterozygous for disruption of the VDAC1 gene, diminishes their survival by accelerating disease onset (in both SOD1G37R/$VDAC1^{+/-}$ and SOD1G37R/$VDAC1^{-/-}$ mice) (Israelson et al., 2010). The observed association of mutant SOD1 with VDAC1 in the OMM in transgenic rats therefore provides the first direct link between misfolded SOD1 and mitochondrial dysfunction in ALS.

1.4.3.2 Oxidative stress and defective oxidative phosphorylation in ALS patients and models

Evidence of oxidative stress has been observed in both ALS patients and models, and has therefore been implicated as part of the pathological process in this disease. For example, in ALS patients, increased levels of ROS have been found in the blood (Siciliano et al., 2002) and increased concentrations of 3-nitrotyrosine (indicative of peroxynitrite mediated nitration of protein tyrosine residues) have been observed in the CSF (Hideo Tohgi et al., 1999). Furthermore, increased carbonylation of proteins as well as peroxidation of lipids in the mitochondrial membrane has been observed in motor neurons in mixed spinal cord cultures derived from $SOD1^{G93A}$ mice (Kruman et al., 1999) and in mitochondria directly isolated from the brains and spinal cords of these animals (Mattiazzi et al., 2002). Although free radicals released by activated microglia and astrocytes are likely to play a significant role in

bringing about oxidative stress in the spinal cords of ALS patients and models (see above), free radicals released as a consequence of defective oxidative phosphorylation in the mitochondria of motor neurons may also contribute to this process. In support of this, evidence of decreased activity of respiratory chain complexes I, II, II and IV has been found in post mortem CNS tissues of sporadic ALS patients by Wiedemann and colleagues (Wiedemann et al., 2002). However it must be noted that Wiedemann and colleagues also identified reduced numbers of mitochondria compared to controls in these samples and suggested this may have been largely responsible for the impaired respiratory chain activities seen. However decreased activity of complex 1V has also been observed in the motor neurons in the spinal cords of ALS patients by Borthwick and colleagues (Borthwick et al., 1999). In $SOD1^{G93A}$ mice, a decrease in the activity of mitochondrial complex I can be seen in ventral horn motor neurons in presymptomatic stages, followed by a decreased function of complex IV after disease onset (Mattiazzi et al., 2002, Jung et al., 2002). Furthermore, reduced ATP levels have been seen in the CNS in $SOD1^{G93A}$ mice at both presymptomatic (Browne et al., 2006) and symptomatic stages (Mattiazzi et al., 2002). However defects in the electron transport chain and ATP synthesis are not seen in all mutant SOD1 based models (Damiano et al., 2006) and therefore the role of the electron transport chain in ALS pathogenesis requires further research.

1.4.3.3 Impaired calcium buffering

In addition to producing ATP, mitochondria carry out the critically important function of buffering intracellular surges of Ca^{2+} in excitable cells such as motor neurons. Mitochondrial uptake of calcium relies on the existence of a negative membrane potential across the IMM that is maintained by the action of the electron transport chain (Graier et al., 2007). Impaired mitochondrial Ca^{2+} buffering can lead to increased intracellular Ca^{2+} levels and associated cellular damage (Graier et al., 2007). In support of a role for impaired calcium handling by motor neuron mitochondria in ALS, mitochondrial buffering capacity has been found to be impaired as early as 35 days of age in the spinal cords of $SOD1^{G93A}$ mice and has also been shown to be impaired in $SOD1^{G85R}$ mice (Damiano et al., 2006). Furthermore, $SOD1^{G93A}$ mice crossed with mice genetically modified to have a decreased calcium permeability of alpha-amino-3-hydroxy-5-methyl-4-isoxazolepropionic acid (AMPA) receptors in spinal motor neurons, have been shown to have a significantly delayed onset of ALS symptoms (Tateno et al., 2004). As mentioned above, it is hypothesised that glutamate excitotoxicity in motor neurons may contribute to ALS pathogenesis (owing to impaired clearance of synaptic glutamate by astrocytes **(Figure 2A)**) (Ilieva et al., 2009). Impaired calcium buffering by motor neurons could both result from and accentuate this process (Duffy et al., 2011).

1.4.3.4 Altered mitochondrial morphology and distribution

Disturbed mitochondrial morphology and in some cases distribution has been observed in the motor neurons (and muscles (Afifi et al., 1966)) of both sporadic (Hirano et al., 1984b, Sasaki and Iwata, 1996, Sasaki and Iwata, 2007) and familial (Hirano et al., 1984c) ALS patients and this has raised the possibility that mitochondrial fission/fusion and/ or transport of mitochondria through the cell may be impaired in affected tissues in ALS patents. In order to

investigate this possibility further Vande Velde and colleagues have generated transgenic mice expressing mitochondrially targeted enhanced green fluorescent protein in motor neurons (Hb9-MitoEGFP) and crossed them to $SOD1^{G37R}$ and $SOD1^{G85R}$ mice (Vande Velde et al., 2011). Interestingly, visualization of mitochondria in the motor neurons of these animals has revealed that axonal mitochondria are increasingly spheroid and clustered at the proximal side of Schmidt-Lanterman incisures (funnel-shaped interruptions in the compact myelin sheath formed around motor neuron axons by Schwann cells (Arroyo and Scherer, 2000, Tricaud et al., 2005)) in $SOD1^{G37R}$ mice, whereas axonal mitochondria are aberrantly elongated in $SOD1^{G85R}$ mice. Both mutations resulted in the swelling of mitochondria in motor neuron cell bodies and a more irregular distribution of mitochondria in motor neuron axons (Vande Velde et al., 2011). These observations support the hypothesis of an impaired ability of mitochondria to regulate their morphology and localization in ALS. This is also supported by the fact that mitochondria in primary motor neurons from $SOD1^{G93A}$ mice (De Vos et al., 2007) and in $SOD1^{G93A}$-expressing NSC-34 cells (Tradewell et al., 2011) have been shown to become abnormally rounded. This rounded morphology is indicative of reduced fusion and/or increased fission (Knott et al., 2008), which can be influenced by elevated Ca^{2+} levels (Breckenridge et al., 2003) or by a loss of mitochondrial membrane potential (Geisler et al., 2010), both of which may occur in ALS.

As described, Vande Velde and colleagues observed a more irregular distribution of mitochondria in motor neuron axons in both $SOD1^{G37R}$ and $SOD1^{G85R}$ mice. This could be indicative of impaired axonal transport of mitochondria in the motor neurons of these mice. In support of this, anterograde transport of mitochondria has been shown to be selectively impaired in motor neurons from $SOD1^{G93A}$ mice and in primary cortical neurons transfected

with four different SOD1 mutants (De Vos et al., 2007). Furthermore in NSC-34 cells, expression of mutant SOD1 that is specifically targeted to the mitochondrial IMS, is sufficient to bring about the fragmentation (rounding) and defective axonal transport of mitochondria (both anterograde and retrograde) (Magrané et al., 2009). Interestingly, increased calcium levels have been shown to bring about the inhibition of both anterograde and retrograde mitochondrial axonal transport in cardiac myoblasts (Yi et al., 2004). Although this cannot explain the anterograde-specific mitochondrial defects observed in primary motor neurons from $SOD1^{G93A}$ mice (De Vos et al., 2007) it suggests that defects in mitochondrial axon transport seen in *in vitro* models of ALS may at least in part be influenced by impaired calcium buffering in these cells.

1.4.3.5 Mitochondrial apoptosis in ALS

Considering observations by Gould and colleagues that a complete rescue of motor neurons from death in $SOD1^{G93A}$ mice, by deletion of the pro-apoptotic factor Bax, was unable to prevent neuromuscular denervation and ALS-like pathology (Gould et al., 2006), it seems unlikely that mitochondrially induced apoptosis plays a primary role in ALS pathology. This is further supported by the absence of motor neuron cell body degeneration until symptomatic phases of pathology in both $SOD1^{G93A}$ (Fischer et al., 2004) and $SOD1^{G85R}$ (Bruijn et al., 1997) mice. However, it must be noted that in ALS patients, biochemical markers of apoptosis have been observed at the end stage of the disease (Yoshiyama et al., 1994) and in $SOD1^{G93A}$ (Li et al., 2000), $SOD1^{G85R}$ and $SOD1^{G77R}$ (Pasinelli et al., 2000) mice, sequential activation of caspases 1 and 3 has been observed in the spinal cord (however, with caspase 3 activation not occurring until symptomatic stages in all cases). Considering the defective mitochondrial processes (including impaired mitochondrial electron transport, impaired

calcium buffering and disturbed morphology and distribution) observed in the motor neurons of ALS patents and models, it is possible that the activation of mitochondrial apoptosis in motor neurons may arise in response to these defective processes. However, should the widely favored dying back hypothesis for motor neuron degeneration in ALS be correct (Dadon-Nachum et al., 2011) this is likely to occur once denervation of muscles and axonal degeneration has already occurred.

1.4.3.6 Hypermetabolism in ALS

Although denervation-induced muscle wasting would be assumed to lead to hypometabolism owing to the loss of a major site of nutrient consumption, increased energy expenditure has been demonstrated in patients with both familial and sporadic ALS (Desport et al., 2001, Desport et al., 2005, Funalot et al., 2009). In support of a negative role for this hypermetabolism in ALS patients, hyperlipidaemia (Dupuis et al., 2008) and increased concentrations of circulating apolipoprotein E are positively correlated with survival in ALS (Lacomblez et al., 2002), which suggests that increased availability of lipids in blood is beneficial. As with ALS patients, muscle metabolism is higher and bodyweight and fat mass are lower in $SOD1^{G93A}$ mice compared to WT mice (Dupuis et al., 2004). As these metabolic changes occur weeks before disease onset in $SOD1^{G93A}$ mice, it has been suggested that hypermetabolism and energy deficiency may be intrinsic to ALS pathogenesis. In support of this, providing $SOD1^{G93A}$ mice with a high-fat diet has been shown to delay disease onset, increase lifespan, reduce muscle denervation, and improve motor neuron survival (Dupuis et al., 2004, Mattson et al., 2007) Conversely, caloric restriction of $SOD1^{G93A}$ mice has been shown to accelerate disease onset and shorten lifespan (Patel et al., 2010, Hamadeh and Tarnopolsky, 2006). Dupuis and colleagues have suggested that defects in muscle energy

metabolism may be the direct cause of energy deficit and hypermetabolism in mutant SOD1 mice (Dupuis et al., 2003). In support of this cellular levels of ATP are decreased and expression of mitochondrial uncoupling proteins is increased in the muscles of mutant SOD1 mice (Dupuis et al., 2003). Furthermore mitochondrial defects have been observed in the muscles of ALS patients (Crugnola et al., 2010, Echaniz-Laguna et al., 2006). Finally, mice overexpressing the mitochondrial brown fat uncoupling protein 1 (UCP1) in muscles, as a model of muscle-restricted hypermetabolism, have been observed to undergo a progressive deterioration in neuromuscular junctions that eventually leads to a mild, late-onset motor neuron pathology (Dupuis et al., 2009). It has thus been suggested that providing trophic/metabolic support to the muscles of ALS patients/models may slow denervation and prolong survival (Dupuis et al., 2011). However it must also be noted that in experiments involving muscle restricted expression of mutant SOD1 in mice, no signs of denervation or motor neuron degeneration were observed, despite the occurrence of severe atrophy and mitochondrial defects in the muscles of these animals (Dobrowolny et al., 2008). This could suggest a number of things; 1) that muscle hypermetabolism is not sufficient to bring about damage to motor neurons 2) that expression of mutant SOD1 in other cells in addition to muscle is required to bring about hypermetabolism in muscle 3) that muscle hypermetabolism requires a background of other toxic processes in order to contribute to pathology or 4) systemic hypermetabolism is required for hypermetabolism-induced motor neuron injury. Unfortunately, Dobrowolny and colleagues did not discuss whether or not mice with muscle restricted expression of mutant SOD1 showed muscle hypermetabolism and therefore it is difficult to conclude which of these possibilities or combination of them may be correct. However, at this stage it cannot be ruled out that hyper-metabolism/energy deficiency play a role in ALS pathology.

1.4.4 ALS genetics

1.4.4.1 An update on mutations identified in familial and sporadic ALS

As described above, the fist gene identified to be involved in typical familial ALS was the *SOD1* gene, which encodes copper/zinc superoxide dismutase 1 (Rosen et al., 1993a). Mutations in *SOD1* are thought to occur in 15-20% of familial ALS and for a long time these were the most common of the known mutations in familial ALS. Recently the field of ALS research has taken a large step forward in the discovery of several other frequently mutated genes in familial ALS patients. The first of these were the *TARDBP* (TAR DNA binding protein 43) (Gitcho et al., 2008, Kabashi et al., 2008a, Sreedharan et al., 2008, Yokoseki et al., 2008) and *FUS* (fused in sarcoma) (Kwiatkowski et al., 2009, Vance et al., 2009) genes, mutations in which are thought to account for 5–10% and 5% of classic familial ALS respectively. Interestingly, *TARDBP and FUS* both encode proteins involved in RNA-metabolism, which has lead to the intriguing hypothesis that defects in RNA metabolism may be associated with ALS pathology. Together mutations in *SOD1, TARDBP and FUS* only account for ~30% of familial ALS cases, however in October 2011 the percentage of familial ALS cases whose mutations could be accounted for hugely increased with the discovery by two independent groups that a large hexanucleotide (GGGGCC) repeat expansion in the first intron of the *C9ORF72* gene on the short arm of chromosome 9 is causative for ALS and Frontotemporal Dementia (FTD) (see section 1.4.2.2 for a discussion of FDT and its relationship to ALS). DeJesus-Hernandez et al. identified the GGGGCC repeat expansion in 12% of familial FTD and 22.5% of familial ALS in their American sample set. Likewise, Renton et al. found it in 46% of familial ALS, 21.1% of sporadic ALS, and 29.3% of FTD in

the Finnish population and in **one third** of ALS patients of outbred European decent (Renton et al., 2011, DeJesus-Hernandez et al., 2011). This mutation is therefore the most common genetic cause of ALS identified to date. Although it is not yet clear how the hexanucleotide repeat expansion in the non-coding region of the *C9ORF72* gene can cause ALS and FTD, Renton and colleagues propose that it may affect the function of C9ORF72, whose cellular role is as yet unknown. However, they also hypothesise that RNA generated from the repeat expansions could disrupt transcription by sequestering normal RNA and proteins involved in transcription regulation, as has previously been proposed for other repeat expansion mutations (Wojciechowska and Krzyzosiak, 2011).

In addition to these commonly occurring mutations, mutations in several other genes have been reported as rare causes of ALS, these are as follows: A single mutation (P56S) was discovered in the *VAPB* gene, encoding VAMP (vesicle associated membrane protein) associated protein B, in Brazilian kindreds who shared a common founder from the time of the Portuguese colonisation of Brazil (Nishimura et al., 2004, Nishimura et al., 2005). Deleterious mutations in another protein involved in vesicle trafficking, FIG4, have also been found (Chow et al., 2009). FIG4 is a phosphoinositide 5-phosphatase that regulates the cellular abundance of $PI(3,5)P_2$, a signaling lipid located on the cytosolic surface of membranes of the late endosomal compartment. Mutations in this gene have also been identified as responsible for the recessive peripheral-nerve disorder CMT4J a severe form of Charcot-Marie-Tooth disease (CMT) (Chow et al., 2009). Mutations in the *ANG* gene which encodes angiogenin, another protein with RNA processing abilities have also been found. This further highlights the potential role of RNA processing in ALS (Crabtree et al., 2007). More recently ALS causing mutations which abolish the inhibition of NFκB activation, have

been discovered in the *OPTN* (optineurin) gene, which is also a causative gene of primary open-angle glaucoma (Maruyama et al., 2010). Furthermore, a unique mutation in the D-amino acid oxidase gene (R199W DAO) which was associated with classical adult onset familial amyotrophic lateral sclerosis in a three generational FALS kindred has recently been discovered (Mitchell et al., 2010). Work is currently underway to establish whether this mutation is causative for the disease, although early indications suggest so (Mitchell et al., 2010). Finally several mutations have been identified which implicate the ubiquitin proteasome system in ALS. Specifically, using exome sequencing a p.R191Q amino acid change in the *valosin-containing protein* (*VCP*) gene was discovered in an Italian family with autosomal dominantly inherited amyotrophic lateral sclerosis (ALS) (Johnson et al., 2010). This lead to the screening by Johnson and colleagues of *VCP* in a cohort of 210 familial ALS cases and 78 autopsy-proven ALS cases, which lead to the identification of four additional mutations in this gene. VCP protein plays a critical role in the maturation of ubiquitin-containing autophagosomes, and mutant VCP toxicity has been identified by Johnson and colleagues to likely be mediated at least partially through toxic effects onTDP-43 protein (Johnson et al., 2010). Interestingly, mutations in *VCP* have previously been found in families with Inclusion Body Myopathy, Paget's disease and FTD (Johnson et al., 2010). Mutations in *UBQLN2*, which encodes the ubiquitin-like protein ubiquilin 2, have also been discovered to be capable of causing dominantly inherited, chromosome-X-linked ALS and ALS/FTD (Deng et al., 2011).

In addition to the genes described above, additional loci have been reported for classical familial ALS, including: ALS3 on 18q identified in a single family (Hand et al., 2002) and ALS7 on chromosome 20p (Sapp et al., 2003). Furthermore, several genes whose mutation

causes rare, atypical forms of ALS have been discovered, these include: the alsin gene, associated with juvenile onset recessive ALS (Hadano et al., 2001); the senataxin gene, which is associated with a slowly progressive form of juvenile onset ALS, (Chen et al., 2004a); the spatacsin gene (of unknown function, whose mutation is the single most common cause of autosomal recessive hereditary spastic paraplegia with thin corpus callosum) in which 12 sequence alterations were identified by Orlacchio and colleagues in 10 unrelated pedigrees with autosomal recessive juvenile amyotrophic lateral sclerosis and long-term survival (Orlacchio et al., 2010) and the σ Non-opioid receptor 1 (*SIGMAR1*) gene in which a mutation was found in a consanguineous family segregating juvenile ALS in an autosomal recessive pattern (Al-Saif et al., 2011). Interestingly, mutations in *SIGMAR1* have also recently been identified in patients presenting with FTD-MND (frontotemporal dementia–motor neuron disease) with no known mutations in known dementia genes , which further highlights that ALS and FTD represent a clinico-pathologically related spectrum of diseases (see section 1.4.2.2 for further discussion of this relationship) (Luty et al., 2010). Table 2 below summarizes the various genes/loci in which ALS-causing mutations have been identified to date.

Table 2: Summary of genes/loci in which ALS-causing mutations have been identified to date

Genetic subtype	Chromosomal locus	Gene	Onset/inheritance	Reference
Abbreviations: AD, autosomal dominant; ALS, amyotrophic lateral sclerosis; AR, autosomal recessive; FTD, frontotemporal dementia				
Oxidative stress				
ALS1	21q22	Superoxide dismutase 1 (*SOD1*)	Adult/AD	(Rosen et al., 1993a)
RNA processing				
ALS4	9q34	Senataxin (*SETX*)	Juvenile/AD	(Chen et al., 2004b)
ALS6	16p11.2	Fused in sarcoma (*FUS*)	Adult/AD	(Kwiatkowski et al., 2009, Vance et al., 2009)
ALS9	14q11.2	Angiogenin (*ANG*)	Adult/AD	(Greenway et al., 2006)
ALS10	1p36.2	TAR DNA-binding protein (*TARDBP*)	Adult/AD	(Sreedharan et al., 2008)
Endosomal trafficking and cell signaling				
ALS2	2q33	Alsin (*ALS2*)	Juvenile/AR	(Yang et al., 2001)
ALS11	6q21	Polyphosphoinositide phosphatase (*FIG4*)	Adult/AD	(Chow et al., 2009)
ALS8	20q13.3	Vesicle-associated membrane protein-associated protein B (*VAPB*)	Adult/AD	(Nishimura et al., 2004)
ALS12	10p13	Optineurin (*OPTN*)	Adult/AD and AR	(Maruyama et al., 2010)
ALS–FTD	3p11.2	Charged multivesicular protein 2B (*CHMP2B)*	Adult/AD	(Cox et al., 2010)
Glutamate excitotoxicity				
ND	12q24	d-amino acid oxidase	Adult/AD	(Mitchell et al., 2010)

Genetic subtype	Chromosomal locus	Gene	Onset/inheritance	Reference
		(*DAO*)		
Ubiquitin/protein degradation				
ND	9p13–p12	Valosin-containing protein (*VCP*)	Adult/AD	(Johnson et al., 2010)
ALSX	Xp11	Ubiquilin 2 (*UBQLN2*)	Adult/X-linked	(Deng et al., 2011)
Other genes				
ALS5	15q15–q21	Spatacsin (*SPG11*)	Juvenile/AR	(Orlacchio et al., 2010)
ALS–FTD	9p13.3	σ Non-opioid receptor 1 (*SIGMAR1*)	Adult/AD Juvenile/AR	(Luty et al., 2010, Al-Saif et al., 2011)
ALS–FTD	9q21–q22	Chromosome 9 open reading frame 72 (*C9ORF72*)	Adult/AD	(Hosler et al., 2000, Renton et al., 2011, DeJesus-Hernandez et al., 2011)
Unknown genes				
ALS3	18q21	Unknown	Adult/AD	(Hand et al., 2002)
ALS7	20ptel–p13	Unknown	Adult/AD	(Sapp et al., 2003)

Table adapted from (Ince et al., 2011)

1.4.4.2 Convergent and divergent pathways in familial and sporadic ALS

As described above, in approximately 90% of cases, ALS manifests as a sporadic disorder with no clear inheritance, whereas the remaining ~10 % of cases are familial and usually display autosomal dominant inheritance. It is frequently stated that as sporadic and familial ALS share common clinical features, they are likely to share common pathophysiological mechanisms (Turner and Talbot, 2008). In support of this, many of the potentially toxic processes such as reactive astrogliosis (Papadimitriou et al., 2010) , mitochondrial abnormalities (Duffy et al., 2011), ER stress (Atkin et al., 2008, Atkin et al., 2006) and

oxidative stress (Cova et al., 2010) described above for the $SOD1^{G93A}$ mouse are observed in both sporadic and familial ALS cases. Furthermore, in recent times the presence of TDP-43 aggregates has been identified as a unifying feature in the majority of sporadic ALS cases as well as in familial ALS-cases arising from mutations in several genes including *TARDBP* itself (predominantly ALS cases) (Da Cruz and Cleveland, 2011), *C9ORF72* (ALS and FTD cases) (DeJesus-Hernandez et al., 2011, Renton et al., 2011), *VAPB* (predominantly ALS cases) (Tudor et al., 2010) and *UBQLN2* (X-linked ALS and ALS/FTD) (Deng et al., 2011). ‘‘TDP-proteinopathy’’ therefore now represents a key pathological feature associated with both familial and sporadic ALS (Ince et al., 2011). However it must be noted that there are exceptions to this rule, in particular, cases of familial ALS caused by mutations in SOD1 have to date not been associated with TDP-43-related pathology. This suggests that although familial patients with mutations in SOD1 may share common downstream toxic processes with sporadic ALS patients and other fALS patients (such as astrogliosis, oxidative stress, ER stress and mitochondrial abnormalities) the upstream mechanisms leading to these processes are likely to be different. FUS proteinopathy was also initially considered to be independent of TDP-43 proteinopathy as no abnormal localisation or accumulations of TDP-43 were observed in familial ALS patients with mutations in FUS nor in FUS-accumulated FTLD-U (Neumann et al., 2009, Munoz et al., 2009). However, sporadic ALS patients with accumulations that are positive for both FUS and TDP-43 have recently been reported (Deng et al., 2010) and this, combined with the fact that these proteins are both RNA-binding proteins with potentially similar functions raises the possibility that they may constitute a common pathologic cascade of the ALS/FTLD-U disease spectrum. In support of this both TDP-43 and FUS show cytoplasmic mislocation as well as recruitment to stress granules in affected tissues in ALS/FTLD-U patients and models (stress granules are small dense

cytoplasmic domains in which specific mRNAs can be translationally arrested when cells are under stress (Anderson and Kedersha, 2008)).

To lend further weight to the notion of TDP-43 pathology as a central feature for non SOD1-related ALS and FTLD-U pathology, several other proteins identified to be mutated in ALS and/or FTLD-U have been shown to influence TDP-43 cell biology. Specifically, mutations in the progranulin gene (*PGRN*) have been identified as causative for familial FTLD-U and it has subsequently been shown that decreases in progranulin can lead to pathological processing of TDP-43 by caspase-3 (Zhang et al., 2007b). Furthermore the toxicity of ALS-causing VCP mutations is thought to be mediated at least partially through toxic effects on TDP-43 as mutant VCP expression has been shown to lead to redistribution of TDP-43 from the nucleus to the cytoplasm both *in vitro* and *in vivo* (Johnson et al., 2010). Finally, Elden and colleagues have recently discovered that intermediate-length polyglutamne expansions in ataxin-2, which normally contains a polyglutamine tract of 22 residues, are associated with an increased risk of ALS (Elden et al., 2010). They have also shown that overexpression or reduced expression of *ATXN2*, the gene coding for ataxin-2, enhances or attenuates TDP-43 toxicity respectively in the retina of flies (Elden et al., 2010). Furthermore they have identified that ataxin-2 and TDP-43 form a complex in an RNA-dependent manner. These data, combined with the fact that ataxin-2 is known to be a constituent component of stress granules (Nonhoff et al., 2007) suggest that ataxin2 may contribute to a common ALS-causing pathologic cascade formed by TDP-43 and potentially FUS.

1.5 Development of therapeutics for ALS

1.5.1 Therapeutics previously tested in mutant SOD1 murine models of ALS.

Appendix 1 summarises the effects on disease onset and survival of the majority of therapeutics tested in mutant SOD1 murine models between 1996 and the present. This table represents an updated version of a table produced by Turner and Talbot, which spanned the period between 1996 and 2007 (Turner and Talbot, 2008). Changes/clarifications made to information provided by Turner and Talbot following the reading of the relevant references, are identified in bold type. Entries added for the period between 2007 and the present are in bold type and are italicized. Abbreviations used are summarized below the table and relevant references are cited. Therapies tested between 2007 and the present were identified using the following search in PubMed: ALS AND treatment AND SOD1. While performing other searches (such as ALS AND therapeutics AND SOD1 or ALS AND drug AND SOD1) appeared to generate the same list of results, we cannot guarantee that we did not miss any therapeutics. However, regardless of this, the table provides an extensive documentation of the nature of therapeutics tested for ALS and the magnitudes of the disease onset and survival benefits that have been achieved. The drugs described in the table are grouped as far as possible according to their primary therapeutic action, although some drugs could have been placed in multiple categories. These categories include: anti-oxidants, anti-excitotoxins, anti-aggregation compounds, anti-apoptotics, anti-inflammatory agents, neurotrophic agents, gene and antisense therapies, cell transplantation therapies and finally combinatorial therapies. Therapies not falling into these categories are listed in a separate section of the table. It is also important to note that while crossing SOD1 mice with other lines of transgenic mice can give useful information about the potential value of certain therapeutic strategies, the expression

of the additional transgene during development may generate effects that cannot be achieved by postnatal treatment. We have therefore focused on postnatal treatments in this table.

1.5.2 The disparity between preclinical and clinical results for potential ALS therapeutics.

As can be seen in **Appendix 1**, a huge number of therapeutics have been tested in murine models of ALS, targeting many of the potential toxic mechanisms described in section 1.4. However, despite a large number of these therapeutics showing significant beneficial effects on disease onset and survival in mutant SOD1 mice, Riluzole has been the only drug to date to show any protection against disease progression in ALS patients (Bensimon et al., 1994, Lacomblez et al., 1996). Several potential reasons for this disparity have been put forward (Philips and Robberecht, 2011, Ludolph et al., 2010), including the following:

1. The preclinical testing of potential therapeutics for ALS is usually performed in mutant SOD1 based murine models, which represent a model for familial ALS. However, the majority of patients enrolled in clinical trials have sporadic ALS, which could potentially involve different pathological mechanisms.

2. Cohorts of mice used in preclinical studies are usually fairly uniform in terms of their environment, food intake and age etc, whereas the population of ALS patients used in clinical trials is frequently more heterogeneous.

3. Reported effects in preclinical studies are often related to disease onset and survival, whereas disease progression is the most relevant parameter to ALS patients who already have the disease when treatment is commenced. Hence if a drug does not affect disease progression in preclinical tests, it may not have any benefit in ALS patients.

4. Differences in corticospinal anatomy, pharmacokinetics and pharmacodynamics exist between mice and humans which may not be fully taken into account when designing dosing regimes in humans.

5. The $SOD1^{G93A}$ mouse expresses much higher levels of mutant SOD1 than human fALS patients (owing to multiple transgene copies) which may lead to different disease characteristics in these mice compared to fALS patients.

In addition to the potential reasons for failed clinical trials above, critical work by Scott and colleagues in 2008 revealed that multiple confounding variables can lead to false positives in survival studies performed in $SOD1^{G93A}$ mice if not adequately controlled for (Scott et al., 2008). These variables include, in order of impact: the occurrence of non-ALS deaths, the incidence of low copy transgenics, genetic background or epigenetic influences causing littermate clustering and a slight gender effect (Scott et al., 2008). Identification of these variables has lead to the production of guidelines for the preclinical testing of therapeutics for ALS, which aim to control for these variables and increase study validity (Ludolph et al., 2010, Scott et al., 2008). In terms of these guidelines, Scott and colleagues have shown using a specially designed computer model (SimLIMS) and data from 2241 control $SOD1^{G93A}$ mice on a mixed hybrid genetic background (maintained by breeding hemizygous B6SJLTg ($SOD1^{G93A}$) males to B6SJLF1 dams), that with an n-number of 24 mice per cohort (12 males and 12 females), and the employment of same-gender litter matching as well as exclusion of mice experiencing non-ALS deaths or loss of transgene copies, noise within survival studies can be reduced to a virtual zero (Scott et al., 2008). It is therefore highly recommended that these conditions are met when performing survival studies in $SOD1^{G93A}$ mice. The

importance of this was highlighted when Scott and colleagues used their optimized study design to re-test a number of therapeutics that had previously been shown to be beneficial in $SOD1^{G93A}$ mice and found that none of the therapeutics significantly attenuated pathology. These therapeutics included; minocycline, creatine, celecoxib, sodium phenylbutyrate, ceftriaxone, WHI-P131, thalidomide and surprisingly riluzole. The original studies in which these therapeutics were tested are listed in **Appendix 1** and are underlined. In light of these results, we decided to include the n-numbers used for all studies following the publication of this optimised study design in **Appendix 1** and were surprised to see that very few studies (only those highlighted in grey in **Appendix 1**) met the n-numbers suggested by Scott and colleagues. Furthermore it was even more unusual to find details of whether or not experimental groups were balanced for litter or sex, or if non-ALS deaths were excluded. However, we were encouraged to see that copy number assessment is now more routinely being employed in preclinical studies in $SOD1^{G93A}$ mice.

1.5.3 Therapeutic strategies currently under investigation in the ALS clinic

As described in section 1.4, studies in ALS patient samples and in mutant SOD1-based animal models have revealed multiple toxic mechanisms that may contribute to motor neuron degeneration in ALS. As understanding of these mechanisms has progressed, further potential therapeutic strategies have emerged. A number of these therapeutic strategies will be discussed below, with a particular focus on compounds which are currently under clinical trial.

1.5.3.1 Anti-glutamatergic strategies

In light of observations that astrocytic clearance of glutamate is impaired in ALS patients and SOD1-based rodent models, due to a loss of the astrocytic EAAT2/GLT1 transporter (Rothstein et al., 1995, Bruijn, 1997, Howland et al., 2002, Yang et al., 2009) Rothstein and colleagues performed a blinded *in vitro* screen of 1040 medications approved by the US Food and Drug Administration to look for compounds which may influence the expression of this transporter (Rothstein et al., 2005). This screen revealed that many β-lactam antibiotics are potent stimulators of GLT1 expression and lead to the testing of the β-lactam, ceftriaxone, in the $SOD1^{G93A}$ mouse. Interestingly, in this initial study, treatment of $SOD1^{G93A}$ mice with ceftriaxone from the pre-symptomatic time-point of 42 days, resulted in a delay in disease onset and a 12% increase in survival. However, when this drug was re-tested by Scott and colleagues using a study design created to minimise error, no significant beneficial effects of ceftriaxone could be found, despite using the same dose and administration route (Scott et al., 2008). Regardless of this discrepancy, a novel phase 1-3 trial with an adaptive design to test intravenous ceftriaxone against placebo is in its final phase and ALS patients are actively being recruited across the USA and Canada, (ClinicalTrials.gov, 2011a). It will therefore be interesting to see the outcome of this study in order to understand how much we can rely on pre-clinical studies in the $SOD1^{G93A}$ mouse, even when they are carefully constructed to minimise error, to indicate the potential for therapeutic benefit in humans.

1.5.3.2 Targeting protein misfolding and accumulation

The occurrence of protein misfolding and aggregation in motor neurons is a hallmark of ALS and as described in section 1.4.2, various mechanisms have been identified by which these misfolded/aggregated species might contribute to motor neuron degeneration in this disease.

Consequently, therapeutics targeting protein misfolding/aggregation are attractive candidates for preclinical testing for ALS. Heat shock proteins (HSPs) are important for the maintenance of cellular function and the stabilisation of proteins under conditions of stress, such as those experienced by motor neurons in ALS. As molecular chaperones, HSPs facilitate the folding of nascent peptides, help to transport proteins between cellular compartments and target misfolded or damaged proteins for proteasomal and lysosomal degradation. As would be expected, HSPs are upregulated in human ALS patient tissue (Garofalo et al., 1991) (Vleminckx et al., 2002) and in *SOD1*^{G93A} mice . However, it is thought that in the motor neurons of SOD1^{G93A} mice, misfolded/aggregated mutant SOD1 species may interact with and reduce the availability of HSPs, thereby disrupting their normal protective functions (Shinder et al., 2001, Okado-Matsumoto and Fridovich, 2002). It has therefore been hypothesized that increasing levels of HSPs may be beneficial in ALS models and patients. Arimoclomol is an orally bioavailable compound that amplifies expression of *HSPA4* and *HSP90AA1*, which encode HSPs HSP70 and HSP90 respectively. Interestingly, Arimoclomol has been shown to delay disease progression and substantially extended survival (by 22%) in SOD1^{G93A} mice (Kieran et al., 2004). Furthermore, placebo-controlled studies have shown that orally administered Arimoclomol reaches the CSF and is safe in ALS patients (Cudkowicz et al., 2008). Efficacy studies investigating the potential benefits of Arimoclamol treatment in patients with familial ALS are therefore underway and are actively recruiting participants (ClinicalTrials.gov, 2011b)

1.5.3.3 Knockdown of mutant SOD1 proteins

Administration of antisense oligonucleotides (Smith et al., 2006) or small inhibitory RNA molecules (Raoul et al., 2005, Wang et al., 2008a) to lower concentrations of mutant SOD1

messenger RNA, has been shown to delay disease progression and/or increase survival in mutant SOD1 rodents, a model of familial ALS. Although these strategies are targeted at familial ALS patients with gain of function mutations in SOD1, the techniques used are likely to be transferrable to the knockdown of other potentially harmful proteins should they be shown to be successful in SOD1 familial ALS patients. In light of this, a phase 1 human trial investigating the safety, tolerability, and pharmacokinetics of antisense SOD1 oligonucleotides administered intrathecally to patients with *SOD1* familial ALS is currently underway (ClinicalTrials.gov, 2010a).

1.5.3.4 Improving/maintaining mitochondrial function

As discussed in section 1.4.3, abnormalities in mitochondrial distribution and morphology and in some cases function can be seen in both ALS patients and mutant SOD1 based models. This has lead to the suggestion that mitochondrial abnormalities may play a role in motor neuron degeneration in ALS. In direct support of this, misfolded SOD1 has recently been shown to directly impair mitochondrial function in the spinal cords of several rodent mutant SOD1 models by binding to, and inhibiting the function of the VDAC1 transporter in the OMM (Israelson et al., 2010). In 2007, Bordet and colleagues published the results of a study in which they screened approximately 40,000 low-molecular-weight compounds for the ability to prevent motor neuron cell death *in vitro*. In this study, they identified that cholest-4-en-3-one, oxime (referred to as Olesoxime or TRO19622) could bring about motor neuron survival in the absence of trophic support in a dose-dependent manner (Bordet et al., 2007). They then went on to show that olesoxime could rescue motor neurons from axotomy-induced cell death in neonatal rats and also promote nerve regeneration following sciatic nerve crush in mice. Furthermore, olesoxime was able to delay disease onset and extended

survival in SOD1^{G93A} mice (although disease progression was not affected) (Bordet et al., 2007). Interestingly Bordet and colleagues identified that olesoxime binds directly to VDAC and another component of the mitochondrial permeability transition pore, translocator protein 18 kDa (or peripheral benzodiazepine receptor) (Bordet et al., 2007). This suggests that its beneficial effects on motor neuron survival may be derived at least in part through stabilising mitochondria and further highlights a potential involvement for VDAC in ALS pathogenesis. In light of its beneficial effects in various models of motor neuron damage, olesoxime is now being tested in a phase 2/3 clinical trial in Europe (ClinicalTrials.gov, 2010b).

In addition to olesoxime, another compound, dexpramipexole, which has been shown to cross the blood brain barrier, accumulate in mitochondria and bring about the detoxification of ROS (Danzeisen et al., 2006), is currently being tested in a large phase 3 clinical trial (Zinman and Cudkowicz, 2011). This compound was shown to significantly increase the survival of SOD1^{G93A} mice when administered in the diet (Danzeisen et al., 2006) and has already been shown to be safe and well tolerated at single and multiple doses in 54 healthy adult human subjects (both males and females) (Bozik et al., 2011)

1.5.3.5 Administration of growth factors.

Many neurotrophic growth factors are known to promote the survival of neurons and foster regeneration in the central nervous system (Henriques et al., 2010). Consequently a number of neurotrophic factors have been tested both pre-clinically and clinically for ALS. Unfortunately, despite showing promising results in many preclinical studies (see Neurotrophic factors section in **Appendix 1**), phase III clinical trials involving growth factor administration to ALS patients have to date been disappointing (Zinman and Cudkowicz,

2011, Henriques et al., 2010). Several reasons have been proposed for this including; inadequate pre-clinical testing of the compounds prior to administration in patients (including infrequent determination of whether or not these growth factors can stabilise the neuromuscular junction or whether they only preserve the motor neuron cell body), failure to achieve sufficiently high and constant doses of administered growth factors in the CNS of treated patients and finally, problems encountered with the design or execution of the clinical trials (Henriques et al., 2010). In light of these potential shortcomings with previous studies, growth factors have not been ruled out as potential therapeutics for ALS and still represent an attractive prospect for further, more robust testing. Consequently, a phase 1/2 clinical trial is currently underway to test intracerebroventricular administration of VEGF in patients with ALS (ClinicalTrials.gov, 2011c). VEGF has received much interest in the ALS field, owing to the observation that transgenic mice with a homozygous deletion in the VEGF promoter develop a pathology resembling motor neuron disease (Oosthuyse et al., 2001). Furthermore, several preclinical studies in $SOD1^{G93A}$ rodents have shown promising effects with VEGF therapy. These are as follows:

1) intraperitoneal injection of VEGF in female $SOD1^{G93A}$ mice from 74 days of age (Zheng et al., 2004) has been shown to significantly delay disease onset and extend survival in these animals.

2. Administration of VEGF using either an EIAV (intramuscular administration) or AAV (intracerebroventricular administration) viral vector close to disease onset has been shown to significantly extend survival in $SOD1^{G93A}$ mice (Azzouz et al., 2004b, Dodge et al., 2010).

3. Intracerebroventricular delivery of recombinant VEGF via osmotic minipump from 60 days onwards in a $SOD1^{G93A}$ rat model of ALS as been shown to significantly delay onset of paralysis, improve motor performance and prolong survival (Storkebaum et al., 2005).

4. Intrathecal transplantation of immortalised human neural stem cells overexpressing the human VEGF gene at 70 days of age has been shown to significantly delay disease onset and prolong survival in $SOD1^{G93A}$ mice (Hwang et al., 2009)

1.5.3.6 Targeting the muscles of ALS patients

Although ALS is a motor neuron disease, it has been hypothesised that compounds which strengthen the diaphragm and other muscles may have clinical benefits by targeting denervation induced muscle wasting and weakness. Strengthening the diaphragm is a particularly attractive prospect as the major cause of mortality and a large contributor to morbidity in ALS patients is respiratory failure (Hardiman, 2011). In light of this a compound, CK-2017357, which selectively activates the fast skeletal muscle troponin complex (by increasing sensitivity to calcium) and therefore increases muscle force has been tested in ALS patients (ClinicalTrials.gov, 2011d). In this phase IIa study CK-2017357 was given orally to ALS patients at two different doses. The treatment was well tolerated and fatigue, strength and pulmonary function improved in a dose dependent manor compared to placebo (Zinman and Cudkowicz, 2011). Cytokinetics, the company who designed this drug, are therefore conducting two further Phase II clinical trials in patients with ALS and it will be interesting to see whether these also show positive results (www.cytokinetics.com).

1.6 Specific aims of this thesis

Although studies in ALS patients and in mutant SOD1-based models have been instrumental in indentifying targetable mechanisms which may contribute to motor neuron degeneration in ALS, an urgent unmet need still persists for effective therapies for this disease. The

overarching aim of this thesis was therefore to carry out the preclinical testing of therapeutics which may provide effective relief to the suffering of ALS patients. As the need for effective therapeutics is so critical, we decided to test therapeutics that have already been confirmed to be safe in humans, as should successful results be seen in our preclinical studies, these therapeutics could quickly be taken to clinical trial (Traynor et al., 2006). Considering the large number of therapeutics that have failed at clinical trial in ALS patients, despite showing promise in preclinical studies, it was important to us to design our preclinical tests in such a way that false positives were avoided and data produced were meaningful. We therefore followed guidelines produced by Scott and colleagues (Scott et al., 2008) and Ludolph and colleagues (Ludolph et al., 2010), intended to improve research methodology in preclinical studies for ALS, when designing and analyzing our experiments. Furthermore, the most relevant parameter when assessing the potential of a therapeutic for the treatment of ALS in preclinical studies is the effect of the therapeutic on disease progression from onset to end stage. This is because ALS patients have usually already experienced disease onset upon diagnosis and therefore if a therapeutic delays disease onset but not progression from onset to death, it may not confer significant benefit to them. We therefore decided that our preclinical studies should be designed in such a way that disease onset, progression and duration could be easily determined. Finally, we decided to conduct our studies in the $SOD1^{G93A}$ model of ALS as this is the most frequently used pre-clinical model of the disease (Scott et al., 2008). Moreover, $SOD1^{G93A}$ mice were already available and well characterized in our laboratory. During the timeframe represented by this thesis, two potential therapeutics for ALS were tested; the anti-type II diabetes drug, metformin and the chemical chaperone and inducer of autophagy, trehalose. Our reasoning behind the selection of these therapeutics is discussed in more detail below.

1.6.1 Metformin

Metformin is a small molecule activator of the metabolic regulator, AMP-activated protein kinase (AMPK), which is routinely used for the treatment of type II diabetes (Hawley et al., 2002, Zhou et al., 2001) and is therefore known to be safe for administration to humans. Metformin was originally prescribed for diabetes on the basis of its ability to reduce hepatic glucose production and increase insulin sensitivity (Cho and Kieffer, 2011), but it has subsequently been found to have potent anti-inflammatory (Dandona et al., 2004, Isoda et al., 2006, Lin et al., 2000) and antioxidant (Lin et al., 2000, Ouslimani et al., 2005, Srividhya et al., 2002) properties, as well as the ability to bring about mitochondrial biogenesis (Kukidome et al., 2006) and to cross the blood brain barrier (BBB) (Chen et al., 2009, Ma et al., 2007). As described in section 1.4, inflammation and toxic glial activation as well as oxidative stress and mitochondrial damage are thought to contribute to the degeneration of motor neurons in ALS. We therefore hypothesised that metformin may be protective for motor neurons in ALS patients by targeting these toxic processes.

We were encouraged in our hypothesis by the fact that metformin therapy has been shown to be beneficial in mouse models of both Huntington's disease and multiple sclerosis in which, like in ALS, inflammation, oxidative stress and mitochondrial defects are thought to be contributing factors to pathology (Beal and Ferrante, 2004, Stadelmann, 2011) Specifically, oral administration of metformin was shown to increase lifespan and improve motor performance in male mice in the R6/2 model of Huntington's disease (Ma et al., 2007). Whereas in the murine Experimental Autoimmune Encephalomyelitis (EAE) model of multiple sclerosis, metformin was shown slow disease progression and inhibit the expression

of pro-inflammatory cytokines (IFN-γ, TNF-α, IL-6, IL-17) as well as inducible NO synthase (iNOS) in the CNS (Nath et al., 2009). Furthermore, in this study, Nath and colleagues, revealed that metformin treatment could significantly attenuate LPS-induced production of NO and proinflammatory cytokines (IFN-γ, TNF-α, IL-6) in primary macrophages from the spleens of C57B1/6 mice (Nath et al., 2009). These results led us to hypothesise that metformin would also attenuate the production of proinflammatory cytokines and NO by microglia and astrocytes in the spinal cords of $SOD1^{G93A}$ mice and therefore afford protection to the motor neurons in these animals.

The antioxidant properties of metformin as well as its ability to bring about mitochondrial biogenesis are thought to derive from its ability to bring about the activation and upregulation of peroxisome-proliferator activated receptor coactivator 1 (PGC1-α) (Kukidome et al., 2006), which lies downstream of AMPK (Jäger et al., 2007, Cantó and Auwerx, 2009). PGC-1α belongs to a small family of transcriptional coactivators (including PGC-1β and PRC) that are involved in the regulation of mitochondrial physiology (Rodgers et al., 2008) and is thought to be intimately involved in mitochondrial biogenesis (Narkar et al., 2008) and the regulation of cellular defense against ROS (St-Pierre et al., 2006). In addition to these effects, PGC1-α is thought to be involved in the adaptation of muscles to endurance exercise by driving slow type I fiber myosin isoform expression (Lin et al., 2002). Interestingly, crossing $SOD1^{G93A}$ mice with mice overexpressing PGC1-α has recently been shown to significantly improve their motor function and increase survival as well to restore mitochondrial electron transport chain activities in their spinal cords (Zhao et al., 2011). Although this study was published after the completion of our experiments, it highlights that

activation of PGC1-α is a relevant parameter when considering therapeutics which may be protective to motor neurons in $SOD1^{G93A}$ mice.

Although, we were ultimately interested in the effects of metformin on disease onset, progression and duration in $SOD1^{G93A}$ mice, we decided to perform an initial study investigating a single symptomatic time point, in order to investigate whether metformin was indeed protective to motor neurons in $SOD1^{G93A}$ mice. To do this we tested the effects of treatment with 2mg/ml metformin in the drinking water from the presymptomatic time point of 35 days, on motor unit survival as well as muscle strength and fatigability in the hindlimbs of male and female $SOD1^{G93A}$ mice (via *in vivo* electrophysiology) at the symptomatic time point of 100 days of age. 2mg/ml was selected as administration of this dose via the drinking water was shown to be protective in the R 6/2 murine model of Huntington's disease. This study is discussed in detail in Chapter 3. Following promising results in this study, we continued to test the effects of three different doses of metformin (0.5, 2 and 5mg/ml) metformin administered via the drinking water from 35 days) on disease onset, progression and survival in male and female $SOD1^{G93A}$ mice. This study is discussed in detail in Chapter 4. Should successful results have been seen with metformin in this dose-response survival study, we would also have performed a survival study in which the most successful dose was administered at a symptomatic time point (which would be more relevant to ALS patients who would probably not receive the drug until symptom onset). However, metformin was not shown to exert beneficial effects in our initial survival study and therefore a second survival study was not performed.

1.6.2 Trehalose

Trehalose is natural, non-reducing disaccharide found in many non-mammalian species (Singer and Lindquist, 1998). In these organisms it functions to protect cells against environmental insults such as heat, cold, dehydration and oxidation, through its ability to act as a chemical chaperone and prevent protein denaturation and aggregation (Chen and Haddad, 2004, Singer and Lindquist, 1998). The stabilization of proteins by trehalose is thought to be derived at least in part from its ability to increase solvent surface tension. This increase in surface tension is thought to raise the energy required by proteins to bring about cavity formation within the solvent in order to accommodate their enlarged surface area upon denaturation (Kaushik and Bhat, 2003). Critically, trehalose is used in many food stuffs in Japan and has been shown to be well tolerated at high doses in humans (Richards et al., 2002).

Protein aggregation is a unifying theme in many neurodegenerative disorders including Alzheimer's disease, prion diseases, Parkinson's disease, and polyglutamine disorders such as Huntington's disease (Sarkar and Rubinsztein, 2008). As a result of its protein stabilizing properties, and also its proven safety for consumption in humans (Richards et al., 2002), trehalose has been evaluated as a potential therapeutic for a number of these disorders. It has for example been shown to prevent aggregation of β-amyloid species associated with Alzheimer's disease (Liu et al., 2009, Izmitli et al., 2011), to impair prion protein aggregation in prion infected cells (Béranger et al., 2008), to ameliorate dopaminergic and tau pathology in parkin deleted/tau overexpressing mice (Rodríguez-Navarro et al., 2010) and also to improve motor function and extend lifespan in the R6/2 model of Huntington's disease (Tanaka et al., 2004). In addition to being successful in these models of neurodegenerative

disorders, trehalose has also been shown to reduce aggregate formation and delay pathology in a transgenic mouse model of Oculopharyngeal Muscular Dystrophy (OPMD) (Davies et al., 2006), a disease in which aggregation of mutant poly(A) binding protein nuclear 1 (PABPN1) in the nuclei of muscle cells is a characteristic feature.

In addition to its actions as a chemical chaperone, trehalose has more recently been shown to have the ability to activate autophagy in an mTOR-independent fashion (Sarkar et al., 2007). As discussed in section 1.4.2.1.3 , autophagy has been shown to play an essential role in the removal of toxic/aggregated proteins and damaged organelles such as mitochondria that may cause toxicity to cells under conditions of stress (Metcalf et al.). It is therefore not surprising that the afore-mentioned beneficial effects of trehalose on the clearance of aggregates in cellular models of Huntington's disease and on dopaminergic and tau pathology in parkin deleted/tau overexpressing mice, were proposed to be derived from autophagy activation as well as protein stabilisation (Sarkar et al., 2007, Rodríguez-Navarro et al., 2010)

As discussed in detail in section 1.4.2, protein misfolding and aggregation is a hallmark of both sporadic and familial ALS and may contribute to pathology. In line with this, investigations in mutant SOD1-based models of familial ALS have revealed several mechanisms by which SOD1 misfolding/aggregation may cause toxicity to motor neurons, including; prolonged induction of ER stress, impairment of axonal transport, inhibition of the proteasome and activation of microglia upon secretion by motor neurons (Ilieva et al., 2009). Far less is known about whether aggregates of TDP-43 or FUS/TLS (or intermediates in the aggregation process) found in sporadic ALS patients or familial ALS patients with mutations

in these genes, may be toxic to motor neurons, however, as with SOD1, this remains a strong possibility.

In light of the documented beneficial effects of trehalose in culture and *in vivo* models of various neurodegenerative diseases involving protein aggregation (Béranger et al., 2008, Liu et al., 2009, Rodríguez-Navarro et al., 2010, Sarkar et al., 2007, Tanaka et al., 2004), and the various mechanisms by which misfolded/aggregated mutant SOD1 has been suggested to damage motor neurons, we hypothesized that trehalose may delay disease onset and progression and increase survival in the $SOD1^{G93A}$ mouse model of ALS. This hypothesis was supported by experiments in which treatment of NSC-34 cells (a mouse motor-neuron-like cell line) transiently transfected with human $SOD1^{G93A}$, brought about a significant reduction in mutant SOD1 aggregate formation and detergent insolubility (Gomes et al., 2010). Furthermore, treatment of $SOD1^{G93A}$ mice with arimoclamol, an orally bioavalable compound that increases the expression of HSPs, HSP70 and HSP90, has been shown to delay disease progression and substantially extended survival (by 22%) in $SOD1^{G93A}$ mice, which supports the idea that stabilising proteins and preventing their misfolding/aggregation may be beneficial in these animals (Kieran et al., 2004).

We decided to test our hypothesis by investigating the effects of treatment with three different doses of trehalose from 35 days, on disease onset, progression and survival in male and female $SOD1^{G93A}$ mice using a similar survival study format to that used for the preclinical testing of metformin. We then planned to take the most successful dose onto a second survival study with administration of trehalose from disease onset, should this be relevant. Trehalose doses selected were 0.5%, 2% and 5% via the drinking water. This dose

range was selected as it encompassed doses previously shown to be therapeutic in models of parkinsonism/tauopathies (1%) (Rodríguez-Navarro et al., 2010) and Huntington's disease (2%) (Tanaka et al., 2004). The results of these investigations are discussed in detail in Chapter 6.

When researching trehalose as a potential therapeutic for ALS, we hypothesised that if TDP-43 or FUS/TLS aggregates or soluble oligomers were found to be toxic to neurons, and trehalose treatment was able to bring about beneficial effects in our $SOD1^{G93A}$ mice, then trehalose may also have beneficial effects in recently developed TDP-43 and FUS/TLS models. We reasoned that if trehalose was shown to be beneficial in SOD1, TDP-43 and FUS/TLS- related models, then this would make it an exciting therapeutic to take forward to clinical trial as it would have the potential to be of benefit to patients with sporadic and familial ALS.

2. Materials and Methods

2.1 Materials

2.1.1 Reagents

Agarose (Ultrapure): Invitrogen

Anhydrous monobasic sodium phosphate (NaH_2PO_4): BDH

Anhydrous disodium hydrogen orthophosphate (Na_2HPO_4): BDH

Boric acid: Fischer Scientific

4.0 Braided surgical silk: Harvard apparatus

Bromophenol Blue: BDH

Chromic potassium sulphate: Sigma

Cryo M-bed: Bright

2.5mM dNTPs: Invitrogen

DPX: VWR

EDTA: BDH

Ethanol: Fisher Scientific

Fentanal/fluanisone (Hypnorm): Vetapharma Ltd

Ficoll: Sigma

Gallocyanin: Aldrich

Gelatin type A from porcine skin: Sigma

Isopentane: Alfa aesar

Metformin (1,1-Dimethylbiguanide): MP Biomedicals, USA

Midazolam (Hypnovel): Roche

Nonidet P40: BDH

Paraformaldehyde (PFA): BDH

Pentobarbital: Merial, UK

Phosphate Buffered Saline (PBS): OXOID

Potassium chloride (KCl): AnalaR (part of VWR)

Primers: all primers were purchased from Invitrogen

Proteinase K: Roche

SIGMA*FAST*™ 3,3′-Diaminobenzidine tablets: Sigma

Sodium hydroxide (NaOH): BDH

Sucrose: Sigma

Superfrost plus glass slides: VWR

SYBR safe stain concentrate: Invitrogen

Trehalose: MP Biomedicals, USA

Tris (ultrapure): Invitrogen

Tween 20: BDH

Xylene: VWR

Xylene Cyanol: Sigma

2.1.2 Kits

Avidin/Biotin blocking kit: Vector Laboratories, UK

Brilliant SYBR green QPCR master mix reagent (Stratagene)

Brilliant II SYBR green QPCR master mix reagent (Stratagene)

DNeasy blood and tissue kit: QIAGEN

PCR enhancer system: Invitrogen

Taq DNA polymerase, recombinant: Invitrogen

Vectastain ABC kit: Vector Laboratories, UK

2.1.3 Antibodies

2.1.3.1 Primary antibodies

Polyclonal anti choline acetyltransferase (ChAT): AB144P, Chemicon, Chandlers Ford, UK

USOD: kindly donated to us by Dr Avijit Chakrabartty, University of Toronto

2.1.3.2 Secondary antibodies

Polyclonal rabbit anti goat-biotinylated: E0466, Dako

Polyclonal swine anti rabbit-biotinylated: E0353, Dako

2.1.4 Equipment

Agarose gel imaging system (AlphaDigiDoc^{TM} RT imaging system): Alpha Innotech

Bench Centrifuge (Biofuge Pico): Heraeus

Chromo4 Real Time PCR-Detector: Biorad

Cryostat: Bright (Model OTF)

305B Dual-mode servomotor transducer: Aurora Scientific, Ontario, Canada

Mx3000p Q-PCR system: Stratagene

Nanodrop ND-1000 Spectrophotometer: Thermo Scientific

PCR machine: Techne TC-512

701A Stimulator: Aurora Scientific, Ontario, Canada

Strain gauge (Dynamometer): UFI devices

Thermo pad: Harvard apparatus

2.2 Methods

2.2.1 Solutions

2.2.1.1 Genotyping

2.2.1.1.1 10x Stock of Ear Homogenisation Buffer

- 500mM KCl
- 100mM Tris-HCl pH8.3
- 0.1mg/ml Gelatin
- 0.45% v/v Tween 20

- 0.45% v/v Nonidet P40
- + 5mg/mL Proteinase K (added following autoclaving the above buffer)

2.2.1.1.2 6X Stock of DNA gel loading buffer (10ml)

Dissolve 1.5 Ficall (glycerol) in 10ml RO (Reverse Osmosis) water by incubation in water bath for ~4hours at 60°C. Once dissolved, add a few crystals of bromophenol blue and a few crystals of xylene cyanol (by touching the end of a separate pipette tip into each powder and then into the ficall solution). Mix well and aliquot, then store at room temperature.

2.2.1.1.3 5X Stock of TBE Buffer (1 litre)

- 54g Tris Base
- 27.5g Boric Acid
- 40ml, 0.5M EDTA

Dissolve above ingredients in 700ml RO water with gentle heating and stirring to aid dissolving, then top up volume to 1 litre.

2.2.1.2 Immunohistochemistry

2.2.1.2.1 4% paraformaldehyde (PFA) (1 litre)

In the fume hood, dissolve 40g PFA in 800ml RO water (preheated to 60°C), maintain temperature at 60°C whilst dissolving (heating above 70°C can bring about degradation of the PFA). Once solution has a milk-like aspect, add concentrated NaOH dropwise until solution turns clear. Add 100ml of 10X PBS and allow solution to cool. Bring pH down to 7.4 then top up volume to 1litre with RO water. Aliquot and freeze for future use.

2.2.1.2.2 Gelatin solution for embedding spinal cords (1 litre)

- 6g anhydrous NaH_2PO_4
- 26.9g anhydrous Na_2HPO_4
- 100g Sucrose (10% final concentration in 1L)
- 75g Gelatin from Porcine skin (7.5% final concentration in 1L)

Dissolve all ingredients in 500 ml of RO water preheated to approximately 70°C (Note: add ingredients little by little to the RO water with stirring to avoid clumping of the gelatin).

Make the volume up to 1L with pre-heated RO water then bring to the boil. Allow to cool then aliquot and freeze.

2.2.1.2.3 Nissl Stain (500ml)

- 1.5g gallocyanin
- 50g Chromic potassium sulphate

Dissolve chromic potassium sulphate in 500ml RO water preheated to approximately 70°C (heating and stirring is required in order for the chromic potassium sulphate to dissolve). Add gallocyanin, bring to the boil and simmer for at least 30 minutes with stirring. To avoid excessive evaporation of solution during boiling and simmering, make solution in a conical flask and insert an additional, smaller conical flask upside down into the neck of the conical flask to act as a condenser. Following simmering, allow the solution to cool and then filter before storing in a sealed bottle at room temperature. Always filter solution before use.

2.2.2 Animals

All animal experiments were carried out under license from the Home Office (UK) in accordance with The Animals (Scientific Procedures) Act 1986 and were approved by Imperial College/Royal Veterinary College ethical committees.

2.2.2.1 SOD1 ^{G93A} mouse breeding and maintenance

For all experiments, mice were housed in a minimal disease facility, with a 12:12 hour light: dark cycle and food and water ad libitum. Male mice overexpressing human SOD1 with the ALS-causing G93A mutation [B6SJL-TgN SOD1^{G93A} 1 Gur/J, Stock number 002726]

(Gurney et al., 1994) were originally purchased from the Jackson Laboratory (Bar Harbour, ME). They have subsequently been maintained (for over 28 generations), as hemizygotes through breeding with wild-type F1 hybrid C57Bl/6 x CBA/Ca females. Mice on this background (Sharp et al., 2008) have similar lifespans (Azzouz et al., 2004a, Chengyun et al., 2004) and disease progression characteristics (as measured by hindlimb electrophysiological parameters (Sharp et al., 2008, Hegedus et al., 2007) and longitudinal monitoring of weight and neurological score (Gill et al., 2009, Kaneb et al., 2011)), to mice on the original B6SJL background. No changes in disease progression or lifespan have been seen with successive generations in our laboratory.

2.2.2.2 Genotyping of SOD1^{G93A} transgenic mice.

Following weaning (or at two weeks of age in our trehalose survival study (2.2.3.4.1)), an ear biopsy of ~1.5-3mm^2 tissue was taken from each animal. DNA was extracted via incubation of the tissue overnight at 55°C in 50µl 1x ear homogenisation buffer (2.2.1.1.1). Once ear samples were completely digested, they were heated at 100°C to deactivate proteinase K and then stored at 4°C until genotyping PCR was performed. The PCR recipe for a single genotyping reaction along with the primer sequences and PCR cycling conditions used are summarised below:

PCR recipe for a single reaction

9.35 µl PCR-grade water

2 µl 10x PCR buffer minus Mg^{2+} (From Invitrogen Taq DNA Polymerase recombinant kit)

2µl PCR Enhancer (From Invitrogen PCR enhancer system kit)

0.8µl 2.5mM dNTPs

2µl 10 pmol/µl Forward Primer

2µl 10 pmol/µl Reverse Primer

0.6µl 50mM $MgCl_2$ (From Invitrogen Taq DNA Polymerase recombinant kit)

0.25µl Taq DNA Polymerase, recombinant

1µl digested ear sample

Primer sequences for the amplification of the human $SOD1^{G93A}$ transgene

Forward: 5'-CATCAGCCCTAATCCATCTGA-3'

Reverse: 5'-CGCGACTAACAATCAAAGTGA-3'

These primers amplify a 236 base pair section of exon 4 of the human SOD1 gene (Rosen et al., 1993b).

$SOD1^{G93A}$ PCR cycling conditions

Initial denaturation at 95°C for 3min

Then 35 cycles of:

95°C for 30s

60°C for 30s

72°C for 45s

Final extension at 72°C for 2mins, then hold at 4°C

Agarose gel electrophoresis

PCR products from SOD1^{G93A} genotyping reactions were electrophoresed on a 1% agarose gel (w/v, in 0.5x TBE buffer, (2.2.1.1.3)). Five µl of PCR product were loaded in each well with 1µl of 6x DNA gel loading buffer (2.2.1.1.2). Agarose gels contained 10,000X SYBR® Safe stain concentrate (Invitrogen, diluted 1:20000 in gel) to allow the visualisation of amplified DNA fragments with the AlphaDigiDoc^{TM} RT imaging system (Alpha Innotech).

2.2.2.3 Assessment of potential variations in copy number in SOD1^{G93A} transgenic mice.

2.2.2.3.1 Quantitative PCR for assessment of potential variations in copy number-background

A quantitative PCR (Q-PCR) method, developed by Alexander et al., was used for assessment of potential variations in copy number in SOD1^{G93A} mice in our experiments (Alexander et al., 2004). In this method, the amount of PCR product produced at each cycle is tracked via the intensity of fluorescence produced by SYBR green. SYBR green is a fluorescent dye that is included in the PCR reaction and emits florescence as a result of its intercalation between the strands of double-stranded DNA (Schneeberger et al., 1995). Variations in transgene copy number were identified by determining the difference in cycle threshold (ΔCT) between a reaction set up to amplify the human SOD1^{G93A} transgene and a reaction set up to amplify an endogenous reference gene (interleukin 2 (IL2)) with a known copy number of 2. Cycle threshold (CT) represents the cycle at which a significant increase in SYBR fluorescence compared to baseline is first detected. SOD1^{G93A} mice used in our colony have ~25 copies of the human SOD1^{G93A} transgene. Consequently, CT values

measured for reactions amplifying the transgene, should be lower than those amplifying the IL2-refernce gene. Lower ΔCT values (calculated by subtraction of the $SOD1^{G93A}$ CT from the IL2 CT) indicate a lower $SOD1^{G93A}$ copy number, whereas higher ΔCT values indicate a higher $SOD1^{G93A}$ copy number.

2.2.2.3.2 Quantitative –PCR protocol for assessment of potential variations in copy number in $SOD1^{G93A}$ mice

Upon death (or prior to perfusion under deep anaesthesia), a 0.5cm tail tip was removed from each experimental mouse for potential use in transgene copy number variation assessment. DNA was extracted from tail tips of mice selected for copy number variation assessment using a DNeasy blood and tissue kit (QIAGEN) as per the manufacturer's instructions. The concentration and purity of the extracted DNA was measured using a nanodrop spectrophotometer (ND-1000, Thermo Scientific). Primer sequences for the human $SOD1^{G93A}$ transgene and the IL2 reference gene were identical to those used and optimised by Alexander et al. (Alexander et al., 2004) and were as follows:

5′-CATCAGCCCTAATCCATCTGA-3′ ($SOD1^{G93A}$ forward)

5′-CGCGACTAACAATCAAAGTGA-3′ ($SOD1^{G93A}$ reverse)

5′-CTAGGCCACAGAATTGAAAGATCT-3′ (IL2 forward)

5′-GTAGGTGGAAATTCTAGCATCATCC-3′ (IL2 reverse)

Either Brilliant® SYBR Green QPCR Master Mix reagent (Stratagene) or Brilliant® II SYBR Green QPCR Master Mix reagent (Stratagene) were used for the real-time amplification and the recipe for a single 30µl reaction was as follows:

- 2ng template DNA in a volume of 9µl H_2O

- 15µl of Brilliant SYBR green (I or II) Q-PCR master mix
- 3 µl forward primer
- 3 µl reverse primer

Optimal final concentrations of forward and reverse primers in the reaction mixture were determined by Alexander et al., to be 0.4 µM for human $SOD1^{G93A}$ and 0.5µM for mIL and were therefore used in our experiments. All primers were Q-PCR grade and were purchased from Invitrogen. Cycling conditions used were as follows: initial activation of Sure Start® Taq polymerase at 95 °C for 10 minutes, then 40 cycles of 95 °C for 30 seconds, 60 °C for 1 minute and 72 °C for 30 seconds. Assays were performed in duplicate using either of two detection systems; the Mx3000p Q-PCR system (Stratagene) (metformin electrophysiology study) or the Chromo4 Real Time PCR-Detector (Biorad) (metformin survival study). A no template control was performed for both human $SOD1^{G93A}$ and mIL2 primers in each Q-PCR experiment to rule out contamination of the master mix with genomic DNA. Average cycle threshold (CT) values for human $SOD1^{G93A}$ and mIL2 were determined for each sample by the detection systems used. In our metformin electrophysiology study, assessment of potential variation in copy number was performed for all mice as they were culled before it could be determined whether they had outlying survival characteristics. In our metformin survival study, potential variations in copy number were investigated in any mice displaying outlying survival characteristics with respect to their treatment group and the ΔCT values obtained were compared to those of a subset of 4 male and 4 female control mice displaying normal survival. Any mice with a ΔCT value that differed by more than 2 standard deviations from the mean ΔCT of these control mice were to be excluded although no mice met this criteria. In our trehalose survival study, no mice were observed to display an outlying

survival time compared to the other mice in their experimental group and hence copy number variation assessments were not performed.

2.2.3 SOD1^{G93A} mouse treatment protocols

2.2.3.1 Metformin electrophysiology study

Male and female SOD1^{G93A} mice and their wild type (WT) littermates were treated with 2mg/ml metformin in the drinking water from 35 days of age. Water bottles containing metformin solution were changed weekly. Mice were treated with metformin until they reached 100 days of age +/-1 day when the effect of metformin treatment on the severity of pathology was analysed via measurement of the following parameters by *in vivo* electrophysiology:

- The number of functional motor units in the right Tibialis Anterior (TA) and Extensor Digitorum Longis (EDL) muscles of SOD1^{G93A} mice and the right EDL muscles of WT mice
- The maximal and specific forces of the right TA and EDL muscles of SOD1^{G93A} and WT mice.
- The resistance to fatigue of the right EDL muscles of SOD1^{G93A} and WT mice.

Control SOD1^{G93A} and WT mice received normal drinking water throughout the experiment and were subjected to the same electrophysiological analyses to treated mice at 100 days of age +/- 1. A subset of mice from each group were weighed every five days from 55 days of age in order to investigate the effects of metformin treatment of bodyweight. Any mice that became injured as a result of fighting or unwell through a non-ALS related mechanism were excluded from the study as these factors may have influenced the results obtained (Scott et al., 2008).

2.2.3.2 Metformin dose-response survival study

2.2.3.2.1 Experimental groups

Twenty breeding trios each consisting of one $SOD1^{G93A}$ transgenic male and two F1 hybrid C57B110 x CBA/Ca females were set up simultaneously to generate a large cohort of 286 age matched pups to provide $SOD1^{G93A}$ mice for enrolment in the survival study. Females were separated when pregnant to allow tracking of the lineage of resultant litters. Following genotyping and when the resultant male and female $SOD1^{G93A}$ pups reached 35 days of age (+/- 2 days), they were separated into four groups which were balanced with respect to age (+/- 2 days), gender (14 males and 15 females per group) and body weight within gender (mean starting weights for all groups were within 0.5g of each other). In order to ensure consistency in genetic background across the groups, transgenic mice from each litter were distributed evenly between the four groups in a gender specific fashion. Mice were housed within their groups in cages of either 4 or 5 mice for males and 5 mice for females.

2.2.3.2.2 Metformin treatment regime

$SOD1^{G93A}$ mice were chronically treated with 0.5, 2 or 5mg/ml metformin in the drinking water from 35 days of age until they reached the endpoint of the inability to right themselves within 30s of being placed on a side. Metformin solutions were freshly prepared in sterilised bottles and changed twice weekly. Control mice received normal drinking water throughout the experiment. The identities of control and treatment groups were blinded to animal technicians and the investigator and were only revealed once all data analysis had been completed.

2.2.3.3 Metformin blood collection study

SOD1^{G93A} and WT female mice (n=6-7 , per group) were treated with 2mg/ml metformin in the drinking water from 35 days of age (the time point at which treatment commenced in all other metformin experiments performed). A separate control group of SOD1^{G93A} and WT females (n=7-10 per group) received normal drinking water throughout. At 70 days of age blood samples were collected from all mice via cardiac puncture in order to measure the effect of metformin treatment on serum β-oestradiol levels (see detailed β-oestradiol assay method below (section 2.2.8)). For the purposes of cardiac punctures, female mice were first anesthetized via a lethal intraperitoneal injection of 100µl of a 20mg/ml solution of pentobarbital (Merial, UK). Cardiac punctures were not performed until the mice had lost their pedal reflex. Following blood collection, mice were culled via cervical dislocation. Blood samples were allowed to clot overnight at 4°C, before serum was collected via centrifugation (13000 rpm for 5 minutes) and then stored at -80°C. Unfortunately, cardiac punctures for two metformin-treated SOD1^{G93A} mice were not successful and this reduced the n-number for this group to 4.

2.2.3.4 Trehalose dose-response survival study

2.2.3.4.1 Experimental groups

Twenty two breeding trios each consisting of one SOD1^{G93A} transgenic male and two F1 hybrid C57B110 x CBA/Ca females were set up simultaneously to generate a large cohort of 299 age-matched pups to provide SOD1^{G93A} mice for enrolment in the survival study. Females were separated when pregnant to allow tracking of the lineage of resultant litters. A small ear biopsy (~1.5-3mm^2 tissue) was taken from each mouse at 14 days of age (prior to

weaning) for the purposes of genotyping. Genotyping at this early stage permitted weaning of mice into four, littermate-balanced groups of 15 mice per sex at 21 days of age. This had the advantage of preventing the fighting that can occur when introducing older, more sexually mature mice (particularly males) from different litters into the same cages (Van Loo et al., 2003). Male mice were weaned into cages of 3 to reduce the incidence of fighting (mice in cages of 3 have been shown to fight less than those in cages of 5 or 8 mice (Van Loo et al., 2001, Van Loo et al., 2003)). Female mice were weaned into cages of 5. At 35 days of age (+/- 2 days), immediately prior to the initiation of trehalose treatment, mice were weighed and the average weights of all male and females groups were determined. At this stage, a small number of cages of mice were swapped between groups (whilst maintaining littermate balancing) to ensure the best balancing of starting weight between groups possible. Following this adjustment all male groups were within 0.35g of each other whereas all female groups were within 0.27g of each other.

2.2.3.4.2 Trehalose treatments

Mice were chronically treated with 0.5, 2 or 5% (w/v) trehalose in sterile drinking water from 35 days of age (+/- 2 days) until they reached the endpoint of the inability to right themselves within 20s of being placed on a side. Trehalose solutions were freshly prepared in sterilised bottles and changed twice weekly. Control mice received normal sterilised drinking water throughout the experiment. The identities of control and treatment groups were blinded to animal technicians and the investigator and were only revealed once all data analysis had been completed. Bottles containing control and trehalose solutions were wrapped in foil in order to maintain blinding as the presence of trehalose in solution could be detected by eye.

2.2.3.5 Trehalose spinal cord histology experiment

An additional cohort of SOD1^{G93A} mice were treated with 5% trehalose in sterile drinking water or sterile drinking water alone from 35 days of age for the purposes of spinal cord collection for histology (n=4 males and n=6 females per group). Solutions were freshly prepared in sterilised, foil wrapped bottles and changed twice-weekly and the identity of the groups was blinded to the animal technicians and the investigator. We had hoped to follow the guidelines for preclinical animal research in ALS/MND proposed by Ludolph et al., (Ludolph et al., 2010) and have a minimum n-number of 5 mice per sex, per group for these histological experiments, but unfortunately we did not have sufficient age-matched males available for this. Additionally, genotyping could not be performed in these mice prior to weaning due to time constrains and therefore full littermate and weight balancing could only be performed female mice, which can be mixed post-weaning without fighting issues (Jennings et al., 1998). Female mice were organized into two cages of three mice per group. Male mice were organized into cages of 2, with each cage containing a pair of SOD1^{G93A} mice from the same litter. These cages of mice were then distributed between male groups in a manner that provided the best possible balancing of litter and weight at 35 days of age. A time-point of 75 days of age was selected for spinal cord collection as we wished to investigate SOD1 aggregation in the spinal cord samples and at this time SOD1 aggregates are usually visible but are not so numerous that they become difficult to quantify (Sharp et al., 2008). At 75 days of age mice were terminally anaesthetized with an intraperitoneal injection of 100µl of a 20mg/ml solution of pentobarbital (Merial, UK) and transcardially perfused with 1x phosphate buffered saline (PBS) followed by 4% paraformaldehyde (PFA) in 1x PBS for the purposes of spinal cord extraction (see detailed perfusion and spinal cord extraction method below (section 2.2.6)).

2.2.4 In vivo electrophysiology

2.2.4.1 Surgical preparation for in vivo electrophysiology

Mice were deeply anesthetized via intra peritoneal injection of fentanyl/fluanisone (Hypnorm, Vetapharma Ltd.), midazolam (Hypnovel, Roche) and water (1:1:2 by volume) at a dosage of 9 ml/kg. Careful monitoring of the mice was performed throughout the experiment and additional doses of anesthetic were administered as required to ensure that there was no reflex response to toe pinch. The distal tendons of the right TA and EDL muscles were dissected free from surrounding tissue, individually tied with 4.0 braided surgical silk (Harvard Apparatus) and then cut at their most distal ends. The sciatic nerve was exposed and all its branches cut except for the common peroneal nerve (CPN), which innervates the TA and EDL muscles. The mouse was placed on a thermopad (Harvard Apparatus) to maintain body temperature at 37 °C. The right foot was secured to a platform and the knee immobilized using a stainless steel pin.

2.2.4.2 Measurement of TA and EDL maximum and specific forces

The right TA and EDL tendons of experimental mice were individually attached to the lever arm of a 305B dual-mode servomotor transducer (Aurora Scientific, Ontario, Canada) via a custom-made steel s-hook. TA and EDL muscle contractions were then elicited by stimulating the distal part of the deep peroneal nerve (DPN) via bipolar platinum electrodes, using supramaximal square-wave pulses of 0.02 ms (701A stimulator; Aurora Scientific). Data acquisition and control of the servomotors were conducted using a Lab-View-based DMC program (Dynamic muscle control and Data Acquisition; Aurora Scientific). Optimal muscle length (Lo) was determined by incrementally stretching the muscle using

micromanipulators until the maximum isometric twitch force was achieved. Maximum isometric tetanic force (Po) (referred to as maximal force from this point forward) was determined from the plateau of the force–frequency relationship following a series of stimulations at 10, 30, 40, 50, 80, 100, 120, 150, and 180 Hz. A 1-minute resting period was allowed between each tetanic contraction. Muscle length was measured using digital calipers based on well-defined anatomical landmarks near the knee and the ankle. The TA and EDL specific forces (N/cm2) were calculated by dividing Po by muscle cross-sectional area. Overall cross-sectional area was estimated for the TA and the EDL muscles using the following formulae:

TA: muscle weight (g)/ [[L_o (cm) × 0.6] × 1.06 (g/cm^3)]

EDL: muscle weight (g)/ [[(L_o (cm) × 0.45] ×1.06 (g/cm^3)]

Where 0.6 and 0.45 represent the fiber length/muscle length ratios of intact TA and EDL muscles respectively and 1.06 g/cm^3 represents the density of mammalian skeletal muscle (Brooks and Faulkner, 1988).

2.2.4.3 Measurement of motor unit number

The TA and EDL muscle tendons were individually attached to a strain gauge (Dynamometer, UFI Devices) to record muscle twitch forces. Isometric twitch contractions were elicited by stimulating the distal part of the DPN via bipolar silver electrodes using square wave pulses of 0.02 ms. The stimulation voltage and subsequently the length of the muscle was adjusted to produce the maximum isometric twitch force. The stimulus amplitude

was then set to 0 V and manually increased over a range of 0-2 V. This resulted in discrete increments in twitch force due to the successive recruitment of motor units. With each increment in force the stimulus amplitude was held at constant voltage for at least 5 stimuli and then increased manually to elicit a larger twitch. This procedure was repeated until there was no further increase in force, indicating that all motor units were recruited. The number of step-wise increments of force was counted in a blinded fashion and taken as an estimate of the number of motor units in the TA and EDL muscles. Force output was recorded using an analogue to digital converter interfaced with a computer running the appropriate software (Cambridge Electronics Design Ltd).

2.2.4.4 Fatigue test

Following the recording of the number of motor units in the EDL muscles of experimental animals and while the distal tendon of the EDL muscle was still attached to the strain gauge, the DPN was stimulated at a frequency of 40 Hz for 250 ms of every second for 3 min using the same electrodes as used for the motor unit assessment protocol. The EDL force output over the 3min time period was recorded using an analogue to digital converter interfaced with a computer running the appropriate software (Cambridge Electronics Design Ltd), to produce a fatigue trace. The decrease in force after 3 min of stimulation was measured and the fatigue index (FI) was calculated by the division of the final force by the initial force. FI results closer to 1 represent muscles that are more resistant to fatigue.

2.2.4.5 Tissue collection following in vivo electrophysiology

At the end of the fatigue test, whilst mice were still deeply anesthetised, the right TA and EDL muscles were removed and weighed (for the purposes of specific force calculations). The TA and EDL muscles were then separately mounted on cork blocks with cryo M-bed and snap frozen in liquid nitrogen-cooled isopentane before being stored at -80°C for future cryosectioning and immunohistochemistry should this be required. Tail samples were collected and snap frozen in liquid nitrogen for DNA extraction for future copy number variation assessments. Finally, animals were perfused through the left ventricle of the heart with 1x PBS followed by 4% PFA in 1X PBS for the purposes of spinal cord extraction for histology should this be required (see detailed perfusion and spinal cord extraction method below **(Section 2.2.6)).**

2.2.4.6 Statistical analyses for metformin in vivo electrophysiology experiments

Comparisons between untreated SOD1 and WT mice were made using one-way ANOVA analyses with post-hoc Bonferroni tests. Where metformin treatment effects were being analyzed, the only statistical comparisons made were between treated and untreated mice of the same sex and genotype e.g. SOD1^{G93A} male vs. metformin treated SOD1^{G93A} male mice. These analyses were performed via individual unpaired t-tests following the testing of the data for normality. All statistical analyses were performed using Graphpad Prism 5 software.

2.2.5 Dose-response survival studies in SOD1^{G93A} mice

2.2.5.1 Cage conditions, food and water

Mice were treated with either normal drinking water or one of 3 doses of metformin or trehalose in the drinking water from 35 days of age. When mice reached 100 days of age and began to show neurological symptoms, cages were fitted with long sipper tubes (Techniplast, UK) and mice were provided daily with a standard amount of mashed diet prepared with the relevant water/drug solution. A standard number of dry food pellets were left on the bedding in addition to in the food hoppers throughout the experiment and cage conditions including bedding and enrichment were kept consistent across groups. Specifically, for the metformin survival study, all cages contained a covering of golden chips bedding (Lillico) on their base as well as two fun tunnels (Lillico) and a handful of paper wool (Lillico). Paper wool and cardboard tubes were removed for all female mice at 110 days of age and once any male mice in a cage started having difficulty walking. Once paper wool and cardboard tubes were removed, each cage was provided with two nestlets (Lillico) for the remainder of the study. For the trehalose survival study, all cage bottoms were covered with a layer of alpha dri bedding Lillico and contained two fun tunnels as well as two nestlets. Fun tunnels were removed at 100 days of age. For all studies, cages were cleaned on a weekly basis. A detailed discussion of the reasons behind the bedding and enrichment choices made is given in Chapter 5.

2.2.5.2 Analysis of disease onset, progression and survival

2.2.5.2.1 Neurological Score

Neurological scores for both hind limbs were assessed twice weekly for each mouse from 41 days of age (metformin survival study) or 46 days of age (trehalose survival study). Neurological scores were assigned using a scale of 0-4 developed by the ALSTDI through detailed observations of $SOD1^{G93A}$ mouse pathology (Scott et al., 2008, Gill et al., 2009, Lincecum et al., 2010). Criteria used to assign each score level were:

0 Full extension of hind legs away from lateral midline when mouse is suspended by it tail and mouse can hold this for 2 seconds, suspended 2-3 times.

1 Collapse or partial collapse of leg extension towards lateral midline (weakness) or trembling of hind legs during tail suspension.

2 Toes curl under at least twice during walking of 12 inches or any part of foot is dragging along cage bottom (a clean cage containing no bedding was used for this analysis to permit easy viewing of the toes).

3 Rigid paralysis or minimal joint movement, foot not being used for forward motion.

4 Mouse cannot right itself within 30s (metformin survival study) or 20s (trehalose survival study) of being placed on a side (this test was performed in a clean cage containing the same type and amount of bedding as present in the mouse's home cage).

2.2.5.2.2 Body Weight

Body weight for all mice was measured twice weekly from 35 days of age (metformin survival study) or 46 days of age (trehalose survival study). This provided an additional, non-invasive, measure of disease onset and progression and also allowed monitoring of the general health of the mice. Weight-loss in high copy $SOD1^{G93A}$ mice is normally a gradual process that begins at approximately 90 days of age and continues until death. Rapid losses of weight over a short number of days that do not fit the normal pattern can therefore be indicative of non-ALS related or drug-induced maladies (Scott et al., 2008).

2.2.5.2.3 Survival

For humane reasons, a uniform end point of the inability of a mouse to right itself within 30s of being placed on a side (metformin survival study) or 20s of being placed on a side (trehalose survival study) was employed for all mice. From 100 days of age, the righting reflex of each mouse from each side was tested twice daily to ensure that the end point of each mouse was accurately determined. Once mice reached their end point, they were euthanized via cervical dislocation and the date and the cause of their death was recorded. Following death, a tail tip was taken from each mouse for assessment of potential variations in copy number via Q-PCR.

2.2.5.3 Graphical representation of data and statistical analyses

As the time course of pathology in male and female $SOD1^{G93A}$ mice has been shown to be different (Choi et al., 2008) and administered therapeutics may behave differently in male and female systems, all graphical representations and statistical analyses were performed

separately for males and females. In order to visualise overall changes in body weight and neurological score, mean body weight and mean neurological score were plotted for each group over time until the time point at which the last mouse in the group died. To prevent decomposition of mean weight and neurological score values as mice reached their end stage, final weight and neurological score values for individual mice were carried forward until the time point at which the last mouse in their group died. This is a practice routinely used when performing survival analyses with longitudinal monitoring of weight and neurological score (Gill et al., 2009, Lincecum et al., 2010). In order to avoid the loss of statistical validity that can occur when performing repeated analyses on correlated serial measurements for the same subjects, we selected relevant summary measures for weight and neurological score data as advised by Matthews, et al. (Matthews et al., 1990) and performed statistical analyses on these. Summary measures selected were time to attain peak weight (the earliest indicator of disease onset), time from peak weight to death (an indicator of disease progression), time to attain a neurological score of 2 in both hind limbs (defined as the definitive onset of symptomatic neurological disease) and finally time to reach a score of 4 (the uniform end point selected for this study, which was taken to represent survival). These summary measures all represent 'time to event measures' and were analyzed using Kaplan Meier survival fit analyses and the Logrank test for statistical significance. This test investigates the null hypothesis that the Kaplan Meier curves for all groups are identical (i.e. that the treatment did not change the time taken to reach the event being analysed). Low P-values are therefore indicative of differences between curves that did not occur due to chance. As multiple groups were being compared and they could be arranged in order of increasing drug dose, we were also able to compare groups using the log rank test for trend. This test generates a P-value for the null hypothesis that there is no linear trend between group order

and median time to event. Low P-values are therefore indicative of a significant trend between increasing drug dose and the event being analysed. The threshold for significance for all analyses was set at $P<0.05$. As has previously been described, in order to establish the age at which each mouse reached its peak weight, successive weight values for each mouse were subjected to spline smoothing and the time at which the maximum of the weight curve occurred was recorded (Gill et al., 2009, Lincecum et al., 2010). If the smoothed body weight curve for an individual mouse had multiple equal peaks, the time point at which the final peak occurred was taken. Spline smoothing of weight curves as well as all Kaplan Meier survival analyses were carried out using Graphpad Prism 5 software.

2.2.6 Mouse spinal cord extraction and preparation for cryosectioning

Following transcardial perfusion of mice with 1X PBS followed by 4% PFA (in 1X PBS), the spinal columns of perfused mice were removed and post-fixed overnight in the same fixative. Spinal cords were then dissected free from their spinal columns and cryoprotected in sucrose (30% in 0.1 M PBS) until the time point at which they sank within the sucrose solution. The lumbar regions of the spinal cords were then isolated, set (on ice) in cubes of a jelly composed of 10% sucrose and 7.5% gelatin in 0.12M phosphate buffer , pH 7.4 (Section 2.2.1.2.2) and mounted on cork blocks with cryo M-bed. During the mounting process the spinal cord was oriented vertically with the most caudal end closest to the cork block. The location of the ventral side of the spinal cord was marked on the cork to allow orientation of the block within the cryostat in order for the ventral side to meet the knife first. Mounted spinal cords were snap frozen in isopentane at -55 +/- 5°C and stored at -80°C for future cryosectioning (20μm per section) and histology.

2.2.7 Histological analysis of trehalose-treated SOD1^{G93A} mouse spinal cords

2.2.7.1 Cryosectioning and immunostaining for trehalose survival study

20 µm sections were cut from L3-L5 of the lumbar spinal cord, with serial sections mounted onto superfrost plus glass slides at 200-µm intervals (every 10th section). Sections were immunostained for either misfolded SOD1 (USOD ; 0.3 µg/ml, kindly donated to us by Dr Avijit Chakrabartty, University of Toronto) or choline acetyltransferase (ChAT; 1:100, AB144P ; Chemicon, Chandlers Ford, UK). Before incubation with primary antibodies, sections were air dried for 30 minutes and endogenous biotin was blocked using an avidin/biotin blocking kit (Vector Laboratories,UK). In order to reduce nonspecific binding of the primary antibody, sections were incubated for 30 minutes in a 5% nonfat milk solution diluted in 1X PBS/0.05% Tween-20. Sections were incubated overnight at 4°C in primary antibody, after which they were incubated for 30 minutes with an appropriate biotinylated secondary antibody (Dako, Ely, UK). Immunoreactivity was visualized using peroxidase detection (Vectastain ABC kit; Vector Laboratories and SIGMA*FAST*™ 3,3′-Diaminobenzidine tablets; Sigma). Following immunodetection, sections were briefly counter-stained (30s) with Nissl stain (Section 2.2.1.2.3), then dipped in distilled water to remove excess Nissl, dehydrated in graded alcohols, cleared in xylene, and coverslipped with DPX. When staining was performed it was ensured that slides for all male mice and slides for all female mice were stained together. This ensured that sections from any mice that were to be directly compared were manipulated identically. Relevant positive and negative controls were included in all stains to ensure the validity of the results obtained. Specifically, for ChAT staining, equivalent spinal cord sections from an age-matched WT mouse to those being analysed for SOD1^{G93A} mice, were used as positive controls. These sections (as well as those from SOD1^{G93A} mice) also acted as negative controls as if any cells in regions of the

spinal cord known not to contain motor neurons (such as the dorsal horns) showed ChAT staining, then this would indicate that non-specific staining was occurring. We confirmed the appropriate localisation of motor neurons in spinal cord levels being analysed using an annotated atlas of the mouse spinal cord (Watson et al., 2008) as well as the results of a comprehensive mapping of the motor nuclei supplying the hindlimb muscles of the mouse by McHanwell and Biscoe (McHanwell and Biscoe, 1981). For USOD staining, equivalent sections from an end-stage $SOD1^{G93A}$ mouse to those being analysed for 75 day old experimental $SOD1^{G93A}$ mice were initially used as positive controls as at end stage we could be sure that misfolded/aggregated mutant SOD1 would be present in the lumbar spinal cord. After USOD staining had been performed several times, sections from an experimental mouse that had previously shown substantial USOD staining were used as positive controls. Equivalent spinal cord sections from an age-matched WT mouse to those being analysed for experimental $SOD1^{G93A}$ mice, were used as negative controls for USOD staining.

2.2.7.2 Quantification of USOD positive motor neurons and surviving motor neurons in the sciatic motor pool of trehalose-treated mice

The localization of the motor nuclei supplying the hindlimb muscles of the mouse, that lie in the sciatic motor pool, has been comprehensively mapped using retrograde transport of horseradish peroxidase (McHanwell and Biscoe, 1981). Specifically, sciatic motor nuclei have been determined to lie in the dorsolateral portion of the ventral horn, forming a longitudinal column starting at L3 and terminating at the L5–L6 boundary (McHanwell and Biscoe, 1981). In order to quantify the relative numbers of motor neurons in the sciatic motor pool containing misfolded/aggregated SOD1, we counted the number of USOD positive sciatic motor neurons in equivalent sections L3-L5 in control and treated $SOD1^{G93A}$ mice. As

staining was performed on every 10th section L3-L5, we were not concerned about counting the same motor neurons twice. In order to confirm that any changes in the number of USOD positive motor neurons in control and 5% trehalose-treated mice were not the result of a change in the number of surviving motor neurons, we counted the number of ChAT/Nissl double stained motor neurons in the sciatic motor pool in equivalent sections to those used for USOD quantification. All USOD and ChAT counts were performed in a blinded fashion by the same investigator and results for males and females were tested separately for statistical significance using the Mann-Whitney test, with the threshold for statistical significance set at $P<0.05$.

2.2.8 17β-oestradiol radioimmunoassay (RIA)

Following collection of blood plasma from metformin-treated and control SOD1^{G93A} and WT mice at 70 days of age (as described in section 2.2.3.3), serum samples were frozen at -80°C and sent on dry ice to Dr Zhangrui Cheng in the department of Veterinary Basic Sciences at the Royal Veterinary College for performance of a 125 iodine-based 17β-oestradiol radioimmunoassay. Dr Zhangrui analysed serum 17β-oestradiol levels in these samples using the following assay procedure produced from guidelines provided in the estradiol MAIA kit used (see below). Measured 17β-oestradiol levels were compared between control and treated SOD1^{G93A} mice and control and treated WT mice via individual unpaired t-tests. The threshold for significance was set as $P\leq0.05$

2.2.8.1 Radioimmunoassay principles

In RIAs, a fixed concentration of radio-labeled antigen in trace amounts is incubated with a constant amount of antiserum. The amount of antiserum present is such that only 30–50% of the total radio-labeled antigen can be bound to antibody in the absence of unlabeled antigen. When unlabeled antigen, either in the form of a standard or test sample is introduced, there is competition between radio-labeled antigen and unlabeled antigen for the limited constant number of binding sites on the antibody. The amount of radio-labeled antigen bound to antibody therefore decreases as the concentration of unlabeled antigen increases. In RIAs, following incubation of assay components for an optimized time period at an appropriate temperature, radio-labeled antigen bound to antibody is separated from unbound radio-labeled antigen (this can be performed by several methods, including the use of a second antibody that recognizes the first antibody). Following this separation process, the bound or free fraction of radio-labeled antigen is counted using a Geiger counter with appropriate settings for the particular radioisotope. Thereafter a standard curve is generated with a set of unlabeled standards of known concentration and from this curve the amount of antigen in unknown samples can be calculated (Millipore, 2011)

2.2.8.2 Chemicals and reagents

Estradiol MAIA kit

Supplied by: Alere Ltd, Pepper Road, Hazel Grove, Stockport, Cheshire, SK7 5BW

RIA buffer preparation:

Gelatin 1 g

Sodium azide 0.25 g

Tris HCl 6.61 g

Tris base 0.97 g

Dissolve gelatin in 800 ml RO water, then add remaining reagents and adjust volume to 1L with RO water. Adjust pH to 7.4 by adding 1 M HCl or NaOH. Warming is required to dissolve gelatin.

Standard Preparation

A 17β-oestradiol standard is provided in the oestradiol MAIA kit. The following dilutions of the standard must be made in preparation for the assay: 1, 2, 4, 8, 16, 32, 64, 125 pg/ml in RIA buffer.

Note: stock solutions of 1 mg/ml and 1 μg/ml can be kept at 20 °C for an extended period. Working dilutions can be kept at 4 °C for 20 days.

2.2.8.3 Assay protocol

Prepare total count (Tc), buffer blank (NSB), zero standard (B0), standard and sample tubes for the assay in duplicate according to the recipes provided in **Table 3.** Vortex tubes thoroughly and incubate at 4 °C for 4 hours. Add 200 µl Estradiol MAIA Separation Reagent to all tubes except total counts. Vortex and incubate at room temperature for 10 minutes. Centrifuge at 3000 × g for 10 minutes. Remove supernatant and measure the counts per minute (cpm) of the cellulose precipitate formed using a γ counter.

Following performance of the assay, calculate the mean cpm for each experimental condition (i.e. Tc, NSB, Bo, each standard and each sample), then calculate the percentage binding of the radioactive tracer to the first antibody (B/B0) in each standard and each sample using the following formula:

%B/B0 = (Mean standard or sample cpm - mean NSB cpm) ÷ (mean B0 cpm – mean NSB cpm) x100

Plot a standard curve of %B/Bo against 17β-oestradiol standard concentration and then use a multiple semi-log regression to calculate the 17β-oestradiol concentration in each unknown sample from this standard curve. (Note: the total counts tubes in this assay are used to confirm that (a) a sufficient amount of radio-labelled antigen is being used in the assay (b) that the amount of antibody being used is appropriate.)

Reagents	**Total count tubes**	**Buffer blank tubes**	**Zero standard tubes**	**Standard tubes**	**Experimental sample tubes**
Standard	-	-	-	100 µl	-
Blood serum sample	-	-	-	-	5ul
Buffer		405 µl	405 µl	305	400
First antibody	-	-	10 µl	10µl	10µl
Tracer	20µl	20 µl	20µl	20µl	20 µl

Table 3: Sample preparation for 17β-oestradiol radioimmunoassay (RIA)

3.1 Metformin electrophysiology study

3.1 Introduction

Amyotrophic Lateral Sclerosis (ALS) is a fatal neurodegenerative disorder associated with the selective degeneration of upper and lower motor neurons, for which there are currently no effective therapeutics (Cozzolino et al., 2008a). Although the majority of ALS cases are sporadic approximately 10% have a familial origin and of these, 15-20% are caused by gain of function mutations in the copper/zinc superoxide dismutase (SOD1) gene (Rosen et al., 1993c). The primary triggers for motor neuron degeneration in ALS remain elusive, however research in patients and mutant SOD1 based models has revealed several processes that are likely to contribute to pathology, including but not limited to: inflammation and toxic glial activation (Papadimitriou et al., 2010, Ilieva et al., 2009, Philips and Robberecht, 2011), mitochondrial dysfunction (Duffy et al., 2011) and oxidative stress (Papadimitriou et al., 2010, Duffy et al., 2011).

Metformin is a small molecule activator of the metabolic regulator, AMP-activated protein kinase (AMPK), which is routinely used for the treatment of type II diabetes (Hawley et al., 2002, Zhou et al., 2001). Metformin was originally prescribed for diabetes on the basis of its ability to reduce hepatic glucose production and increase insulin sensitivity (Cho and Kieffer, 2011), but it has subsequently been found to have potent anti-inflammatory (Dandona et al., 2004, Isoda et al., 2006, Lin et al., 2000) and antioxidant (Lin et al., 2000, Ouslimani et al., 2005, Srividhya et al., 2002) properties, as well as the ability to bring about mitochondrial biogenesis (Kukidome et al., 2006) and to cross the blood brain barrier (BBB) (Chen et al., 2009, Ma et al., 2007). In recent years it has emerged that peroxisome-proliferator activated

receptor coactivator 1 (PGC1-α) is an important mediator of the downstream effects of AMPK activation and that AMPK can directly enhance PGC1alpha activity via its phosphorylation (Jäger et al., 2007, Cantó and Auwerx, 2009). Furthermore, metformin treatment has been shown to increase the levels of PGC1α protein in skeletal muscles (Suwa et al., 2006) and it is thought that the antioxidant properties of this drug in addition to its ability to bring about mitochondrial biogenesis are derived from activation of AMPK-PGC-1α pathway (Kukidome et al., 2006).

Metformin therapy has been successfully tested in mouse models of both Huntington's disease and multiple sclerosis in which, as in ALS, inflammation, oxidative stress and mitochondrial defects are thought to be contributing factors to pathology (Beal and Ferrante, 2004, Stadelmann, 2011) Specifically, oral administration of metformin has been shown to increase lifespan and improve motor performance in male mice in the R6/2 model of Huntington's disease (Ma et al., 2007) and to attenuate pathology and inhibit the expression of pro-inflammatory mediators in the murine Experimental Autoimmune Encephalomyelitis (EAE) model of multiple sclerosis (Nath et al., 2009). In light of the observed beneficial effects of metformin therapy in these disease models of neurodegeneration, we hypothesised that metformin therapy would also attenuate motor neuron degeneration in the $SOD1^{G93A}$ mouse model of ALS (Gurney et al., 1994).

We tested the potential neuroprotective properties of metformin by treating male and female $SOD1^{G93A}$ mice with 2mg/ml metformin in the drinking water from 35 days of age and measuring the number of surviving functional motor units as well as strength and resistance to fatigue in their right TA and EDL muscles via *in vivo* electrophysiology. An early

symptomatic timepoint of 100 days, when substantial motor unit loss has occurred (Hegedus et al., 2007) but mice are not so sick that they struggle under anaesthetic, was selected for these electrophysiological assessments. Control SOD1^{G93A} mice received normal drinking water throughout and were analysed via the same electrophysiological parameters at 100 days of age. To ensure that metformin did not have any detrimental effects on the parameters being investigated in normal conditions and to compare the pathology of untreated SOD^{G93A} mice to age-matched WT mice, we replicated the experiment in WT litter mates. A subset of mice in all treatment groups were weighed approximately every 5 days to allow monitoring of metformin treatment on mouse weight. All experiments were performed in both male and female mice and data collected for the two sexes was considered separately as the onset of disease, survival time and response to therapeutic interventions has been shown differ between male and female SOD1G93A mice (Veldink et al., 2003).

3.2 Methods and n-numbers

All methods are described in detail in the materials and methods chapter. N-numbers for the electrophysiological parameters tested in all experimental groups are summarized in **Table 4**. N-numbers for the motor unit assessment protocol in SOD1^{G93A} male and female control mice are lower than for other groups as a file containing raw motor unit assessment data for several mice in these groups became corrupted and unfortunately the data could not be retrieved. Although, the male SOD1^{G93A} metformin treatment group originally contained 11 mice, rather than the 9 stated in **Table 4**, data collected from two of these mice were excluded, as they were suspected to have lost copies of the SOD1^{G93A} transgene (see below). TA motor unit assessment for WT mice was not performed in this study as a suitable force transducer for this purpose was not available.

Experimental Group	TA maximum force	TA specific force	TA motor units	EDL maximum force	EDL specific force	EDL motor units	EDL fatigue test
SOD1 M	11	11	7	11	11	7	11
SOD1 M tx	9	9	9	9	9	9	9
SOD1 F	11	11	6	11	11	6	11
SOD1 F tx	15	15	15	14	14	15	15
WT M	6	NA	6	6	6	6	6
WT M tx	6	NA	6	6	6	6	5
WT F	6	NA	6	6	6	6	6
WT F tx	7	NA	7	7	7	7	7

Table 4: Summary of the n-numbers used in metformin electrophysiology study

M = Male, F = Female, tx = treated with 2mg/ml metformin via the drinking water from 35 days of age.

3.3 Results

3.3.1 Assessment of potential variations in copy number

Assessment of potential copy number variation was performed for all mice enrolled in the metformin electrophysiology study via Q-PCR. Mice were analysed across three separate 96 well plates and results are summarized in **Table 5.** Metformin treated (tx) male $SOD1^{G93A}$ mice, SOD1 302 and SOD1 321, were analysed for potential copy number variations on two occasions, as they showed highly outlying electrophysiological characteristics for their group (substantially higher muscle forces and motor unit numbers than their peers) **(Table 5)** and were suspected to have lost copies of the transgene. As Q-PCR reactions are highly sensitive, it is not possible to compare samples accurately between plates, as the experimental conditions could have been slightly different for individual plates. Consequently, the ΔCT values for individual mice were only compared to the mean ΔCT value of mice analysed within the same plate. This was especially important in this study as a modified, more sensitive version of the Brilliant® SYBR Green QPCR Master Mix reagent (Stratagene) was used for plates 2 and 3 and therefore ΔCT values were overall lower in these plates. If the ΔCT value of an individual mouse differed by more than 2 standard deviations from the mean ΔCT for the plate, it was considered to have experienced a change in transgene copy number and was excluded from the study. One of the metformin treated male mice suspected to have lost copies of the transgene, SOD1 302, had a ΔCT value that was more than 2 standard deviations lower than the mean ΔCT and was therefore excluded. Although SOD1 312 did not have a ΔCT value that differed by more than two standard deviations from the mean in either plate 1 or 2, its ΔCT values were close to reaching this threshold. In light of this and the highly outlying electrophysiological measurements recorded for this mouse **(see Table 6)**, a decision was made to exclude it from the study. Although several other mice showed ΔCT

values that were also approaching the threshold of differing by more than 2 standard deviations from the plate mean (highlighted in light grey), the electrophysiological recordings made for these mice were not outlying **(see Table 6)** and therefore they were not excluded from the study.

Plate 1			Plate 2			Plate 3		
Mouse no.	ΔCT	Mean ΔCT - ΔCT	Mouse no.	ΔCT	Mean ΔCT - ΔCT	Mouse no.	ΔCT	Mean ΔCT – ΔCT
SOD1 302	**10.50**	**0.90**	**SOD1 302**	**7.14**	**0.79**	SOD1 334	8.74	0.07
SOD1 321	**10.80**	**0.60**	**SOD1 321**	**7.53**	**0.40**	SOD1 339	8.73	0.08
SOD1 304	11.36	0.04	SOD1 368	7.79	0.14	SOD1 371	8.34	0.47
SOD1 303	11.27	0.13	SOD1 370	7.87	0.06	SOD1 333	8.44	0.37
SOD1 309	11.58	-0.18	SOD1 350	8.14	-0.21	SOD1 356	8.77	0.04
SOD1 312	11.21	0.19	SOD1 353	8.07	-0.14	SOD1 358	8.54	0.27
SOD1 299	11.57	-0.17	SOD1 348	7.88	0.05	SOD1 145	8.30	0.51
SOD1 315	12.04	-0.64	SOD1 157	8.01	-0.08	SOD1 161	8.73	0.08
SOD1 316	11.33	0.07	SOD1 175	7.52	0.41	SOD1 162	9.16	-0.35
SOD1 318	11.74	-0.34	SOD1 176	7.91	0.02	SOD1 164	8.62	0.19
SOD1 319	11.51	-0.11	SOD1 179	7.74	0.19	SOD1 172	9.16	-0.35
SOD1 308	11.52	-0.12	SOD1 182	8.14	-0.21	SOD1 191	8.89	-0.08
SOD1 323	11.72	-0.32	SOD1 187	7.91	0.02	SOD1 203	9.36	-0.55
SOD1 324	11.38	0.02	SOD1 206	8.12	-0.19	SOD1 205	9.08	-0.27
			SOD1 241	8.08	-0.15	SOD1 208	9.19	-0.38
			SOD1 242	8.27	-0.34	SOD1 143	9.06	-0.25
			SOD1 244	8.26	-0.33	SOD1 140	8.80	0.01
			SOD1 169	8.26	-0.33	SOD1 156	8.71	0.10
			SOD1 190	8.12	-0.19			
Mean ΔCT	**11.40**			**7.93**			**8.81**	
SDEV	**0.39**			**0.29**			**0.31**	
2x SDEV	**0.77**			**0.59**			**0.61**	

Table 5: Summary of Δ CT values obtained for SOD1^{G93A} mice in metformin electrophysiology study

SOD1^{G93A} mice enrolled in the metformin electrophysiology study were analysed for potential variations in transgene copy number across 3 separate Q-PCR plates. Brilliant® SYBR Green QPCR Master Mix reagent (Stratagene) was used for plate 1 whereas the more sensitive Brilliant® II SYBR Green QPCR Master Mix reagent (Stratagene) was used for plate 2. If the ΔCT value for a particular mouse differed by more than 2 standard deviations (SDEV) from the mean ΔCT value for all other mice analysed in the same plate, it was considered to have experienced a copy number change and was excluded from the study. SOD1^{G93A} mice 302 and 321 (highlighted in dark grey) displayed outlying electrophysiological characteristics **(see Table 6)** and were suspected to have lost copies of the transgene. They were therefore analysed on two occasions. Although mouse no. 321 did not have ΔCT values that differed by more than 2 standard deviations from the means for the individual plates, it was close to reaching this threshold and was therefore excluded from the study on the basis of its outlying electrophysiological measurements. Mice highlighted in light grey also had ΔCT values approaching this threshold but were not excluded as they did not display outlying electrophysiological results **(see Table 6).**

A.

SOD1 Males							SOD1 females						
Mouse no.	TA tetanic tension (N)	TA specific force N/cm2	EDL tetanic tension (N)	EDL specific force N/cm2	EDL MU	TA MU	Mouse no.	TA tetanic tension (N)	TA specific force N/cm2	EDL tetanic tension (N)	EDL specific force N/cm2	EDL MU	TA MU
145	0.25	5.65	0.12	8.53	N/A	N/A	143	0.33	8.11	0.18	15.13	N/A	N/A
161	0.41	8.35	0.14	12.03	N/A	N/A	140	0.23	6.03	0.13	11.67	N/A	N/A
162	0.50	9.46	0.21	12.07	N/A	N/A	144	0.49	16.32	0.22	28.45	N/A	N/A
164	0.59	12.44	0.25	14.28	N/A	N/A	156	0.07	2.22	0.05	5.08	N/A	N/A
169	0.10	3.01	0.06	4.42	10	10	157	0.20	6.07	0.18	14.43	N/A	N/A
172	0.14	3.72	0.06	4.32	12	12	175	0.22	8.56	0.10	7.47	14	13
190	0.52	9.55	0.28	15.98	17	23	176	0.29	9.47	0.25	19.09	11	17
191	0.58	12.72	0.25	15.12	20	21	179	0.26	9.76	0.16	13.77	14	13
203	0.22	5.95	0.19	12.48	10	14	182	0.22	7.31	0.15	12.45	15	11
205	0.14	4.61	0.19	15.21	11	18	187	0.40	10.53	0.16	12.93	17	13
208	0.37	9.49	0.15	10.94	20	14	206	0.38	10.27	0.24	15.45	27	21

B.

Metformin-treated SOD1G93A males							Metformin-treated SOD1G93A females						
Mouse no.	TA tetanic tension (N)	TA specific force N/cm2	EDL tetanic tension (N)	EDL specific force N/cm2	EDL MU	TA MU	Mouse no.	TA tetanic tension (N)	TA specific force N/cm2	EDL tetanic tension (N)	EDL specific force N/cm2	EDL MU	TA MU
304	0.27	8.11	0.16	11.54	15	11	299	0.29	8.87	0.24	17.04	23	26
303	0.07	2.28	0.09	7.71	24	11	315	0.25	7.16	0.11	11.42	21	18
302	0.81	15.42	0.51	22.56	N/A	N/A	316	0.10	3.65	0.10	8.60	17	21
321	1.55	24.63	0.51	27.75	36	26	318	0.25	9.39	0.14	16.57	14	15
309	0.14	3.58	0.12	10.34	22	13	319	0.14	5.58	0.08	8.97	16	22
312	0.41	10.34	0.26	15.86	29	30	308	0.10	3.40	0.10	8.44	23	14
334	0.57	12.22	0.17	11.49	19	27	323	0.09	3.14	0.17	15.19	26	29
339	0.69	13.25	0.19	10.51	20	8	324	0.40	11.64	0.07	5.60	24	18
371	0.49	11.36	0.20	15.23	34	37	325	0.61	22.22	N/A	N/A	14	22
368	0.77	22.87	0.34	23.64	34	31	333	0.37	10.57	0.14	11.27	29	31
370	0.22	7.08	0.08	7.44	20	16	356	0.44	10.73	0.20	16.12	21	20
							358	0.46	12.19	0.31	20.88	36	25
							350	0.57	17.54	0.16	15.56	22	26
							353	0.06	2.76	0.08	9.63	18	14
							348	0.36	15.56	0.16	19.50	29	17

Table 6 A & B: Summary of results obtained for electrophysiological analysis of (A) control and (B) metformin-treated SOD1^{G93A} TA and EDL muscles at 100 days of age

Mice highlighted in dark grey (302 and 321) performed better than all others in electrophysiological assessments and were suspected to have lost copies of the transgene. Mice highlighted in light grey, did not show outlying characteristics in electrophysiological assessments but had ΔCT values that were close to differing by 2 standard deviations from the mean ΔCT value of mice analysed for potential copy number variations in the same Q-PCR setup. Mice highlighted in dark grey (302 and 321) were excluded from the study whereas all other mice were included. (N/A= not available, MU=motor units)

3.3.2 The effect of metformin treatment on the weights of SOD1^{G93A} and WT mice between 55 and 99 days of age.

Once the study was underway, a decision was made to weigh mice in all groups approximately every 5 days in order to allow monitoring of their general health and also to gain insight into the effect of metformin treatment on bodyweight. Unfortunately, deciding to collect weight data part way through the study meant that this data was not collected from some of the first mice enrolled in the study. Additionally, in order to be able to perform *in vivo* electrophysiology on large numbers of mice at the same age point, it was not possible to use large cohorts of animals with the same birth dates. For this reason, individual mice could not always be weighed at exactly the same age points as their counterparts. It was therefore necessary to group weight data into 5-day age brackets when performing averaging for graphical representation. In this averaging process, some age brackets had more data values than others, depending on how many mice were weighed at ages that fell into those brackets. The number of mice used to collect data for each age bracket was always 4 or more. In light of the variation in n-numbers from one time point to the next, weight data presented here can only be used as qualitative guide of the effect of metformin treatment on the weight of male and female SOD1^{G93A} and WT mice rather than a quantitative data set that robust statistical analyses can be performed on.

The weights of control SOD1^{G93A} and WT mice between 55 and 99 days of age are summarized in **Figure 3**.Within the timeframe studied, SOD1^{G93A} female mice, as would be expected, did not put on weight at as quickly as WT female mice **(Figure 3).** SOD1^{G93A} male mice put on weight at a similar rate to WT males until 95-99 days when WT mice showed a more rapid increase in weight. The effects of metformin treatment on the weights of

SOD1^{G93A} and WT mice between 55 and 99 days of age are presented in **Figures 4 and 5** respectively. Metformin was observed to have no effect on weight in SOD1^{G93A} female **(Figure 4)** or WT male mice **(Figure 5)** but appeared to bring about decreased weight in metformin treated male SOD1^{G93A} mice **(Figure 4)** and increased weight in WT female mice throughout the period studied **(Figure 5)**.

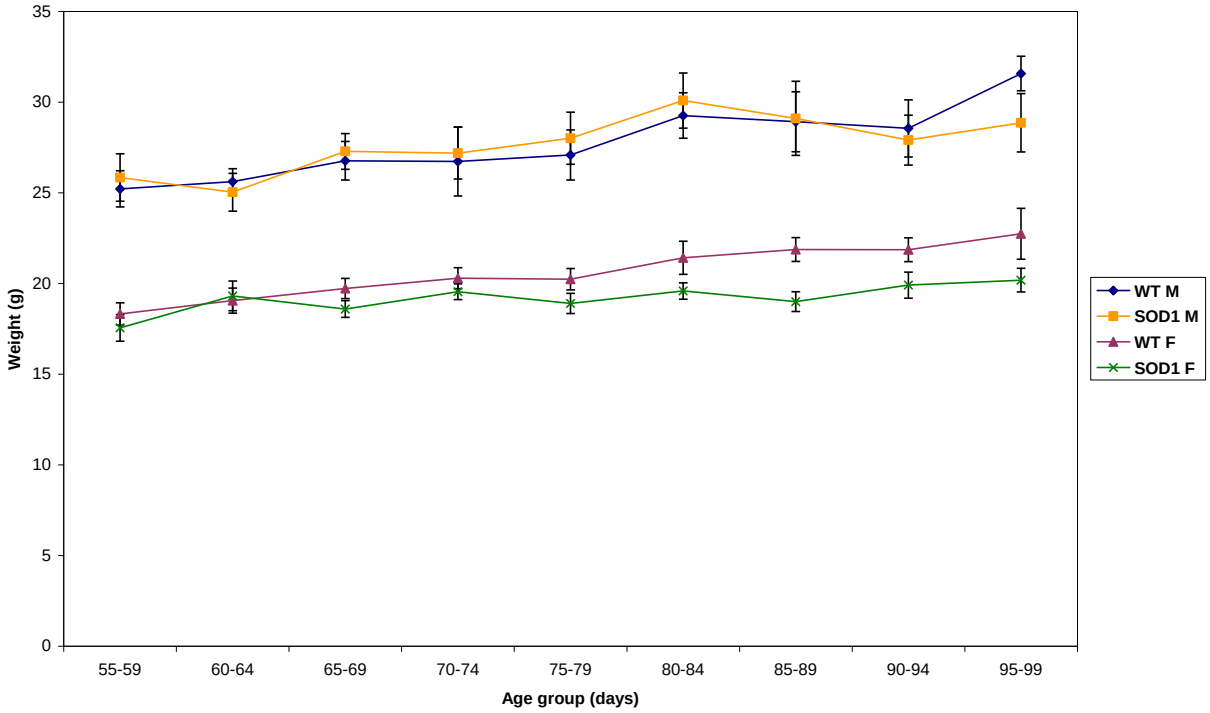


Figure 3: Comparison of the weights of WT and SOD1^{G93A} mice between 55 and 99 days of age.

Male SOD1^{G93A} mice put on weight at a similar rate to male WT mice until 95-99 days when WT males showed a large increase in weight that was not matched by their male SOD1^{G93A} counterparts. Female SOD1^{G93A} mice began to show a lower weight compared to WT females from 75-79 days onwards, an earlier time point than the SOD1^{G93A} males. Error bars represent SEM, WT M (WT males)-minimum n=4, SOD1 M (SOD1^{G93A} males)-minimum n=4, WT F (WT females)-minimum n=5, SOD1 F (SOD1^{G93A} females)-minimum n=4. Although only minimum n- numbers for each group are displayed, n-numbers for female mice were on average ~two fold higher than for male mice, as is shown by the female weight curves being smoother than those of the males.

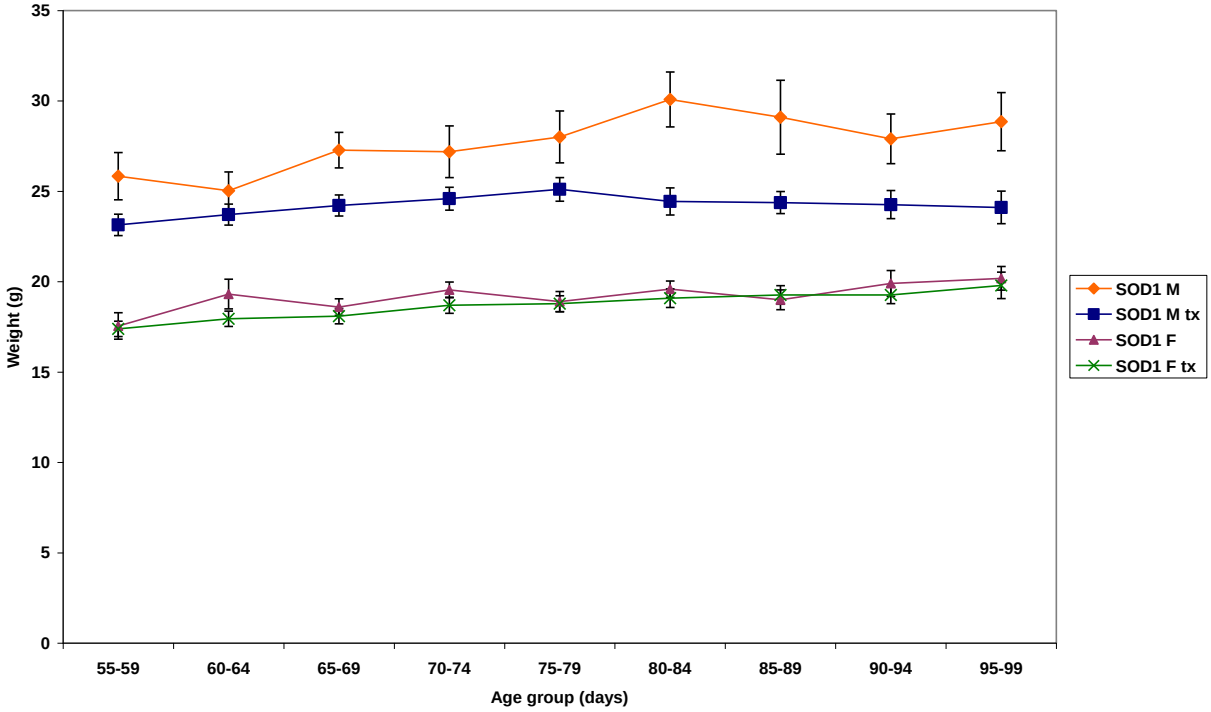


Figure 4: The effect of metformin treatment on the weight of SOD1^{G93A} mice between 55 and 99 days of age.

Male SOD1^{G93A} mice treated with metformin were lighter than their untreated counterparts throughout the time period studied, with the exception of the period between 60 and 64 days when there was no obvious difference between metformin treated and untreated male SOD1 mice (although this could be an artifact of n-number in this time bracket or the time of day at which the mice were weighed with respect to eating/drinking times). Metformin treatment had no effect on the weight of female SOD1^{G93A} mice thought the period investigated. Error bars represent SEM, SOD1 M (SOD1^{G93A} males)-minimum n=4, SOD1 M tx (metformin treated SOD1^{G93A} males)-minimum n=13, SOD F (SOD1^{G93A} females)-minimum n=5, SOD1 F tx (metformin treated SOD1^{G93A} females)-minimum n=7. Although only minimum n-numbers for each group are displayed, n-numbers for all female mice and metformin treated SOD1^{G93A} male mice were on average at least two fold higher than for untreated SOD1^{G93A} male mice, as is shown by the SOD1^{G93A} male weight curve being less smooth than the other weight curves.

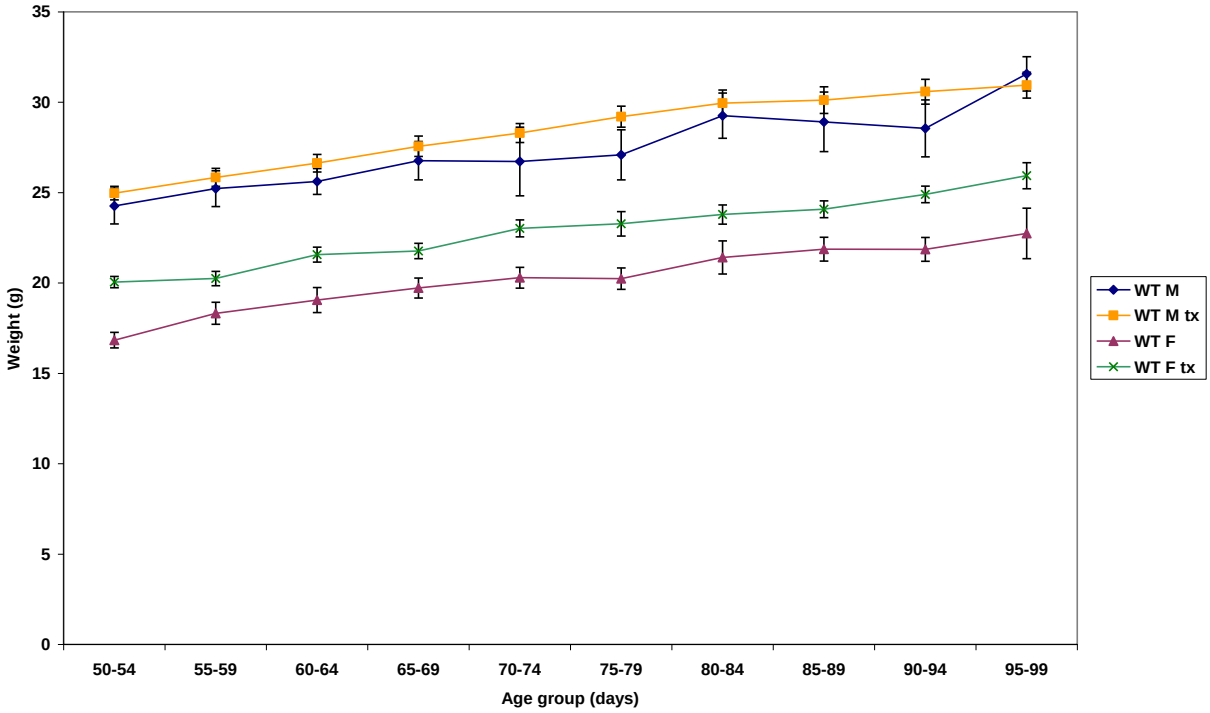


Figure 5: The effect of metformin treatment on the weight of WT mice between 55 and 99 days of age.

Metformin treatment caused an increase in the weight of female WT mice compared to their untreated counterparts throughout the time period investigated. There was a minor trend towards metformin-treated WT males being heavier than their untreated counterparts, but this was not as pronounced as for the females. Error bars represent SEM, WT M (WT males)-minimum n=4, WT M tx (metformin treated WT males)-minimum n=16, WT F (WT females)-minimum n=5, WT F tx (metformin treated WT females)-minimum n=7. Although only minimum n- numbers for each group are displayed, n-numbers for all female mice and metformin treated WT male mice were on average at least two fold higher than for untreated WT male mice, as is shown by the WT male weight curve being less smooth than the other weight curves.

3.3.3 Functional motor unit measurements

Estimation of the number of functional motor units (MUs) in the TA and EDL muscles of experimental animals at 100 days of age was carried out by counting the number of stepwise increments in twitch force produced in each muscle by stimulation of the deep peroneal nerve with pulses of increasing intensity. Motor unit counting was performed in a blinded fashion.

3.3.3.1 $SOD1^{G93A}$ EDL muscles have significantly fewer motor units than their WT counterparts at 100 days.

The ultimate cause of death in SOD1 mice is the occurrence of pathological processes in their motor neurons that lead to the malfunctioning and retraction of their distal motor axons and therefore denervation (Gould et al., 2006). In accordance with this we saw a significant loss of functional motor units in $SOD1^{G93A}$ male (M) EDL muscles compared to WT male EDL muscles at 100 days of age (14 +/- 2 MUs $SOD1^{G93A}$ M vs. 54 +/- 4 MUs WT M, $P < 0.001$) **(Figures 6 and 7)**. We also saw a significant loss of functional motor units in $SOD1^{G93A}$ female (F) EDL muscles compared to WT female EDL muscles at 100 days of age (16 +/- 2 MUs $SOD1^{G93A}$ F vs. 47 +/- 4 MUs WT F, $P < 0.0002$) **(Figure 7)**.

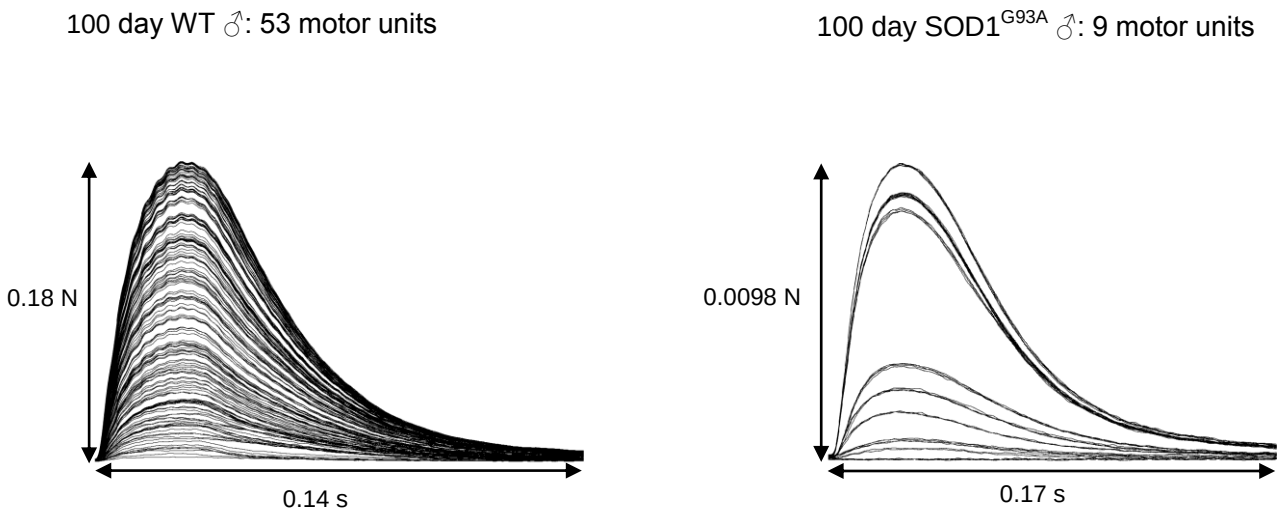


Figure 6: Typical traces recorded for motor unit assessment protocol in WT and SOD1^{G93A} male EDL muscles at 100 days of age.

Estimation of the number of functional motor units (MUs) in the TA and EDL muscles of experimental animals at 100 days of age was carried out by counting the number of stepwise increments in twitch force produced in each muscle by stimulation of the deep peroneal nerve with pulses of increasing intensity (from 0-4V). This figure shows typical twitch-force traces produced in the motor unit assessment protocol for WT and SOD1^{G93A} male EDL muscles at 100 days of age and highlights the significantly reduced numbers of functional motor units present in SOD1^{G93A} EDL muscles at 100 days of age compared to WT.

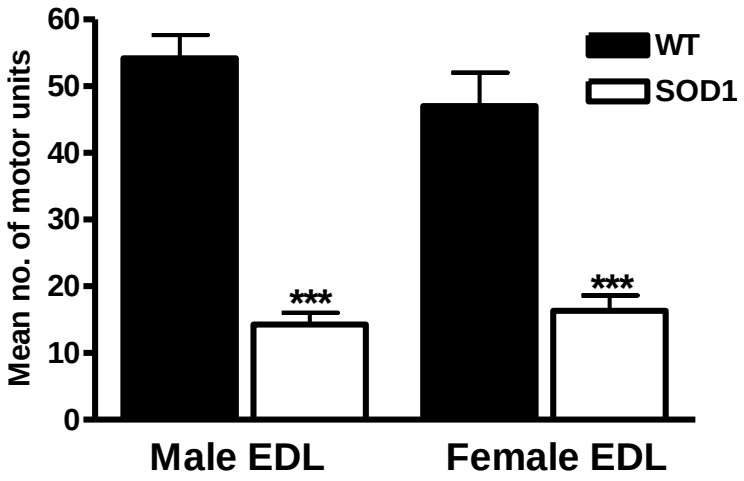


Figure 7: Comparison of the number of functional motor units in the EDL muscles of SOD1^{G93A} mice and WT mice at 100 days.

Determination of the number of functional motor units in the EDL muscles of SOD1^{G93A} (SOD1) and WT mice via *in vivo* electrophysiology, revealed significantly lower numbers of remaining motor units in the EDL muscles of both SOD1^{G93A} male mice and SOD1^{G93A} female mice compared to their WT counterparts at 100 days of age. n=7 SOD1^{G93A} males, n=6 SOD1^{G93A} females, n=6 WT males, n=5 WT females, error bars represent SEM, (SOD1^{G93A} M vs. WT M, $P < 0.0001$ (***)), (SOD1^{G93A} F vs. WT F, $P < 0.0002$ (***)).

3.3.3.2 Metformin treatment brought about a significant preservation of motor units in SOD1^{G93A} male EDL muscles and SOD1^{G93A} female TA muscles.

Measurement of the number of remaining functional motor units in the right TA and EDL muscles of metformin treated and untreated SOD1^{G93A} mice at 100 days of age revealed a significant preservation of functional motor units in the EDL muscles of metformin treated male SOD1^{G93A} mice compared to their untreated counterparts (24 +/- 2 MUs SOD1^{G93A} tx M vs. 14 +/- 2 SOD1^{G93A} M, $p<0.005$) **(Figures 8 and 9)** and an almost significant preservation of functional motor units in the EDL muscles of metformin treated female SOD1^{G93A} mice compared to their untreated counterparts (22 +/- 2 MUs SOD1^{G93A} tx F vs. 16 +/- 2 SOD1^{G93A} F. P = 0.056) **(Figure 9)**. A significant preservation of functional motor units was also seen in the TA muscles of metformin-treated female SOD1^{G93A} mice compared to untreated female SOD1^{G93A} mice (21 +/- 1 MUs SOD1 tx F vs. 15 +/- 2 SOD1^{G93A} F, P = 0.0134) (**Figure 10)** and although there was a strong trend towards the preservation of functional motor units in the TA muscles of metformin-treated male mice compared to untreated male mice (20 +/- 4 MUs SOD1^{G93A} tx M vs. 16 +/- 2 SOD1^{G93A} M), this did not reach significance **(Figure 10)**.

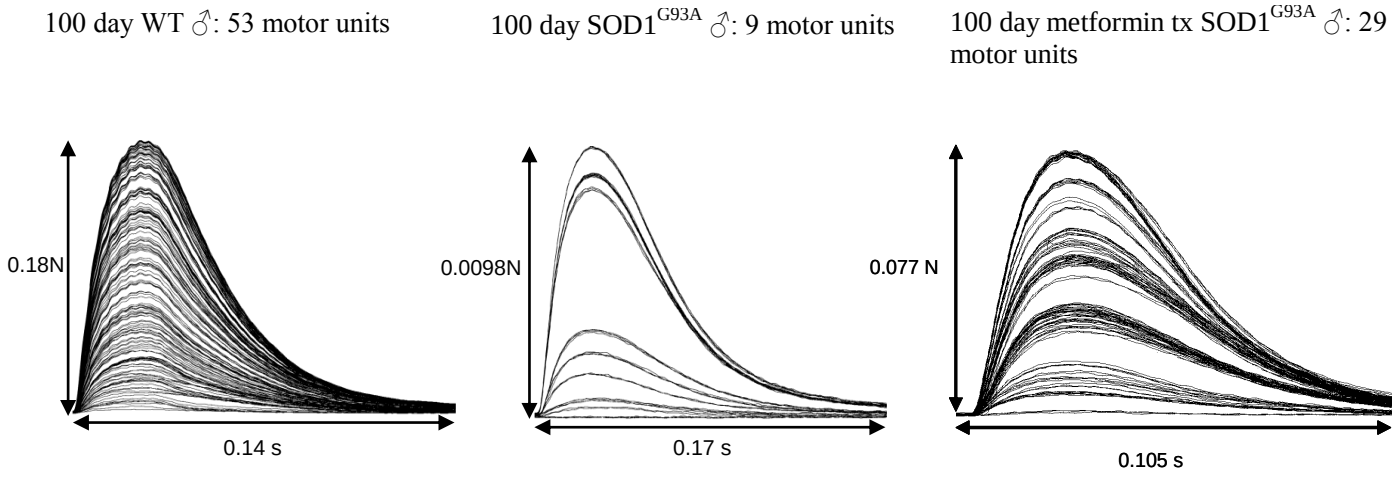


Figure 8: Typical traces recorded for motor unit assessment protocol in WT and metformin treated and untreated SOD1^{G93A} male EDL muscles at 100 days of age.

Estimation of the number of functional motor units (MUs) in the TA and EDL muscles of experimental animals at 100 days of age was carried out by counting the number of stepwise increments in twitch force produced in each muscle by stimulation of the deep peroneal nerve with pulses of increasing intensity (from 0-4V). This figure shows typical twitch-force traces produced in the motor unit assessment protocol for WT, untreated SOD1^{G93A} and metformin treated (tx) SOD1^{G93A} male EDL muscles at 100 days of age (Note that the WT and untreated SOD1^{G93A} traces shown in this figure are the same traces as shown in Figure 3.4). This figure highlights the significantly increased numbers of functional motor units present in metformin treated male SOD1^{G9A} EDL muscles at 100 days of age compared to their untreated counterparts.

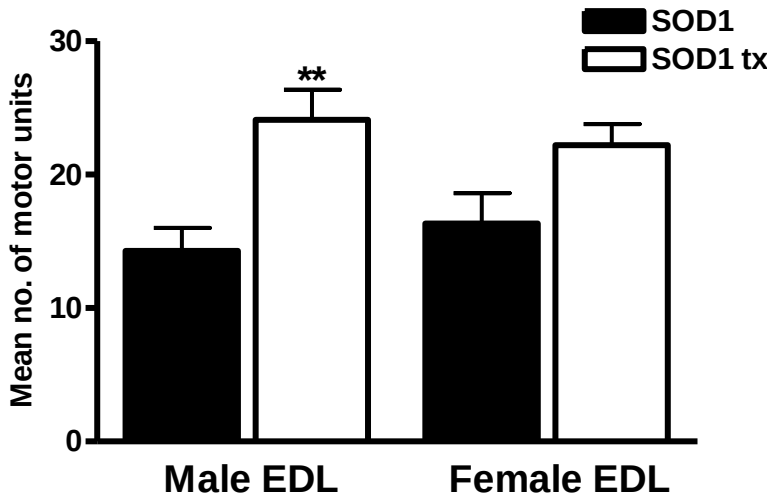


Figure 9: Comparison of the number of functional motor units in the EDL muscles of metformin treated and untreated SOD1^{G93A} mice at 100 days.

Determination of the number of functional motor units in the right EDL muscles of metformin treated (SOD1 tx) and untreated (SOD1) SOD1^{G93A} mice via *in vivo* electrophysiology, revealed a significant preservation of functional motor units in the EDL muscles of metformin treated male SOD1^{G93A} mice compared to untreated male SOD1^{G93A} mice and an almost significant preservation of functional motor units in the EDL muscles of metformin treated female SOD1^{G93A} mice compared to untreated female SOD1^{G93A} mice. n=7 SOD1^{G93A} males, n=6 SOD1^{G93A} females, n=9 metformin treated SOD1^{G93A} males and n=15 metformin treated SOD1^{G93A} females, error bars represent SEM, (SOD1^{G93A} M vs. SOD1^{G93A} tx M, P = 0.005 (**)), (SOD1^{G93A} F vs. SOD1^{G93A} tx F, P = 0.056).

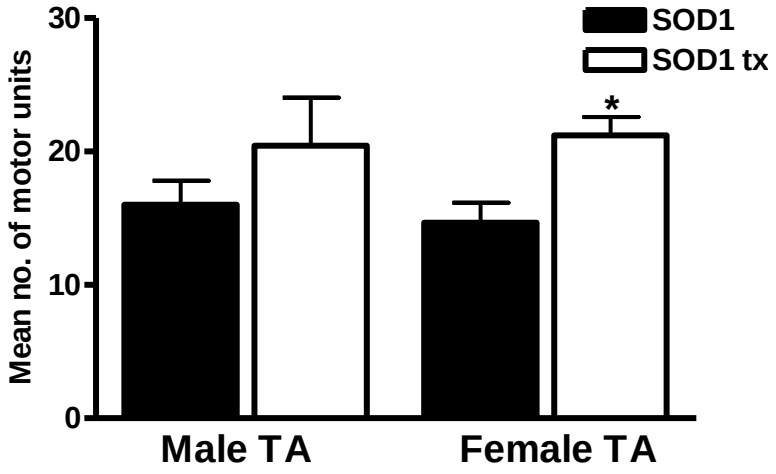


Figure 10: Comparison of the number of functional motor units in the TA muscles of metformin treated and untreated SOD1^{G93A} mice at 100 days.

Determination of the number of functional motor units in the right TA muscles of metformin treated (SOD1 tx) and untreated (SOD1) SOD1^{G93A} mice via *in vivo* electrophysiology, revealed a significant preservation of functional motor units in the TA muscles of metformin treated female SOD1^{G93A} mice compared to untreated female SOD1^{G93A} mice. There was a trend towards motor neuron preservation in the TA muscles of metformin treated male SOD1^{G93A} mice compared to untreated male SOD1^{G93A} mice but this was not significant. n=7 SOD1^{G93A} males, n=6 SOD1^{G93A} females, n=9 metformin treated SOD1^{G93A} males and n=15 metformin treated SOD1^{G93A} females, error bars represent SEM, (SOD1^{G93A} F vs. SOD1^{G93A} tx F, P = 0.0134 (*))

3.3.3.3 Metformin treatment did not affect motor unit number in WT mice.

As expected, metformin treatment did not have a significant effect on the number of functional motor units present in the EDL muscles of WT mice at 100 days of age **(Figure 11)**. The average number of motor units measured for metformin treated and untreated WT mice were as follows:

WT male: 54 +/- 4 MUs

Metformin treated WT male: 61 +/- 4 MUs

WT Female: 47 +/- 4 MUs

Metformin treated WT female: 53 +/- 6 MUs

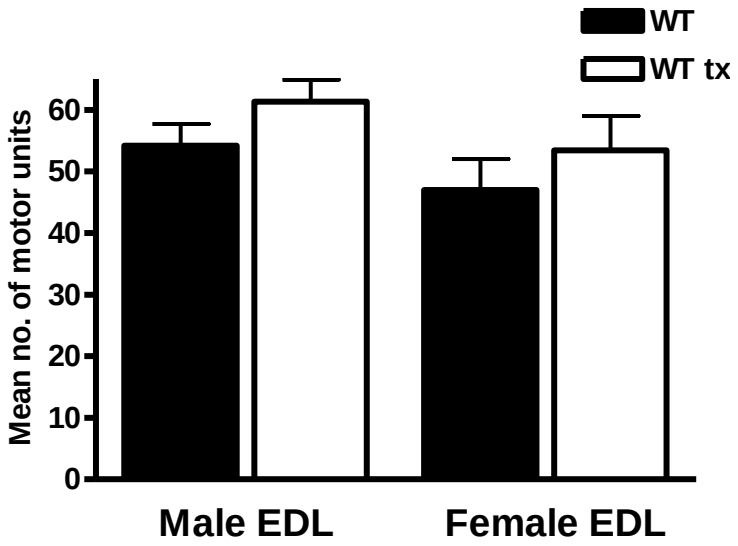


Figure 11: Comparison of the number of functional motor units in the EDL muscles of metformin-treated and untreated WT mice at 100 days.

Determination of the number of functional motor units in the right EDL muscles of metformin treated (WT tx) and untreated (WT) WT mice via *in vivo* electrophysiology, revealed no significant effect of metformin treatment on the number of functional motor units in the EDL muscles of WT male or WT female mice. n=6 WT males, n=5 WT females, n=6 metformin treated WT males and n=7 metformin treated WT females, error bars represent SEM.

3.3.4 Maximal force and specific force measurements

3.3.4.1 The TA and EDL muscles of SOD1^{G93A} mice are significantly weaker than those of WT mice at 100 days.

The denervation of muscles that occurs in SOD1^{G93A} pathology, leads to progressive muscle atrophy and therefore loss of muscle strength. In accordance with this we observed a significant reduction in both the maximal **(Figures 12A and 12B)** and specific forces (**Figure 13)** of both SOD1^{G93A} male and SOD1^{G93A} female TA and EDL muscles compared to WT at 100 days of age. Mean maximum force and specific force values for all muscles measured are summarised in **Table 7** ($P<0.0001$ for male TAs, male EDLs and female TAs when comparing maximal forces of SOD1^{G93A} mice to WT mice, $P<0.0002$ for female EDLs when comparing maximal forces of SOD1^{G93A} mice to WT mice, $P<0.0001$ for male TAs, male EDLs and female TAs when comparing specific forces of WT mice to SOD1^{G93A} mice and $P<0.05$ for female EDLs when comparing specific forces of WT mice to SOD1^{G93A} mice). Interestingly, the loss of maximal force **(Figures 12A and 12B)** and specific force **(Figure 13)** in both male and female SOD1^{G93A} mice compared to WT mice was more pronounced in the TA muscles than the EDL muscles. Indeed, the percentage loss of maximal force in SOD1^{G93A} male TA muscles compared to WT was ~20% higher than in their EDL muscles and the percentage loss of maximal force in SOD1^{G93A} female TA muscles compared to WT was ~ 32% higher than in their EDL muscles. Likewise, the percentage loss of specific force in SOD1^{G93A} male TA muscles compared to WT was ~25% higher than in their EDL muscles and the percentage loss of specific force in SOD1^{G93A} female TA muscles compared to WT was ~ 35% higher than in their EDL muscles. Finally no significant differences were found when comparing the specific forces of male and female WT TA muscles, male and female

WT EDL muscles, male and female SOD1^{G93A} TA muscles or male and female SOD1^{G93A} EDL muscles.

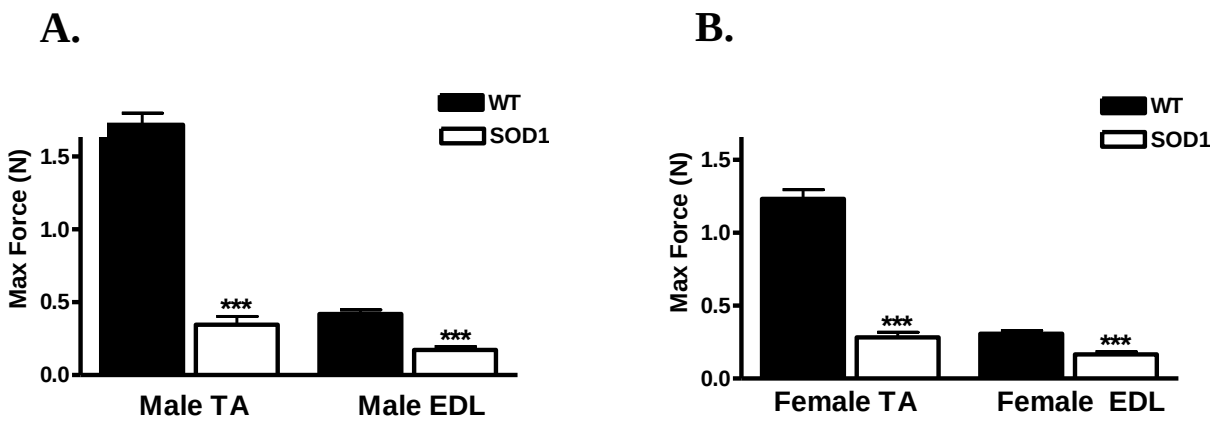


Figure 12: Comparison of the maximal forces of the right TA and EDL muscles of (A) male and (B) female, WT and SOD1^{G93A} mice at 100 days of age.

Determination of the maximal forces of the right TA and EDL muscles of WT and SOD1^{G93A} (SOD1) mice at 100 days of age via *in vivo* electrophysiology revealed that both SOD1^{G93A} male and SOD1^{G93A} female mice have significantly weaker TA and EDL muscles than their WT counterparts at 100 days of age. n=11 SOD1^{G93A} males, n=11 SOD1^{G93A} females, n=6 WT males, n=6 WT females, error bars represent SEM. ($P<0.0001$ (***) for male TA, male EDL and female TA when comparing WT to SOD1^{G93A}), ($P<0.0002$ (***) for female EDL when comparing WT to SOD1^{G93A}).

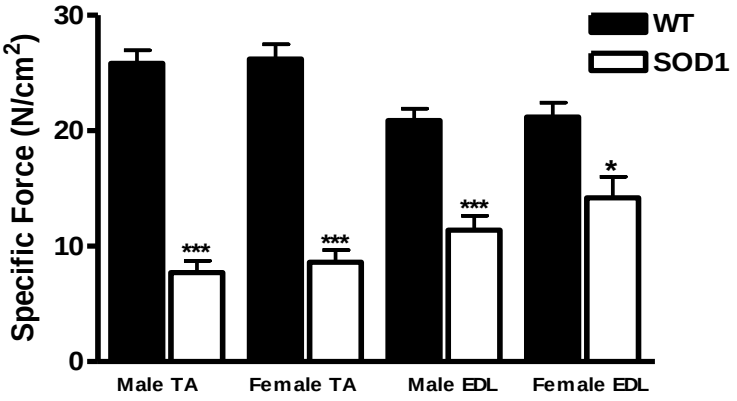


Figure 13: Comparison of the specific forces of the right TA and EDL muscles of WT and SOD1^{G93A} mice at 100 days of age.

Determination of the specific forces of the right TA and EDL muscles of WT and SOD1^{G93A} (SOD1) mice at 100 days of age via *in vivo* electrophysiology, revealed that both SOD1^{G93A} male and SOD1^{G93A} female TA and EDL muscles produce a significantly weaker force per unit cross-sectional area than the TA and EDL muscles of their WT counterparts at this time point. There were no significant differences between the specific forces of WT male and female TA muscles, WT male and female EDL muscles, SOD1^{G93A} male and female TA muscles and SOD1^{G93A} male and female EDL muscles at this time-point. Statistical analyses were performed via a one-way ANOVA with post-hoc Bonferroni tests. n=11 SOD1^{G93A} males, n=11 SOD1^{G93A} females, n=6 WT males, n=6 WT females, error bars represent SEM. ($P<0.0001$ (***) for male TA, male EDL and female TA when comparing WT to SOD1^{G93A}), ($P<0.05$ (*) for female EDL when comparing WT to SOD1^{G93A}). Specific force was calculated by dividing the maximal force of each muscle by its cross sectional area.

Treatment Group	Mean TA max force (N) + SEM	Mean TA specific force (N/cm^2) + SEM	Mean EDL max force (N) + SEM	Mean EDL specific force (N/cm^2) + SEM
WT M	1.7 +/- 0.082	25.84 +/- 1.12	0.42 +/- 0.028	20.88 +/- 1.04
WT F	1.23 +/- 0.064	26.22 +/- 1.26	0.31 +/- 0.022	21.19 +/- 1.25
SOD1 M	0.35 +/- 0.055	7.72 +/- 1.01	0.17 +/- 0.022	11.40 +/- 1.23
SOD1 F	0.28 +/- 0.035	8.60 +/- 1.06	0.17 +/- 0.018	14.18 +/- 1.83
Metformin-treated SOD1 M	0.40 +/- 0.083	10.12 +/- 2.03	0.18 +/- 0.028	12.64 +/- 1.67
Metformin-treated SOD1 F	0.30 +/- 0.046	9.63 +/- 1.47	0.15 +/- 0.018	13.20 +/- 1.25
Metformin-treated WT M	1.65 +/- 0.042	26.69 +/- 1.07	0.45 +/- 0.0088	24.19 +/- 1.17
Metformin-treated WT F	1.42 +/- 0.085	27.51 +/- 1.26	0.41 +/- 0.025	27.82 +/- 1.23

Table 7: Summary of the mean maximum and specific force values measured for metformin-treated and control WT and $SOD1^{G93A}$ (SOD1) TA and EDL muscles, via in vivo electrophysiology.

M = Male, F = Female

3.3.4.2 Metformin treatment did not increase the maximal or specific forces of SOD1^{G93A} - TA and EDL muscles.

Despite the significant preservation of functional motor units observed in SOD1^{G93A} male EDL muscles and SOD1^{G93A} female TA muscles with metformin treatment, there were no significant improvements in the maximal forces **(Figures 14A and 14B)** nor specific forces **(Figure 15)** of metformin treated SOD1^{G93A} male or female muscles compared to the muscles of untreated SOD1^{G93A} mice at 100 days of age. The mean maximum forces and specific forces of the TA and EDL muscles of metformin-treated and control SOD1^{G93A} mice are summarised in **Table 7**.

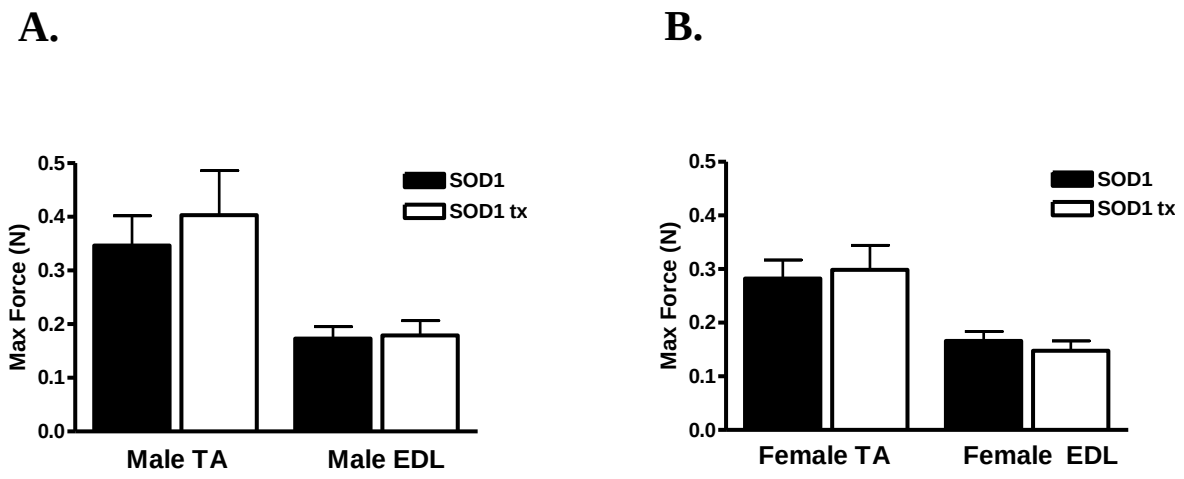


Figure 14: Comparison of the maximal forces of the right TA and EDL muscles of (A) male and (B) female metformin-treated and control SOD1^{G93A} mice at 100 days of age.

Determination of the maximal forces of the right TA and EDL muscles of metformin-treated (SOD1 tx) and control (SOD1) SOD1^{G93A} mice at 100 days of age via *in vivo* electrophysiology revealed that metformin treatment had no significant effect on the maximal forces of SOD1^{G93A} male or female TA or EDL muscles at the dose investigated. n=11 SOD1^{G93A} males, n=11 SOD1^{G93A} females, n=9 metformin treated SOD1^{G93A} males, n=14 metformin treated SOD1^{G93A} females, error bars represent SEM.

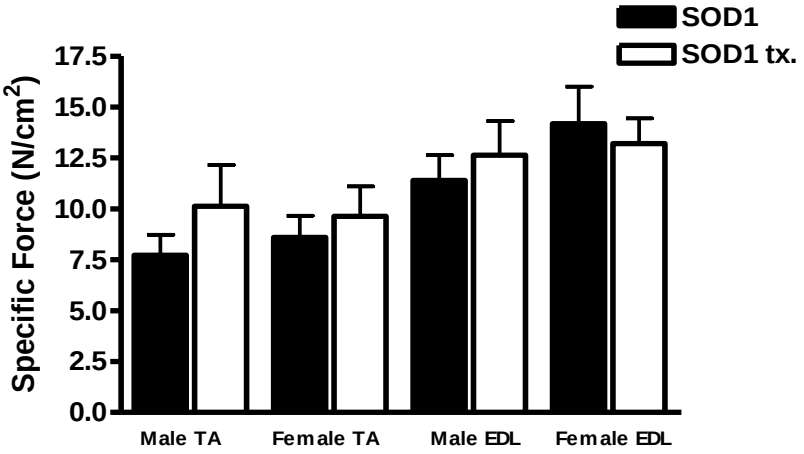


Figure 15: Comparison of the specific forces of the right TA and EDL muscles of metformin-treated and untreated SOD1^{G93A} mice at 100 days of age.

Determination of the specific forces of the right TA and EDL muscles of metformin-treated (SOD1 tx) and untreated (SOD1) SOD1^{G93A} mice at 100 days of age via *in vivo* electrophysiology, revealed that metformin treatment had no significant effect on the force per unit cross-sectional area of the TA and EDL muscles of SOD1^{G93A} mice at the dose investigated. n=11 SOD1^{G93A} males, n=11 SOD1^{G93A} females, n=9 metformin treated SOD1^{G93A} males, n=15 metformin treated SOD1^{G93A} female TA muscles, n=14 metformin treated SOD1^{G93A} female EDL muscles. Error bars represent SEM. Specific force was calculated by dividing the maximal force of each muscle by its cross sectional area.

3.3.4.3 Metformin treatment significantly increased the maximal and specific forces of WT female EDL but not TA muscles and had no effect on WT male muscles.

Metformin treatment had no effect on the maximal **(Figures 16A and 16B)** or specific forces **(Figure 17)** of WT male TA or EDL muscles at 100 days of age. It also had no effect on the maximal or specific forces of WT female TA muscles at this time point. Female WT mice treated with metformin however showed significantly increased maximal and specific forces in their EDL muscles (WT female EDL vs. metformin-treated WT female EDL, P = 0.0094). The mean maximum forces and specific forces of the TA and EDL muscles of metformin-treated and control WT mice are summarised in **Table 7**.

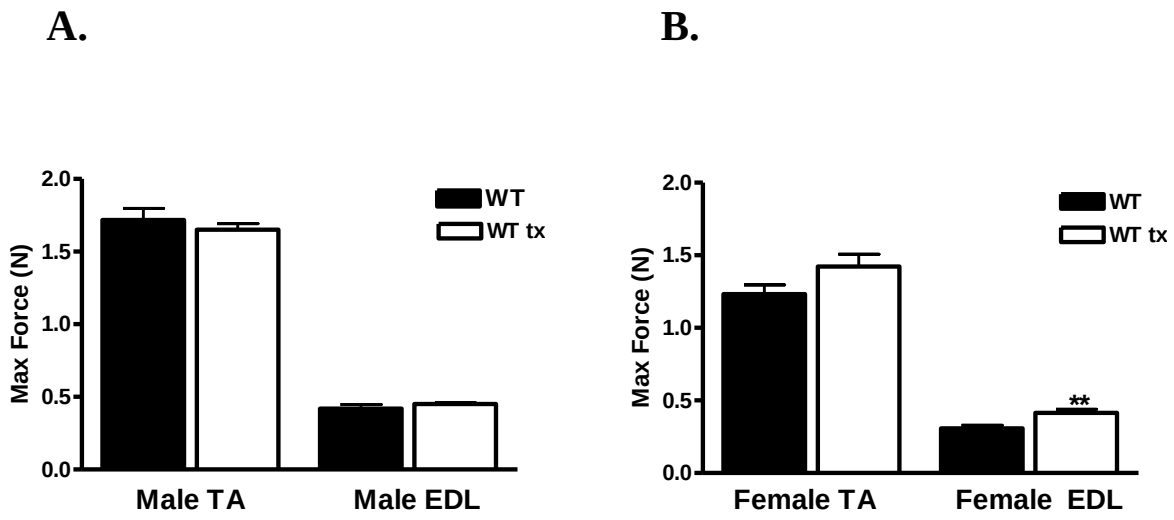


Figure 16: Comparison of the maximal forces of the right TA and EDL muscles of (A) male and (B) female metformin-treated and untreated WT mice at 100 days of age.

Determination of the maximal forces of the right TA and EDL muscles of metformin-treated (WT tx) and untreated (WT) WT mice at 100 days of age via *in vivo* electrophysiology revealed that metformin treatment had no significant effect on the maximal forces of male EDL and TA muscles or female TA muscles at the dose investigated. However, metformin treatment did bring about a significant increase in the maximal force of female EDL muscles . n=6 WT males, n=6 WT females, n=6 metformin treated WT males and n=7 metformin treated WT females, error bars represent SEM, (WT female EDL vs. metformin-treated WT female EDL, P = 0.0094 (**)).

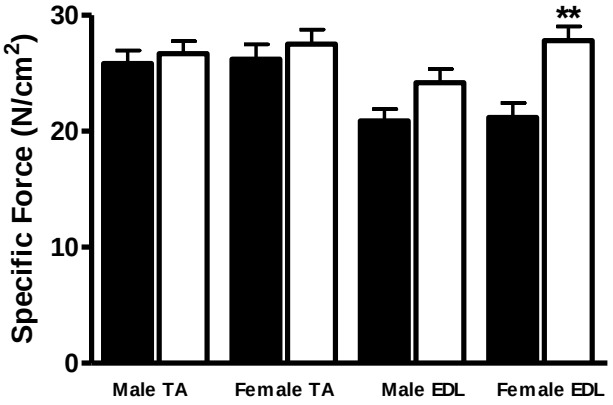


Figure 17: Comparison of the specific forces of the right TA and EDL muscles of metformin-treated and untreated WT mice at 100 days of age.

Determination of the specific forces of the right TA and EDL muscles of metformin-treated (WT tx) and untreated (WT) WT mice at 100 days of age via *in vivo* electrophysiology, revealed that metformin treatment had no significant effect on the maximal force per unit cross-sectional area of male EDL and TA muscles nor female TA muscles at the dose investigated. However, metformin treatment did bring about a significant increase in the maximal force per unit cross sectional area of female EDL muscles at the dose investigated. n=6 WT males, n=6 WT females, n=6 metformin treated WT males and n=7 metformin treated WT females, error bars represent SEM, (WT female EDL vs. metformin-treated WT female EDL, P = 0.0032 (**)). Specific force was calculated by dividing the maximal force of each muscle by its cross sectional area.

3.3.5 Muscle fatigability measurements

3.3.5.1 SOD1 EDL muscles are significantly more resistant to fatigue than WT EDL muscles at 100 days of age.

In SOD1 mice, large motor neurons innervating large motor units in fast twitch muscles are the first to undergo denervation and degenerate, whereas smaller motor neurons innervating small motor units in slow twitch muscles are more resistant to mutant SOD1-mediated toxicity and survive until the latter stages of the disease (Hegedus et al., 2007). This results in the muscles of SOD1G93A mice adopting a progressively slower, more fatigue resistant phenotype. In accordance with this, we observed a significant increase in the resistance to fatigue (represented by a higher fatigue index) of the right EDL muscles of both $SOD1^{G93A}$ male mice and $SOD1^{G93A}$ female mice compared to their WT counterparts at 100 days of age (0.4 +/- 0.06 $SOD1^{G93A}$ M vs. 0.17 +/- 0.04 WT M, P = 0.0174) (0.5 +/- 0.06 $SOD1^{G93A}$ F vs. 0.24 +/- 0.04 WT F, P = 0.0069) **(Figures 18 and 19)**.

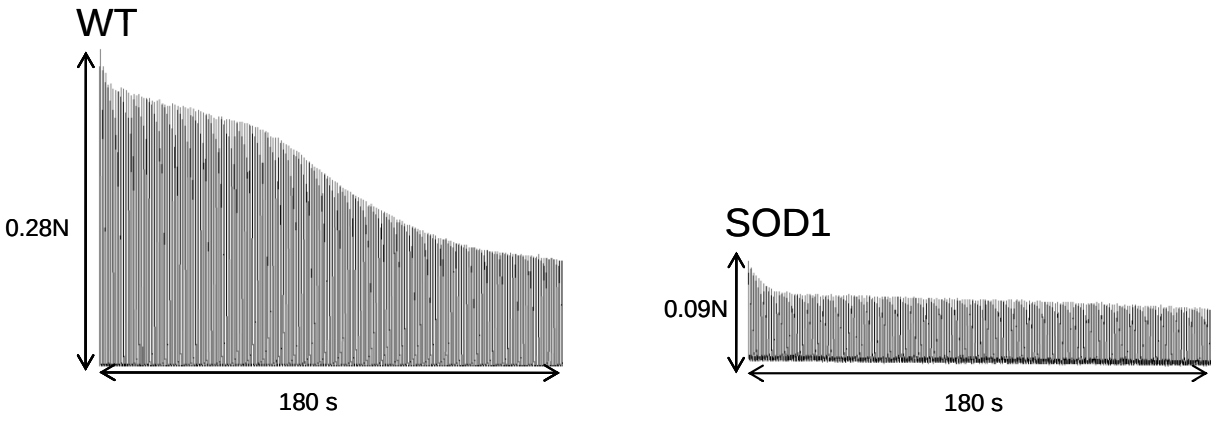


Figure 18: Typical fatigue traces for the EDL muscles of SOD1^{G93A} mice and WT mice at 100 days.

Fatigue traces were generated by stimulating the Deep Peroneal Nerve (DPN) at 40Hz for 250ms of every second for 3 minutes and digitally recording the forces of the resultant EDL contractions throughout the 3 minute period. This figure shows representative fatigue traces for the EDL muscles of male WT and SOD1^{G93A} (SOD1) mice at 100 days of age and highlights that SOD1^{G93A} mice are significantly more resistant to fatigue than their WT counterparts.

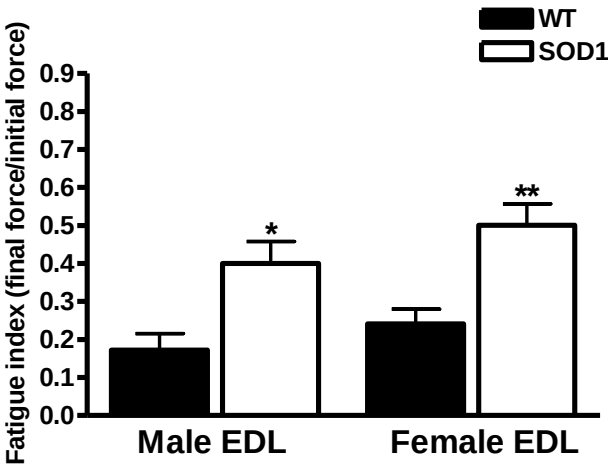


Figure 19: Comparison of the fatigue index of the right EDL muscles of SOD1^{G93A} mice and WT mice at 100 days.

The fatigue index of each muscle investigated was determined by stimulating the muscle at 40Hz for 250ms of every second for 3 minutes and then dividing the final force recorded by the initial force. Higher fatigue index values represent an increased resistance to fatigue. Calculation of the fatigue index for the EDL muscles of SOD1^{G93A} (SOD1) and WT mice revealed that the EDL muscles of both SOD1^{G93A} male mice and SOD^{G93A} female mice are significantly more resistant to fatigue than their WT counterparts at 100 days of age. n=11 SOD1^{G93A} males, n=11 SOD1^{G93A} females, n=6 WT males, n=6 WT females, error bars represent SEM. (SOD1^{G93A} Males vs. WT Males, P = 0.0174 (*)), (SOD1^{G93A} Females vs. WT Females, P = 0.0069 (**)).

3.3.5.2 Metformin treatment brought about a significant increase in the resistance to fatigue of male SOD1^{G93A} EDL muscles.

Metformin treatment significantly increased the resistance to fatigue (represented by a higher fatigue index) of SOD1^{G93A} male EDL muscles compared to untreated SOD1^{G93A} male EDL control muscles at the dose tested (0.77 +/- 0.09 metformin treated SOD1^{G93A} M vs. 0.40 +/- 0.09 SOD1^{G93A} M, P = 0.0019) **(Figure 20)**. Although there was a trend towards increased resistance to fatigue in female EDL muscles with metformin treatment, this was not significant (0.61 +/- 0.06 metformin treated SOD1^{G93A} F vs. 0.50 +/- 0.06 SOD1^{G93A} F) **(Figure 20)**.

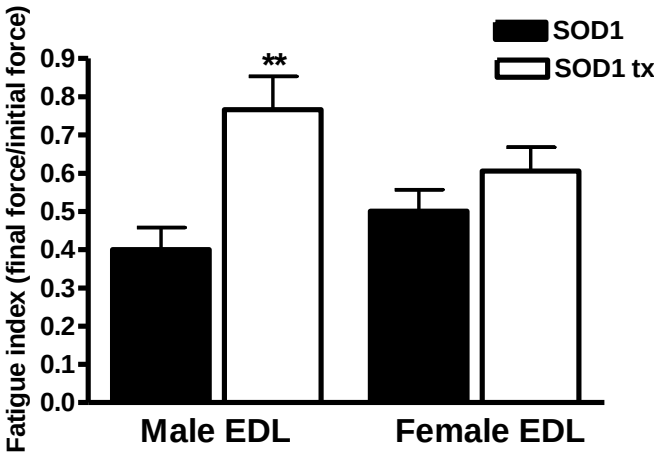


Figure 20: Comparison of the fatigue index of the right EDL muscles of metformin-treated and untreated SOD1^{G93A} mice at 100 days.

The fatigue index of each muscle investigated was determined by stimulating the muscle at 40Hz for 250ms of every second for 3 minutes and then dividing the final force recorded by the initial force. Higher fatigue index values represent an increased resistance to fatigue. Calculation of the fatigue index for the EDL muscles of metformin-treated (SOD1 tx) and control (SOD1) SOD1^{G93A} mice revealed that metformin treatment significantly increased the resistance to fatigue of SOD1^{G93A} male EDL muscles compared to untreated SOD1^{G93A} male EDL muscles. Although there was a trend towards increased resistance to fatigue in female EDL muscles with metformin treatment, this was not significant. n=11 SOD1^{G93A} males, n=11 SOD1^{G93A} females, n=9 metformin treated SOD1^{G93A} males, n=15 metformin treated SOD1^{G93A} females, error bars represent SEM. (SOD1^{G93A} Males vs. Metformin-treated SOD1^{G93A} Males, P = 0.0019 (**))

3.3.5.3 Metformin treatment did not significantly increase the resistance to fatigue of WT EDL muscles at 100 days of age, despite a trend towards this effect.

Measurement of the resistance to fatigue of the EDL muscles of metformin-treated and untreated WT mice, revealed a strong trend towards increased resistance to fatigue (represented by a higher fatigue index) in both WT male and female EDL muscles with metformin treatment, however, these trends did not reach statistical significance (0.28+/- 0.057 metformin treated WT M vs. 0.17 +/- 0.04 WT M) (0.35+/-0.036 metformin-treated WT F vs. 0.24 +/- 0.04 WT F) **(Figure 21)**.

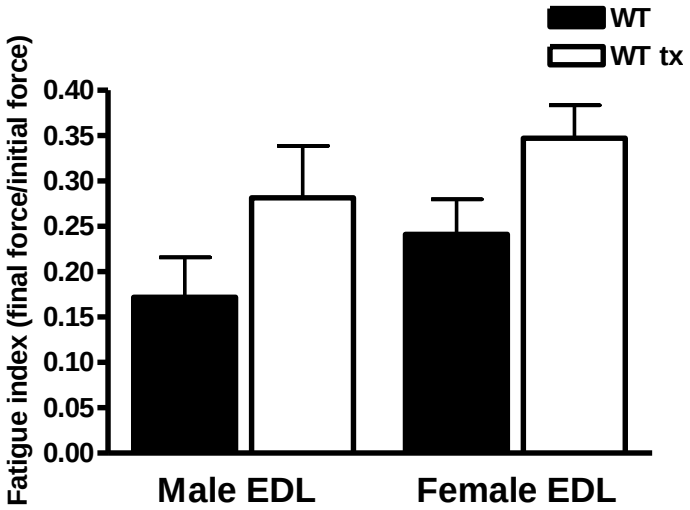


Figure 21: Comparison of the fatigue index of the right EDL muscles of metformin-treated and untreated WT mice at 100 days.

The fatigue index of each muscle investigated was determined by stimulating the muscle at 40Hz for 250ms of every second for 3 minutes and then dividing the final force recorded by the initial force. Higher fatigue index values represent an increased resistance to fatigue. Calculation of the fatigue index for the EDL muscles of metformin-treated (WT tx) and control (WT) WT mice revealed a strong trend towards increased resistance to fatigue in both male and female EDL muscles with metformin treatment, however, these trends failed to reach statistical significance. n=6 WT males, n=6 WT females, n=5 metformin treated WT males and n=7 metformin treated WT females, error bars represent SEM.

3.4 Discussion

Although the ultimate trigger or triggers of the selective damage and degeneration of motor neurons in ALS remain to be elucidated, several pathological mechanisms have been identified which may contribute this process. These mechanisms include, amongst others; inflammation and toxic glial activation (Papadimitriou et al., 2010, Ilieva et al., 2009, Philips and Robberecht, 2011), mitochondrial dysfunction (Duffy et al., 2011) and oxidative stress (Papadimitriou et al., 2010, Duffy et al., 2011). Metformin is a routinely used anti-type II diabetes drug, which has been shown to have anti-inflammatory (Dandona et al., 2004, Isoda et al., 2006, Lin et al., 2000) and antioxidant (Lin et al., 2000, Ouslimani et al., 2005, Srividhya et al., 2002) properties as well as the ability to bring about mitochondrial biogenesis (Kukidome et al., 2006). Furthermore, it has been shown to attenuate pathology in mouse models of both Huntington's disease (Ma et al., 2007) and multiple sclerosis (Nath et al., 2009) which, like ALS models, show central nervous system (CNS)-based inflammation, oxidative stress and mitochondrial abnormalities (Beal and Ferrante, 2004, Stadelmann, 2011, Ilieva et al., 2009). We therefore hypothesised that metformin would also attenuate pathology in the $SOD1^{G93A}$ mouse model of ALS. We tested this hypothesis by treating male and female $SOD1^{G93A}$ mice with 2mg/ml metformin in their drinking water from the presymptomatic time point of 35 days of age and analysed the effects of the drug on functional motor unit number, muscle strength and muscle fatigability via *in vivo* electrophysiology at 100 days of age.

3.4.1 Conclusions drawn from control data

The inclusion of untreated $SOD1^{G93A}$ and WT mice in this study allowed us characterise the pathology of our high copy $SOD1^{G93A}$ mice compared to WT mice at 100 days of age and to

compare the results obtained with those published by other groups performing *in vivo* electrophysiology in this model. As would be expected for mice undergoing denervation, motor neuron degeneration and resultant muscle atrophy (Gurney et al., 1994), we saw a significant reduction in the number of functional motor units and the maximal and specific forces of $SOD1^{G93A}$ muscles compared to WT muscles at 100 days of age. We also saw a significant increase in the resistance to fatigue of $SOD1^{G93A}$ EDL muscles compared to WT, which is consistent with the finding that fast fatigable motor units are the first to degenerate in $SOD1^{G93A}$ mice (Hegedus et al., 2007, Hegedus et al., 2008). All results obtained for electrophysiological parameters in control $SOD1^{G93A}$ mice were consistent with those published by Sharp and colleagues, (Sharp et al., 2005, Sharp et al., 2008) who are experienced with electrophysiological assessments in this model. This confirmed that our $SOD1^{G93A}$ mice were exhibiting normal pathology at 100 days and that our electrophysiological methods were working correctly.

Our electrophysiological results for WT mice we also consistent with those previously published by Sharp and collaborators, with the exception of the number of functional motor units in WT male EDL muscles. In this study we determined the mean no of motor units in the EDL muscles of WT male mice at 100 days of age to be 54+/-4, whereas Sharp and colleagues previously measured this to be 26.6 +/- 0.4 in adult male WT mice. This discrepancy could have arisen from the use of different criteria for the identification of motor units during the counting process. Alternatively, it is possible that an overestimation of the number of motor units occurred owing to the phenomenon of alternation, which is associated with the manual incremental stimulation method for motor unit stimulation used (Brown and Milner-Brown, 1976). Specifically the threshold for nerve fiber excitation is often not a

discrete value and instead the probability of motor unit activation is spread over a range that often overlaps with neighboring motor axons (Rashidipour and Chan, 2008). This means that an increase in muscle force elicited by stimulation of the nerve with a higher intensity pulse may not in every case indicate activation of the original lower threshold motor unit(s) with an additional new motor unit. Rather, force increases may in some instances occur as a result of activation of another motor unit with a slightly higher but overlapping threshold rather than the original motor unit(s). This phenomenon, referred to as alternation, can lead to overestimation of motor unit number (Rashidipour and Chan, 2008). Although alternation could have resulted in overestimation of motor unit numbers in WT mice in this study, this is likely to have been less of an issue in $SOD1^{G93A}$ mice where the low numbers of surviving motor units would have reduced the likelihood of overlapping thresholds for motor unit activation. Another issue that could have lead to overestimation of motor unit numbers in WT mice is baseline shifts in the motor unit traces, which we have recently been informed can occur when using this technique. However during our motor unit estimation experiments we did not see evidence of substantial baseline shifts and therefore feel that it is unlikely that our results were affected by this problem.

In light of the problems associated with the manual incremental stimulation method for motor unit estimation, several other methods for motor unit number estimation (MUNE) have been developed and trialed, in particular for use in human subjects for diagnosis of neuromuscular disease. MUNE in human subjects is more challenging than in mice as the number of motor units present in muscles of interest is too large to be measured directly. In light of this, MUNE methods used for humans involve an initial determination of the size of the surface detected action potential generated by all the motor units in the muscle in response to a

supramaximal stimulus delivered to the motor nerve, followed by the determination of the average size of the action potential of a small but representative sample of motor units in the muscle. An estimate of the total number of motor units within the muscle is then derived using the following formula:

$$\text{MUNE: } \frac{\text{size of the maximum compound muscle action potential}}{\text{Size of the average surface detected motor unit action potential}}$$

The main way in which methods for MUNE in humans differ from each other is the way in which the size of the average surface detected motor unit action potential (SMUAP) is determined. The main methods available for MUNE in humans other than the manual incremental stimulation method used in this study are discussed below:

Multiple point stimulation method:

This method involves stimulation of the motor nerve of interest at multiple sites along its length. Here the nerve is subjected to finely graded stimuli at each site in order to find the lowest threshold axon as indicated by the occurrence of an all or none response of the associated surface detected motor unit action potential (Doherty and Brown, 1993). Importantly, for each surface detected motor unit action potential to be accepted as indicative of a single motor unit, there must be no change in the shape or latency of the detected response in response to successive stimuli as such changes could suggest the presence of two or more axons with overlapping thresholds (Rashidipour and Chan, 2008). In doing this and only accepting the lowest threshold motor units at each stimulation site, the problem of alternation is avoided. The disadvantages of this technique are that it requires considerable operator skill and experience and also that it is not applicable to proximal muscles. Collection of surface detected motor unit action potentials at multiple sites is also more time consuming.

Spike-triggered averaging method:

In contrast to the two other methods discussed, which both use electrical stimulation to stimulate the motor nerve, this method uses voluntary muscle contraction to activate motor units. This method has the advantage that it can be used on proximal muscle groups where the nerve cannot easily be reached for electrical stimulation. In this method, a needle EMG electrode is used to detect motor unit activation. The motor unit spike is then used to synchronize the accumulation of an ensemble average of surface action potentials (Brown et al., 1988). The position of the EMG needle is changed several times in order to collect a sample of ten or more single motor unit action potentials. The MUNE is calculated by dividing the average surface detected motor unit action potential into the maximum action potential. The disadvantages of this method are that it is invasive because it requires a needle electrode, it is time consuming and it also requires some patient cooperation.

Statistical method:

This method was proposed by Daube, who reasoned that because the sizes of surface detected motor unit action potentials in a muscle follow a Poisson distribution, the variance of the motor unit potential should be equal to the mean motor unit action potential (Daube, 1995). In this method the nerve is stimulated electrically as with the manual incremental stimulation and multiple point stimulation methods. In order to make a measurement an initial scan is performed in which 30 computer controlled stimuli at 1Hz are delivered at intensities that increase at equally spaced increments from just below threshold to just maximal. The amplitude differences between successive responses are then used to determine optimal stimulus intensities for use in the determination of mean motor unit action potential. A

sequence of 30 submaximal stimuli is then given at each stimulus intensity. During this process, the inherent variability of the threshold of individual axons leads to their intermittent firing which leads to variations in the size of the compound muscle action potential that are used to determine the mean motor unit action potential. As a result of this method employing a statistical measurement, a slightly different result is found with each series of stimuli. This means that multiple trials are needed to make an accurate measurement. A decision to stop recording is normally made after four to nine trials if the standard error of surface motor unit action potentials is less than 10% of the mean. This process is repeated for all other pre-chosen stimulus intensity levels and the final MUNE is derived from the average of the MUNEs calculated from all of the trials performed. The major problem associated with this method is that decrement of motor unit action potential with repetitive stimulation, if not identified, can severely affect MUNE results. In light of the fact that motor unit action potential decrement is more likely to occur in dysfunctional motor units and its presence cannon be identified using the statistical method, this method is no longer widely used for diagnostics in humans.

As is clear from the above sections, each of the methods described has advantages and disadvantages and may be better for some applications over others. Currently, the most widely used method for studying distal muscles is the multiple point stimulation method whereas spike triggered averaging is frequently used for the investigation of proximal muscles whose innervating nerve is not readily accessible. Interestingly Shefner and colleagues conducted a comparison in $SOD1^{G93A}$ mice of the incremental stimulation method for MUNE used in this study with the multiple point stimulation method. They found both methods to yield similar motor unit estimates and concluded that both methods were equally

effective in documenting the progression of lower motor neuron degeneration in SOD1^{G93A} mice (Shefner et al., 2002). This highlights that the incremental stimulation method was an appropriate method to use in our study.

In addition to revealing reductions in the maximum and specific forces of the TA and EDL muscles of SOD1^{G93A} mice that are consistent with the literature, analysis of control SOD1^{G93A} mice in this study, revealed that at 100 days of age, the TA muscles of both male and female SOD1^{G93A} mice are more severely affected in terms of loss of maximal and specific force, than the EDL muscles. This suggests that the signal to noise ratio for analysis of the efficacy of therapeutic strategies, may be better in the TA muscle than in the EDL muscle. Additionally, we saw no significant differences between the specific forces of male and female WT muscles or between the specific forces of male and female SOD1^{G93A} muscles, indicating that by 100 days of age, female SOD1^{G93A} mice have lost an identical amount of force per unit cross sectional area to male SOD1^{G93A} mice.

When working with the SOD1^{G93A} murine model, it is common to monitor the weights of the mice as this can be a good indicator of disease onset and progression as well as the general health of the animals (Scott et al., 2008). As would be expected for mice experiencing denervation and associated muscle wasting as well as a hyper-metabolic rate (Dupuis et al., 2011) , female SOD1^{G93A} mice were considerably lighter than female WT mice from 75-79 days onwards. We were surprised to see no difference between the weights of WT and SOD1^{G93A} male mice until 95-99 days of age, which is later than has previously been described by colleagues working with the same colony of SOD1^{G93A} mice (Sharp et al., 2008). However, the decision to collect weight data in this study was unfortunately made

once the study had already commenced and therefore the n-numbers for weight data presented for male WT and SOD1^{G93A} mice were not as high as we would have liked. Consequently, if the four male SOD1^{G93A} mice from which weight data were collected for this study were on the heavier end of the spectrum of male SOD1^{G93A} mice, the data collected for these mice may not have been representative of male SOD1^{G93A} mice as a whole. If this was the case then it could explain the surprising lack of difference between the weights of male WT and SOD1^{G93A} mice before 95-99 days of age. N-numbers for female SOD1^{G93A} and WT mice used for weight data in this study were on average at least two-fold higher than for males and this may explain why the results for female mice are more in line with what we would have expected.

3.4.2 The effect of metformin treatment on disease severity in SOD1G93A mice at 100 days of age.

In this study, we hypothesised that treatment of SOD1^{G93A} mice with the synthetic activator of AMPK, metformin, would be protective for the motor neurons in their spinal cords and therefore reduce the severity of their pathology at 100 days of age. In direct support of this we observed a significant increase in the survival of functional motor units as measured by *in vivo* electrophysiology, in metformin-treated male EDL muscles compared to their untreated counterparts at 100 days of age (24 +/- 2 vs. 14 +/- 2 motor units, $p<0.005$). When comparing these results to those obtained for the number of functional motor units in wild type (WT) male EDL muscles at 100 days of age (54 +/-4 motor units) this represented a considerable increase in motor unit survival from approximately 26% of WT motor units to 44%. We also observed a significant increase in the number of surviving motor units in metformin-treated female TA muscles compared to their untreated counterparts (21 +/- 1 vs. 15 +/- 2 motor

units, P = 0.0134) at 100 days of age. The number of functional motor units in the TA muscles of WT mice has previously been determined by Hegedus et al., to be 95 +/- 12.4 (Hegedus et al., 2008). Taking this into consideration, the increase in survival of functional motor units seen in the TA muscles of metformin-treated female mice represented an increase from approximately 16% of WT motor units to 22%. We were also encouraged to see strong trends towards increased survival of motor units in male TA muscles and female EDL muscles. Although the increases in motor unit survival seen were not sufficient to restore motor unit numbers to levels comparable to WT, they suggested that metformin was having a trophic effect on motor neuron health in $SOD1^{G93A}$ mice at 100 days of age and highlighted the possibility that motor unit survival may be further enhanced with a different dose of metformin.

In light of the increased survival of motor units seen in male and female $SOD1^{G93A}$ mice with metformin treatment, we were surprised not to see a resultant increase in the maximal forces of the TA and EDL muscles of these animals. However, activation of AMPK by metformin has previously been shown to increase the expression of PGC1α in skeletal muscles and over-expression of this transcription factor in the skeletal muscles of transgenic mice has been shown to drive slow myosin isoform expression, increase aerobic capacity and increase running performance (Lin et al., 2002). We therefore hypothesized that if metformin brought about increased PGC1α expression in the skeletal muscles of out $SOD1^{G93A}$ mice, this may have encouraged muscles to adopt a slower, more fatigue resistant and thus weaker phenotype. If this was the case, then it could have acted in opposition to any increases in muscle force brought about by increased motor unit survival. This is supported by the finding that the muscles of metformin-treated male $SOD1^{G93A}$ mice were significantly more resistant

to fatigue (a feature of slow muscles) than their untreated counterparts and by the fact that that the EDL muscles of female SOD1^{G93A} mice also showed a trend towards becoming more fatigue resistant.

In addition to performing electrophysiology on metformin treated SOD1^{G93A} mice, we also weighed these mice approximately every 5 days from 55 days of age onwards. Comparison of the weight curves produced for metformin treated mice with those of untreated controls, revealed that metformin had no effect on the weights of female SOD1^{G93A} mice, but appeared to bring about a reduction in the weight of male SOD1^{G93A} mice throughout the time period studied. Although the number of untreated SOD1^{G93A} male mice from which weight data were derived was only 4 (much lower than for metformin-treated male SOD1^{G93A} mice) and we could therefore not be certain of the validity of this trend, we considered it important to investigate this possibility further in future studies with greater n-numbers and age-matched controls. Interestingly, treatment of the R6/2 murine model of Huntington's disease with the same dose of metformin via the same method, did not correct disease associated weight loss in these mice, despite bringing about a significant increase in the lifespan in male mice (Ma et al., 2007). These observations correlate with the absence of a beneficial effect of metformin treatment on weight in our mice.

4.3 The effect of metformin treatment on WT mice

In order to analyse whether metformin had any negative effects in healthy mice and to observe its physiological effects in an environment not clouded by disease pathology, we treated WT mice with metformin from 35 days of age and analysed the effects of treatment via the same electrophysiological methods as for SOD1^{G93A} mice. Throughout the period of

treatment, WT mice were seen to be in good health and were indistinguishable from their untreated WT littermates. Additionally, as would be expected for mice with no motor neuron pathology, metformin had no effect on the number of functional motor units measured in the EDL muscles of WT mice at 100 days of age.

In light of our hypothesis that the absence of force increases in $SOD1^{G93A}$ mice with metformin treatment resulted from their muscles adopting a slower, more fatigue resistant phenotype, it seemed likely that we would observe a loss of maximum /specific force or no substantial change in these parameters in metformin treated WT mice (depending on the degree of PGC1α upregulation achieved and the other regulatory pathways in operation). In accordance with this, we saw no changes in the maximal or specific forces of the TA or EDL muscles of metformin-treated WT male mice. We were however surprised to see an increase in both the maximal force and the specific force of metformin-treated WT female EDL muscles and a trend towards this in their TA muscles. This suggests that our hypothesised metformin-induced drive towards the adoption of slower muscle phenotypes may not have been as applicable in WT mice as in $SOD1^{G93A}$ mice, where there is already a favoring of the slower muscle phenotype. This is supported by the fact that in metformin-treated WT mice, unlike in treated $SOD1^{G93A}$ mice, we did not see a significant increase in the resistance to fatigue in the EDL muscles.

In addition to seeing increased muscle strength in metformin-treated WT female mice, we were also surprised to see a pronounced increase in bodyweight in these animals. This effect was not matched in metformin treated male WT mice. This suggests that metformin may have interacted differently with the female hormone system to the male hormone system in

our experiments. Alternatively, the female WT mice that were treated with metformin in this study could have been naturally heavier and stronger than those selected to be controls. This possibility is one that should not be overlooked, considering the mixed-hybrid genetic background used for this study and the fact that metformin has been reported to be either weight neutral or to bring about weight loss in patients with type II diabetes (Mitri and Hamdy, 2009). Despite the surprising increases in weight and muscle force in metformin-treated female WT mice, we were encouraged to see that metformin-treatment had no obvious detrimental effects (particularly on the motor system) in healthy mice and were therefore happy to continue our investigations with this drug.

In conclusion, in this study we hypothesised that treatment of $SOD1^{G93A}$ mice with the synthetic, blood brain barrier crossing, AMPK activator, metformin from 35 days of age would reduce the severity of their pathology at 100 days of age. In direct support of this we observed a significant preservation of functional motor units in $SOD1^{G93A}$ male EDL muscles and female TA muscles and a strong trend towards functional motor unit preservation in $SOD1^{G93A}$ female EDL muscles and male TA muscles with metformin treatment. As the ultimate cause of death in $SOD1^{G93A}$ mice is the malfunctioning and retraction of their distal motor axons and therefore the loss of functional motor units (Gould et al., 2006), we hypothesized that metformin treatment may also bring about increased survival in these mice. In order to test this hypothesis and to investigate whether the beneficial effects of metformin could be augmented with a different dose, we performed a dose-response survival study in $SOD1^{G93A}$ mice. This study is discussed in detail in Chapter 4.

4. Metformin dose-response survival study

4.1 Introduction

ALS is a devastating neurodegenerative disorder that is in desperate need of suitable treatments. Consequently, FDA-approved drugs that are routinely used for the treatment of other diseases, represent attractive candidates for research as potential ALS therapeutics, as their previous safety, toxicity and pharmacological testing would speed up their passage into clinical trial (Traynor et al., 2006). Metformin is a routinely used anti-type II diabetes drug, which has been shown to have anti-inflammatory (Dandona et al., 2004, Isoda et al., 2006, Lin et al., 2000) and antioxidant (Lin et al., 2000, Ouslimani et al., 2005, Srividhya et al., 2002) properties as well as the ability to bring about mitochondrial biogenesis (Kukidome et al., 2006) and to cross the blood brain barrier (BBB) (Chen et al., 2009, Ma et al., 2007). In recent years, metformin has been shown to attenuate pathology in mouse models of both Huntington's disease (Ma et al., 2007) and multiple sclerosis (Nath et al., 2009) which, like ALS models, show central nervous system (CNS)-based inflammation, oxidative stress and mitochondrial abnormalities (Beal and Ferrante, 2004, Stadelmann, 2011, Ilieva et al., 2009). We therefore hypothesised that metformin would also attenuate pathology in the $SOD1^{G93A}$ mouse model of ALS. We tested this hypothesis through an initial study involving the treatment of male and female $SOD1^{G93A}$ mice with 2mg/ml metformin in the drinking water from 35 days of age (Chapter 3). We analysed the strength and number of surviving functional motor units in the right TA and EDL muscles of these mice as well as the resistance to fatigue of their right EDL muscles via *in vivo* electrophysiology at 100 days of age. In direct support of our hypothesis we saw a significant increase in the survival of functional motor units in metformin-treated male EDL muscles (24 +/- 2 vs. 14 +/- 2 motor

units, $p<0.005$) as well as in metformin-treated female TA muscles (21 +/- 1 vs. 15 +/- 2 motor units, $P = 0.0134$). A strong trend towards increased motor unit survival was also observed in female EDL muscles and male TA muscles. We were surprised not to see a resultant increase in the maximal and/or specific forces of the muscles of metformin-treated $SOD1^{G93A}$ mice, but hypothesized that this may have been the result of muscles adopting an even slower, more fatigue resistant (and thus weaker) phenotype than is already seen in $SOD1^{G93A}$ mice. We hypothesized that this may have occurred through a metformin-inducted activation/upregulation of PGC1α. This hypothesis was supported by the EDL muscles of metformin treated male $SOD1^{G93A}$ mice showing a significantly increased resistance to fatigue compared to their untreated counterparts, and the EDL muscles of treated females also showing a strong trend towards this.

The ultimate cause of death in $SOD1^{G93A}$ mice is the retraction of distal motor axons and denervation of skeletal muscles (Gould et al., 2006, Dadon-Nachum et al., 2011). Consequently, bringing about the preservation of functional motor units, in which the motor neuron is not only present but also forming functional neuromuscular junctions, is likely to be a key requirement for prolonging survival in ALS models and patients. As we observed metformin to be able to bring about increased motor unit survival in $SOD1^{G93A}$ mice at the early symptomatic time point of 100 days of age, we hypothesized that it may also bring about an increase in survival in these mice. We therefore decided to perform a dose-response survival study to test this.

Metformin doses selected for our survival study were 0.5, 2 and 5mg/ml via the drinking water from 35 days of age. The 2mg/ml dose was selected because this was the dose with

which we saw a beneficial effect on motor neuron survival in male and female SOD^{G93A} mice at 100 days of age. The 0.5 and 5mg/ml doses were selected as they flanked the 2 mg/ml dose and would therefore allow us to analyse whether any beneficial effects seen at 2mg/ml could be further improved or equalled by a higher or lower dose. When considering which doses to test, we also considered approximately what these doses would correspond to in humans. To do this we made use of the body surface area (BSA) normalisation method which is recommended by the Food and Drug Administration (FDA) (Reagan-Shaw et al., 2008). This method employs the following formula:

Human equivalent dose (HED) = Mouse dose x (Mouse K_m/Human K_m)

Where the K_m factor (body weight (kg) divided by BSA (m^2) is used to convert the mg/kg dose used in a study into a mg/m^2 dose. The K_m values provided by the FDA (Reagan-Shaw et al., 2008), based on average BSA calculations for various species are summarised in **Table 8**. Based on the values specified for mice and human adults in **Table 8** and on data from Bachmanov and colleagues, describing the average water intake across 28 strains of mice to be 5.8+/-2 ml/mouse/day(Bachmanov et al., 2002), we calculated the following HEDs for the metformin doses tested:

0.5 mg/ml = 11.7 mg/kg/day

2 mg/ml = 47 mg/kg/kg/day

5 mg/ml = 117.4 mg/kg/day

The maximum daily dose of metformin in adult humans with type II diabetes is 2g (33.3 mg/kg/day assuming the average adult human weighs 60kg) (information taken from the

British National Formulary, edition 21, March 2011). Therefore the doses selected for our metformin survival study were in an appropriate range to be informative with respect to humans.

Table 8: Conversion of animal doses to Human Equivalent Doses (HED) based on Body Surface Area (BSA)

Species	Weight (kg)	BSA (m^2)	K_m factor
Human adult	60	1.6	37
Human child	20	0.8	25
Baboon	12	0.6	20
Dog	10	0.5	20
Monkey	3	0.24	12
Rabbit	1.8	0.15	12
Guinea pig	0.4	0.05	8
Rat	0.15	0.025	6
Hamster	0.08	0.02	5
Mouse	0.02	0.007	3

Values based on data from FDA Draft Guidelines (Reagan-Shaw et al., 2008). To convert dose in mg/kg to dose in mg/m^2, multiply by K_m *value.*

Despite many therapeutics being documented to bring about significant increases in survival in the SOD1^{G93A} mouse, Riluzole has been the only drug to show any, albeit small, beneficial effect in ALS patients (Ludolph and Jesse, 2009). Investigations into the potential reasons for this disparity have revealed several confounding variables that may lead to false positives in survival experiments in SOD1^{G93A} mice (Scott et al., 2008). These variables include, in order of impact: the occurrence of non-ALS deaths, the incidence of low copy transgenics, genetic background or epigenetic influences causing littermate clustering and a slight gender effect (Scott et al., 2008). Identification of these variables has lead to the production of guidelines for the preclinical testing of therapeutics for ALS, which aim to control for these variables and increase study validity (Ludolph et al., 2010, Scott et al., 2008). Indeed, Scott and colleagues have shown using a specially designed computer model (SimLIMS) and data from 2241 control SOD1^{G93A} mice on a mixed hybrid genetic background (maintained by breeding hemizygous B6SJLTg (SOD1^{G93A}) males to B6SJLF1 dams), that with an n-number of 24 mice per cohort (12 males and 12 females), and the employment of same-gender litter matching as well as exclusion of mice experiencing non-ALS deaths or loss of transgene copies, noise within survival studies can be reduced to a virtual zero (Scott et al., 2008). We carefully followed these guidelines when designing our metformin dose-response survival study in order to ensure as far as possible, the accurate determination of the potential of metformin as a therapy for ALS. Specifically, in order to control for the variability introduced by non-ALS deaths, we closely monitored the health of all mice throughout the study and excluded relevant data from any mice observed to experience a non-ALS death. In order to control for transgene copy number losses, we investigated the possibility of copy number variation (via Q-PCR) in any mice displaying outlying disease progression or survival characteristics (Alexander et al., 2004) and were prepared to exclude any mice which had lost

copies of the transgene. We balanced all experimental groups in the study for age, starting weight and litter and considered data from all male and female mice separately to negate any sex-effect. Furthermore, we used an n-number of 14 males and 15 females per group.

As we enrolled a total of 116 age-matched mice in our survival study and wanted to monitor disease onset, progression and survival in all mice at the same time of day an in a minimally invasive and consistent fashion, it was important that we selected the techniques used to measure these parameters carefully. Although the rotarod is routinely used for assessment of disease onset and progression in $SOD1^{G93A}$ mice (Ralph et al., 2005, Sharp et al., 2008, Towne et al., 2008), conversations with colleagues who had previously performed rotarod assessments, lead us to believe that it would be difficult to process the large numbers of mice enrolled in our study with this technique (owing to the time required to process each mouse). Additionally, these colleagues described difficulties with some mice (even healthy WT animals) failing to learn how to run on the rotarod even after a period of training. In light of the critical importance of litter balancing and high n-numbers in our survival study, we could not afford to lose information from mice that did not perform well on the rotarod task or to introduce variability into the study through non-disease related differences in rotarod performance between mice. We therefore decided that the rotarod was not a suitable measure of disease onset/progression to use in our study. We also considered using the paw grip endurance test, determined by Weydt and colleagues to be a sensitive and inexpensive alternative to the rotarod test in $SOD1^{G93A}$ mice (Weydt et al., 2003), but were concerned that the results gained from this assessment were likely to be user dependent. Using this technique would therefore have prevented the possibility of a second investigator helping to perform these measurements should this be required. We therefore decided to follow study guidelines

developed and validated by Scott and colleagues at the ALS Therapy Development Institute, in which disease onset and progression are established by longitudinal monitoring of weight and neurological score (Scott et al., 2008, Gill et al., 2009, Lincecum et al., 2010). The neurological scoring system utilised in this study format (described in detail in the materials and methods section) was developed through detailed observations of $SOD1^{G93A}$ mouse pathology and provides a quick, non-invasive and unambiguous measure of disease onset and progression in $SOD1^{G93A}$ mice. (Scott et al., 2008, Gill et al., 2009, Lincecum et al., 2010). As we had not previously performed survival studies in the $SOD1^{G93A}$ mice, we decided to use the most commonly employed endpoint of the inability of mice to right themselves within 30s of being placed on a side (Scott et al., 2008). It was however important to us to make detailed observations of mice at end stage in this study in order to establish whether this end point could be brought forward in future studies, whilst still obtaining meaningful results.

4.2 Results

4.2.1 Assessment of potential variations in transgene copy number

Assessment of potential variation in transgene copy number was performed for four male mice and two female mice whose survival time appeared to be outlying compared to the other mice of the same sex within their treatment group. Although the survival times of these mice only differed slightly from those of their peers, we felt that it was still worth checking whether their copy numbers varied with respect to the rest of their group to be sure that results taken from them were valid. ΔCT values obtained for these mice were compared to those obtained for a subset of 4 male and 4 female control mice whose survival was closest to the median survival calculated for male and female control mice respectively. Any mice with

a ΔCT value that differed by more than 2 standard deviations from the mean ΔCT of these control mice were to be excluded although no mice met this criteria. The median survival for male control mice was 123 days and the median survival for female control mice was 140 days. The survival times of the control and outlying mice for which copy number variation assessment was performed, as well as the ΔCT values obtained for these mice are summarised in **Table 9.**

	Mouse no.	Survival (Days)	∆CT	Mean ΔCT - ΔCT
Average males	198	119	9.25	0.17
	335	121	9.40	0.02
	264	122	9.53	-0.10
	269	123	9.56	-0.14
Average Females	245	127	9.41	0.01
	224	134	9.62	-0.20
	210	135	9.11	0.31
	384	138	9.72	-0.30
Outlying Males	174	147	9.46	-0.04
	294	142	9.30	0.13
	244	141	9.64	-0.22
	312	149	9.06	0.36
	429	141	9.36	0.06
Outlying Females	371	161	9.38	0.04
	172	160	9.61	-0.19
Mean ΔCT of average mice			**9.45**	
SDEV of average mice			**0.20**	
2x SDEV of average mice			**0.40**	

Table 9: Summary of the survival times and Δ CT values of mice for which copy number variation assessments were performed in our metformin survival study

Copy number variation assessments were performed for four male mice and two female mice whose survival time appeared to be outlying compared to the other mice of the same sex within their treatment group. ΔCT values obtained for these mice were compared to those obtained for a subset of 4 male and 4 female control mice whose survival was closest to the median survival calculated for male and female control mice respectively. Any mice with a ΔCT value that differed by more than 2 standard deviations from the mean ΔCT of these control mice were to be excluded although no mice met this criteria. The survival times and ΔCT values obtained for all mice for which copy number variation assessments were performed as well as the mean and standard deviation of the ΔCT values obtained for control mice are summarised in this table. The median survival for male control mice was 123 days and the median survival for female control mice was 140 days.

4.2.2Metformin treatment had no effect on disease onset, progression or survival in male mice.

4.2.2.1 N-numbers, weight balancing and non-ALS deaths in male mice

Four groups of 14 male mice that were balanced for age, litter and body weight were enrolled in this study. The average starting bodyweights for each group were within 0.5g of each other (Control: 20.7g, 0.5mg/ml: 20.5g, 2mg/ml: 20.2g and 5mg/ml: 20.6g). During the study one male from the control group and one male from the 0.5mg/ml group were found dead prior to developing any neurological symptoms. Additionally, one male from the 0.5mg/ml group developed a kidney cyst and was therefore culled prematurely. These mice were all recorded as dying from 'non ALS deaths' and were treated as 'censored' in Kaplan Meier analyses and excluded from weight and neurological score plots. Two males from the 2mg/ml group sustained fighting wounds prior to reaching end stage and were culled for humane reasons. Weight and neurological score data from these mice were included up to the date at which they were culled in weight and neurological score plots and they were treated as censored in Kaplan Meier analyses that required information about end points.

4.2.2.2 Effect of metformin on body weight, disease onset and disease progression in male SOD1^{G93A} mice.

High copy SOD1G93A mice, unlike wild type (WT) mice are unable to maintain body weight from approximately 90 days of age and steadily lose weight from this time point until death. Longitudinal monitoring of weight therefore provides a good indication of disease onset and progression and can reveal important information about the efficacy of potential therapeutics (Scott et al., 2008). The change in mean body weight over time of male mice in

all four groups is plotted in **Figure 22A** from 35 days onwards. Weight curves for male mice in all groups showed a very similar shape with the onset of weight decline, occurring at ~90 days in each group. Consequently, no significant differences were observed in the selected summary measures of time to peak weight **(Figure 22B, Table 10)** and time from peak weight to end stage **(Figure 22C, Table 10).** However mice in all treatment groups appeared to be lighter throughout the study than control mice.

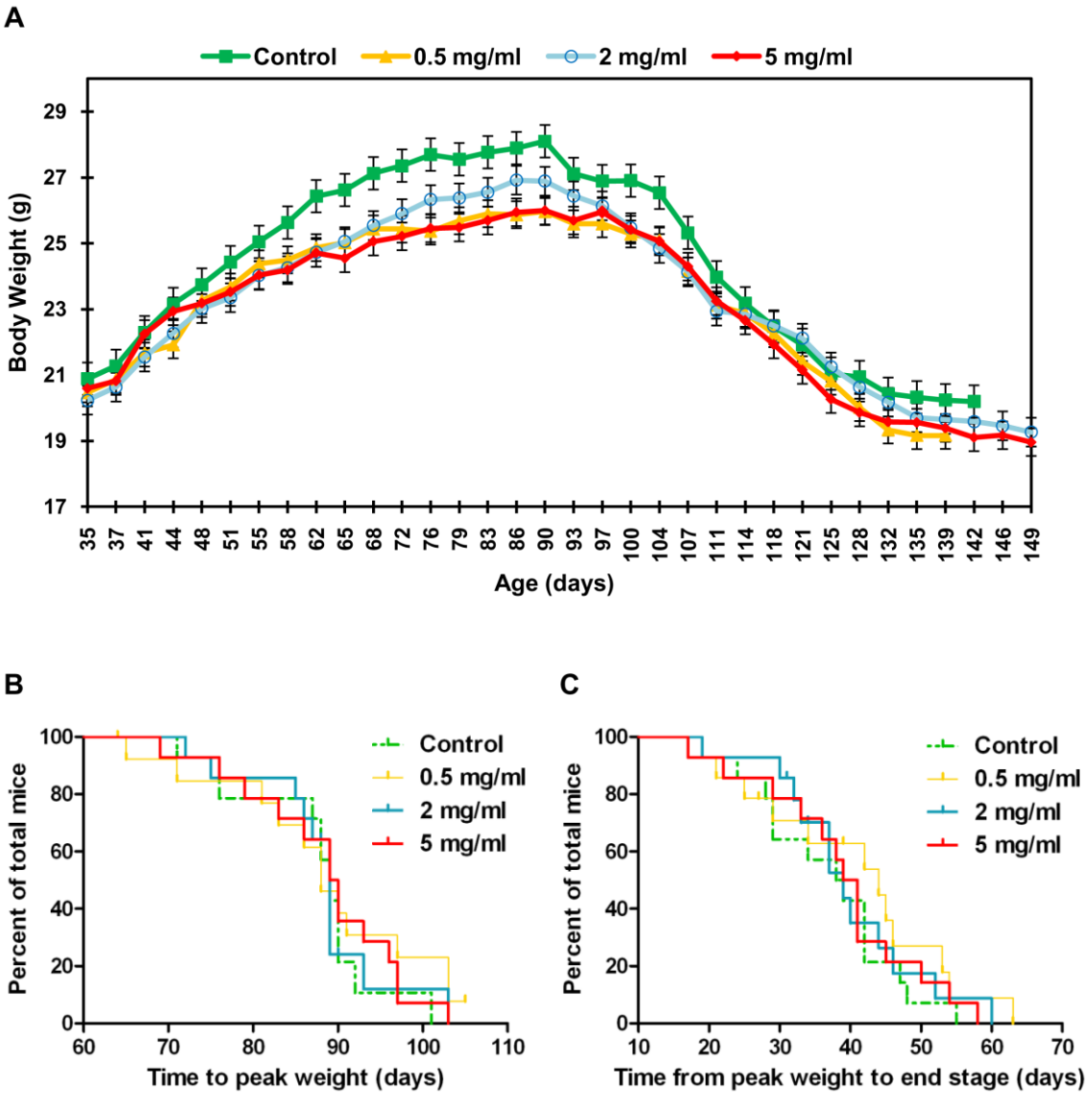


Figure 22: Effect of metformin on body weight, disease onset and disease progression in male SOD1^{G93A} mice.

(A) Mean group body weight plotted for male SOD1^{G93A} mice over time from 35 days of age until the date at which the last death within each individual group occurred. As mice within groups died at different ages, the final weights of all mice were carried forward when calculating group mean values, until the date at which the last mouse within each group died. This prevented decomposition of the mean at later stages. Error bars represent standard error of the mean (SEM). (B) Kaplan-Meier survival plot for time to peak weight (an indicator of disease onset) in male SOD1^{G93A} mice. (C) Kaplan-Meier survival plot for time from peak weight to end stage (an indicator of disease progression) in male SOD1^{G93A} mice. Graphs (A), (B) and (C) present data for male SOD1^{G93A} mice in all four experimental groups: Control = green, 0.5mg/ml metformin = yellow, 2mg/ml metformin = blue, 5mg/ml metformin = red). Results for statistical analyses performed on data presented in (B) and (C) are given in **Table 10**.

Table 10: Kaplan Meier time to event analyses for male SOD1^{G93A} mice [1, 2, 3]

	Median Value (days)				P Value	
	Control	**0.5 mg/ml**	**2 mg/ml**	**5 mg/ml**	**Log-rank**	**Log-rank test for trend**
Time to peak weight	89	88	89	89.5	0.8469	0.8492
Time from peak weight to end stage	38.5	44	39	40	0.6986	0.8963
Time to reach score 2 in both hindlimbs	114	121	114.5	114	0.6942	0.6289
Survival	123	128	126	126	0.8575	0.6597

[1]The Logrank test investigates the null hypothesis that that the Kaplan Meier curves for all groups are identical (i.e. that the treatment did not change the time taken to reach the event being analysed). Low P-values are therefore indicative of differences between curves that did not occur due to chance. The threshold for significance was set at $P<0.05$.

[2] To perform the log-rank test for trend, experimental groups were arranged in order of increasing dose (Control, then 0,5mg/ml, 2mg/ml and 5mg/ml) and a P value testing the null hypothesis that there was no linear trend between group order and median time to event was then calculated. Low P-values are indicative of a significant trend between increasing dose and the event being analysed. The threshold for significance was set at $P<0.05$.

[3]The time at which peak body weight occurred for each mouse was analysed after spline smoothing of each animal's body weight values over time (using Prism 5 software) from the start of the study to the time at which the mouse died. If the smoothed body weight curve for an individual mouse had multiple equal peaks, the time point at which the final peak occurred was taken.

4.2.2.3 Effect of metformin on the definitive onset of neurological disease and the change in neurological score over time in male SOD1^{G93A} mice.

The change in the mean combined neurological score (the sum of the neurological score recorded for left and right hind limbs) for male mice in all four groups from 41 days of age, is plotted in **Figure 23A**. Neurological score curves for all male groups were largely similar in shape. Specifically, scores remained low and fairly constant until approximately 104 days of age when they began to sharply increase, indicating the onset of neurological symptoms. This time point is approximately 14 days later than the onset of weight loss shown in **Figure 22A**, indicating that weight loss precedes overt neurological pathology in our SOD1^{G93A} mice. As has previously been described (Gill et al., 2009, Lincecum et al., 2010), we classified the definitive onset of symptomatic neurological disease as the time point at which a mouse reached a neurological score of two in both hindlimbs. Comparison of the time point at which this occurred in all four males groups revealed no statistically significant differences **(Figure 23B, Table 10).**

4.2.2.4 Effect of metformin on survival in male mice

For humane reasons, a uniform end point of the inability of a mouse to right itself within 30s of being placed on a side was used for all mice in this study. The proportion of male mice surviving over time is shown in **(Figure 23C).** There were no statistically significant differences in survival between any groups indicating that metformin had no effect on survival in male mice **(Table 10).**

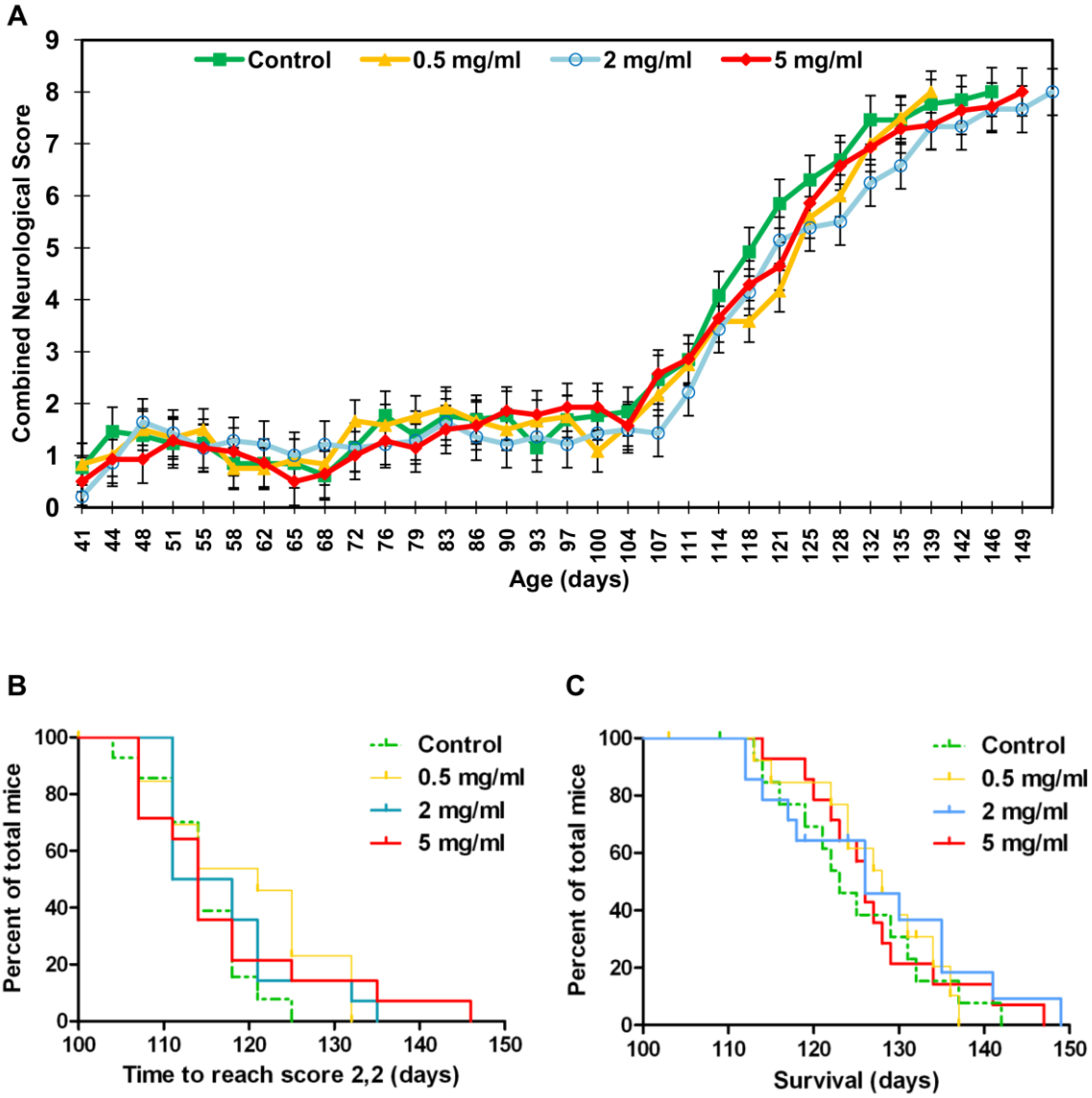


Figure 23: Effect of metformin on neurological score, neurological disease onset and survival in male SOD1^{G93A} mice.

(A) Mean group combined neurological score plotted for male SOD1^{G93A} mice over time from 41 days of age until the date at which the last death within each group occurred. Combined neurological score was calculated for each mouse at each time point through summation of the neurological scores recorded for its left and right hindlimbs. As mice within groups died at different ages, the final combined neurological scores of all mice were carried forward when calculating group mean values, until the date at which the last mouse within each group died. This prevented decomposition of the mean at later stages. Error bars represent standard error of the mean (SEM). (B) Kaplan-Meier survival plot for the time taken for male SOD1^{G93A} mice to reach a neurological score of 2 in both hindlimbs (an indicator of the onset of symptomatic neurological disease). (C) Kaplan-Meier survival plot for the time taken for male SOD1^{G93A} mice to reach the humane end stage of attaining a neurological score of 4 (representative of survival). Graphs (A), (B) and (C) present data for male SOD1^{G93A} mice in all four experimental groups: Control = green, 0.5mg/ml metformin = yellow, 2mg/ml metformin = blue, 5mg/ml metformin = red). Results for statistical analyses performed on data presented in (B) and (C) are given in **Table 10.**

4.2.3 Metformin treatment negatively affected disease onset and progression in female mice in a dose-dependent fashion.

4.2.3.1 N-numbers, weight balancing and non-ALS deaths in female mice

Four groups of 15 female mice that were balanced for age, litter and bodyweight were enrolled in this study. The average starting bodyweights for all groups were within 0.5g of each other (Control: 16.7g, 0.5mg/ml: 16.9g, 2mg/ml: 16.8g and 5mg/ml: 17.2g). Towards the end of the study, one female mouse from the 0.5mg/ml group was injured by a fellow cage mate and was therefore culled. Weight and neurological score data from this mouse were included in weight and neurological score plots up to the date at which she became wounded and she was treated as censored in any Kaplan Meier analyses requiring information about survival. One further female mouse from the 0.5mg/ml group showed abnormally rapid weight loss and signs of discomfort over the course of two days without showing neurological symptoms. She was therefore culled and classed as dying a 'non-ALS death'. Weight and neurological score data from this mouse were not included weight and neurological score plots and she was treated as censored in all Kaplan Meier analyses.

4.2.3.2 Effect of metformin on body weight, disease onset and disease progression in female SOD1^{G93A} mice.

The change in mean body weight over time for female mice in all four groups is plotted in **Figure 24A** from 35 days onwards. As with male mice, weight curves for all groups showed a very similar shape, with the onset of weight decline occurring at approximately 90 days of age. However, female mice in the 0.5 mg/ml group tended to be heavier than mice in other groups between 55 and 135 days of age and female mice in the control group tended to drop

to lower weights at end stage than mice in treatment groups. As with male mice, no significant differences were seen between female groups in the time taken to reach peak weight **(Figure 24B, Table 11)** but unlike male mice, there was a significant association between increasing metformin dose and decreasing time from peak weight to end stage in female mice **(Figure 24C, Table 11, P = 0.0362).** This indicates that metformin had a negative effect on disease progression in female mice.

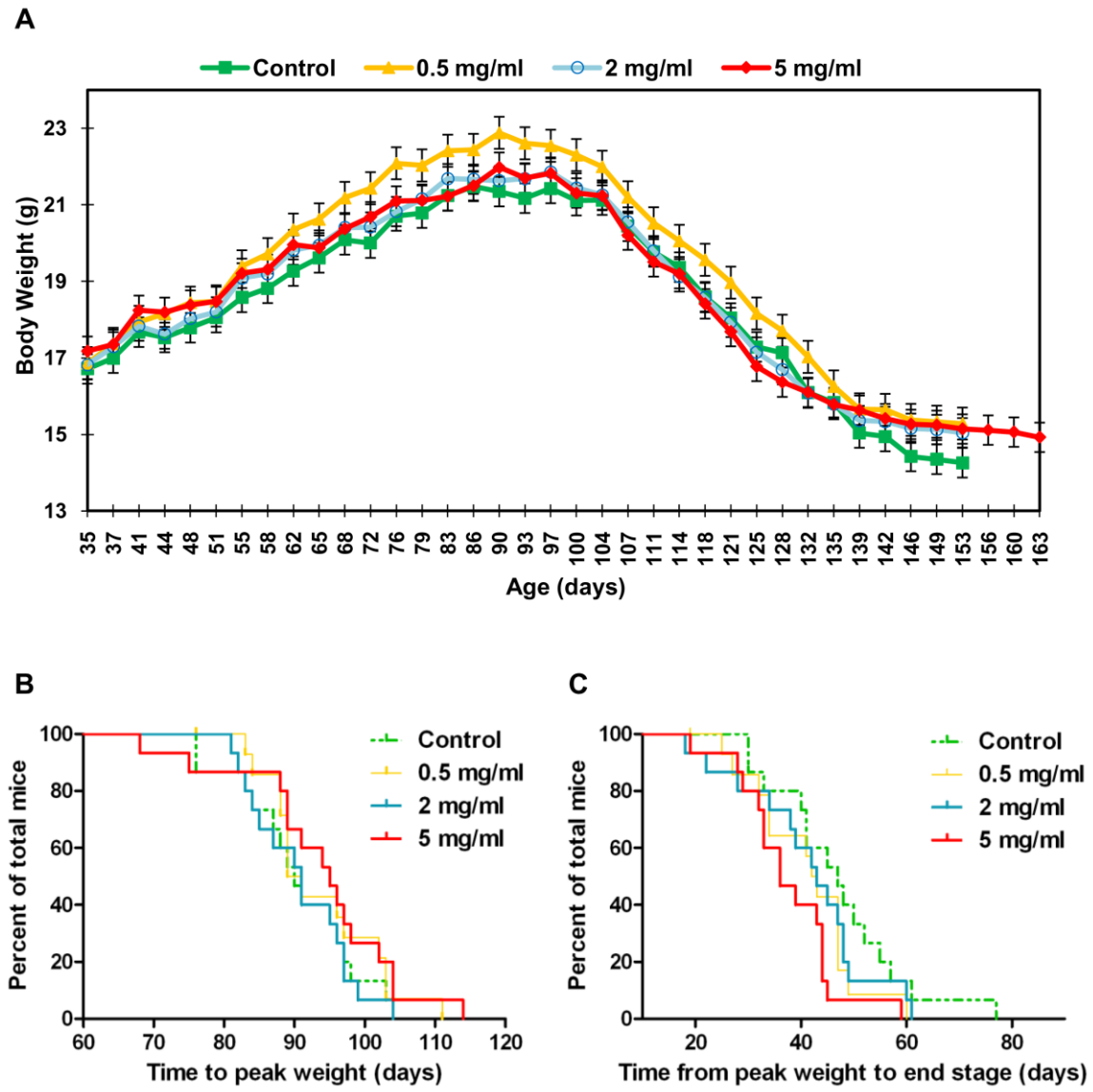


Figure 24: Effect of metformin on body weight, disease onset and disease progression in female SOD1^{G93A} mice.

(A) Mean group body weight plotted for female SOD1^{G93A} mice over time from 35 days of age until the date at which the last death within each individual group occurred. As mice within groups died at different ages, the final weights of all mice were carried forward when calculating group mean values, until the date at which the last mouse within each group died. This prevented decomposition of the mean at later stages. Error bars represent the standard error of the mean (SEM). (B) Kaplan-Meier survival plot for time to peak weight (an indicator of disease onset) in female SOD1^{G93A} mice. (C) Kaplan-Meier survival plot for time from peak weight to end stage (an indicator of disease progression) in female SOD1^{G93A} mice. Graphs (A), (B) and (C) present data for female SOD1^{G93A} mice in all four experimental groups: Control = green, 0.5mg/ml metformin = yellow, 2mg/ml metformin = blue, 5mg/ml metformin = red). Results for statistical analyses performed on data presented in (B) and (C) are given in **Table 11**.

Table 11: Kaplan Meier time to event analyses for female SOD1^{G93A} mice[1, 2, 3]

	Median Value (days)				P Value	
	Control	**0.5 mg/ml**	**2 mg/ml**	**5 mg/ml**	**Log-rank**	**Log-rank test for trend**
Time to peak weight	90	90	91	95	0.5418	0.3664
Time from peak weight to end stage	47	42.5	43	36	0.1149	0.0362 Significant
Time to reach score 2 in both hindlimbs	132	125	118	118	0.0991	0.0236 Significant
Survival	140	136	132	132	0.6216	0.1964

[1]The Logrank test investigates the null hypothesis that that the Kaplan Meier curves for all groups are identical (i.e. that the treatment did not change the time taken to reach the event being analysed). Low P-values are therefore indicative of differences between curves that did not occur due to chance. The threshold for significance was set at $P<0.05$.

[2] To perform the log-rank test for trend, experimental groups were arranged in order of increasing dose (Control, then 0,5mg/ml, 2mg/ml and 5mg/ml) and a P value testing the null hypothesis that there was no linear trend between group order and median time to event was then calculated. Low P-values are indicative of a significant trend between increasing dose and the event being analysed. The threshold for significance was set at $P<0.05$.

[3]The time at which peak body weight occurred for each mouse was analysed after spline smoothing of each animal's body weight values over time (using Prism 5 software) from the start of the study to the time at which the mouse died. If the smoothed body weight curve for an individual mouse had multiple equal peaks, the time point at which the final peak occurred was taken.

4.2.3.3 Effect of metformin on the definitive onset of neurological disease and the change in neurological score over time in female SOD1^{G93A} mice.

The change in the mean combined neurological score (the sum of the neurological score recorded for left and right hind limbs) for female mice in all four groups from 41 days of age, is plotted in **Figure 25A**. Neurological score curves for female mice in all groups were similar in shape until approximately 104 days of age when, as with male mice, the onset of neurological symptoms began. Following this point, however, neurological score curves began to rise more steeply with increasing metformin dose, suggesting a negative effect of metformin on disease progression. In support of this there was a significant association between increasing metformin dose and the time point at which female mice reached a score of 2 in both hindlimbs (the definitive onset of symptomatic disease) **(Figure 25B, Table 11, P = 0.0236).**

4.2.3.4 Effect of metformin on survival in female mice

The proportion of female mice surviving over time is shown in **(Figure 25C)**. Although there were no significant differences in survival between groups **(Table 11)**, there was a trend towards increasing survival with decreasing metformin dose.

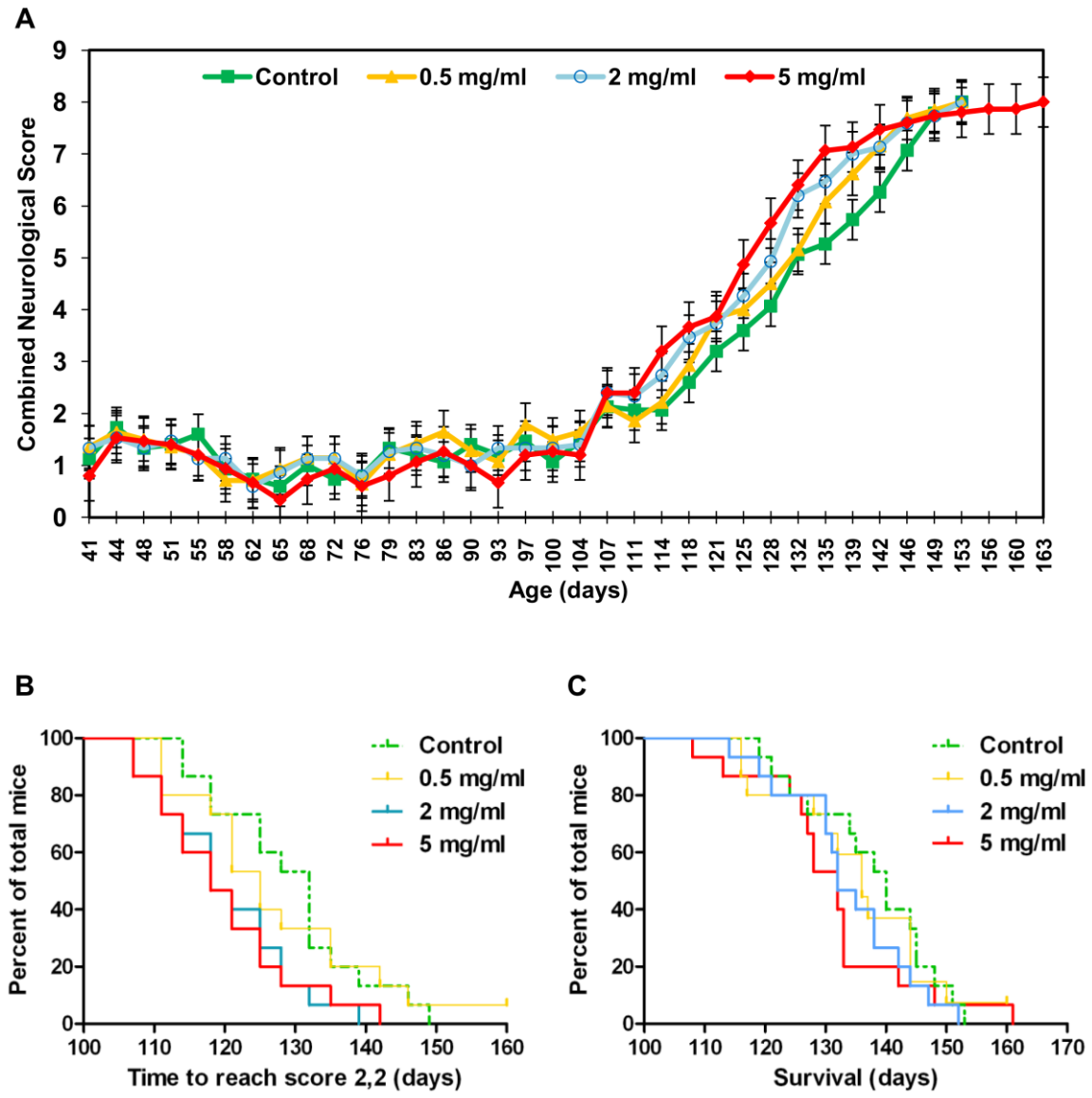


Figure 25: Effect of metformin on neurological score, neurological disease onset and survival in female SOD1^{G93A} mice.

(A) Mean group combined neurological score plotted for female SOD1^{G93A} mice over time from 41 days of age until the date at which the last death within each group occurred. Combined neurological score was calculated for each mouse at each time point through summation of the neurological scores recorded for its left and right hindlimbs. As mice within groups died at different ages, the final combined neurological scores of all mice were carried forward when calculating group mean values, until the date at which the last mouse within each group died. This prevented decomposition of the mean at later stages. Error bars represent standard error of the mean (SEM). (B) Kaplan-Meier survival plot for the time taken for female SOD1^{G93A} mice to reach a neurological score of 2 in both hindlimbs (an indicator of the onset of symptomatic neurological disease). (C) Kaplan-Meier survival plot for the time taken for female SOD1^{G93A} mice to reach the humane end stage of attaining a neurological score of 4 (representative of survival). Graphs (A), (B) and (C) present data for female SOD1^{G93A} mice in all four experimental groups: Control = green, 0.5mg/ml metformin = yellow, 2mg/ml metformin = blue, 5mg/ml metformin = red). Results for statistical analyses performed on data presented in (B) and (C) are given in Table 11.

4.2.4 Effect of metformin on survival in female mice

Our observations of a significant association between increasing metformin dose and earlier onset of symptomatic neurological disease as well as faster disease progression in female $SOD1^{G93A}$ mice suggested to us that metformin may have interacted in a negative fashion with a female specific cellular process that is normally beneficial for motor neuron health. It is well documented that female $SOD1^{G93A}$ mice develop neurological symptoms later and have a longer lifespan than male $SOD1^{G93A}$ mice and this was also found to be the case in our survival study **(Figure 26A and 26B, Tables 12 and 13).** Specifically, median onset of symptomatic neurological disease was 18 days later in control female mice than in their male counterparts (132 vs. 114, P = 0.0001) and median survival was extended by 17 days (140 vs. 123, P = 0.0011). Interestingly, prevention of oestrogen production in female $SOD1^{G93A}$ mice via ovariectomy has been shown to accelerate disease progression (Choi et al., 2008) and also to reduce survival time to levels comparable to male $SOD1^{G93A}$ mice (Groeneveld et al., 2004b, Choi et al., 2008) . Furthermore treatment of these ovariectomised females with 17β-oestradiol (the most potent mammalian form of oestrogen (Barha et al., 2009)) has been shown to rescue these effects (Choi et al., 2008). This suggests that the presence of oestrogen is a large contributing factor to the slower disease progression and increased lifespan of female $SOD1^{G93A}$ mice compared to males. Metformin is increasingly becoming prescribed for the treatment of polycystic ovary syndrome (PCOS) with the aim of reducing the insulin resistance that is associated with the disorder. Interestingly, it has recently been identified that metformin is also able to inhibit basal and insulin-stimulated 17β-ostradiol production and that this may contribute to its beneficial effect in PCOS (Rice et al., 2009, Mansfield et al., 2003). In light of the beneficial effect of oestrogen on disease progression and survival in female $SOD1^{G93A}$ mice and the documented ability of metformin to inhibit 17β-ostradiol

production, it seemed likely to us that the negative effects of metformin seen in female mice in our study were at least in part derived from reduced 17β-ostradiol production. In support of this, treatment of female SOD1^{G93A} mice with either 2 or 5 mg/ml metformin in our survival study, prevented the significant delay in the onset of symptomatic neurological disease seen in female control mice compared to male control mice **(Figure 26A, Table 13)**. Furthermore, treatment of female SOD1^{G93A} mice with metformin at all doses negated the significant increase in survival seen in female control mice compared to male control mice and this effect became more pronounced with increasing metformin dose **(Figure 26B, Table 13).**

In order to test the hypothesis that metformin treatment brought about a reduction in plasma 17β-estradiol levels in female SOD1^{G93A} mice in our survival study, we treated an additional cohort of female SOD1^{G93A} mice with 2mg/ml metformin from 35 days of age and measured the concentration of 17β-estradiol in their blood serum at 70 days of age using a 125 Iodine-based radioimmuno assay (kindly performed for us by Dr Zhangrui Cheng at the Royal Veterinary College). The results of this assay are shown in **Figure 27A**. In support of our hypothesis, metformin treatment brought about a significant reduction in serum 17β-estradiol levels in metformin treated female SOD1^{G93A} mice compared to control female SOD1^{G93A} mice (6.4 +/- 0.2 pg/ml in treated SOD1^{G93A} females (n=4) vs. 7.1 +/- 0.15 pg/ml in control SOD1^{G93A} females (n=8), P =0.0164). We also investigated the effect of metformin treatment via the same dosing regimen on female WT mice at 70 days of age. As with SOD1^{G93A} mice, metformin brought about a significant reduction in plasma 17β-estradiol levels in treated female WT mice compared to control female WT mice (5.9 +/- 0.3 pg/ml in treated WT females (n=7) vs. 6.7 +/- 0.2 pg/ml in control WT females (n=10), P =0.0287) **(Figure 27)**.

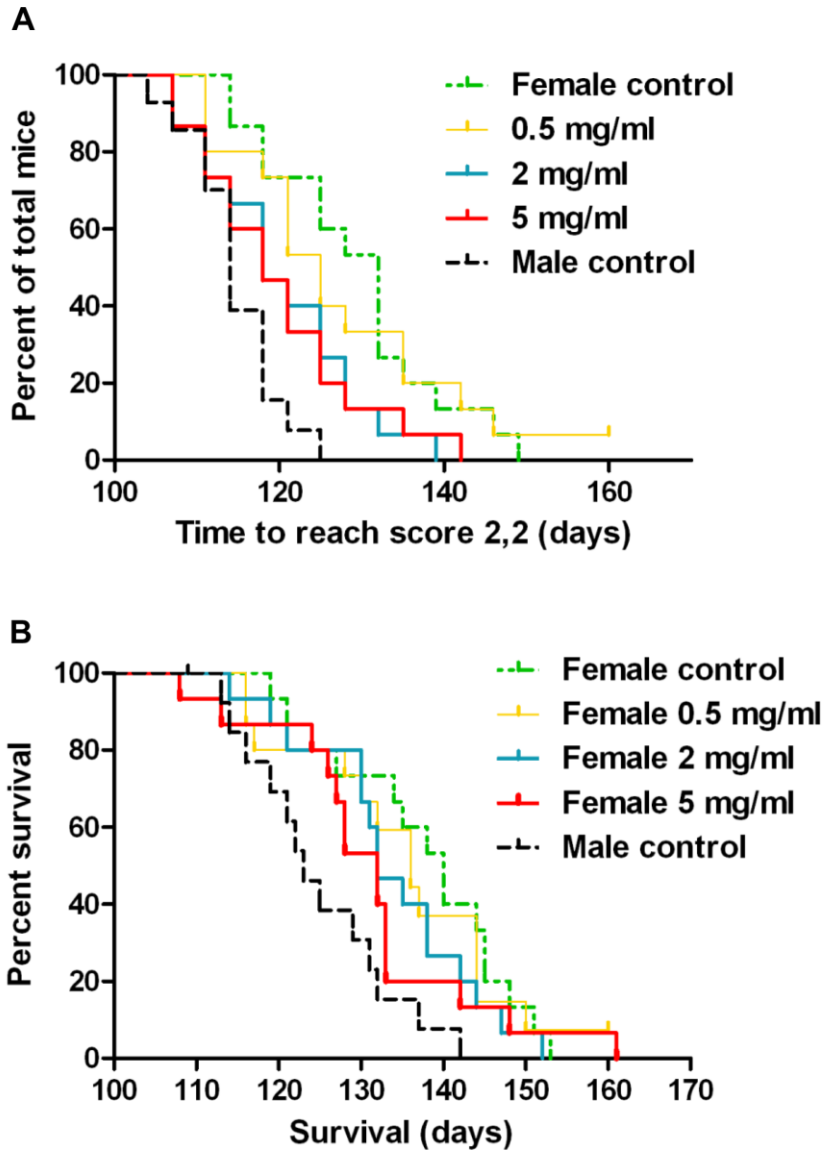


Figure 26: Comparison of the definitive onset of symptomatic neurological disease and survival in control and metformin-treated female mice and male control mice.

Kaplan-Meier time to event plots for (A) time taken for mice to reach a score of 2 in both hindlimbs (the definitive onset of symptomatic neurological disease) and (B) time taken for mice to reach the humane end stage of the inability to right within 30s of being placed on a side (survival) for all female groups and the male control group. Female mice were treated with normal drinking water (control, green) or 0.5 (yellow), 2 (blue) or 5 (red) mg/ml metformin in the drinking water from 35 days of age. Male control mice (black) received normal drinking water throughout.

Table 12: Summary of median time to reach score 2,2 and median survival for all female groups and the male control group.

	Median Value (days)				
	Female control	**Female 0.5mg/ml**	**Female 2mg/ml**	**Female 5mg/ml**	**Male Control**
Time to reach score 2,2	132	125	118	118	114
Survival	140	136	132	132	123

Median values derived from Kaplan Meier analyses for the time taken for mice to reach a score of 2 in both hindlimbs and the time taken for mice to reach the humane end stage of the inability to right within 30s of being placed on a side (survival) for all female groups (control, 0.5, 2 and 5 mg/ml metformin) and the male control group.

Table 13: Summary of statistical analyses performed to compare the time taken for mice to reach a score of 2 in both hindlimbs and the time taken for mice to reach the humane end stage of the inability to right within 30s of being placed on a side between all groups.

	P Value, Time to reach score 2,2, log-rank test	P Value, Survival, log-rank test
All male and female groups	0.0317 Significant	0.0190 Significant
Male control vs. female control	0.0001 Significant	0.0011 Significant
Male control vs. female 0.5mg/ml	0.0014 Significant	0.0078
Male control vs. female 2mg/ml	0.0416	0.0179
Male control vs. female 5 mg/ml	0.0804	0.0870

The Logrank test investigates the null hypothesis that that the Kaplan Meier curves for all groups are identical. Low P-values are therefore indicative of differences between groups that did not occur due to chance. Statistical comparison of the time taken for mice to reach a score of 2 in both hindlimbs and the time taken for mice to reach the humane end stage (survival) in all four male and female groups via a log rank test revealed that there were significant differences between the groups for both measures. The threshold for significance was set at $P<0.05$ for these comparisons. Subsequent post hoc comparisons between pairs of groups for both measures were then performed. Using Bonferroni's correction for multiple comparisons we calculated that P must be less than 0.0018 (i.e. $P= <0.05/28$, where 28 represents the number of possible pairwise comparisons for 8 different experimental groups) in order to be significant in these pairwise comparisons.

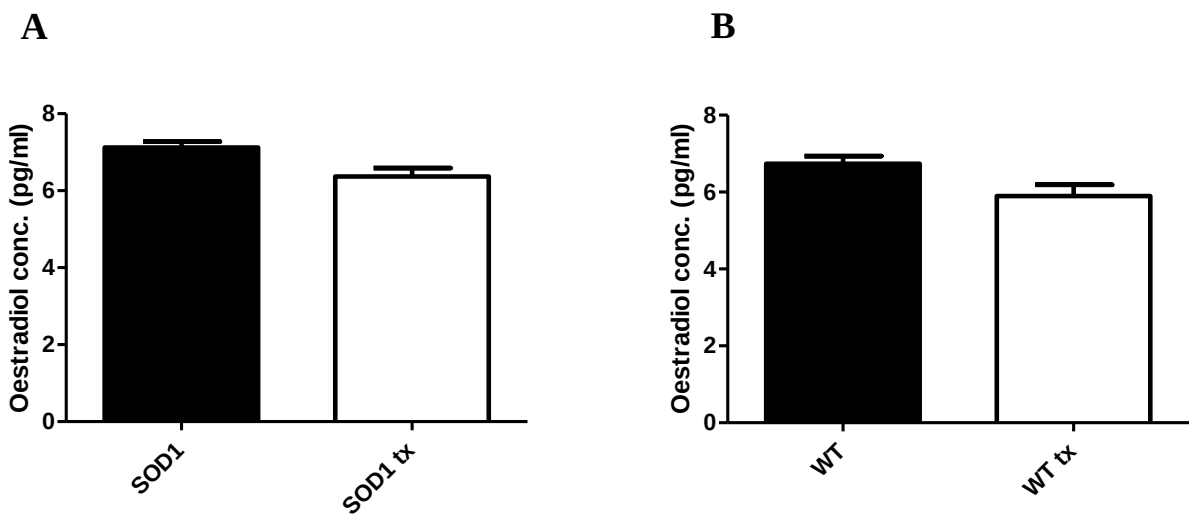


Figure 27: Comparison serum 17β-estradiol levels in control and metformin-treated (A) SOD1^{G93A} and (B) WT female mice at 70 days.

SOD1^{G93A} and WT mice were treated with metformin in the drinking water from 35 days of age. Control SOD1^{G93A} and WT mice received normal drinking water throughout. Plasma 17β-estradiol levels were measured in blood serum collected from all mice at 70 days of age via a 125 Iodine-based radioimmuno assay (RIA). 17β-estradiol levels were compared in control and treated SOD1^{G93A} mice and control and treated WT mice via individual unpaired t-tests. Metformin was shown to significantly reduce plasma 17β-estradiol levels in both SOD1^{G93A} mice and WT mice (7.1 +/- 0.15 pg/ml control SOD1^{G93A} females (n=8) vs. 6.4 +/- 0.2 pg/ml treated SOD1^{G93A} females (n=4), P =0.0164 and 6.7 +/- 0.2 pg/ml control WT females (n=10) vs. 5.9 +/- 0.3 pg/ml treated WT females (n=7), P =0.0287).

4.4 Discussion

The aim of this study was to test the hypothesis that the anti-type II diabetes drug, metformin, could delay disease onset, slow disease progression and increase survival in the $SOD1^{G93A}$ murine model of ALS. Our reasoning behind this hypothesis was that we had previously observed treatment of $SOD1^{G93A}$ mice with 2mg/ml metformin in the drinking water from 35 days of age to bring about a significant increase in the survival of functional motor units in male EDL muscles and female TA muscles. We also observed strong trends towards increased motor unit survival in male TA muscles and female EDL muscles in these studies. As the ultimate cause of death in $SOD1^{G93A}$ mice is the retraction of distal motor axons and denervation of skeletal muscles (Gould et al., 2006, Dadon-Nachum et al., 2011), we felt that increasing the survival of functional motor units in these mice was likely to have an impact on their disease course. Our original decision to test the potential protective properties of metformin in $SOD1^{G93A}$ mice was based on its known anti-inflammatory (Dandona et al., 2004, Isoda et al., 2006, Lin et al., 2000) and antioxidant (Lin et al., 2000, Ouslimani et al., 2005, Srividhya et al., 2002) properties as well as the ability to bring about mitochondrial biogenesis (Kukidome et al., 2006). We were further encouraged by studies documenting the ability of metformin to attenuate pathology in mouse models of Huntington's disease (Ma et al., 2007) and multiple sclerosis (Nath et al., 2009) which, like ALS models, show central nervous system (CNS)-based inflammation, oxidative stress and mitochondrial abnormalities (Beal and Ferrante, 2004, Stadelmann, 2011, Ilieva et al., 2009). In order to test the ability of metformin to delay disease onset, slow disease progression and increase survival in $SOD1^{G93A}$ mice, we performed a blinded, dose-response survival study in which mice were treated with normal drinking water or 0.5, 2 or 5 mg/ml metformin in the drinking water from 35 days of age. Disease onset and progression were analysed via twice weekly monitoring of

weight and neurological score and survival was determined as the age at which mice could no longer right themselves within 30s of being placed on a side.

Despite seeing small but significant increases in motor unit survival with metformin treatment in our initial investigations, we surprised to see no significant beneficial effects of metformin treatment on disease onset, progression or survival in male or female SOD1^{G93A} mice at any of the doses tested. Furthermore, we saw a dose dependent negative effect on the definitive onset of symptomatic neurological disease as well as disease progression in female SOD1^{G93A} mice. This could suggest that the increases in motor unit survival seen in our electrophysiology study were not large enough to have a significant long-term impact on overall pathology or that they could not be maintained long-term. This is supported by the fact that we did not see any significant increases in the maximal or specific forces of the TA and EDL muscles of SOD1^{G93A} mice treated with 2mg/ml metformin in our initial studies. However, we also cannot rule out the possibility that force increases resulting from increased motor unit survival were prevented partially or completely by muscles becoming slower and thus weaker in phenotype, through a metformin-induced activation/upregulation of PGC1α (as discussed in **Chapter 3**). An additional possibility is that at the early symptomatic time point of 100 days of age, when increases in motor unit survival were seen in our initial electrophysiology study, metformin-induced beneficial effects outweighed toxic effects and were therefore able to reduce motor unit loss. Whereas, at the later symptomatic time points reached in our survival study, these metformin-induced trophic effects were overshadowed by advancing and aggressive SOD1^{G93A} pathology and potentially negative drug effects, thus preventing overall beneficial effects on disease course. When considering potential reasons for why metformin was unable to bring about long-term benefits in SOD1^{G93A} mice despite

its anti-inflammatory and anti-oxidant properties and ability to induce mitochondrial biogenesis, it is important to highlight that this drug has been identified as having many other cellular effects in addition to these. It is therefore possible that some of these additional effects could have been detrimental to $SOD1^{G93A}$ mice. Metformin has for example been shown to inhibit mitochondrial complex one (Brunmair et al., 2004), which is already compromised as a result of ALS pathology (Ferri et al., 2006) and also to bring about a reduction in both total-and LDL-cholesterol levels, high levels of which have paradoxically been shown to be a positive prognostic factor in ALS patients (Dupuis et al., 2008).

A final explanation for the surprising absence of beneficial effects of metformin treatment in our survival study is that the increases in motor unit survival seen with metformin treatment in our electrophysiology study were actually the result of inherent variations between mice, rather than a beneficial effect of metformin treatment. We unfortunately did not perform weight and littermate balancing of $SOD1^{G93A}$ mice in this electrophysiology study as the importance of doing this was only established when we began researching optimal experimental designs for our subsequent survival study. Consequently, we cannot rule out the possibility that the results we saw were caused by the effects of litter clustering. Additionally, motor unit data was unfortunately lost from several control $SOD1^{G93A}$ mice in our electrophysiology study, due to files containing this data becoming corrupted. These assessments were therefore not as high powered as we would have liked. In light of this, it is critical that any future electrophysiology studies are high powered and designed to minimize variation associated with performing experiments in mice with a mixed-hybrid genetic background. Regardless of the reason(s) for the disparity between the positive results seen in our initial study and the lack of benefit of metformin treatment in our survival study, these

observations highlight that it is essential to perform robust survival studies with longitudinal monitoring of disease onset and progression to gain a clear picture of the potential of a drug for the treatment of ALS.

Our observations of a significant association between increasing metformin dose and earlier onset of symptomatic neurological disease as well as faster disease progression in female $SOD1^{G93A}$ mice, lead us to investigate the possibility that metformin inhibited the production of 17β-estradiol in treated female $SOD1^{G93A}$ mice. Our reasoning behind this was that metformin has been shown inhibit 17β-estradiol production in cultured human cells (Rice et al., 2009, Mansfield et al., 2003) and 17β-estradiol production in female $SOD1^{G93A}$ mice is thought to be a large contributing factor to their delayed disease onset and increased survival time compared to male $SOD1^{G93A}$ mice (Choi et al., 2008, Groeneveld et al., 2004b). In our experiments we observed that treatment with 2mg/ml metformin in the drinking water from 35 days of age brought about a significant reduction in plasma 17β-estradiol levels in both female $SOD1^{G93A}$ and female WT mice at 70 days of age. Considering the documented protective effects of 17β-estradiol in female SOD1 mice, (Choi et al., 2008, Groeneveld et al., 2004b) it seems likely that the dose-dependent negative effects of metformin in female $SOD1^{G93A}$ mice in our survival study were at least partially derived from a metformin-induced reduction in 17β-estradiol production. It is also interesting to note that despite showing beneficial effects in male mice in the R6/2 model of Huntington's disease, metformin had no beneficial effect in female mice. Furthermore, 17β-estradiol has been postulated to be the reason for a less severe pathology in female rats compared to male rats in a transgenic model of Huntington's disease (Bode et al., 2008) and has been shown reduce oxidative stress in a rodent experimental model of this disease (Túnez et al., 2006). These

observations further support a role for reduced 17β-ostradiol production in the dose-dependent negative effects of metformin in our female SOD1^{G93A} mice.

Finally, it is interesting to note that as with the 2mg/ml metformin dose used in our electrophysiology study, all doses of metformin appeared to bring about an overall reduction in the weight of male SOD1^{G93A} mice in our survival study. Considering the high powered nature of our survival study and the fact that all groups were balanced for weight and litter, it seems highly likely that this is a true trend. Additionally, as in our electrophysiology study, female SOD1^{G93A} mice in our survival did not appear to experience the same overall metformin-induced reduction in weight as male mice. Interestingly, several studies have suggested that metformin may bring about weight loss in obese patients with type II-diabetes though suppression of appetite (Lee and Morley, 1998, Stumvoll et al., 1995). It would therefore be interesting to investigate whether treatment of male SOD1^{G93A} mice with metformin brings about a reduction in food consumption as this could at least partially explain the overall reduction in weight seen in metformin-treated male SOD1^{G93A} mice. Surprisingly however, Stumvoll and colleagues observed a clear metformin-induced reduction in appetite in obese female type II diabetes patients in their study (Stumvoll et al., 1995). Consequently, if a reduction in food consumption was the reason for the lower weights of metformin-treated male SOD1^{G93A} mice in our study, it is surprising that lower weights were not also seen in female SOD1^{G93A} mice. Clearly metformin interacted differently with the gene expression and hormone systems in male and female SOD1^{G93A} mice in our study.

In conclusion, we have shown that despite showing promise in mouse models of Huntington's disease and multiple sclerosis, in which similar pathological process have been

implicated to SOD1^{G93A} mice, metformin is not capable of delaying disease onset, slowing disease progression or increasing survival in these animals. Furthermore, metformin appears to be harmful in female SOD1^{G93A} mice in a dose dependent fashion and we hypothesise that this effect may be derived from its ability to inhibit oestrogen production. This could have implications for the prescription of medication to female ALS patients suffering from type II diabetes as metformin could potentially worsen their prognosis. However this situation is likely to be complex as a recent retrospective study of ALS patients with pre-morbid diabetes mellitus has suggested a positive effect of diabetes on the age of ALS onset (Jawaid et al., 2010) . Further investigations into the relationship between ALS and diabetes and the way in which metformin treatment modifies this relationship are therefore required.

5. Trehalose Survival Study

5.1 Introduction

Amyotrophic Lateral Sclerosis is a fatal neurodegenerative disorder associated with the selective degeneration of upper and lower motor neurons, that is currently lacking in effective therapeutics (Cozzolino et al., 2008b). Although the majority of ALS cases are sporadic, approximately 10% have a familial origin and of these 15-20% are caused by gain of function mutations in the copper/zinc superoxide dismutase (SOD1) gene (OMIM 147450) (Rosen et al., 1993c). The mechanisms by which mutations in SOD1 cause ALS remain unknown, however a common feature of ALS-causing mutant SOD1 proteins is their propensity to misfold and aggregate in motor neurons (Wang et al., 2008b, Shaw et al., 2008, Wang et al., 2002a). SOD1 is a 32 kDa homodimeric enzyme composed of two monomeric eight-stranded beta barrels, each with a binding site for one copper ion and one zinc ion (Rakhit and Chakrabartty, 2006). Aggregation of mutant SOD1 species is thought to be a multi-step process involving sequential protein monomerisation, demetallation and oligomerisation (Khare et al., 2004, Kerman et al., 2010, Rakhit et al., 2007) . Although this remains a matter of debate, several lines of evidence suggest that mutant SOD1 aggregates or intermediates in the aggregation process may be toxic to motor neurons. Wang et al., have for example demonstrated that the aggregation propensity and stability of different mutant forms of SOD1 in a cohort of familial ALS patients, could together account for 69% of the variability in patient survival time (Wang et al., 2008b) and Lindberg et al., have also reported similar results (Lindberg et al., 2005). Furthermore, strong correlations between disease progression and the levels of insoluble mutant SOD1 species present in affected neuromuscular tissues have been observed in various murine SOD1-based models (Johnston et al., 2000, Wang et

al., 2002a, Wang et al., 2005, Turner et al., 2003c). Several mechanisms have been proposed by which misfolded and/or aggregated species of mutant SOD1 in motor neurons may contribute to ALS pathology. These include but are not limited to: aggregation of mutant SOD1 onto the outer mitochondrial membrane and thus potential impairment of mitochondrial function (Vande Velde et al., 2008, Duffy et al., 2011, Pedrini et al., 2010), induction of ER stress (Wang et al., 2011, Atkin et al., 2006) and impairment of axonal transport (Bilsland et al., 2010). Although evidence exists for all of these mechanisms, their relative importance for ALS pathology remains to be confirmed.

Trehalose is natural non-reducing disaccharide found in many non-mammalian species (Singer and Lindquist, 1998). In these organisms it functions to protect cells against environmental insults such as heat, cold, dehydration and oxidation, through its ability to act as a chemical chaperone and prevent protein denaturation and aggregation (Chen and Haddad, 2004, Singer and Lindquist, 1998). The stabilization of proteins by trehalose is thought to be derived at least in part from its ability to increase solvent surface tension. This increase in surface tension is thought to raise the energy required by proteins to bring about cavity formation within the solvent in order to accommodate their enlarged surface area upon denaturation (Kaushik and Bhat, 2003).

Protein aggregation is a unifying theme in many neurodegenerative disorders including Alzheimer's disease, prion diseases, Parkinson's disease, and polyglutamine disorders such as Huntington's disease (Sarkar and Rubinsztein, 2008). As a result of its protein stabilizing properties, and also its proven safety for consumption in humans (Richards et al., 2002), trehalose has been evaluated as a potential therapeutic for a number of these disorders. It has

for example been shown to prevent aggregation of β-amyloid species associated with Alzheimer's disease (Liu et al., 2009, Izmitli et al., 2011), to impair prion protein aggregation (Béranger et al., 2008), to ameliorate dopaminergic and tau pathology in parkin deleted/tau overexpressing mice (Rodríguez-Navarro et al., 2010) and also to improve motor function and extend lifespan in the R6/2 model of Huntington's disease (Tanaka et al., 2004).

In addition to its actions as a chemical chaperone, trehalose has more recently been shown to have the ability to activate macroautophagy (hitherto referred to as autophagy) in an mTOR-independent fashion (Sarkar et al., 2007). Autophagy is a cellular process that involves the formation of double membrane-bound structures called autophagosomes around portions of cytoplasm and associated organelles. These autophagosomes then fuse with lysosomes, in order to permit degradation of their contents (Yang and Klionsky, 2010). Autophagy plays a critical role in intracellular organelle homeostasis and is also employed in conditions of starvation to maintain cellular nutrient levels (Yang and Klionsky, 2010). Furthermore, autophagy has been shown to play an essential role in the removal of toxic/aggregated proteins and damaged organelles such as mitochondria that may cause toxicity to cells under conditions of stress(Metcalf et al., 2010). Consequently, it has been shown that beneficial effects of trehalose on the clearance of aggregates in cellular models of Huntington's disease and on dopaminergic and tau pathology in parkin deleted/tau overexpressing mice, were derived from autophagy activation as well as protein stabilisation (Sarkar et al., 2007, Rodríguez-Navarro et al., 2010)

Like, mutant Huntington and tau, various mutant SOD1 proteins (A4V, G85R, and G93A) have been shown to be degraded by autophagy in vitro (Kabuta et al., 2006) and furthermore,

markers of autophagy have been shown to be increased in the spinal cords of SOD1^{G93A} mice compared to wild-type (WT) mice (Morimoto et al., 2007, Li et al., 2008). Although the exact role of autophagy in the pathology of SOD1^{G93A} mice remains to be established, it has been suggested that upregulation of autophagy could be a protective mechanism to clear potentially toxic mutant SOD1 oligomeric species and aggregates (Kabuta et al., 2006, Morimoto et al., 2007).

In light of the documented beneficial effects of trehalose in culture and *in vivo* models of various neurodegenerative diseases involving protein aggregation (Béranger et al., 2008, Liu et al., 2009, Rodríguez-Navarro et al., 2010, Sarkar et al., 2007, Tanaka et al., 2004), we hypothesized that it may delay disease onset and progression and increase survival in the SOD1^{G93A} mouse model of ALS. This hypothesis was supported by experiments in which treatment of NSC-34 cells (a mouse motor-neuron-like cell line) transiently transfected with human SOD1^{G93A}, brought about a significant reduction in mutant SOD1 aggregate formation and detergent insolubility (Gomes et al., 2010). We tested our hypothesis by treating SOD1^{G93A} mice (n=15 male and 15 female, age weight and litter-mate balanced mice per group) with either normal drinking water or 0.5%, 2% or 5% weight for volume (w/v) trehalose in the drinking water from 35 days of age. Disease onset and progression were assessed in a blinded fashion by twice weekly monitoring of weight and neurological score as previously described (Chapter 4) (Gill et al., 2009, Lincecum et al., 2010). Survival was determined as the time point at which mice could no longer right themselves within 20s of being placed on a side.

Interestingly, protein misfolding and aggregation is not limited to cases of ALS-resulting from mutations in SOD1. Indeed, the formation of inclusion bodies consisting of aggregated and unbiquitinated proteins has long been recognised as a hallmark of both sporadic and familial forms of ALS (Migheli et al., 1990, LEIGH et al., 1991). In recent years it has emerged that the key component of inclusion bodies in the majority of sporadic ALS cases is the RNA-binding protein TDP-43 (Neumann et al., 2006a, Arai et al., 2006b). Furthermore, in those sporadic ALS cases where inclusion bodies are negative for TDP-43, these inclusions are usually largely composed of another RNA-binding protein FUS/TLS (Kwiatkowski et al., 2009, Vance et al., 2009). Although mutations in the genes coding for TDP-43 (*TARDBP)* and FUS/TLS (*FUS/TLS*) are not required to bring about their aggregation in ALS patients, mutations in these genes have subsequently been found to be causative for ALS (Gitcho et al., 2008, Kabashi et al., 2008a, Sreedharan et al., 2008, Yokoseki et al., 2008, Kwiatkowski et al., 2009, Vance et al., 2009). Indeed mutations in *TARDBP* are thought to account for 5–10% of classic familial ALS cases whereas mutations in *FUS/TLS* account for 5% (Kiernan et al., 2011). As with mutant SOD1 aggregates in familial ALS, it is not clear whether TDP-43 or FUS aggregates (or intermediates in the aggregation process) are toxic to motor neurons (see Chapter 1, section 1.4.2.2). However, when researching trehalose as a potential therapeutic for ALS, we hypothesised that if TDP-43 or FUS/TLS aggregates or soluble oligomers were found to be toxic to neurons, and trehalose treatment was able to bring about beneficial effects in our $SOD1^{G93A}$ mice, then trehalose may also have beneficial effects in recently developed TDP-43 and FUS/TLS models. We reasoned that if trehalose was shown to be beneficial in SOD1, TDP-43 and FUS/TLS- related models, then this would make it an exciting therapeutic to take forward to clinical trial as it would have the potential to be of benefit to patients with sporadic and familial ALS.

Surprisingly however, trehalose had no effect on disease onset, progression or survival in female SOD1^{G93A} mice in our study. Additionally, despite bringing about a dose-dependent delay in the onset of weight loss in male mice, trehalose was unable to delay the onset of overt neurological symptoms, slow disease progression or increase survival in these males. Using a conformation-specific antibody (USOD), that specifically recognizes misfolded/aggregated SOD1 species in which the copper ion has been lost, the beta barrel structure is disrupted and the hydrophobic core is exposed (Kerman et al., 2010), we determined that trehalose treatment (5% w/v), was unable to reduce the number of motor neurons containing misfolded/aggregated SOD1 in the sciatic motor pool of SOD1^{G93A} mice at 75 days of age. Instead a trend towards increased numbers of motor neurons containing misfolded/aggregated SOD1 was seen in both male and female SOD1 mice. Motor neuron counts revealed that this was not the result of an increase in the number of surviving motor neurons. We concluded that orally administered trehalose is not protective for the motor neurons of SOD1^{G93A} mice and furthermore that it may increase the accumulation of misfolded/aggregated mutant SOD1, potentially through exacerbation of a pre-existing impairment in the autophagy system. These results are discussed in detail below.

5.2 Results

5.2.1 Copy number variations

No SOD1^{G93A} mice with outlying disease progression or survival characteristics with respect to other mice in their experimental groups were identified in this study. We therefore concluded that copy number variation assessments were not required for mice in this study.

5.2.2 Trehalose treatment had no effect on the onset of neurological symptoms, disease progression or survival in male mice but brought about a dose-dependent delay in weight loss.

5.2.2.1 N-numbers, weight balancing and non-ALS deaths in male mice

Four groups of 15 male mice that were balanced for age, litter and body weight were enrolled in this study. No non-ALS deaths or injuries occurred in male mice and hence data from all male mice were included in analyses. The average starting bodyweights for each group were within 0.35g of each other (Control: 20.55g, 0.5%: 20.77g, 2%: 20.83g and 5%: 20.48g).

5.2.2.2 Effect of trehalose on body weight, disease onset and disease progression in male SOD1^{G93A} mice.

The change in mean body weight over time for all male groups is plotted in **Figure 28A** from 46 days onwards. Although weight curves for all male groups displayed a classic SOD1^{G93A} shape involving weight gain, followed by progressive weight loss from approximately 85 days of age until death, trehalose-treated mice appeared to lose weight at an initially slower rate than control mice. This was confirmed by Kaplan Meier analysis of the time to reach

peak weight in all male groups, in which there was a significant trend between increasing trehalose dose and later onset of weight loss **(Figure 28B, Table 14, P = 0.0353 logrank test for trend).** Although all trehalose-treated male mice appeared to have a shorter time from peak weight to end stage than control mice **(Figure 28C, Table 14)**, this trend was not significant.

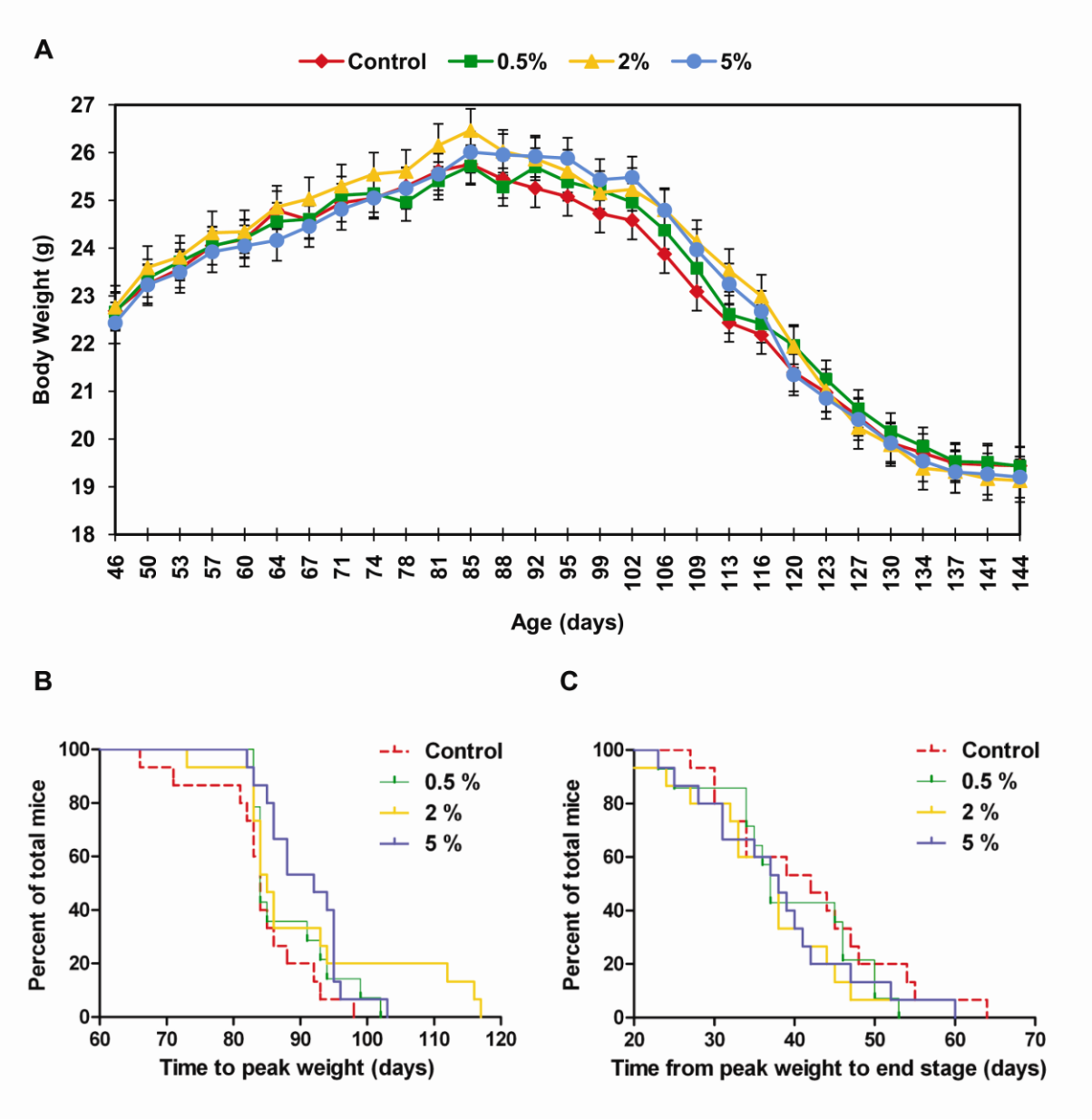


Figure28: Effect of trehalose on body weight, disease onset and disease progression in male SOD1^{G93A} mice.

(A) Mean group body weight plotted for male SOD1^{G93A} mice over time from 46 days of age until the date at which the last death within each individual group occurred. As mice within groups died at different ages, the final weights of all mice were carried forward when calculating group mean values, until the date at which the last mouse within each group died. This prevented decomposition of the mean at later stages. Error bars represent standard error of the mean (SEM). (B) Kaplan-Meier survival plot for time to peak weight (an indicator of disease onset) in male SOD1^{G93A} mice. (C) Kaplan-Meier survival plot for time from peak weight to end stage (an indicator of disease progression) in male SOD1^{G93A} mice. Graphs (A), (B) and (C) present data for male SOD1^{G93A} mice in all four experimental groups: control = red, 0.5% trehalose = green, 2% trehalose = yellow, 5% trehalose = blue. Results for statistical analyses performed on data presented in (B) and (C) are given in **Table 14.**

Table 14: Kaplan Meier time to event analyses for male SOD1G93A mice[1, 2, 3]

	Median Value (days)				P Value	
	Control	**0.5 mg/ml**	**2 mg/ml**	**5 mg/ml**	**Log-rank**	**Log-rank test for trend**
Time to peak weight	84	84	85	92	0.1488	0.0353 significant
Time from peak weight to end stage	42	37	38	38	0.6773	0.2889
Time to reach score 2 in both hindlimbs	113	119.5	116	116	0.5609	0.3105
Survival	127	128.5	126	128	0.8333	0.4719

[1]The Logrank test investigates the null hypothesis that that the Kaplan Meier curves for all groups are identical (i.e. that the treatment did not change the time taken to reach the event being analysed). Low P-values are therefore indicative of differences between curves that did not occur due to chance. The threshold for significance was set at $P<0.05$.

[2] To perform the log-rank test for trend, experimental groups were arranged in order of increasing dose (Control, then 0,5%, 2% and 5% trehalose) and a P value testing the null hypothesis that there was no linear trend between group order and median time to event was then calculated. Low P-values are indicative of a significant trend between increasing dose and the event being analysed. The threshold for significance was set at $P<0.05$.

[3]The time at which peak body weight occurred for each mouse was analysed after spline smoothing of each animal's body weight values over time (using Prism 5 software) from the start of the study to the time at which the mouse died. If the smoothed body weight curve for an individual mouse had multiple equal peaks, the time point at which the final peak occurred was taken.

5.2.2.3 Effect of trehalose on the definitive onset of neurological disease and the change in neurological score over time in male SOD1^{G93A} mice.

The change in the mean combined neurological score (the sum of the neurological score recorded for left and right hind limbs) for male mice in all four groups from 46 days of age, is plotted in **Figure 29A**. Neurological score curves for all male groups rose very slowly between 46 and 102 days after which they rose more steeply, indicating the onset of neurological symptoms. Interestingly, the onset of a steeper decline in weight loss was also seen at 102 days of age in all groups **(Figure 28A)**, further indicating a worsening of pathology at this stage. After 102 days, although curves for all groups rose more steeply, the curve for the control group showed the steepest rise, indicating a trend towards faster disease progression in control mice compared to treated mice. However, when Kaplan Meier analysis of the time point at which mice reached a neurological score of two in both hindlimbs (defined as the definitive onset of symptomatic neurological disease (Gill et al., 2009, Lincecum et al., 2010, Kaneb et al., 2011)) was performed, no significant differences were observed between control and treatment groups **(Figure 29B, Table 14).**

5.2.2.4 Effect of trehalose on survival in male mice

For humane reasons, a uniform end point of the inability of a mouse to right itself within 20s of being placed on a side was used for all mice in this study. The proportion of male mice surviving over time is shown in **(Figure 29C).** There were no statistically significant differences in survival between any groups indicating that trehalose had no effect on survival in male mice, despite bringing about a slower initial decline in weight loss **(Table 14).**

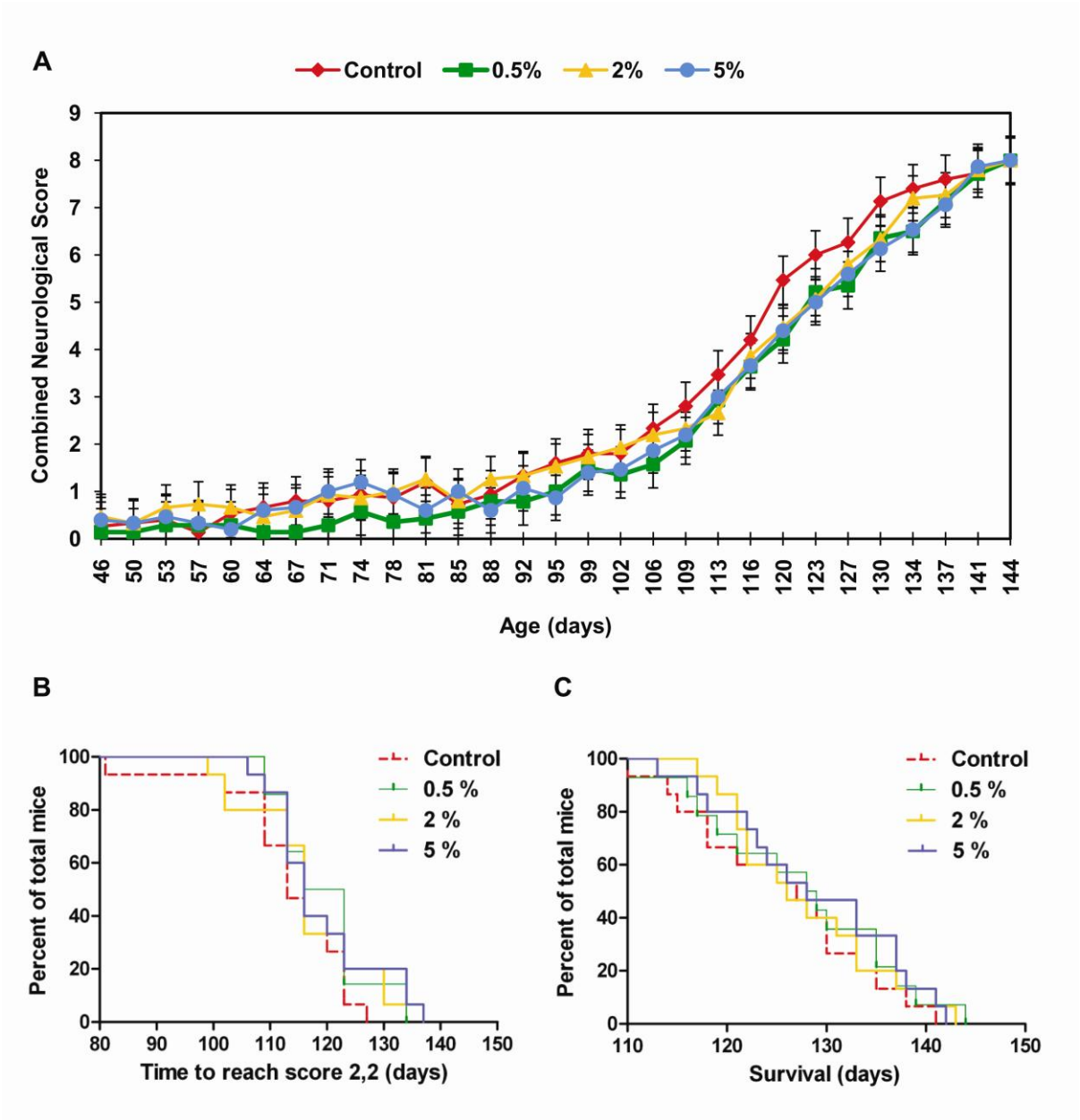


Figure29: Effect of trehalose on neurological score, neurological disease onset and survival in male SOD1^{G93A} mice.

(A) Mean group combined neurological score plotted for male SOD1^{G93A} mice over time from 46 days of age until the date at which the last death within each group occurred. Combined neurological score was calculated for each mouse at each time point through summation of the neurological scores recorded for its left and right hindlimbs. As mice within groups died at different ages, the final combined neurological scores of all mice were carried forward when calculating group mean values, until the date at which the last mouse within each group died. This prevented decomposition of the mean at later stages. Error bars represent standard error of the mean (SEM). (B) Kaplan-Meier survival plot for the time taken for male SOD1^{G93A} mice to reach a neurological score of 2 in both hindlimbs (the definitive onset of symptomatic neurological disease). (C) Kaplan-Meier survival plot for the time taken for male SOD1^{G93A} mice to reach the humane end stage of attaining a neurological score of 4 (representative of survival). Graphs (A), (B) and (C) present data for male SOD1^{G93A} mice in all four experimental groups: control = red, 0.5% trehalose = green, 2% trehalose = yellow, 5% trehalose = blue. Results for statistical analyses performed on data presented in (B) and (C) are given in **Table 14.**

5.2.3 Trehalose treatment had no effect on disease onset, progression or survival in female mice.

5.2.3.1 N-numbers, weight balancing and non-ALS deaths in female mice

Four groups of 15 female mice that were balanced for age, litter and bodyweight were enrolled in this study. Towards the end of the study, one female from the 0.5% group and one female from the 5% group, which had both been displaying a very normal female SOD1^{G93A} disease course but were not yet experiencing hindlimb paralysis, were injured by fellow cage mates and were therefore culled. These injuries appeared to be fighting injuries on the back of the neck, leading us to question whether trehalose may enhance aggression in female mice, as we had never previously seen injuries such as this in females. An additional female from the 0.5% group who had also followed a very normal female SOD1^{G93A} disease course was found dead at this stage. Weight and neurological score data from these three mice were included in weight and neurological score plots up to the date at which they were culled/found dead respectively and they were treated as censored in any Kaplan Meier analyses requiring information about survival. All three females died prior to attaining a neurological score of 2 in both hind limbs (defined as the definitive onset of symptomatic neurological disease) and were therefore also treated as censored in the Kaplan Meir analysis performed to compare time taken to reach this stage. One further female mouse from the 0.5mg/ml group displayed fit-like behavior at 130 days of age prior to developing overt neurological symptoms and was found dead the next day. She was therefore classed as dying a 'non-ALS death' and was excluded completely from the study as it was not clear whether she had another medical condition that could have affected weight and neurological score data. At the very end of the study, one female mouse from the control group remained that had not displayed weight loss or developed neurological symptoms. An ear biopsy was therefore taken from this mouse in

order to confirm her genotype and she was found to be a wild type. She was therefore culled and excluded completely from the study. The average starting bodyweights for all groups were within 0.27g of each other (Control: 16.24g, 0.5%: 16.19g, 2%: 16.45g and 5%: 16.35g).

5.2.3.2 Effect of trehalose on body weight, disease onset and disease progression in female SOD1^{G93A} mice.

The change in mean body weight over time for female mice in all four groups is plotted in **Figure 30A** from 46 days onwards. Weight curves for all groups showed a largely similar shape, with weight rising until approximately 81 days of age, following which the curves reached a plateau. At approximately 102 days, weight in all groups began to steeply decline. Despite all curves showing a largely similar shape, mice in the 0.5% and 5% trehalose groups appeared to be heavier overall than control mice and mice in the 2% trehalose group until approximately 113 days for the 5% group and 120 days for the 0.5% group. Following this, weights in all groups were similar apart from in the 2% trehalose group in which weight appeared to be lower than in all other groups from approximately 120 days onwards. As all weight curves showed a largely similar shape, it was not surprising that there were no significant differences between female groups in the time taken to reach peak weight **(Figure 30B, Table 15)** or the time taken from peak weight to end stage **(Figure 30C, Table 15).**

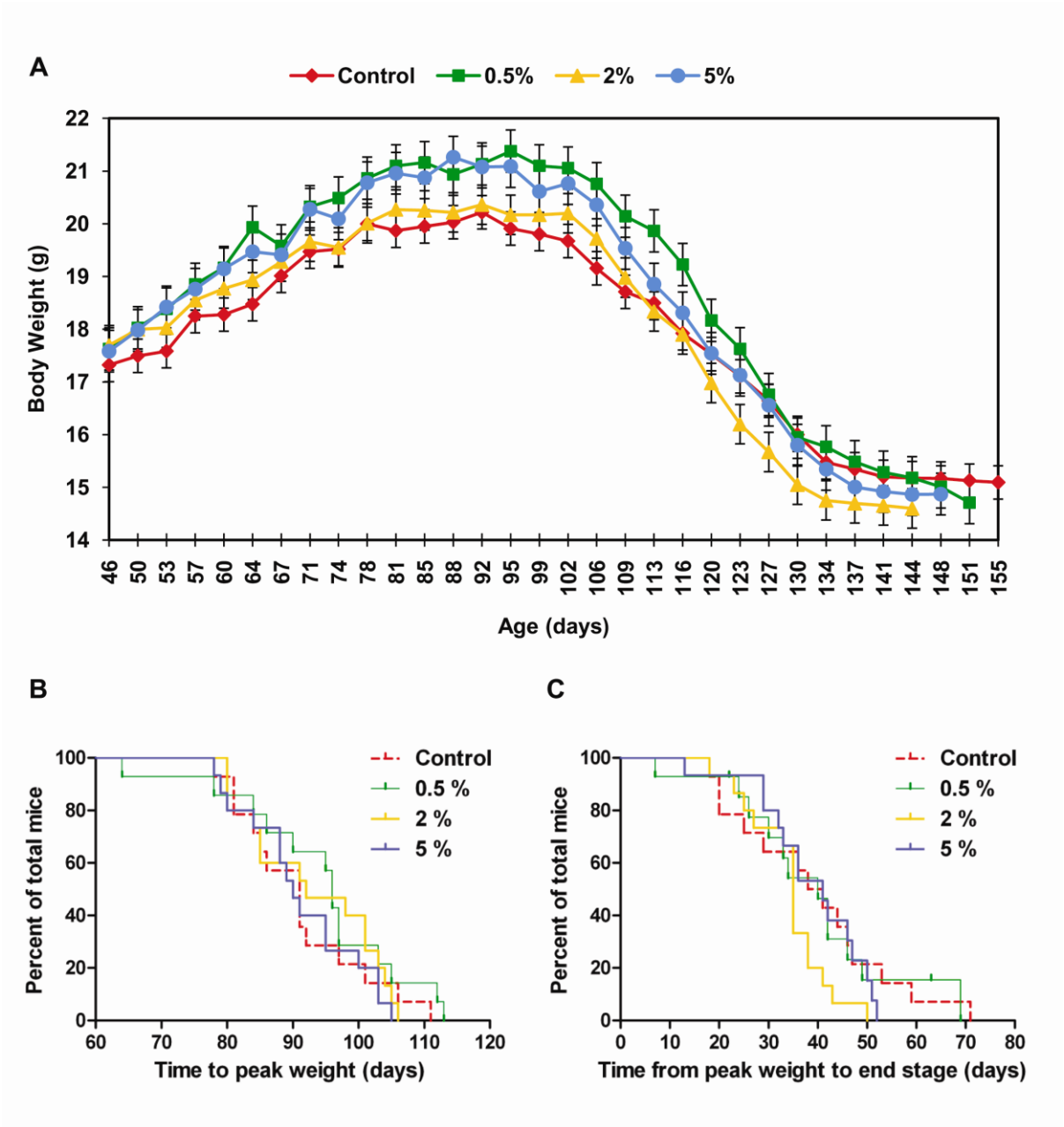


Figure 30: Effect of trehalose on body weight, disease onset and disease progression in female SOD1^{G93A} mice.

(A) Mean group body weight plotted for female SOD1^{G93A} mice over time from 46 days of age until the date at which the last death within each individual group occurred. As mice within groups died at different ages, the final weights of all mice were carried forward when calculating group mean values, until the date at which the last mouse within each group died. This prevented decomposition of the mean at later stages. Error bars represent standard error of the mean (SEM). (B) Kaplan-Meier survival plot for time to peak weight (an indicator of disease onset) in female SOD1^{G93A} mice. (C) Kaplan-Meier survival plot for time from peak weight to end stage (an indicator of disease progression) in female SOD1^{G93A} mice. Graphs (A), (B) and (C) present data for female SOD1^{G93A} mice in all four experimental groups: control = red, 0.5% trehalose = green, 2% trehalose = yellow, 5% trehalose = blue. Results for statistical analyses performed on data presented in (B) and (C) are given in **Table 15.**

Table 15: Kaplan Meier time to event analyses for female SOD1^{G93A} mice[1, 2, 3]

	Median Value (days)				P Value	
	Control	**0.5 mg/ml**	**2 mg/ml**	**5 mg/ml**	**Log-rank**	**Log-rank test for trend**
Time to peak weight	91	96	92	90	0.5817	0.5915
Time from peak weight to end stage	39.5	40	35	41	0.2919	0.4531
Time to reach score 2 in both hindlimbs	123	130	123	123	0.2740	0.6555
Survival	130	130	126	129	0.3480	0.4058

[1]The Logrank test investigates the null hypothesis that that the Kaplan Meier curves for all groups are identical (i.e. that the treatment did not change the time taken to reach the event being analysed). Low P-values are therefore indicative of differences between curves that did not occur due to chance. The threshold for significance was set at $P<0.05$.

[2] To perform the log-rank test for trend, experimental groups were arranged in order of increasing dose (Control, then 0.5%, 2% and 5% trehalose) and a P value testing the null hypothesis that there was no linear trend between group order and median time to event was then calculated. Low P-values are indicative of a significant trend between increasing dose and the event being analysed. The threshold for significance was set at $P<0.05$.

[3]The time at which peak body weight occurred for each mouse was analysed after spline smoothing of each animal's body weight values over time (using Prism 5 software) from the start of the study to the time at which the mouse died. If the smoothed body weight curve for an individual mouse had multiple equal peaks, the time point at which the final peak occurred was taken.

5.2.3.3 Effect of trehalose on the definitive onset of neurological disease and the change in neurological score over time in female SOD1^{G93A} mice.

The change in the mean combined neurological score (the sum of the neurological score recorded for left and right hind limbs) for female mice in all four groups from 46 days of age, is plotted in **Figure 31A**. Neurological score curves for female mice in all groups showed a broadly similar shape. Specifically, scores remained low and constant until approximately 92 days when they began to gradually rise. At 113 days, neurological score curves for all groups began to rise more steeply, with the curve representing the 2% trehalose group showing the steepest rise. Kaplan Meier analysis of the time point at which female mice reached a score of 2 in both hindlimbs (the definitive onset of symptomatic disease (**Figure 31B, Table 15)** revealed no significant differences between groups, indicating that the apparent faster progression of neurological symptoms in the 2% trehalose group was only minor.

5.2.3.4 Effect of trehalose on survival in female mice

The proportion of female mice surviving over time is shown in **(Figure 31C)**. There were no significant differences in survival between groups **(Table 15)**.

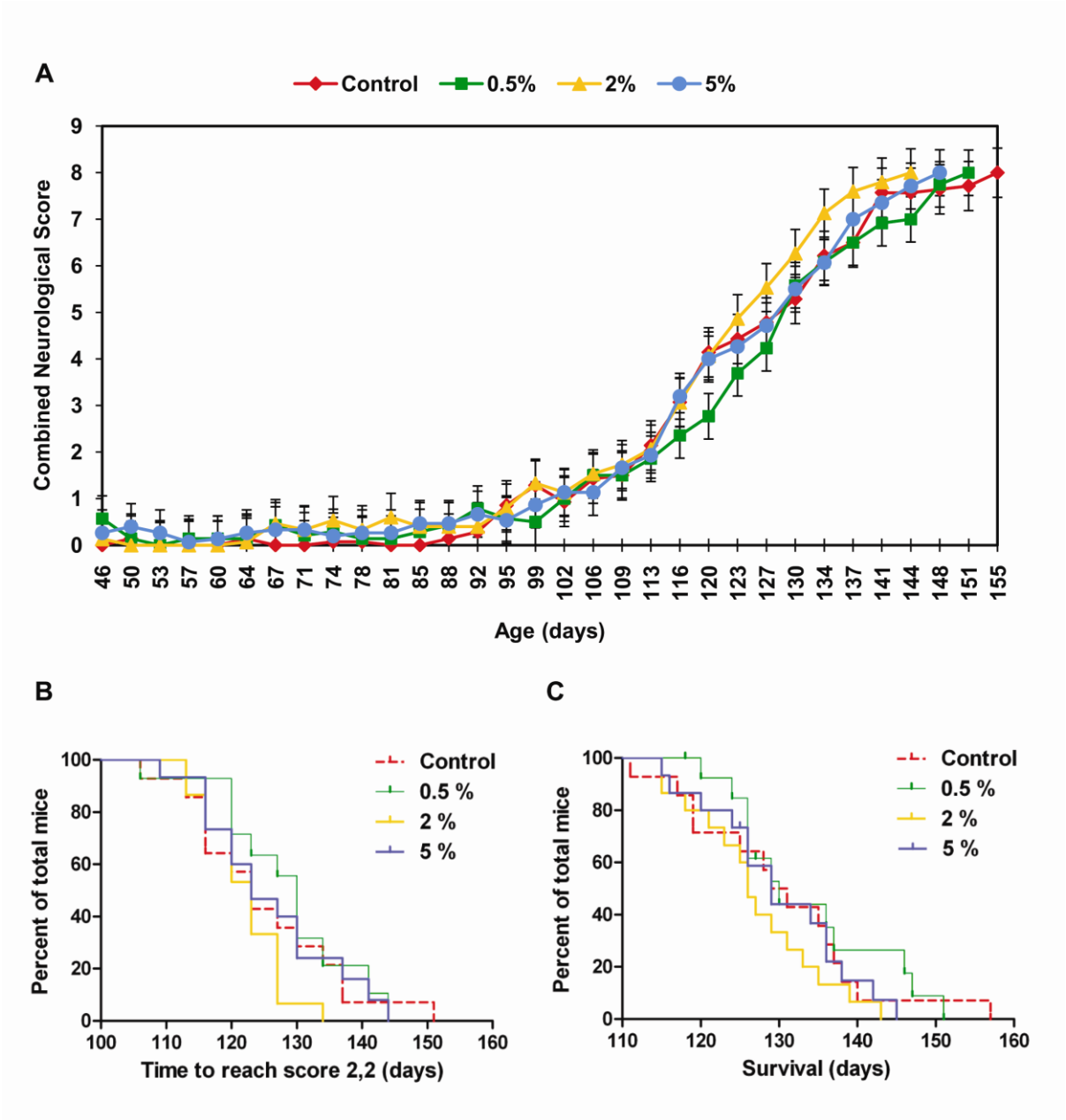


Figure 31: Effect of trehalose on neurological score, neurological disease onset and survival in female SOD1^{G93A} mice.

(A) Mean group combined neurological score plotted for female SOD1^{G93A} mice over time from 46 days of age until the date at which the last death within each group occurred. Combined neurological score was calculated for each mouse at each time point through summation of the neurological scores recorded for its left and right hindlimbs. As mice within groups died at different ages, the final combined neurological scores of all mice were carried forward when calculating group mean values, until the date at which the last mouse within each group died. This prevented decomposition of the mean at later stages. Error bars represent standard error of the mean (SEM). (B) Kaplan-Meier survival plot for the time taken for female SOD1^{G93A} mice to reach a neurological score of 2 in both hindlimbs (the definitive onset of symptomatic neurological disease). (C) Kaplan-Meier survival plot for the time taken for female SOD1^{G93A} mice to reach the humane end stage of attaining a neurological score of 4 (representative of survival). Graphs (A), (B) and (C) present data for female SOD1^{G93A} mice in all four experimental groups: control = red, 0.5% trehalose = green, 2% trehalose = yellow, 5% trehalose = blue. Results for statistical analyses performed on data presented in (B) and (C) are given in **Table 15.**

5.2.4 Trehalose treatment did not reduce the amount of misfolded/aggregated SOD1 in the spinal cords of male or female SOD1^{G93A} mice

Quantification of SOD1 aggregates in motor neurons can be challenging using conventional SOD1 antibodies or ubiquitin antibodies (SOD1 aggregates are usually ubiquitinated (Shaw et al., 2008)) as both SOD1 and ubiquitin are ubiquitously expressed. Consequently, we quantified motor neurons containing misfolded/aggregated SOD1 in the sciatic motor pools of control and treated mice using an antibody specifically targeted to misfolded SOD1 (USOD) (Kerman et al., 2010). In this study we did not detect any USOD staining in the spinal cords of wild type mice (n=3) (**Figures 32A and 32D)** and only saw USOD staining within motor neurons and not other cell types in SOD1^{G93A} mice. Quantification of USOD positive motor neurons was performed in equivalent levels of the sciatic motor pool L3-L5 in control and 5%-trehalose-treated SOD1^{G93A} mice. Visual analysis of USOD staining within the spinal cords of control male SOD1^{G93A} mice (n=4) revealed low overall numbers of USOD positive motor neurons, with many sections showing no staining at all **(Figure 32B)**. When USOD staining did occur in these animals it usually appeared faint and diffuse. Surprisingly, male SOD1^{G93A} mice that were treated with 5% trehalose (n=4) appeared to show moderately increased numbers of USOD positive motor neurons with many USOD positive motor neurons showing punctuate USOD staining and staining around the periphery of intracellular vacuoles **(Figure 32C arrowheads)**. These visual observations were supported by our counts, in which there was a trend towards increased numbers of USOD positive motor neurons in 5% trehalose-treated male mice over control mice, however this trend did not reach significance **(Figure 32G, Table 16)**. Levels of USOD positive motor neurons in control female SOD1^{G93A} mice at 75 days of age (n=4) appeared to be slightly higher than in males with some motor neurons showing faint, diffuse USOD staining but

others showing clear aggregates and staining surrounding vacuoles **(Figure 32E)**. Surprisingly the numbers of USOD positive motor neurons in 5% trehalose-treated female $SOD1^{G93A}$ (n=5) appeared to be substantially higher than in control mice (the spinal cords of treated female mice could usually be identified from control mice in a blinded fashion) with most USOD positive motor neurons showing intense USOD staining throughout the cell body and also surrounding vacuoles **(Figure 32F)**. Consequently there was a strong trend towards increased numbers of USOD positive motor neurons in 5% trehalose-treated $SOD1^{G93A}$ mice compared to control females, however this trend did not reach significance **(Figure 32H, Table 16)**. Interestingly, in trehalose-treated females in particular but also to a certain extent in control females and trehalose-treated males, some extracellular USOD staining was seen in the ventral horns of the spinal cord sections examined **(see Figure 32F)**. This staining is unlikely to be background staining as staining for all mice within each sex (including WT controls) was performed in an identical fashion on the same day and extracellular staining in the ventral horns was only seen in certain (predominantly treated) mice.

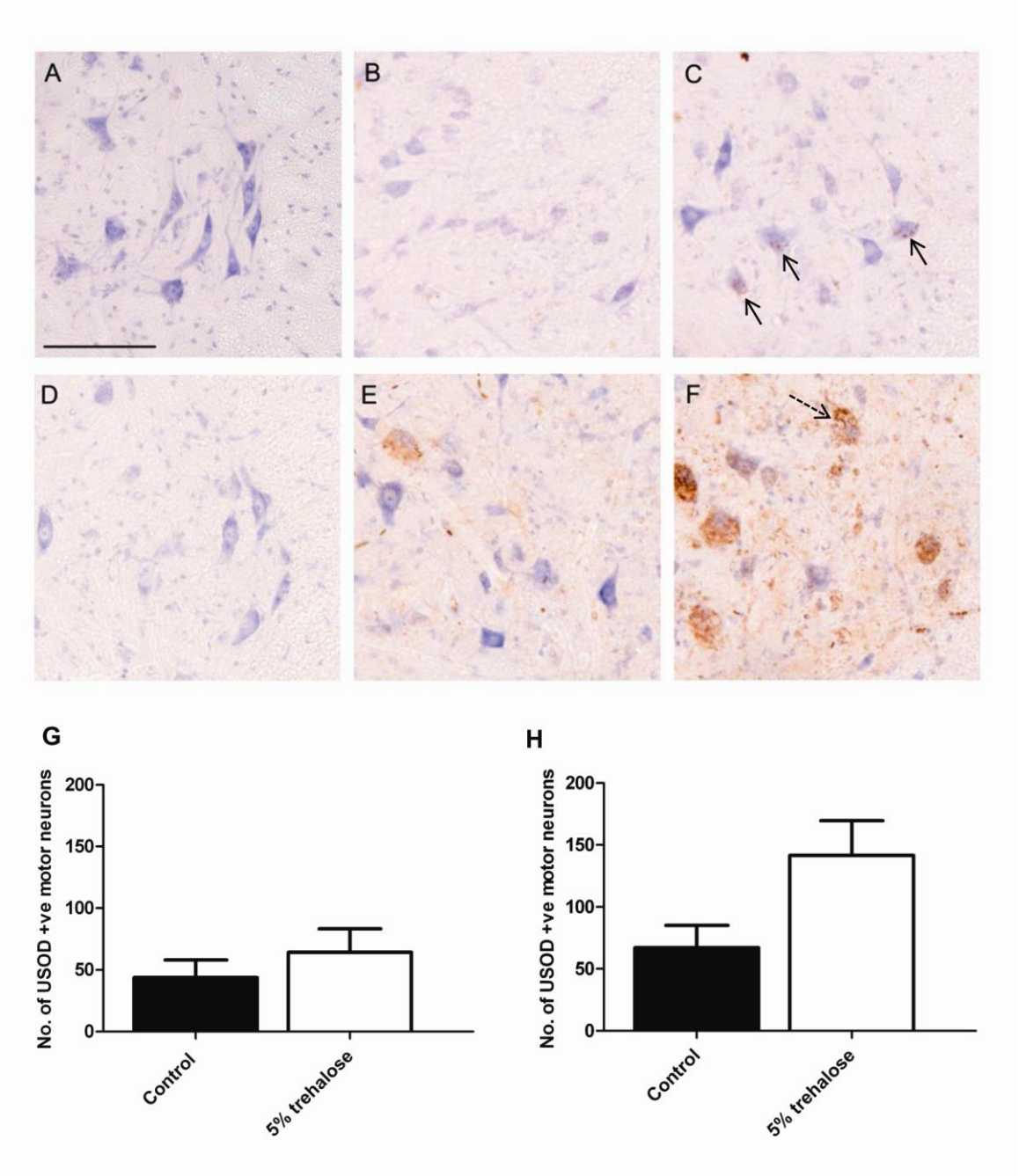


Figure 32: Effect of 5% trehalose on number of USOD positive motor neurons in sciatic motor pool

(A-F) Representative USOD (brown)/Nissl (blue)-stained sections from the ventral horns (lumbar region, L4) of the spinal cords of 75 day old mice: (A) wild type male mouse showing no USOD positive motor neurons, (B) control male $SOD1^{G93A}$ mouse showing minimal USOD staining in motor neurons, (C) 5% trehalose-treated male $SOD1^{G93A}$ mouse showing punctuate USOD staining in some motor neurons (solid arrows), (D) wild type female mouse showing no USOD positive motor neurons, (E) control female $SOD1^{G93A}$ mouse showing intense USOD staining throughout some motor neurons and punctuate or faint staining in others, (F) 5% trehalose-treated female $SOD1^{G93A}$ mouse showing highly intense USOD staining throughout the cell body and surrounding vacuoles in many motor neurons (broken arrow) and apparent extracellular staining which may represent secreted misfolded SOD1. Scale bar in (A) applies to all images (A-F) and represents 100µm. **(G and H)** Graphs showing the mean number of USOD positive motor neurons in equivalent sections L3-L5 in control and 5% trehalose-treated male $SOD1^{G93A}$ mice (G) and in control and 5% trehalose-treated female $SOD1^{G93A}$ mice (H). Error bars in (G) and (H) represent standard error of the mean (SEM). n=4 $SOD1^{G93A}$ males, n=4 $SOD1^{G93A}$ females, n=4 trehalose-treated $SOD1^{G93A}$ males and n=5 trehalose-treated $SOD1^{G93A}$ females. No significant differences were seen between control and trehalose-treated $SOD1^{G93A}$ males or between control and trehalose-treated $SOD1^{G93A}$ females by Mann-Whitney test **(Table 16)**. The threshold for significance was set at $P \leq 0.05$.

Table 16: Summary of mean numbers (+/- SEM) and statistical analyses of USOD and ChAT positive motor neurons in equivalent levels of the sciatic motor pool in control and trehalose treated $SOD1^{G93A}$ mice.

Counts performed	**Control**	**5% trehalose treated**	**P-value Man-Whitney test**
No. of USOD positive motor neurons in male mice	44 +/- 14	64 +/- 19	0.3429
No. of USOD positive motor neurons in female mice	67 +/- 18	142 +/- 28	0.111
No. of ChAT positive motor neurons in male mice	243 +/- 20	254 +/- 9	1.000
No. of ChAT positive motor neurons in female mice	340 +/- 25	313 +/- 38	0.8049

In order to confirm that the trends towards increased numbers of USOD positive motor neurons in the sciatic motor pool seen in 5% trehalose-treated mice were not the result of increased numbers of motor neurons per-se, we counted the number of ChAT/Nissl-stained motor neurons in the sciatic motor pool in equivalent sections to those used for USOD quantification. An example of ChAT/Nissl staining in the ventral horn of the lumbar region (L4) of a 75 day old wild type mouse is shown in **Figure 33A**. Here ChAT staining within motor neurons is diffuse throughout the cell body and nicely overlaid with Nissl. We found ChAT staining within the motor neurons of 75 day old $SOD1^{G93A}$ mice to be less uniform and more punctuate in nature **(Figure 33B solid arrows)** as has been described by others (Tortarolo et al., 2006a), but still easily identifiable. Clearly degenerating motor neurons showing vacuolation and faint Nissl/ChAT staining **(Figure 33B broken arrow)** were included in motor neuron counts as these were often the motor neurons in which USOD staining was observed. Motor neuron counts revealed no significant differences between the number of surviving motor neurons in the sections counted in control (n=3) and trehalose-treated (n=4) male $SOD1^{G93A}$ mice **(Figure 33C Table 16)** or in control (n=4) and trehalose-treated (n=5) female $SOD1^{G93A}$ mice **(Figure 33D Table 16)**. This indicates that the trends towards increased numbers of USOD positive motor neurons seen in male and female trehalose-treated mice were not due to increased numbers of motor neurons per-se.

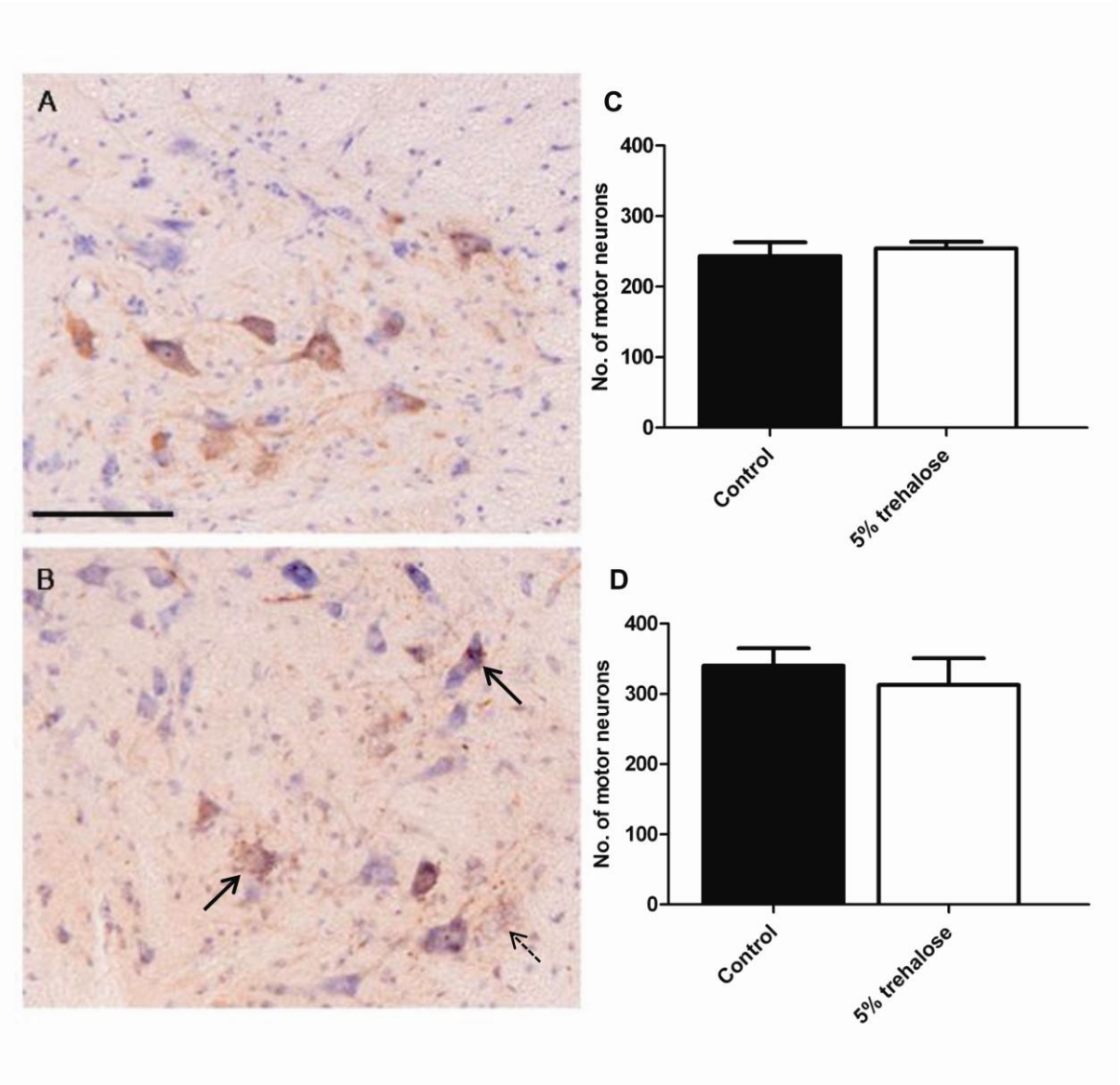


Figure 33: Effect of 5% trehalose on number of ChAT positive motor neurons in sciatic motor pool

(A and B) representative ChAT (brown)/ Nissl (blue)-stained sections from the ventral horns (lumbar region, L4) of (A) a 75 day old WT mouse and (B) a 75 day old SOD1G93A mouse. ChAT staining within motor neurons of WT mice (A) was found to be present throughout the cytoplasm and nicely overlaid with Nissl whereas ChAT staining within the motor neurons of 75 day old SOD1G93A mice (B) was less uniform and often punctuate in nature (solid arrows). Scale bar in (A) applies to both (A) and (B) and represents 100µm. (C and D) graphs showing the mean numbers of ChAT/Nissl positive motor neurons counted in equivalent sections L3-L5 in control and 5% trehalose-treated male SOD1G93A mice (C) and in control and 5% trehalose-treated female SOD1G93A mice (D). Error bars in (C) and (D) represent standard error of the mean (SEM). n=3 SOD1G93A males, n=4 SOD1G93A females, n=4 trehalose-treated SOD1G93A males and n=5 trehalose- treated SOD1G93A females. No significant differences were seen between control and trehalose-treated SOD1G93A males or between control and trehalose-treated SOD1G93A females by Mann-Whitney test (Table 16). The threshold for significance was set at $P<0.05$. Note: clearly degenerating motor neurons showing vacuolation and faint Nissl/ChAT staining (broken arrow in B) were included in motor neuron counts as these were often the motor neurons in which USOD staining was observed.

5.3 Discussion

Trehalose is a naturally occurring disaccharide that has been shown to stabilize proteins in conditions of stress in order to prevent their misfolding/aggregation and also to promote the clearance of aggregated proteins via the induction of autophagy (Béranger et al., 2008, Liu et al., 2009, Sarkar et al., 2007). These properties have been exploited for therapeutic benefit in both parkin deleted/tau overexpressing mice (a model of parkinsonism and tauopathies) (Rodríguez-Navarro et al., 2010) and in the R6/2 model of Huntington's disease (Tanaka et al., 2004). Treatment of 3 month old parkin deleted/tau overexpressing mice with 1% trehalose in the drinking water for 2.5 months improved motor and cognitive behavior, reduced the degeneration of dopaminergic neurons in the ventral midbrain and reduced numbers of tau-positive neuritic plaques and phosphorylated tau levels in various brain regions. Treatment of R6/2 Huntington's mice with 2% trehalose in the drinking water decreased polyglutamine aggregates in the cerebrum and liver, improved motor dysfunction and extended lifespan. Tauopathies, Parkinson's disease and Huntington's disease share a common feature with ALS in that they involve the formation of oligomeric protein species and aggregates in neuronal cells, which may play a causative role in pathology (Sarkar and Rubinsztein, 2008). In light of this we hypothesized that as in models of parkinsonism/tauopathies and Huntington's disease, oral trehalose treatment may be beneficial in the $SOD1^{G93A}$ model of ALS. This hypothesis was supported by experiments performed by Gomes et al., in which treatment of NSC-34 cells (a mouse motor-neuron-like cell line) transiently transfected with human $SOD1^{G93A}$, brought about a significant reduction in mutant SOD1 aggregate formation and detergent insolubility (Gomes et al., 2010). There are currently no effective treatments for ALS and hence trehalose represented an exciting compound to test, as it had already been shown to be safe at high doses in humans and

approved for use in food products in Japan (Richards et al., 2002) and would therefore be relatively easy to take to clinical trial should beneficial effects be seen.

In order to assess the potential therapeutic benefits of trehalose for ALS, we designed a blinded, dose-response survival study in $SOD1^{G93A}$ mice in which all groups contained n=15 male and n=15 female age, weight and littermate balanced mice and any mice experiencing loss of transgene copies or non-ALS deaths were excluded. Studies following this format have previously been shown to reduce any noise resulting from mice being maintained on a mixed-hybrid background to a virtual zero and we were therefore confident in the validity of the results obtained (Scott et al., 2008) Disease onset and progression were assessed by twice weekly monitoring of weight and neurological score (Gill et al., 2009, Lincecum et al., 2010, Kaneb et al., 2011) and survival was determined as the time point at which mice could no longer right themselves within 20s of being placed on a side. Trehalose doses selected were 0.5%, 2% and 5% trehalose via the drinking water. This dose range encompassed doses previously shown to be therapeutic in models of parkinsonism/tauopathies (1%) (Rodríguez-Navarro et al., 2010) and Huntington's disease (2%) (Tanaka et al., 2004).

In our survival study we were surprised to find that trehalose treatment had no beneficial effect at any dose on disease onset, progression or survival in female mice. Furthermore, despite bringing about a significant dose-dependent delay on the onset of weight loss in male mice, this effect was not translated into a significantly delayed onset of definitive neurological symptoms, delayed disease progression or increased survival in males. We therefore hypothesise that the delayed weight loss in males was caused by a feeding effect derived from supplementing the normal diet with a constant supply of sugar, rather than a

delay in the degeneration of motor neurons. $SOD1^{G93A}$ mice have been shown to have a hyper-metabolic rate and therefore providing an additional energy source is likely to be beneficial for the maintenance of weight in these animals (Dupuis et al., 2004, Dupuis et al., 2011). This feeding hypothesis is supported by the fact that female mice in the 0.5% and 5% trehalose groups appeared to be heavier than control mice until approximately 120 days when overt neurological pathology was underway. It is surprising that female mice in the 2% trehalose group did not also show this trend towards increased weight and appeared to do worse than all other female groups following the definitive onset of neurological symptoms. However, as this trend was not significant it seems likely that it was caused by inherent variation between groups (despite our efforts to minimize confounding variables by using high n-numbers, and balancing groups for age, weight and litter (Scott et al., 2008)). If this trend was caused by a true biological effect then it could be that at this dose, trehalose has a particular, as yet unknown negative pharmacological effect in the female $SOD1^{G93A}$ system.

In order to try and understand why trehalose did not show the same beneficial effects in $SOD1^{G93A}$ mice as in murine models of parkinsonism/tauopathies and Huntington's disease, we investigated the effects of trehalose treatment on the misfolding/aggregation of SOD1 in the lumbar regions of the spinal cords of these animals. We did this via immunohistochemistry using the USOD antibody, generated and kindly donated by Dr Avijit Chakrabartty and colleagues, which specifically recognizes misfolded SOD1 species in which the copper ion has been lost, the beta barrel structure is disrupted and the hydrophobic core is exposed (Kerman et al., 2010). Dr Chakrabartty and colleagues have generated an additional SOD1 conformation-specific antibody, SEDI, which recognizes any SOD1 conformation in which the dimer interface of SOD1 has been disrupted. These conformations have been

shown to include both folded monomeric SOD1 and misfolded monomeric SOD1 (Rakhit et al., 2007). Analysis of the staining patterns of USOD and SEDI in the ventral horns of the spinal cords of $SOD1^{G93A}$ mice has been shown to give very similar results (labeled vacuolated structures in the ventral horn and labeling of some axons in the ventral root) (Kerman et al., 2010). This suggests that misfolding of SOD1 in the G93A mouse involves disruption of the SOD1 beta barrel structure and exposure of the hydrophobic core (USOD antibody) as well as disruption of the dimer interface (SEDI antibody). In addition to detecting misfolded SOD1 in inclusion bodies, USOD has also been shown to detect SOD1-species in the detergent-soluble fraction of $SOD1^{G93A}$ mouse spinal cord tissue, indicating that it recognizes misfolded SOD1 species at different stages of the aggregation process (Kerman et al., 2010). In light of the extensive characterization of the USOD antibody for the detection of misfolded SOD1 species at various stages in the aggregation species in $SOD1^{G93A}$ mice, we felt that it would give us a good indication of the effects of trehalose-treatment on SOD1 misfolding and aggregation in these animals.

We selected 75 days as a suitable time point to assess the effects of trehalose-treatment on SOD1 misfolding as at this time point clear aggregates can be seen in the spinal cords of $SOD1^{G93A}$ mice but they are not so numerous that they become difficult to quantify (Sharp et al., 2008). We chose to analyze the effects of the highest trehalose dose used (5% trehalose), as no negative effects were seen with this dose in our survival study and we felt that it was the most likely to show us whether or not trehalose had the ability to reduce SOD1 misfolding/aggregation. As would be expected, we did not see any USOD staining in the spinal cords of WT mice at 75 days of age, indicating the specificity of this antibody. Furthermore, in control female $SOD1^{G93A}$ mice at 75 days of age, we saw the typical USOD

staining around vacuoles in motor neurons in the ventral horn and in some axons in the ventral root described by Dr Chakrabartty and colleagues (Kerman et al., 2010). Staining in male control SOD1^{G93A} at this time point was also localized in motor neurons in the ventral horn, as would be expected, however USOD-positive motor neurons appeared less numerous and staining appeared fainter and more diffuse than in females. This could be due to a prior loss of unhealthy USOD-positive motor neurons in male mice that still remain in female mice at this time point, as disease onset has been shown to be later in female SOD1^{G93A} mice (Veldink et al., 2003). The selectivity of USOD staining for motor neurons and axons in our SOD1^{G93A} mice clearly aligns with observations of a motor neuron specific localization of aggregates in the spinal cords of other murine SOD1-based ALS models (Vande Velde et al., 2011) and highlights that misfolding/aggregation of SOD1 is largely restricted to the very cells that degenerate in ALS pathology.

When looking at USOD-stained sections from the lumbar regions (L3-L5) of the spinal cords of 5%-trehalose treated SOD1^{G93A} mice, we were surprised to see an apparent increase in the number of USOD positive motor neurons in both male and female mice compared to controls, although this increase appeared more pronounced in females. Furthermore, the intensity of USOD staining within USOD positive motor neurons and the proportion of the motor neuron cell body covered by intense USOD staining, appeared to be moderately increased in trehalose-treated male mice and further increased in trehalose-treated female mice compared to their respective controls. We also observed apparent extracellular USOD staining exclusively in the ventral horns of the spinal cord in trehalose-treated females and to a lesser extent in control females and trehalose-treated males. We hypothesize that this extracellular staining may represent secreted misfolded SOD1 species which are increasingly

becoming associated with ALS pathology (Münch et al., 2011, Urushitani et al., 2006, Urushitani et al., 2007). If this was the case then it could potentially indicate higher levels of misfolded and/or aggregated SOD1 in the motor neurons of these animals and therefore greater secretion of these misfolded/aggregated species into the extracellular space. In order to analyze these observations quantitatively, we counted the number of USOD positive motor neurons in equivalent levels L3-L5 of the sciatic motor pole in control and trehalose treated male and female $SOD1^{G93A}$ mice. As with our survival study we analyzed male and female mice separately to account for any sex differences. We also confirmed by counting the number ChAT positive motor neurons in equivalent sections to those used for USOD counts, that the number of motor neurons in these sections was not significantly different between control and treated mice. This allowed us to confirm that any differences seen in the number of USOD positive motor neurons were not due to overall changes in the number of motor neurons present. Although we saw a moderate trend towards increased numbers of USOD positive motor neurons in trehalose-treated male $SOD1^{G93A}$ mice and a strong trend towards this in trehalose-treated female $SOD1^{G93A}$ mice, in keeping with our visual observations, these trends were not significant. However in light of the increased intensity and broader distribution of USOD staining within USOD positive motor neurons in trehalose treated female mice, coupled with the increased observation of potential extracellular USOD species in these animals, we feel that in female mice, this trend was probably not the result of chance or inherent variation between the mice alone. Additionally, as outlined by Ludolph and colleagues, it is important to use an n of at least five per group, with each group representing the same proportion of each gender, when performing histological analyses in $SOD1^{G93A}$ mice (Ludolph et al., 2010). Although n-numbers used for USOD positive motor neuron counts in this study met this criterion (n=4 $SOD1^{G93A}$ males, n=4 $SOD1^{G93A}$ females, n=4

trehalose-treated SOD1^{G93A} males and n=5 trehalose-treated SOD1^{G93A} females), we felt that it was important to consider male and female data separately as trehalose may interact differently with the male and female systems. Consequently our n-numbers were lower than is recommended and this may have contributed to the lack of significant results when comparing numbers of USOD positive motor neurons between control and treated (particularly female) mice. Regardless of whether or not the increased numbers of USOD positive motor neurons seen in our trehalose-treated animals were due to chance, the results of our counts suggest that trehalose was unable to reduce SOD1 misfolding and aggregation in the motor neurons of these mice. It is therefore not surprising that trehalose was unable to delay the onset or progression of neurological symptoms in these mice or to increase survival.

Considering the documented ability of trehalose to prevent the aggregation of SOD1^{G93A} species in NSC-34 cells (Gomes et al., 2010) and the aggregation of many other proteins associated with neurodegenerative disorders *in vitro* (Béranger et al., 2008, Liu et al., 2009, Sarkar et al., 2007) and *in vivo* (Tanaka et al., 2004, Rodríguez-Navarro et al., 2010) it is interesting that trehalose-treatment was unable to reduce SOD1 misfolding and aggregation in our SOD1^{G93A} mice. This suggests that there may have been additional cellular and/or organismal processes in play that prevented the administered trehalose from stabilizing mutant SOD1 species and/or promoting their successful clearance by autophagy. Interestingly, it has recently been shown by Zhang and colleagues that the mTOR dependent autophagy enhancer, rapamycin, accelerates motor neuron degeneration, increases SOD1 aggregation and shortens lifespan in SOD1^{G93A} mice (Zhang et al., 2011). In this study Zhang and collaborators performed a systematic assessment of the autophagy system in control SOD1^{G93A} mice and demonstrated that the autophagic protein marker LC3-II and also

p62/SQSTM1, a marker of autophagic flux, are markedly and specifically increased in the spinal cord motor neurons of these animals in a manner that correlates closely with disease progression. Furthermore, autophagic vacuoles are significantly accumulated in the dystrophic axons of motor neurons of these mice. Interestingly, these effects were all exacerbated by rapamycin treatment. This combined with the observed toxicity of rapamycin, lead the authors to suggest that the autophagy system may be impaired in $SOD1^{G93A}$ mice and that this impairment may be augmented by treatment with the autophagy enhancer rapamycin. Although this remains to be proven, Zhang and colleagues suggest that this impairment in autophagy could be associated with defective autophagosomal degradation, potentially through impaired retrograde transport of these vesicles from their site of synthesis at the axonal terminal (Yue, 2007). It must however be highlighted that the target of rapamycin, mTOR, controls many other important cellular processes (including cell growth and translation), and therefore the observed toxicity of rapamycin could have resulted from perturbation of one or more of these processes instead of, or in addition to, augmentation of a potentially defective autophagy system.

If the autophagy system is indeed impaired in $SOD1^{G93A}$ mice then this could explain the lack of therapeutic benefit of trehalose, a known enhancer of autophagy, in our mice. However, we did not see toxicity in our mice and this would either suggest that further activating autophagy is not toxic to $SOD1^{G93A}$ mice (and that rapamycin toxicity was caused by an alternative mechanism) or that autophagy was not activated as significantly with trehalose-treatment as with rapamycin treatment. If clearance of autophagic vesicles is indeed defective in $SOD1^{G93A}$ mice then this could explain the trend towards increased aggregation of SOD1 observed in our mice and with rapamycin treatment. As this observation was more

pronounced in females in this study, it would also be interesting to investigate the potential impairment of the autophagy system in SOD1^{G93A} mice further and to see whether this impairment, if found to be existent, is equal in male and female mice. Given more time we would investigate these possibilities by measurement of the levels of LC3-II as well as p62/SQSTM1 in the spinal cords in male and female, control and 5% trehalose treated mice via western blot. We would do this at equivalent time points to those investigated by Zhang and colleagues (Zhang et al., 2011) and compare the results obtained. During autophagy, the cytoplasmic form of LC3 (LC3 I) is processed and recruited to the autophagosomes, where LC3 II is generated by site specific proteolysis and lipidation near to the C-terminus. The amount of LC3 II present is therefore a commonly used indicator of the level of autophagy activation (although it must be noted that an accumulation of LC3-II can also indicate an impairment in autophagosome-lysosome fusion or lysosomal degradation of autophagic vesicle contents and therefore results obtained with this marker should be interpreted with care, as is discussed further in the final discussion chapter)(Barth et al., 2010). p62/SQSTM1 interacts with poly-ubiquitinated protein aggregates through a ubiquitin-binding domain and with LC3 through its LC3-binding domain, thereby targeting these aggregates for degradation at the autolysosome. Accumulation of this protein is therefore a good measure of defects in autophagy of ubiquitinated aggregates. Consequently, through analysis of LC3-II levels and p62/SQSTM1 levels in control and trehalose-treated mice by western blot we would be able to see whether trehalose treatment augmented the autophagy system in SOD1^{G93A} mice and whether there were sex differences in this effect. Furthermore, looking at p62/SQSTM1levels would give us some indication of the effect of trehalose on autophagic degradation of ubiquitinated aggregates in male and female mice and whether it impaired this process.

Interestingly, lithium, which is thought to activate autophagy in an mTOR independent fashion, through inhibition of inositol monophosphatase (Sarkar et al., 2005), has also been tested for the treatment of ALS. In an initial study, lithium was reported to delay disease onset and extend lifespan in male $SOD1^{G93A}$ mice (B6SJL background) and also to delay disease progression in ALS patients (Fornai et al., 2008). These effects were proposed to be the result of an activation of autophagy, increased numbers of mitochondria in motor neurons and suppressed astrogliosis. Surprisingly however, two subsequent studies, one performed in female $SOD1^{G93A}$ mice on both C57BL/6 and 129S2/Sv backgrounds (Pizzasegola et al., 2009) and one performed in male and female $SOD1^{G93A}$ mice on the B6SJL background (Gill et al., 2009), could not recapitulate these beneficial effects, despite using similar doses and routes of administration. Furthermore, lithium was seen to bring about significantly earlier disease onset and reduced survival in female $SOD1^{G93A}$ mice on the 129/Sv background (Pizzasegola et al., 2009) and has been shown to have no benefit and low tolerability in patients in recent clinical trials (Miller et al., 2011). Unlike the study performed by Fornai and colleagues, the study performed by Gill et al., employed sibling matching, gender balancing, investigator blinding, and transgene copy number verification for each experimental subject . Consequently it seems likely that the results of the Gill and Pizzasegola studies are correct and lithium, like rapamycin and trehalose is not beneficial in the $SOD1^{G93A}$ model of ALS. If this is the case then it would lend further weight to the hypothesis that activation of autophagy is not an appropriate therapeutic strategy for ALS. However it must also be stressed that enhancing autophagy is not the only effect of lithium and hence the lack of benefit of lithium treatment could have resulted from other lithium – induced cellular changes (Pasquali et al., 2010). Should future studies reveal an impairment in autophagosome clearance in $SOD1^{G93A}$ mice, it would be interesting to see whether

rapamycin, lithium and trehalose bring about an exacerbation of this impairment as this may help to explain, at least partially, their observed lack of benefit in this model.

In conclusion, we have shown that the chemical chaperone and enhancer of autophagy, trehalose, is not able to delay the onset or progression of neurological symptoms or increase survival in the $SOD1^{G93A}$ mouse model of ALS when administered orally. This suggests that trehalose represents a poor candidate for clinical trial in ALS. Furthermore, we observed a trend towards increased misfolding/aggregation of SOD1 in the motor neurons of trehalose-treated mice, suggesting confounding cellular or organismal processes preventing trehalose from having its normal protein-stabilizing and aggregate-clearing effects. One of these confounding processes could have been a pre-existing defect in the autophagy system that was exacerbated by trehalose treatment. Clearly additional work is required to ascertain whether or not the autophagy system is impaired in $SOD1^{G93A}$ mice and if so, the relative contribution that this makes to pathology.

6. Future directions

6.1 Continuation of work performed in this thesis

The aim of this thesis was to address the urgent unmet need for effective treatments for ALS via the preclinical testing of two-potential therapeutics in the most commonly used, $SOD1^{G93A}$, murine model of the disease. The therapeutics selected were; metformin, an anti-type II diabetes drug with potent anti-inflammatory (Dandona et al., 2004, Isoda et al., 2006, Lin et al., 2000) and antioxidant (Lin et al., 2000, Ouslimani et al., 2005, Srividhya et al., 2002) properties as well its ability to bring about mitochondrial biogenesis (Kukidome et al., 2006) and trehalose, a natural disaccharide that behaves as a chemical chaperone and enhancer of autophagy (Sarkar et al., 2007). With metformin, we aimed to target the inflammation and toxic glial activation, oxidative stress and mitochondrial defects that have been shown to occur in ALS patients and models. Whereas, with trehalose we aimed to target the potentially toxic misfolding and aggregation of mutant SOD1 that is a hallmark of pathology in familial patients with mutations in SOD1 and in mutant SOD1-based models (Ilieva et al., 2009). When selecting these compounds, we were encouraged by the fact that both had previously been shown to be beneficial in murine models of other neurodegenerative disorders sharing similar proposed pathological mechanisms to ALS (when administered orally) (Ma et al., 2007, Nath et al., 2009, Rodríguez-Navarro et al., 2010, Tanaka et al., 2004) . Furthermore, both compounds had already been shown to be safe for oral administration in humans (Saenz et al., 2005, Richards et al., 2002) and we therefore reasoned that they would be relatively easy to take to clinical trial should beneficial effects be seen in our preclinical studies. When designing our preclinical studies it was critically important to us to ensure that false positives were avoided and confounding variables were

minimized. We therefore followed (as far as possible) guidelines produced by Scott and colleagues (Scott et al., 2008) and Ludolph and colleagues (Ludolph et al., 2010), which were published close to the start of this study in order to improve the quality of data produced from preclinical studies for ALS.

In our preclinical studies we found that neither metformin nor trehalose could significantly slow disease progression or increase survival in the $SOD1^{G93A}$ model of ALS when administered orally (at three different doses). Additionally, metformin had no beneficial effect on disease onset in male or female mice and trehalose had no beneficial effect on disease onset in female mice, although it was observed to bring about a small dose-dependent delay in weight loss in male mice, which we concluded may have been a feeding effect rather than a delay in motor neuron degeneration. Furthermore, metformin was shown to have a dose-dependent negative effect on disease onset and progression in female mice. We hypothesized that this may have been the result of a metformin-induced inhibition of oestrogen production and indeed showed that metformin was able to reduce oestrogen production in female $SOD1^{G93A}$ mice. These results led us to conclude that the case for the testing of oral administration of metformin or trehalose in clinical trials in ALS patients was poor.

During the timeframe represented by this thesis, we elected to carry out dose-response survival studies with metformin and trehalose prior to performing experiments to investigate whether they were able to bring about the biochemical effects in $SOD1^{G93A}$ mice that we were hoping to achieve (AMPK activation, anti inflammatory and antioxidant effects and mitochondrial biogenesis with respect to metformin and reduced protein aggregation and

enhanced autophagy with respect to trehalose). The decision to do this was not taken lightly and was made on the basis of several factors including:

- time constraints with respect to when appropriate cohorts of mice and the space to house them would be available for survival studies as well as when a sufficiently long space of time was available to monitor mice on a daily basis for the extent of their lifespan.
- The published ability of both metformin and trehalose to have the biochemical effects we were hoping to achieve in murine models of several other neurodegenerative disorders with several common pathological processes
- The question of whether potential therapeutic benefits of a compound could be missed if the compound was discarded on the basis of the inability to carry out a particular biological effect at a particular time point. This was especially the case for metfomin which has multiple biological effects and therefore it would be difficult to predict its effect on disease progression and survival on the basis of its effects on isolated cellular processes.

Had more time been available we would have liked to carry out several additional experiments to investigate possible reasons for the inability of metformin and trehalose to slow disease progression and extend survival in $SOD1^{G93A}$ mice, which are outlined below. These experiments center around determining whether or not metformin and trehalose had the biological effects we were hoping to achieve. Although these experiments are presented below as experiments that we would like to perform now having already got the results of our survival studies, they demonstrate the types of techniques that can be used to ensure a drug is

having its proposed effects *in vivo*. In future studies with less intense time constraints, I would elect to perform these drug-target experiments prior to beginning a survival study.

6.1.1 Experiments to establish potential reasons for the lack of benefit of oral metformin treatment in SOD1^{G93A} mice

The following experiments could be performed to analyse potential reasons for the absence of benefit of metformin treatment in SOD1^{G93A} mice:

An additional cohort of SOD1^{G93A} and WT mice (n=6 per sex, per group) could be treated with 2mg/ml metformin in the drinking water from 35 days of age (the time point at which treatment was commenced in all other metformin experiments performed). Various tissues (liver, quadriceps, TA muscles, brain and spinal cord) could then be collected from these mice as well as untreated controls at 70 days of age, for biochemical analysis. The 2mg/ml metformin dose would be an appropriate dose to use as this was the original dose with which we saw a beneficial effect on motor unit survival in male and female SOD1^{G93A} mice. It was also the middle and therefore most representative dose tested in our dose-response survival study. The time point of 70 days of age (after 35 days of metformin treatment) would be appropriate for tissue collection as this would allow sufficient time for any metformin-induced changes in gene expression/protein activation to become apparent given that by 70 days, cellular changes associated with SOD1^{G93A} pathology would have commenced (Turner and Talbot, 2008). Samples collected could be used for the following investigations:

We originally decided to test the therapeutic potential of metformin for ALS on the basis of its anti-inflammatory (Dandona et al., 2004, Isoda et al., 2006, Lin et al., 2000) and

antioxidant (Lin et al., 2000, Ouslimani et al., 2005, Srividhya et al., 2002) properties as well its ability to bring about mitochondrial biogenesis (Kukidome et al., 2006). Metformin is thought to bring about these effects through the activation of the master regulator of cellular and organismal metabolism, AMPK (Zhou et al., 2001, Nath et al., 2009, Kukidome et al., 2006, Sag et al., 2008). Thus it would be useful to investigate the baseline level of AMPK activation in $SOD1^{G93A}$ mice compared to age-matched WT controls (to establish the existence of any disease-related changes in AMPK activation in $SOD1^{G93A}$ mice) and then to investigate whether metformin was able to bring about activation of AMPK in WT and $SOD1^{G93A}$ mice. As the ultimate cause of death in ALS patients is the loss of functional motor neurons, we would be particularly interested in investigating metformin-induced changes in AMPK activation in the spinal cord where the motor neurons are located. However, brain, muscle and liver samples should be collected in the event of changes in AMPK activation (or any other biochemical changes being investigated) not being detected in the spinal cord. Collection of additional tissues would also provide further tissue to work with should the levels of protein and RNA extracted from spinal cords (using Trizol reagent) be too low to perform successful assays with. If metformin was unable to bring about activation of AMPK in the spinal cords of $SOD1^{G93A}$ mice when administered via the drinking water, this could explain at least in part, the absence of beneficial effects of metformin treatment in our survival study.

When investigating changes in AMPK activation, it is common to investigate the phosphorylation status of the Threonine-172 residue of the AMPKα catalytic domain, which is required for its activation (Sag et al., 2008) and also to look at the phosphorylation (Ser 79) status of the AMPK substrate Acetyl-CoA carboxylase (ACC) (Sag et al., 2008, Nath et al.,

2009). Investigation of the phosphorylation state of AMPK and ACC can be performed by western blot using antibodies provided in the frequently used AMPK and ACC Antibody Sampler Kit #9957 from Cell Signaling Technology (Sag et al., 2008, Narkar et al., 2008).

As the antioxidant properties of metformin as well as its ability to bring about mitochondrial biogenesis are thought to be derived from activation of the AMPK-PGC-1α pathway (Kukidome et al., 2006), it would be useful to investigate base-line levels of PGC-1α expression in the spinal cords of WT and $SOD1^{G93A}$ mice to see whether metformin-treatment augmented these levels. Although it would be most illuminating to look at the levels of PGC-1α protein in the spinal cords of treated and control mice via western blot, conversations with colleagues at conferences and internal lab meetings revealed that commercially available antibodies against PGC-1α can be unreliable. Consequently, we would investigate PGC-1α expression at the RNA level via quantitative reverse transcriptase PCR (Q- RT-PCR), as has previously been described (Kukidome et al., 2006). Considering our hypothesis that the absence of metformin-induced increases force in the TA and EDL muscles of $SOD1^{G93A}$ mice were the result of increased PGC1-α expression causing muscles becoming slower and therefore weaker in phenotype, it would also be interesting to measure the expression of PGC1-α in the muscles collected from treated animals.

If metformin treatment did bring about increased PGC1-α expression in our mice, it would also be interesting to see whether this brought about a resultant increase in the levels of antioxidant enzymes and increased mitochondrial biogenesis. It has previously been shown that PGC-1α is responsible for the induction of reactive oxygen species (ROS) scavenging enzymes such as glutathione peroxidase 1 (Gpx1) and catalase in response to oxidative

stressors (St-Pierre et al., 2006). We therefore would investigate the basal levels of these ROS scavenging enzymes in $SOD1^{G93A}$ mouse spinal cords and the effect of metfomin treatment on the expression of these enzymes via Q-RT-PCR, as has been previously described (St-Pierre et al., 2006). The effect of metformin treatment on mitochondrial biogenesis in human umbilical vein endothelial cells has previously been analysed via Q- RT-PCR-mediated measurement of the mRNA levels of mitochondrial DNA transcription factor A (a transcription factor known to regulate mitochondrial DNA copy number in vivo (Larsson et al., 1998)) as well as by measurement of mitochondrial DNA content via quantitative PCR (Kukidome et al., 2006). We therefore would use these techniques to investigate the effects of metformin on mitochondrial biogenesis in our mice.

Inflammation and toxic glial activation are thought to contribute to pathology in ALS patients and SOD1-related ALS models and the pro-inflammatory cytokine, tumour necrosis factor alpha (TNFα) has been shown to be highly upregulated in the spinal cords of $SOD1^{G93A}$ mice (Hensley et al., 2002, Yoshihara et al., 2002) as well as in the spinal cords of ALS patients (Cereda et al., 2008). We therefore reason that investigation of the levels of TNFα expression in metformin treated and control $SOD1^{G93A}$ mice would give us an indication of whether metformin was able to reduce inflammation in these animals. Metformin treatment has previously been shown to reduce TNFα expression in a murine model of multiple sclerosis (Nath et al., 2009). This was established by performance of Q-RT-PCR for TNFα on brain homogenates (Nath et al., 2009). We therefore would perform Q-RT-PCR to assess the levels of TNFα in the spinal cords of metformin treated and control $SOD1^{G93A}$ mice.

Performance of the experiments outlined above should give us an indication of whether the activation of AMPK and the expression of PGC1α are changed as a consequence of pathology in SOD1^{G93A} mice and furthermore whether metformin was able to augment the activation/expression of these proteins respectively. Additionally they would allow us to analyse whether metformin was able to bring about the reductions in inflammation and oxidative stress and the increase in mitochondrial biogenesis that we hypothesised would be protective in SOD1^{G93A} mice. If metformin was not able to bring about these effects then this would help to explain the absence of any long-term benefits in SOD1^{G93A} mice.

6.1.2 Further experiments to establish potential reasons for the lack of benefit of oral trehalose treatment in SOD1^{G93A} mice

6.1.2.1 Re-counting USOD positive motor neurons in SOD1^{G93A} spinal cords using a system accounting for USOD distribution and intensity within motor neurons

In our trehalose dose-response survival study, we observed that trehalose was unable to bring about any beneficial effect on the onset of neurological symptoms, disease progression or survival in SOD1^{G93A} mice. Furthermore, we observed that trehalose was unable to reduce SOD1 misfolding and aggregation in the motor neurons of these mice and instead showed a trend towards increasing SOD1 misfolding/aggregation (particularly in females). Although this trend was not significant, we felt that it may be valid, particularly in females, owing to our observations of an increased intensity and broader distribution of USOD staining within USOD positive motor neurons in treated mice. This conclusion was further reinforced by our observations of increased levels of extracellular USOD staining in trehalose treated female mice, which we hypothesized may represent secreted misfolded SOD1 species. Although this was not possible within the timeframe represented by this thesis, we would have liked to have

recounted USOD-stained sections from 5% trehalose-treated and control SOD1^{G93A} mice using a counting system that took into consideration the intensity and distribution of USOD-staining within motor neurons. This would give us a clearer picture of whether trehalose significantly affected SOD1 misfolding and/or aggregation. In this new counting system we would count the number of motor neurons in equivalent levels of the sciatic motor pool falling into each of the categories outlined below. Statistical analyses would then be performed to compare the number of motor neurons in each category in control and treated mice.

- Motor neurons showing diffuse, low intensity USOD staining throughout
- Motor neurons showing discrete patches or puncta of low intensity USOD staining
- Motor neurons showing discrete patches or puncta of intense USOD staining and/or intense USOD staining around vacuoles.
- Motor neurons showing intense USOD staining throughout the cell body (which may be interrupted by the presence of vacuoles)

Considering our observations of extracellular USOD staining in the ventral horns of the lumbar spinal cords of some, particularly trehalose treated, mice, it would also be interesting to employ a graded counting system for this observation. Possible categories for this could be:

- Spinal cord section contains no extracellular USOD staining in ventral horn
- Spinal cord section contains moderate extracellular USOD staining in ventral horn
- Spinal cord section contains extensive extracellular USOD staining in ventral horn

As outlined by Ludolph and colleagues, it is important to use an n of at least five per group, with each group representing the same proportion of each gender, when performing histological analyses in $SOD1^{G93A}$ mice (Ludolph et al., 2010). Although n-numbers used for USOD positive motor neuron counts in this study met this criterion (n=4 $SOD1^{G93A}$ males, n=4 $SOD1^{G93A}$ females, n=4 trehalose-treated $SOD1^{G93A}$ males and n=5 trehalose-treated $SOD1^{G93A}$ females), we felt that it was important to consider male and female data separately as trehalose may interact differently with the male and female systems. Consequently it would have been preferable to have an n of at least 6 of each sex per group in our study. If more time was available we would therefore treat an additional cohort of mice with 5% trehalose in order to generate more spinal cords for analysis. As before, we would use littermate controls as far as possible for these analyses to minimise the effects of genetic variations between mice. We would also collect spinal cords from 75 day old $SOD1^{G93A}$ mice treated with 0.5% or 2% trehalose from 35 days of age (n=6 males and 6 females for each dose) in order to investigate the possibility of a dose-dependent effect of trehalose on SOD1 misfolding and/or aggregation.

6.1.2.2 Investigating the autophagy system in the motor neurons of $SOD1^{G93A}$ mice

In a recent publication, Zhang and colleagues revealed that the mTOR dependent autophagy enhancer, rapamycin, accelerates motor neuron degeneration, increases SOD1 aggregation and shortens lifespan in $SOD1^{G93A}$ mice (Zhang et al., 2011). As discussed in Chapter 6 section 6.3, they concluded that these negative effects of may have resulted from exacerbation of a pre-existing impairment in the autophagy system (in particular in the clearance of autophagosomes). In light of these observations, we concluded that should an impaired autophagy system exist in $SOD1^{G93A}$ mice, this could have been, at least partially,

responsible for the failure of trehalose to show any benefit in our SOD1^{G93A} mice. Consequently, if more time had been available, we would have liked to investigate whether similar increases in the levels of the autophagic protein marker LC3-II and p62/SQSTM1 (a marker of autophagic flux) could be seen the spinal cord motor neurons of trehalose-treated animals as those reported by Zhang et al., in rapamycin-treated animals. In the short term we would look at these autophagic markers in the spinal cords of the 75 day old 5%-trehalose treated mice that we have available. We would then also investigate the effects of trehalose on these autophagic markers at equivalent time points (90 and 120 days) to those investigated by Zhang and colleagues, in order to afford direct comparison between our data and theirs.

Although, Zhang and colleagues proposed that autophagosomal degradation may be defective in SOD1^{G93A} mice (potentially through impaired retrograde transport of these vesicles from their site of synthesis at the axonal terminal to the lysosomes where they would be degraded), their study did not include any experiments to confirm whether or not this is the case. This is likely to have resulted from the fact are currently few robust assays available for measuring autophagosomal degradation in an *in vivo* setting (Barth et al., 2010). This is however an emerging field and suitable assays are likely to be developed in the near future. Indeed autophagic flux has recently been measured in the TA muscles of live mice via *in vivo* bioluminescent imaging (Ju et al., 2009). This was carried out through electroporation of both polyQ80-luciferase and polyQ19-luciferase expression constructs into these muscles (polyQ = poly glutamine). PolyQ80 readily aggregates and is an autophagy substrate whereas polyQ19 does not form aggregates. Measurement of the change in the ratio of polyQ80-luciferase to polyQ19-luciferase signals in the TA muscles before and after autophagic stimulation or inhibition, therefore allowed measurement of autophagosomal

degradation of polyQ80 in these muscles (Ju et al., 2009). Although this method may not be ideal in SOD1^{G93A} mice, considering the implications of introducing additional protein aggregates into a system already overloaded with aggregated SOD1 and also the challenge of delivering luciferase constructs to motor neurons in the spinal cord, it demonstrates that novel assays are continuously being developed to study autophagy *in vivo*. Should an impairment in autophagy be identified in SOD1^{G93A} mice in future studies, it would also be interesting to investigate this in TDP-43 and FUS/TLS-related animal models. This would give some indication of whether impaired autophagy was solely a feature of ALS caused by mutations in SOD1 or a more widespread defect (potentially occurring in both sporadic and familial cases of ALS). Early evidence in support of widespread defect in autophagy in ALS patients has come from recent reports of increased autophagy (as measured by an increase in double-membraned autophagosomes) in degenerating motor neurons over surviving motor neurons in the spinal cords of 16 sporadic ALS patients and no evidence of autophagy features in controls (Sasaki, 2011). However, much additional work is clearly required before firm conclusions about the role of autophagy in ALS can be drawn.

6.1.2.3 Investigating the levels of trehalose in the spinal cords of trehalose treated and control SOD1^{G93A} mice.

Although the strong trend towards increased SOD1 misfolding/aggregation that we observed in the motor neurons of the sciatic motor pool in trehalose treated SOD1^{G93A} female mice was likely not an artefact, we cannot rule out this possibility. If this trend was indeed an artefact, then this combined with the absence of any trehalose induced benefits on neurological symptoms or survival in SOD1^{G93A} mice could put into question whether trehalose was able to reach the spinal cords of SOD1^{G93A} mice when administered via the drinking water in our

study. This is a particularly important consideration as ingested trehalose is thought to be hydrolyzed in the small intestine by the enzyme trehalase, into two d-glucose molecules, which are subsequently absorbed and metabolized (Richards et al., 2002). Consequently, if trehalose was completely digested to glucose in the small intestines of treated mice before reaching the blood stream, then it would not have reached the spinal cord. However, it is known that there is a small degree of intestinal permeability (though passive diffusion) to other disaccharides, including lactulose and sucrose, in humans (van Elburg et al., 1995). It is therefore possible that a fraction of the trehalose ingested by our $SOD1^{G93A}$ mice reached the bloodstream through this passive diffusion process. However, it must also be noted that trehalase activity has been found in the liver, plasma and kidney in mammals (Richards et al., 2002). Consequently if trehalase is also present in these locations in mice, this could have reduced the levels of any trehalose molecules reaching the bloodstream.

The persistence of some trehalose molecules in the bloodstream, despite the actions of trehalase, would be supported by the fact that trehalose (administered at doses or 1 or 2% via the drinking water) has been shown to have significant beneficial effects in the central nervous systems of mouse models of both parkinsonism/ tauopathies (Rodríguez-Navarro et al., 2010) and Huntington's disease (Tanaka et al., 2004) and also in the muscles of a mouse model of oculopharyngeal muscular dystrophy (Davies et al., 2006). Indeed it was these promising positive results that prompted us to test trehalose in our $SOD1^{G93A}$ mice, despite our concerns over how much trehalose would reach the CNS in these animals and the lack of robust measurements of trehalose levels in target tissues in these previous studies. We were further influenced by experiments in which Tanaka and colleagues showed that treating their R 6/2 mouse model of Huntington's disease with 2% glucose via the drinking water, did not

recapitulate the beneficial effects that they had seen with trehalose in the same model. This suggested to them that the beneficial effects of trehalose seen in R 6/2 mice were not derived from increased glucose absorption through hydrolysis of trehalose to two glucose molecules in the small intestine (Tanaka et al., 2004). However it must be noted that a more appropriate dose of glucose to test in this instance may have been 4% glucose considering that the hydrolysis of trehalose results in the production of two glucose molecules for every one trehalose molecule.

Although we initially tested trehalose in our $SOD1^{G93A}$ mice on the basis of its positive results in models of other disorders involving protein aggregation, the disparity between our results and those of other studies prompted us to consider the formal possibility that the positive results seen in other studies were derived from experimental error rather than genuine positive results. Our reasoning behind this was that if false positives can occur though inappropriate experimental design in $SOD1^{G93A}$ mice, this could also be the case for other disease models. As we took measures to ensure that the chance of obtaining false positives/negatives was kept to a minimum in our studies, we feel confident in the validity of the results obtained. However, without investigating the study designs used in other disease models further, we could not be sure that this was also the case for these studies. We therefore analysed these previous studies in order to investigate whether they had been designed in such a way to keep the possibility of error low.

Although these studies overall appeared to be performed in a reasonable manner, there were some aspects of study design which could have been improved. For example, when studying Trehalose in the R 6/2 model of Huntington's disease (Tanaka et al., 2004), Tanaka and

colleagues used n-numbers that were substantially lower than those recently calculated by Menalled and colleagues to be required for 30% effect using similar behavioural assessments in the same model (Sasaki, 2011). Furthermore they did not perform their study in a blinded fashion and did not mention whether groups were balanced for sex. The absence of sex balancing is worrying considering differences between drug absorption and response to treatment have been observed between male and female R6/2 mice in other pre-clinical studies (Menalled et al., 2009). Additionally, the endpoint used for survival analyses was not described. If a uniform end-point was not used for all mice (as suggested for studies in $SOD1^{G93A}$ mice (Scott et al., 2008)) then this could have introduced error into survival results. Finally, the mutation that causes Huntington's disease is an expansion of a CAG repeat in the first exon of the gene encoding the protein Huntingtin. (MacDonald et al., 1993). It is now known that the CAG repeats in the Huntingtin transgene in R6/2 mice are unstable and that this can result in drifts in CAG length in individual colonies (Menalled et al., 2010). Such changes in the number of CAG repeats have been identified to bring about changes in the onset and severity of disease in R6/2 mice (Dragatsis et al., 2009). It has therefore recently been recommended that CAG lengths for individual R6/2 mice in preclinical studies are measured and balanced across groups (in addition to groups being balanced for gender, litter and weight) to avoid the occurrence false positives or negatives (Menalled et al., 2010). Consequently if CAG length was not accounted for in experiments performed by Tanaka and colleagues and groups were not appropriately balanced, this could have been a potential source of error.

Studies performed with Trehalose in OPMD mice and in parkin-deleted/tau overexpressing mice by Davies and Colleagues and Rodriguez-Navarro and colleagues respectively were

more difficult to analyse as both were performed using transgenic mouse lines that were generated in house and are therefore less well characterised in terms of appropriate n-numbers and potential sources of error (Davies et al., 2006, Rodríguez-Navarro et al., 2010). However, we identified certain aspects of experimental design which could have been improved upon, for example, neither study appeared to balance experimental groups for litter and both studies used very low n-numbers (as low as 2 in one study) for certain important histological analyses. N-numbers for behavioural analyses were initially reasonably high in both studies (≥15) but dropped to less appropriate numbers at later time points. Finally behavioural analyses performed by Rodrigues Navarro and colleagues did not appear to be performed in a blinded fashion (Rodríguez-Navarro et al., 2010).

As described above, each of the studies in which trehalose had previously been shown to have a beneficial effect on disease pathology had some short-comings in experimental design. If these shortcomings did result in false positives then this would lend weight to the possibility that trehalose may not reach the CNS at therapeutic levels when administered via the drinking water. In light of this possibility, it would be interesting to carry out experiments to measure trehalose levels in the brains and spinal cords of trehalose-treated and control $SOD1^{G93A}$ mice. However, it must also be noted that if trehalose was found not to reach the CNS in $SOD1^{G93A}$ mice, this may not necessarily mean that this would also be the case in the other disease models discussed. Indeed it may be that there are strain and model specific differences in the degree of absorption of trehalose into the bloodstream and indeed in the response to trehalose, which could have resulted in the discrepancy between our results and those in other disease models. However, if trehalose was determined to reach the CNS in our $SOD1^{G93A}$ mice, then this would lend support to our hypothesis that the apparent increases in

SOD1 misfolding/aggregation in the motor neurons of trehalose treated animals were a direct result of trehalose-treatment and not chance.

When researching possible methods for measuring trehalose levels in target tissues, we identified that it might be possible to carry out direct measurements via high performance liquid chromatography (HPLC) followed by electrochemical detection, as has previously been described (Wannet et al., 2000). However, a discussion with Dr Terry D. Butters at the Oxford Glycobiology Institute revealed that quantification of trehalose in tissues using such a chromatography method presents several difficulties, including extraction efficiency, separation of potential cross-contaminants and detection of low levels (which would probably be the case in the brains and spinal cords of $SOD1^{G93A}$ mice). Performance of these HPLC experiments would therefore require considerable optimisation time in order to gain meaningful results. Consequently, we have considered other methods for trehalose detection which may be more cost and time effective.

As discussed in above, trehalose treatment has been tested in the R6/2 model of Huntington's disease by Tanaka and colleagues (Tanaka et al., 2004). In this publication, Tanaka and collaborators claimed that they confirmed the presence of trehalose in brain homogenates of treated mice to be 0.11 ± 0.02 nmol/μg protein and in the livers of these mice to be 11.6 ± 1.1 nmol/μg protein. These values were determined by measuring glucose concentrations in brain and liver homogenates of trehalose-treated mice before and after treatment with the enzyme trehalase. As trehalose is composed of two glucose molecules, halving the increase in glucose derived from trehalase treatment would indicate the amount of trehalose present (providing all other metabolic processes that may change glucose concentration were

disabled during the assay). Unfortunately however, these measurements were only made in trehalose-treated mice and therefore baseline levels of trehalose in these tissues were not established. Furthermore, n-numbers used were not described and an in depth discussion of methodology was not made. We therefore contacted Tanaka and colleagues to establish further information about their methodology and controls used, however they could not offer any further clarification. We therefore feel that these measurements require further confirmation. The method used by Tanaka and colleagues to measure trehalose levels has been used by several other groups in *saccharomyces cervisiae* (Kienle et al., 1993, Lee and Goldberg, 1998). On the basis of these results, we reasoned that provided appropriate controls were put in place, this could be a relatively simple method to investigate the levels of trehalose reaching the spinal cords of our mice. The methods that we would use for optimising this assay are outlined in appendix 3:

6.2 Future perspectives for the development of effective therapeutics for ALS

As discussed throughout this document, a huge number of therapeutics have been tested and shown to be moderately successful in pre-clinical studies of ALS, however, all but one of these therapeutics (Riluzole) have failed to show any benefit in ALS patients in the clinic. Furthermore, Riluzole is at best only able to prolong the survival of patients by a few months (Miller et al., 2007). Various reasons have been proposed for the discrepancy between successful preclinical results and failed clinical trials, including but not limited to: a failure to design preclinical studies in such a way that false positives are avoided (Scott et al., 2008), the testing of therapeutics in the clinic that were unable to alter disease progression in preclinical studies (Zinman and Cudkowicz, 2011), a potential inconsistency between disease

characteristics in high copy $SOD1^{G93A}$ mice and familial ALS patients (who would only have one copy of the mutant SOD1 gene) and additionally between disease characteristics in $SOD1^{G93A}$ mice and sporadic ALS patients without mutations in SOD1, and finally, a failure to account for differences in corticospinal anatomy, pharmacokinetics and pharmacodynamics between mice and humans when designing dosing and administration regimes for clinical trial.

The failure of so many therapeutics in the ALS clinic to date also indicates that we have likely not yet managed to elucidate and target toxic mechanisms far enough upstream in disease pathology to have significant therapeutic effect in ALS patients. Furthermore, many of the toxic processes implicated in motor neuron degeneration in ALS have been shown to be interrelated and to exacerbate each other. It may therefore be that targeting a number of these toxic processes at the same time is required to bring about a successful treatment effect (in the absence of a therapy that can address the primary trigger(s) for motor neuron degeneration in this disease).

Although the most upstream mechanisms leading to motor neuron degeneration have to date been elusive, I feel that we are entering a time in ALS research, where the possibility of their elucidation is stronger than ever. This is largely the result of the recent discoveries of causative mutations in the RNA-binding proteins TDP-43 and FUS/TLS in both familial and sporadic ALS patients, coupled with the discovery that one or other of these proteins aggregates in most sporadic ALS patients. These discoveries have lead to the development of various new models in which to carry out ALS research and have also opened up a new avenue of research, in terms of the role of RNA-metabolism in ALS. Furthermore, very

recently the field of ALS research has taken a huge leap forward in the discovery by Renton and collaborators and DeJesus-Hernandez and colleagues that a large hexanucleotide (GGGGCC) repeat expansion in the first intron of the *C9ORF72* gene on the short arm of chromosome 9 is causative for ALS and responsible for approximately a third of familial ALS cases (Renton et al., 2011, DeJesus-Hernandez et al., 2011). Although it is not yet clear how the hexanucleotide repeat expansion in the non-coding region of the *C9ORF72* gene can cause ALS and FTD, Renton and colleagues propose that it may affect the function of C9ORF72, whose cellular role is as yet unknown. However, they also hypothesise that RNA generated from the repeat expansions could disrupt transcription by sequestering normal RNA and proteins involved in transcription regulation, as has previously been proposed for other repeat expansion mutations (Wojciechowska and Krzyzosiak, 2011). This hypothesis fits nicely into the increasingly proposed role for defects in RNA metabolism in ALS. Indeed in a previous publication by Lin and colleagues, samples from ALS patients in a family that have subsequently been shown to possess the chromosome 9 hexanucleotide mutation, showed evidence of aberrant RNA metabolism of the astroglial EAAT2 glutamate transporter (Lin et al., 1998), whose altered expression levels have implicated as a potential pathological mechanism in ALS (Ilieva et al., 2009).

In addition to the exciting discovery of hexanucleotide mutations in chromosome 9 in familial ALS patients, mutations in *UBQLN2*, which encodes the ubiquitin-like protein ubiquilin 2, have recently been discovered to be capable of causing dominantly inherited, chromosome-X-linked ALS and ALS/FTD (Deng et al., 2011). Ubiquilin 2 is a member of the ubiquilin family, which regulates the degradation of ubiquitinated proteins. Accordingly, functional analysis performed by Deng and colleagues, showed that mutations in *UBQLN2*

lead to an impairment of protein degradation *in vitro* and the formation of intracellular aggregates in the spinal cords of patients with these mutations. Interestingly, these intracellular aggregates were found to be positive for ubiquilin 2 as well as TDP43 and FUS but not SOD1 in post-mortem samples from affected patients. This lead Deng and colleagues investigate whether ubiquilin 2 was a component of intracellular inclusions in other types of ALS. To do this they examined 47 post-mortem spinal-cord samples, including cases of sporadic ALS (n = 23), familial ALS without mutations in *SOD1*, *TDP43* and *FUS* (n = 5), ALS with dementia (n = 5), familial ALS with *SOD1* mutations (n = 7 (A4V, n = 4; G85R, n = 2; E100G, n = 1)), familial ALS with a G298S mutation in *TARDBP* (n = 1), and controls without ALS (n = 6). Fascinatingly they discovered ubiquilin-2-positive inclusions in all ALS cases investigated, indicating that ubiquilin 2 is a common component of proteinaceous inclusions in a wide variety of ALS. These observations strongly support a contributory role for impaired protein turnover in ALS and also suggest that defects in protein turnover and perturbations in RNA-processing in ALS may be interrelated.

Discoveries of repeat expansion mutations in chromosome 9 and x-linked *UBQLN2* mutations in familial ALS will undoubtedly lead to the generation of murine models harboring these mutations. Once these models are established, their comparison to models expressing mutant or WT forms of TDP-43, FUS/TLS and SOD1 is likely to be instrumental in allowing researchers to tease out the primary mechanisms responsible for ALS. In particular, if common pathological processes can be identified in these models, then these are likely to play important roles in ALS pathology as a whole. Early experiments in two different transgenic mouse models made to express human WT TDP-43 in the CNS have already provided one example of this. Specifically, these investigations revealed alterations in

mitochondrial ultrastructure as well as clusters of swollen mitochondria in motor neuron cell bodies and reduced numbers of mitochondria at motor neuron terminals (Shan et al., 2010, Xu et al., 2010), that are remarkably similar to defects in mitochondrial morphology and distribution recently characterised by Vande Velde and colleagues in $SOD1^{G37R}$ and $SOD1^{G85R}$ mice, crossed to mice expressing mitochondrially targeted eGFP (Hb9-MitoEGFP mice) (Vande Velde et al., 2011). This suggests a potential common defect in the ability of mitochondria within motor neurons to regulate their size, morphology and distribution in these models, which I plan to investigate further in my post doctoral studies with the Vande Velde group.

As mutations in proteins involved in the processes of mitochondrial fission and fusion, can themselves cause neurodegenerative disorders such as Charcot-Marie-Tooth type 2A (a peripheral neuropathy affecting sensory and motor neurons of the distal extremities (Zuchner et al., 2004)) and autosomal dominant optic atrophy (a degeneration of retinal ganglia cells that leads to optic nerve atrophy (Alexander et al., 2000)), it seems likely that defects in mitochondrial fission and fusion could play a primary role in ALS pathology if these are found to be a common occurrence in TDP-43 and SOD1 models. Furthermore, should common mitochondrial defects be found in TDP-43 and SOD1 models it would also be interesting to investigate the potential existence of these defects in FUS/TLS models (although the production and characterisation of FUS/TLS models is at this stage slightly less advanced than the production/characterisation of TDP-43 models (Da Cruz and Cleveland, 2011))

Should commonalities in pathological mechanisms occurring in SOD1, TDP-43 and FUS/TLS models (and potentially in novel models harbouring repeat expansion mutations in chromosome 9 or *UBQLN2* mutations) be found in the future and therapeutics be identified to target them, then the ability to test these therapeutics in a number of these models rather than just SOD1-related models will be highly advantageous. Specifically, if a therapeutic is shown to be successful in robust preclinical studies set up in multiple models, it is probably more likely to show success in the clinic than a therapeutic that only shows success in one model (unless it is specifically targeted to a particular mutation). Furthermore, WT TDP-43 and FUS-overexpressing models may provide a better representation of pathology in sporadic ALS-patients than SOD1 models and this could be beneficial considering that the majority of ALS patients enrolled in clinical trials have sporadic forms of the disease. However the upmost care must be taken to design meaningful studies for the testing of potential compounds for these studies, in terms of ensuring that; analysis of optimal dosing is performed, adequate n-numbers are used, confounding variables are controlled for and relevant parameters for ALS patients (particularly the effect of therapeutics on disease progression) are addressed.

Interestingly, in a recent publication, Mead and colleagues proposed a novel method for the preclinical testing of therapeutics for ALS which they suggest may increase throughput for reduced costs, whilst reducing the severity of the experimental procedures involved (Mead et al., 2011). In this publication they described the production of an inbred C57BL/6 mouse line from the original mixed background (SJLxC57BL/6) $SOD1^{G93A}$ transgenic line and revealed that these mice were less prone to background noise than mice on the mixed genetic backgrounds. In line with this, power calculations revealed that less than half of the mice

required on the mixed genetic background were required on the inbred background to obtain a 10% effect on survival (Mead et al., 2011). Although using inbred genetic backgrounds has the disadvantage that some potential therapeutic effects may be missed, the ability to use fewer mice and to have a lower risk of noise in experiments is clearly advantageous (providing that sources of error associated with genetic drift are controlled for (Taft et al., 2006)). Mead and colleagues revealed that in these mice, a robust and reproducible, decline in motor function as measured by rotarod performance could be detected at the very early time point of 40 days of age, over a month prior to the onset of visible clinical signs of disease. They also detected early and progressive changes in hind-limb muscle volumes using magnetic resonance imaging (MRI) and in certain aspects of gait using a catwalk gait analysis system (Mead et al., 2011). On the basis of these observations they propose the use of the following pre-clinical screening protocol to assess the potential of therapeutics in this early window of loss of motor function and hind-limb muscle innervations. They suggest that implementing this screening process would reduce the number of animal experiments that would need to be taken through to phases of disease in which $SOD1^{G93A}$ mice would experience the most distress (i.e. symptomatic and end stages) (Mead et al., 2011).

1) Use 14 litter and sex matched mice in each of two groups (control dosed and active dosed), dosed from day 21 onwards (weaning), with weighing at each dose.

2) Assess from day 35 twice per week for motor performance using rotarod testing following 3 days consecutive training on ~days 30–33.

3) At day 60 assess hind-limb muscle volumes using MRI in 7 mice per group and collect tissue from the same mice to assess percentage innervation of motor end-plates in the gastrocnemius muscle.

4) Assess the remaining 7 mice per group, 3 times per week for onset of clinical signs from 60 days of age to day 90 (if necessary) and gait analysis using the catwalk gait analysis system at 63, 77 and 91 days of age (9, 11, and 13 weeks). Collect tissue at day 91 for further analysis of histological readouts.

Although we feel strongly about implementing methods in ALS research that minimise the number of animals required and the distress caused to the animals by these methods, we are concerned that this screening protocol may not be the most meaningful for ALS patients. As **Appendix 1** shows, there is little correlation between the ability of therapeutics to influence disease onset and survival in $SOD1^{G93A}$ mice. Consequently, if therapeutics were shown to have benefit at the early time points investigated in the screening protocol proposed by Mead and colleagues, this would give little information about whether they would have any effect on the most relevant parameter for ALS patients, disease progression. Furthermore if therapeutics were shown **not** to be beneficial at these early stages, this would not necessarily mean that they wouldn't have an effect on disease progression and this could lead to therapeutics with the potential to help ALS patients being missed. Finally, any therapeutics that were found to be beneficial at the early time points involved in the Mead et al., protocol would have to be tested at later time-points in an additional cohort of mice before they could be used in clinical trials, which would effectively double the number of mice required. I therefore feel that the guidelines for preclinical testing of therapeutics for ALS proposed by

Scott and colleagues and used in this thesis are still the best to follow (Scott et al., 2008). However, these could be supplemented by the early assessment of rotarod performance proposed by Mead and colleagues as well as longitudinal catwalk analysis should the facilities for this be available, as knowledge of the effect of therapeutics early on in the disease course would be useful. Furthermore the use of inbred lines, as suggested by Mead and colleagues, would permit the use of fewer mice which would make performance of more lengthy tests such as rotarod and catwalk analysis more manageable (particularly when testing multiple doses). As MRI facilities are expensive and not readily accessible to many researchers we consider that these would not be essential, however, they would be interesting if facilities and finances were available. In addition to the longitudinal monitoring of neurological symptoms, histological and biochemical analyses of the mechanisms of action of therapeutics being tested in tissues collected from an additional cohort of mice would be beneficial.

Finally, in addition to improving preclinical studies of potential therapeutics for ALS, it will also be important to work on improving the clinical testing of these compounds. One area with great potential for the improvement of the clinical testing of therapeutics for ALS is the elucidation of relevant biomarkers to permit the earlier diagnosis of ALS as well as the tracking of disease progression in ALS patients. Historically, the most frequently used primary outcome measure in phase-III clinical trials in ALS patients has been survival (de Carvalho and Swash, 2011). However, using survival as the primary outcome measure, makes for long and expensive trials which may cause patients and their families considerable stress if the therapeutic appears not to work (de Carvalho and Swash, 2011). Furthermore, the possibility of receiving placebo in these clinical trials is understandably a great concern for

ALS patients as they would then have no hope of increased survival, although the potential use of historical controls in such studies is being debated as a potential measure to avoid this problem (Zinman and Cudkowicz, 2011). Should suitable biomarkers for ALS pathology be identified in the future then this would permit the investigation of whether potential therapeutics interact with their intended targets, are being administered at the most appropriate dose and/or affect disease progression in smaller, shorter, early-phase trials. This would mean that only those therapeutics and dosing regimens shown to be efficacious in these quicker screening studies would need to be tested in long and expensive Phase III studies. Biomarkers could then further be used to provide supportive or even primary evidence for efficacy in these late-phase trials (and potentially facilitate decisions to terminate trials should sufficient modulation of disease progression not be seen) (Hersch and Rosas, 2011) . Furthermore, if relevant ALS biomarkers were to be found, these may allow the earlier diagnosis and therefore earlier recruitment of patients into clinical trials as well as potentially facilitating the selection of more homogeneous cohorts of patients for clinical trials (Zinman and Cudkowicz, 2011). Although we are not yet at a stage where suitable biomarkers for ALS have been fully characterized, several candidates, or panels of candidates that may provide an ALS signature are under investigation (de Carvalho and Swash, 2011). For example Ganesalingam and colleagues recently conducted a study in which they measured and compared levels of various cytoskeletal proteins and inflammatory markers in the cerebrospinal fluid (CSF) of ALS patients, disease controls and healthy subjects. Through these analyses they found that the ratio of the levels of phosphorylated neurofilament heavy chain compared to complement C3 (pNFH/C3) could identify ALS samples with 87.3% sensitivity and 94.6% specificity in a total of 71 ALS subjects, 52 disease control subjects and 40 healthy subjects. They also revealed that the level of CSF

pNFH correlated with survival of ALS patients (Ganesalingam et al., 2011). Although these initial results are promising, future prospective studies incorporating pNFH and pNFH/C3 analysis of CSF will be important to establish the diagnostic accuracy and clinical utility of these biomarkers.

6.3 Optimising the design of my future preclinical studies for ALS Performing two survival studies in $SOD1^{G93A}$ mice during this PhD has instilled in me the fact that pathology in SOD1 mice (and likely ALS patients) is highly aggressive and hence without elucidating toxic processes that are early on in the pathological cascade in this disease we are unlikely to identify highly effective therapeutics. It is therefore my aim to work on the elucidation of the most upstream mechanisms leading to ALS in my postdoctoral studies and to only carry out the preclinical testing of therapeutics once I have identified a mechanism to target that I feel is sufficiently far upstream. Following identification of such a mechanism I would plan to employ a high throughput screening method to identify compounds which most robustly target this toxic mechanism. Various model systems are adaptable to high throughput screens including, cell based systems (Benmohamed et al., 2011) as well as zebrafish(Walker et al., 2012) and c-elegans (Desalermos et al., 2011). If efficacious compounds were found in such a high throughput screen I would then plan to test them in the most relevant murine models of ALS available. Although this was something that was not done during this PhD owing to logistical and time constraints, I would select biochemical analyses that would give me the best possible indication of whether my candidate compounds could target the toxic mechanism in question in the transgenic line(s) selected. These could involve techniques such as Q-PCR and western blots on tissue samples collected from treated animals to look for changes in expression of key molecules and could also be used to aid selection of optimal doses. However it would have to be ensured that these drug-target studies were designed in

such a way that they were sufficiently powered and avoided any confounding variables associated with the model in question. Should several candidate drugs be tested in these drug-target studies, the most effective drug would be selected for a full survival study. Considering the lower n-numbers required for inbred strains over those on missed backgrounds in survival studies, I would use an inbred strain as this would free up more time for performing additional longitudinal analyses on top of those performed in this study. I feel that the longitudinal analyses performed in the studies in this document are sensitive and highly capable of detecting positive and negative effects of administered therapeutics, in particular when employed in dose-response studies. However, there has not been a published study in which these longitudinal analyses have been directly compared to other, more traditional longitudinal analyses such as rotarod and grip strength. I would therefore like to incorporate the rotarod test from an early timepoint as suggested by Mead and colleagues in order to compare whether the data that can be obtained from the different longitudinal analyses are complementary. This will be of great benefit to the ALS field. Finally, as would have been performed for the studies described in this thesis had more time been available, I will carry out histological and biochemical analyses, to back up the results from the longitudinal analyses performed during survival studies. For example if slowed disease progression is found in a survival then this will be backed up by motor neuron counts at key time points etc. Finally if I perform motor unit estimation via electrophysiology again, I will ensure that the baseline for measurements remains constant, that motor units are counted during as well as after the measurement procedure and that the phenomenon of alternation is taken into consideration,

6.4 Overall conclusions

This study has permitted the designing and implementation in our laboratory of an optimised study format for the preclinical testing of potential therapeutics for ALS in the $SOD1^{G93A}$ murine model of this disease. In this study design, optimal mouse husbandry conditions are outlined to ensure the generation of consistent results and the minimisation of animal suffering. Using this study format we were able to identify that metformin and trehalose, when administered orally, do not represent promising candidates for clinical trial in ALS, despite showing promise in models of other neurodegenerative diseases. Furthermore, we identified several themes for continued research, including (1) the relationship between ALS and diabetes and the way in which metformin treatment modifies this relationship and (2) the role of autophagy in the pathogenesis of ALS. Finally, performing these preclinical studies has instilled in me the critical importance of identifying the primary triggers/mechanisms responsible for motor neuron degeneration in ALS in order to have more likelihood of identifying therapeutics that will be successful in ALS patients. The emergence of new models of ALS through identification of mutations/alterations in TDP-43, FUS/TLS, C9ORF72 and ubiquilin 2 biology in ALS will undoubtedly help with the identification of these primary mechanisms. Furthermore a commitment to improving the preclinical testing of therapeutics for ALS as well as the efficiency of clinical trials for this disease will be instrumental in tackling the urgent need for suitable therapeutics for ALS patients.

7. Appendices

7.1 Appendix 1: Summary of therapies tested to date in mutant SOD1-based murine models of ALS

Agent	Model	Gender	Dosology	Start (days)	Onset change (%)	Survival change (%)	Reference
Anti-oxidant							
N-acetylcysteine	SOD1$^{G93A\ G1L}$	m/f	500 mg/kg/d, sc	120	ns	ns	(Jaarsma et al., 1998)
	SOD1$^{G93A\ G1L}$	m/f	10 mg/ml, water	120	ns	ns	(Jaarsma et al., 1998)
	SOD1^{G93A}	nd	2 mg/kg/d, water	28–35	↑	↑ 7	(Andreassen et al., 2000)
Apocynin	***SOD1^{G93A}***	***m/f (n=13-63)***	***20, 150, 300, water***	***14***	***↑***	***↑45^{c}, 65^{c}, 90^{c}***	***(Harraz et al., 2008)***
AR-R 17338, 18512	SOD1^{G93A}	nd	250, 150 mg/ml, water	30	ns	ns	(Upton-Rice et al., 1999a)
AR-R 17477	SOD1^{G93A}	nd	40 µg/ml, water	30–40	nd	↑ 10	(Facchinetti et al., 1999)
	SOD1$^{G93A\ G1L}$	nd	40 µg/ml, water	30–40	nd	↑ 13	(Facchinetti et al., 1999)
Ascorbate	SOD1^{G93A}	m	0.8% diet	50	ns	↑ 8	(Nagano et al., 2003)
Aspirin	SOD1^{G93A}	m	100–160 mg/kg/d, water	35	↑	ns	(Barnéoud and Curet, 1999)
Aspirin	**SOD1^{G93A}**	**m**	**100–160 mg/kg/d, water**	**91**	**ns**	**ns**	**(Barnéoud and Curet, 1999)**
Baicalein	SOD1^{G93A}	m/f	3.7, 7.4 nmol/kg/d for 5 weeks, sc	63–77	nd	nd	(Ignacio et al., 2005)
Carnitine	SOD1$^{G93A\ G1L}$	m/f	50 mg/kg/d, water	112	↑	↑	(Kira et al., 2006)
	SOD1$^{G93A\ G1L}$	m/f	5 mg/kg/2d, sc	Onset	nd	↑	(Kira et al., 2006)
Carnosine	SOD1^{G93A}	m/f	2.2, 11 µmol/kg/d for 5 weeks, ip	63–77	nd	nd	(Ignacio et al., 2005)
Carnosic acid	***SOD1^{G93A}***	***f (n=13-22)***	***0.13 mg/kg, ip, twice weekly***	***63***	***ns***	***ns***	***(Shimojo et al., 2010)***
Catalase	SOD1^{G93A}	m/f	720–900 U/d, sc	30–46	↑ 12	ns	(Reinholz et al., 1999)
	SOD1$^{G93A\ G1L}$	m/f	60,000 U/kg, 2 times a week, ip	30–45	↑ 7	ns	(Reinholz et al., 1999)
Catalase-putrescine	SOD1^{G93A}	m/f	720–900 U/d, sc	30–46	↑ 26	ns	(Reinholz et al., 1999)
	SOD1$^{G93A\ G1L}$	m/f (n=13-18)	60,000 U/kg, 2 times a week, ip	30–45	↑ 15	ns	(Reinholz et al., 1999)

Agent	Model	Gender	Dosology	Start (days)	Onset change (%)	Survival change (%)	Reference
	SOD1$^{G93A\ G1L}$	nd	450 U/d, sc	35–42	↑ 6	↑ 12	(Poduslo et al., 2000)
CDDO ethylamide (Nrf2/ARE activator)	***SOD1^{G93A}***	***m/f (n=18)***	***80 mg/kg/day diet***	***30, onset (80-90)***	***nd***	***↑17, ↑14***	***(Neymotin et al., 2011)***
CDDO trifluoroethylamide (Nrf2/ARE activator)	***SOD1^{G93A}***	***m/f (n=18)***	***80 mg/kg/day diet***	***30, onset (80-90)***	***nd***	***↑ 14, ↑***	***(Neymotin et al., 2011)***
Celastrol	SOD1^{G93A}	nd	2, 8 mg/kg/d, diet	30	↑ 15, nd	↑ 9, 13	(Kiaei et al., 2005b)
Creatine	SOD1^{G93A}	nd	1, 2% diet	70	nd	↑ 9, 18	(Klivenyi et al., 1999)
	SOD1^{G93A}	***nd n=25-32***	***2% diet***	***76-80***	***nd***	***nd***	***(Choi et al., 2009)***
DMPO	SOD1^{G93A}	nd	5 mg, 3 times a week, ip	70	nd	↑	(Liu et al., 2002)
DP-109, DP-460	SOD1^{G93A}	nd	**5, 10 mg/kg/d, water for DP-109 and DP-460 respectively**	30	**↑ 8, 10 for DP-109 and DP-460 respectively**	**↑ 10, 9 for DP-109 and DP-460 respectively**	(Petri et al., 2007)
Genistein	SOD1$^{G93A\ G1L}$	m/f	16 mg/kg, 2 times a day for 5 × week, ip	nd	↑ m	↑ m	(Trieu and Uckun, 1999)
Ginko biloba	SOD1^{G93A}	m/f	200, 400 mg/kg/d, diet	21	nd	↑ 9, 10 m	(Ferrante et al., 2001)
Ginseng	**SOD1^{G93A}**	**nd**	**40, 80 mg/kg/d, water**	**30**	**↑ 19^{d}**	**↑ 5^{d}**	**(Jiang et al., 2000)**
Green tea	SOD1^{G93A}	nd	2.9, 5.8 mg/kg/d, po	60	↑ 12, 11	↑ 16, 17	(Koh et al., 2006)
	SOD1^{G93A}	nd	10 mg/kg/d, po	42	↑ 9	↑ 11	(Xu et al., 2006)
Light	***SOD1^{G93A}***	***nd (n=11-12)***	***140-mW output power, 1.4 cm2 spot size, 120s treatment, 12 J/cm2 energy density per treatment site/day (3 treatment sites across CNS and spinal cord)***	***51***	***nd***	***ns***	***(Moges et al., 2009)***
Lipoic acid	SOD1^{G93A}	nd	100 mg/kg/d, diet	28	nd	↑ 6	(Andreassen et al., 2001)
Melatonin	SOD1^{G93A}	f	0.5 mg/ml, water	28	ns	↑ 5	(Weishaupt et al., 2006)
L-NAME	SOD1^{G93A}	nd	50, 200 µg/ml water	30	nd	ns	(Facchinetti et al., 1999)
	SOD1^{G93A}	***m (n=10)***	***3.3mg/d, sc***	***60***	***nd^{f}***	***nd***	***(Martinez et al., 2008)***
	SOD1^{G93A}	***m (n=10)***	***3.3mg/d, in***	***60***	***nd^{f}***	***nd***	***(Martinez et al., 2008)***
Neu2000	SOD1^{G93A}	nd	30 mg/kg/d, diet	56	↑ 14	↑ 15	(Shin et al., 2007)
7-nitroindazole	SOD1^{G93A}	nd	25 mg/kg, 2 times a	60	nd	ns	(Facchinetti et

Agent	Model	Gender	Dosology	Start (days)	Onset change (%)	Survival change (%)	Reference
			day, sc				al., 1999)
D-penicillamine	SOD1^{G93A}	nd	0.1 g/kg, 5 times a week, po	30	↑ 8	↑ 8	(Hottinger et al., 1997)
	SOD1^{G93A}	nd	0.1% diet	30	ns	↑ 7	(Hottinger et al., 1997)
Fe-porphyrin	SOD1^{G93A}	nd	1 mg/kg/d, ip	40	nd	↑ 5	(Wu et al., 2003)
	SOD1^{G93A}	nd	1 mg/kg, 2 times a day, ip	Onset	na	↑	(Wu et al., 2003)
Mn-porphyrin	SOD1^{G93A}	nd	**5mg/kg loading dose on 1st day of symptom onset then daily maintenance dose of** 2.5 mg/kg/d, ip	Onset	na	↑ 26	(Crow et al., 2005)
	SOD1^{G93A}	nd	2.5 mg/kg/d, ip	Onset	na	↑ 11	(Petri et al., 2006b)
	SOD1^{G93A}	nd	**5mg/kg loading dose on 1st day of symptom onset then daily maintenance dose of** 2.5 mg/kg/d, sc	Onset	na	↑ 28	(Crow et al., 2005)
Pyruvate	SOD1^{G93A}	nd	1 g/kg/week, ip	70	ns	↑ 10	(Park et al., 2007)
	SOD1^{G93A}	nd	500 mg/kg/d, ip	70	ns	ns	(Esposito et al., 2007)
Co-enzyme Q_{10}	SOD1^{G93A}	nd	200 mg/kg, diet	50	nd	↑	(Matthews et al., 1998)
Red wine	SOD1^{G93A}	nd	20 mg/d, po	43–66	nd	↑ 6	(Esposito et al., 2000)
	SOD1^{G93A}	nd	20 mg/d, po	30–40	nd	↑ 15	(Amodio et al., 2006)
Riboflavin	***SOD1^{G93A}***	***nd (n=11-12)***	***12 mg/kg diet***	***51***	***nd***	***ns***	***(Moges et al., 2009)***
Rosemary extract	***SOD1^{G93A}***	***f (n=22-24)***	***3 mg/kg, ip, twice weekly***	***63***	***ns***	***↑***	***(Shimojo et al., 2010)***
Rosmarinic acid	***SOD1^{G93A}***	***f (n=14-22)***	***0.13 mg/kg, ip, twice weekly***	***63***	***ns***	***↑***	***(Shimojo et al., 2010)***
salicylaldehyde isonicotinoyl hydrazone (an iron chelator)	***SOD1^{G37R}***	***m/f (n=12-18)***	***50mg/kg, ip, once weekly or twice weekly***	***~240***	***nd***	***↑7, 10***	***(Jeong et al., 2009)***
SK-PC-B70M	***SOD1^{G93A}***	***nd (n=6-9)***	***100 ,400 mg/kg/day***	***56***	***ns, ↑***	***nd***	***(Seo et al., 2011)***
SS-31	SOD1^{G93A}	m/f	5 mg/kg/d, ip	30	↑ 8	↑ 9	(Petri et al., 2006a)
SOD1-catalase mimetic	SOD1$^{G93A\ G1L}$	nd	33 mg/kg, 3 times a week, ip	60	ns	↑ 10	(Jung et al., 2001)
Trientine	SOD1^{G93A}	nd	400, 800 mg/kg/d, water	28	nd	↑ 6, 8	(Andreassen et al., 2001)

Agent	Model	Gender	Dosology	Start (days)	Onset change (%)	Survival change (%)	Reference
	SOD1^{G93A}	m	0.5% water	50	ns	↑ 5	(Nagano et al., 2003)
	SOD1^{G93A}	**m**	**0.5% water**	**Onset of hindlimb weakness**	**ns**	**ns**	**(Nagano et al., 2003)**
Tomato	SOD1^{G93A}	nd	10% diet	29	ns	ns	(Esposito et al., 2007)
Vitamin E	SOD1^{G93A}	m/f	**200 IU/kg diet**	30	↑ 14	ns	(Gurney et al., 1996)
Anti-glutamatergic							
Carboxyfullerene	SOD1^{G93A}	nd	15 mg/kg/d, ip **(continuous infusion via mini osmotic pump)**	73	↑	↑	(Dugan et al., 1997)
Ceftriaxone	SOD1^{G93A}	nd	200 mg/kg/d, ip	42	↑	↑ 11	(Rothstein et al., 2005)
Gabapentin	SOD1^{G93A}	m/f	3% diet	50	ns	ns	(Gurney et al., 1996)
	SOD1$^{G93A\ G1L}$	m/f	3% diet	50	nd	↑ 5	(Gurney et al., 1996)
GCPII inhibitor	SOD1$^{G93A\ G1L}$	nd	30 mg/kg/d, po	37–39	↑	↑ 15[c]	(Ghadge et al., 2003)
GPI-1046	SOD1$^{G93A\ G1L}$	nd	50 mg/kg, 2 times a day, po	150	ns	↑ 12	(Ganel et al., 2006)
Ivermectin	SOD1^{G93A}	m/f	4.8, 12 mg/L, water	50	nd	↑ 6, 9	(Andries et al., 2007)
L-arginine	***SOD1^{G93A}***	***m (n=20)***	***6%, water***	***30, 70***	***↑, na***	***↑ 20, 9***	***(Lee et al., 2009)***
L-745,870 (dopamine receptor antagonist)	***SOD1^{H46R}***	***nd (n=13-17)***	***10, 20 mg/kg/d, ig***	***84***	↑4, 4	↑10, 7	***(Tanaka et al., 2008)***
	SOD1^{H46R}	***nd (n=12-16)***	***4, 10, 20 mg/kg/d, ig***	***~126 (onset)***	***na***	↑6, 8, 6	***(Tanaka et al., 2008)***
Memantine	SOD1^{G93A}	nd	10 mg/kg, 2 times a day, sc	70	ns	↑ 7	(Wang and Zhang, 2005)
	SOD1^{G93A}	nd (n=10)	30, 90 mg/kg/d, water	75	na	↑ 5	(Joo et al., 2007)
Mg pidolate	SOD1^{G93A}	nd	5.2, 10.3 mg/d, water	42	ns	ns	(Pamphlett et al., 2003)
methionine sulfoximine (glutamine synthetase inhibitor)	***SOD1^{G93A}***	***nd (n=15)***	***20 mg/kg thrice weekly***	***50 +/- 2***	***nd***	***↑ 8***	***(Ghoddoussi et al., 2010)***
NBQX	SOD1^{G93A}	nd	8 mg/kg, 5 times a week, ip	70	↑	↑ 10	(Van Damme et al., 2003)
Nordihydroguaiaretic acid	***SOD1^{G93A}***	***m/f (n=17)***	***1mg/d for 30d, via sc implant***	***90***	***na***	***ns***	***(Boston-Howes et al., 2008)***
Riluzole	SOD1^{G93A}	m/f	50 mg/kg/d, po	50	ns	↑ 10	(Gurney et al., 1996)
	SOD1^{G93A}	m/f	24, 44 mg/kg/d, diet	42–43	↑	↑ 10, 9	(Gurney et al., 1998)
	SOD1^{G93A}	***m/f (n=10-***	***25mg/kg/d, po***	***49***	***ns***	***nd***	***(Sekiya et al.,***

Agent	Model	Gender	Dosology	Start (days)	Onset change (%)	Survival change (%)	Reference
		22)					***2009)***
RPR 119990	SOD1^{G93A}	nd	**3 or 2 × 3 mg/kg/d, sc**	50	↑	↑ 7, 13	(Canton et al., 2001)
Topiramate	SOD1^{G93A}	nd	50 mg/kg, po	30	nd	ns	(Maragakis et al., 2003)
ZK 187638	SOD1^{G93A}	nd	140 mg/kg, once in 2 days, po	77	↑	↑	(Tortarolo et al., 2006b)
Anti-aggregation							
Arimoclomol	SOD1^{G93A}	m/f	10 mg/kg/d, ip	35	↑	↑ 22	(Kieran et al., 2004)
	SOD1^{G93A}	m/f	10 mg/kg/d, ip	70	nd	↑ 18	(Kieran et al., 2004)
	SOD1^{G93A}	m/f	10 mg/kg/d, ip	**75,90**	**na**	**↑ 8 m ↑ 9 f**	**(Kalmar et al., 2008)**
Hsp70	SOD1^{G93A}	m/f	20 µg, 3 times a week, ip	50	↑ 12	↑ 7	(Gifondorwa et al., 2007)
	SOD1^{G93A}	m/f	20 µg, 3 times a week, ip	30	↑	↑ 12	(Gifondorwa et al., 2007)
	SOD1^{G93A}	m/f	20 µg, 3 times a week, ip	**90**	**na**	**ns**	**(Gifondorwa et al., 2007)**
Noscapine	SOD1^{G93A}	m/f	100 mg/kg/d, ip	70	ns	↑ 14	(Fanara et al., 2007)
Rapamycin	***SOD1^{G93A}***	***nd(n=10)***	***2mg/kg/d, ip***	***64***	***↓ 8***	***↓ 18***	***(Zhang et al., 2011)***
Anti-apoptotic							
CGP3466	SOD1^{G93A}	nd	0.1 mg/kg, po	28	nd	ns	(Andreassen et al., 2001)
	SOD1^{G93A}	m/f	0.39–390 µg/kg, 3 times a week, sc	50	ns	ns	(Groeneveld et al., 2004a)
Desmethylselegiline	SOD1^{G93A}	nd	10 mg/kg/d, sc	28	nd	ns	(Andreassen et al., 2001)
Lithium	SOD1^{G93A}	nd	200 mg/kg/d, diet	56	↑ 16	↑ 6	(Shin et al., 2007)
	SOD1^{G93A}	***m/f (n=6 sex and littermate balanced)***	***60 mg/kg twice daily, ip***	***30***	↑ 9	***ns***	***(Feng et al., 2008)***
	SOD1^{G93A}	***m***	***6.94 mg/kg/d , ip***	***75***	***↑ 8***	***↑ 34***	***(Fornai et al., 2008)***
	SOD1^{G93A}	***m and f (n=27-28 age, sex, weight, littermate balanced)***	***6.94 mg/kg/d , ip***	***50***	***ns m or f***	***ns m or f***	***(Gill et al., 2009)***
	SOD1^{G93A}	***f***	***6.94 mg/kg/d , ip***	***75***	***ns***	***ns***	***(Pizzasegola et al., 2009)***
PARP inhibitor	SOD1^{G93A}	nd	40 mg/kg/d, diet	28	nd	ns	(Andreassen et al., 2001)
Rasagiline	SOD1$^{G93A\ G1L}$	nd	2 mg/kg/d, po	60	nd	↑ 14	(Waibel et al.,

Agent	Model	Gender	Dosology	Start (days)	Onset change (%)	Survival change (%)	Reference
							2004)
PBA	SOD1^{G93A}	m	200, 400 mg/kg, ip	21	↑	↑ 9, 22	(Ryu et al., 2005)
	SOD1^{G93A}	nd	400 mg/kg/d, ip	Onset	na	↑ 13	(Petri et al., 2006b)
Semapimod	SOD1^{G93A}	nd	4 mg/kg, 5 times a week, ip	70	ns	↑ 5	(Dewil et al., 2007)
TAT-modified BCL-X_L	***SOD1^{G93A}***	***m (n=12-15)***	***1.4 nmol, it over 28 days via mini pump***	***91***	***↑10***	***↑11***	***(Ohta et al., 2008)***
WHI-P131	SOD1^{G93A}	nd	12.5 mg/kg, 5 times a week, ip	60	nd	↑ 49[c]	(Trieu et al., 2000)
zVAD-fmk	SOD1^{G93A}	nd	15 mg/kg, for 2 months, icv	60	↑ 20	↑ 22	(Li et al., 2000)
VPA	SOD1$^{G93A\ G1L}$	m	460–600 mg/kg/d, po	45	ns	↑ 8	(Sugai et al., 2004)
	SOD1$^{G93A\ G1L}$	**m**	**460–600 mg/kg/d, po**	**Onset**	**ns**	**ns**	**(Sugai et al., 2004)**
	SOD1^{G86R}	nd	150–400 mg/kg/d, ip	60	↑	ns	(Rouaux et al., 2007)
	SOD1^{G93A}	***m/f (n=6 sex and littermate balanced)***	***300 mg/kg twice daily, ip***	***30***	ns	↑ 10	***(Feng et al., 2008)***
Immunomodulatory							
Celecoxib	SOD1^{G93A}	nd	1,500 ppm diet	28	↑	↑ 25	(Drachman et al., 2002)
	SOD1^{G93A}	m/f	0.012% diet	30	nd	↑ 19	(Klivenyi et al., 2004)
CD40L-blocking monoclonal antibody MR1	***SOD1^{G93A}***	***m/f (n=44-45)***	***loading dose of 5.22 mg/ kg in f and 6.75 mg/kg in m, then weekly injections of 1.0 and 1.34 mg/kg in f and m, respectively***	***50***	***ns***	***↑ 7***	***(Lincecum et al., 2010)***
	SOD1^{G93A}	***m/f (n=?)***	***loading dose of 5.22 mg/ kg in f and 6.75 mg/kg in m, then weekly injections of 1.0 and 1.34 mg/kg in f and m, respectively***	***80***	***ns***	***ns***	***(Lincecum et al., 2010)***
Cyclosporin-A	SOD1^{G93A}	nd	25 µg/2 d, icv	Onset	na	↑	(Keep et al., 2001)
	SOD1^{G93A}	nd	0.8–1 mg/kg/week, icv	65	↑ 10	↑ 13	(Karlsson et al., 2004)
	SOD1^{G93Aa}	**m and f**	4 mg/kg, once in 2 days, ip	35	nd	**↑ 12m ns f**	(Kirkinezos et al., 2004)
FK506	SOD1^{G93A}	nd	1, 5 mg/kg/d, ip	Onset	ns	ns	(Anneser et al., 2001)
Folic Acid	***SOD1^{G93A}***	***nd (n=9)***	***4mg/kg/d, po***	***42***	***↑ 6***	***↑ 7***	***(Zhang et al., 2008)***
Glatiramer acetate	SOD1^{G93Ab}	nd	**75 µg, sc initial**	60	↑	↑ 25	(Angelov et al.,

Agent	Model	Gender	Dosology	Start (days)	Onset change (%)	Survival change (%)	Reference
			injection then 12.5 mg/kg/d, water				2003)
	SOD1^{G93A}	m/f	75, 150 µg, sc every 28 days	45	nd	ns	(Habisch et al., 2007a)
	SOD1^{G93A}	m/f	**75 µg/week or month, sc**	50	ns	ns	(Haenggeli et al., 2007)
	SOD1^{G93Ab}	m/f	**75–500 µg/week or month, sc**	42	nd	ns	(Haenggeli et al., 2007)
	SOD1^{G37R}	nd	**75 µg/week or month, sc**	180–270	nd	ns	(Haenggeli et al., 2007)
GSK-3 inhibitor	SOD1^{G93A}	nd	2,4 mg/kg, 5 times a week, ip	60	↑ 12, 16	↑ 12, 17	(Koh et al., 2007a)
IL-1 receptor antagonist	***SOD1^{G93A}***	***nd (n=?)***	***150, 75 mg/kg/d ip***	***70***	***nd***	***↑ 3, 4***	***(Meissner et al., 2010)***
Lenalidomide	SOD1^{G93A}	nd	100 mg/kg/d, po	30	↑	↑ 19	(Kiaei et al., 2006)
	SOD1^{G93A}	***nd (n=18)***	***100 mg/kg/d, diet***	***80-90***	***na***	***↑12***	***(Neymotin et al., 2009)***
LPS	SOD1^{G37R}	nd	1 mg/kg, once in fortnight for 2 months, ip	180	nd	↓ 8	(Nguyen et al., 2004)
Mellitin (peptide in bee venom)	***SOD1^{G93A}***	***m (n =11)***	***100 µg/kg, sc***	***98***	***nd***	***ns***	***(Yang et al., 2011a)***
Bee Venom	***SOD1^{G93A}***	***m (n=11)***	**0.1 µg/g, sc twice weekly**	***98***	***nd***	***↑12***	***(Yang et al., 2010)***
Minocycline	SOD1^{G37R}	nd	1 g/kg diet	210–270	ns	↑ 6	(Kriz et al., 2002)
	SOD1^{G93A}	nd	10 mg/kg/d, ip	35	↑ 21	↑ 9	(Zhu et al., 2002)
	SOD1^{G93A}	nd	11 mg/kg/d, ip	42	nd	↑ 10	(Zhu et al., 2002)
	SOD1^{G93A}	f	25, 50 mg/kg, 5 times a week, ip	70	↑	↑ 10, 16	(Van Den Bosch et al., 2002)
	GFAP-luc/SOD1^{G93A}	***m/f (n=8)***	***100mg/kg in diet***	***75***	***nd***	***↑ 7***	***(Keller et al., 2011)***
	GFAP-luc/SOD1^{G93A}	***m/f (n12-17)***	***100mg/kg in diet***	***90, 105***	***nd***	***ns***	***(Keller et al., 2011)***
Monoclonal antibody against misfolded SOD1 (D5H5 antibody)	***SOD1^{G93A}***	***f (n=8)***	***3.6µg/d for 42 and 26 days, respectively, icv***	***65, 85***	***↑, nd***	***↑,↑***	***(Gros-Louis et al., 2010)***
Fab fragment of monoclonal antibody against misfolded SOD1 (D5H5 antibody)	***SOD1^{G93A}***	***f (n=8***	***3.6µg/d for 42 days, icv***	***65***	***nd***	***↑***	***(Gros-Louis et al., 2010)***
Monoclonal antibody against misfolded SOD1 (A5C3 antibody)	***SOD1^{G93A}***	***f (n=8)***	***3.6µg/d for 42 days, icv***	***65***	***nd***	***ns***	***(Gros-Louis et al., 2010)***
Myostatin mAb	SOD1^{G93A}	m	20–40 mg/kg/week, ip	28	nd	ns	(Holzbaur et al., 2006)

Agent	Model	Gender	Dosology	Start (days)	Onset change (%)	Survival change (%)	Reference
NDGA	SOD1^{G93A}	m/f	2,500 ppm diet	90	↑	↑	(West et al., 2004)
Nimesulide	SOD1^{G93A}	nd	1,500 mg/kg diet	49	↑	ns	(Pompl et al., 2003)
Pioglitazone	SOD1^{G93A}	nd	1,200 ppm diet	30	↑	↑ 13	(Kiaei et al., 2005a)
	SOD1^{G93A}	m	40 mg/kg/d, diet	57	↑ 10	↑ 8	(Schutz et al., 2005)
Resveratrol	***SOD1^{G93A}***	***m/f (n=10-11)***	***25 mg/kg/d, diet***	***47***	***ns***	***ns***	***(Markert et al., 2010)***
Rofecoxib	SOD1^{G93A}	m/f	0.005% diet	30	nd	↑ 21	(Klivenyi et al., 2004)
	SOD1^{G93A}	f	2.5, 5 mg/kg, 3 times a week, ip	60	↑	ns	(Azari et al., 2005)
Ro 28-2653	SOD1^{G93A}	nd	100 mg/kg/d, po	30	↑ 7	↑ 11	(Lorenzl et al., 2006)
	SOD1^{G93A}	nd	100 mg/kg/d, po	90	nd	ns	(Lorenzl et al., 2006)
SOD1^{G93A} vaccination	SOD1^{G37R}	m/f	**50 µg initial dose then 2 further 50 µg doses at 3 week intervals then 50µg dose at 180 days, sc**	60	↑ 6	↑ 8	(Urushitani et al., 2007)
	SOD1^{G93A}	nd	**Described as same protocol as for SOD1^{G37R} mice above but presume final dose was not possible as mice would not have been alive at 180 days.**	60	ns	ns	(Urushitani et al., 2007)
SOD1$^{G93A\ apo}$ vaccination	***SOD1$^{G93A\ G1L}$***	***nd (n=9-13)***	***50 µg initial dose then 2 further 50 µg doses at 3 week intervals then 50µg dose at 180 days, sc***	***60***	***↑ 9***	***↑ 4***	***(Takeuchi et al., 2010)***
SOD1$^{WT\ apo}$ vaccination	***SOD1$^{G93A\ G1L}$***	***nd (n=12-13)***	***50 µg initial dose then 2 further 50 µg doses at 3 week intervals then 50µg dose at 180 days, sc***	***60***	***ns***	***↑ 7***	***(Takeuchi et al., 2010)***
SOD1 pAb	SOD1^{G93A}	nd	1.8 µg/d/mo, icv	85	nd	↑ 6	(Urushitani et al., 2007)
Sulindac	SOD1^{G93A}	nd	300 ppm diet	30	↑	↑ 10	(Kiaei et al., 2005c)
Thalidomide	SOD1^{G93A}	nd	50, 100 mg/kg/d, po	30	↑	↑ 12, 16	(Kiaei et al., 2006)
uPA inhibitor	SOD1^{G93A}	nd	10 mg/kg/d, ip	30	ns	↑ 7	(Glas et al., 2007)
Vincristine	SOD1^{G93A}	nd	0.1 mg/kg/fortnight, ip	68	ns	↑ 12	(Bruce et al., 2004)
Vitamin B12	***SOD1^{G93A}***	***nd (n=9)***	***0.2mg/kg/d, po***	***42***	***ns***	***ns***	***(Zhang et al.,***

Agent	Model	Gender	Dosology	Start (days)	Onset change (%)	Survival change (%)	Reference
							2008)
Wen-Pi-Tang	SOD1^{G93A}	m/f (n=22)	100, 200 mg/kg/d, po	49	ns, ↑ 8	ns	(Sekiya et al., 2009)
Neurotrophic							
ADNF	SOD1^{G93A}	m/f	30 nmol/2d, icv	80	↑	ns	(Chiba et al., 2004)
	SOD1^{G93A}	m/f	30 nmol/2d, icv	80	↑ 6	ns	(Chiba et al., 2006)
ADNF (colivelin)	SOD1^{G93A}	m/f	0.01, 1 nmol/2d, icv	80	↑ 9, 11	↑ 8, 6	(Chiba et al., 2006)
AIT-082	SOD1^{G93A}	m/f	1–100 mg/kg/d, water	30	ns	ns	(Jiang et al., 2006)
BMP-7	SOD1^{G93A}	nd	10 µg, single, ic	80	ns	ns	(Dreibelbis et al., 2002)
EGF	SOD1^{G93A}	nd	0.5 µg/d/week, is	100	na	nd	(Ohta et al., 2006)
FGF2	SOD1^{G93A}	nd	0.5 µg/d/week, is	100	na	nd	(Ohta et al., 2006)
EGF + FGF2	SOD1^{G93A}	nd	0.5 µg/d/week, is	100	na	nd	(Ohta et al., 2006)
Erythropoietin	SOD1^{G93A}	m/f	8.3 µg/kg, 2 times a week, ip	47	**↑ f ns m**	ns	(Grunfeld et al., 2007)
	SOD1^{G93A}	f	4000 U/kg/d, sc	49	nd	ns	(Grignaschi et al., 2007)
	SOD1^{G93A}	nd	2500, 5000 U/kg/fortnight, ip	60	ns, ↑ 8	↑ 8, 10	(Koh et al., 2007b)
bFGF	SOD1^{G93A}	nd	15–500 µg/kg, 2 times a week, ip	30	ns	ns	(Upton-Rice et al., 1999b)
Galectin-1 oxidised	SOD1^{H46R}	nd	0.25 mg/kg, 1 times a week, im	70	↑ 4	↑ 7	(Chang-Hong et al., 2005)
GCSF (Pegfilgrastim)	***SOD1^{G93Ab}***	***m (n=8-9) littermate balanced***	***300µg/kg/weekly, ip***	***84***	***ns***	***7***	***(Pollari et al., 2011)***
GCSF (filgrastim)	***SOD1^{G93Ab}***	***f (n=17-18) littermate balanced***	***30µg/kg/d, sc, osmotic pump, for 8 weeks***	***77***	↑ 20	↑ 7	***(Pitzer et al., 2008)***
IGF-1	SOD1$^{G93A\ G1L}$	nd	0.1, 1 mg/kg/d, is	140	↑ 10, 15	↑ 8, 11	(Nagano et al., 2005)
IGF-1 plasmid	***SOD1^{G93A}***	***nd***	***200 µl (1 µg/µl) plasmid, im***	***70***	***na***	***na, but increased muscle strength, motor unit and motor neuron number at 120 d***	***(Riddoch-Contreras et al., 2009)***
IGF-1:TTC fusion protein	***SOD1^{G93A}***	***f (n = 7-11)***	***0.4, 1.2, 4 mg, im at 60 days and 70days***	***60***	***ns***	***ns***	***(Chian et al., 2009)***
IGF-1:TTC fusion	***SOD1^{G93A}***	***m (n =8-***	***25, 110 µg/d, it***	***60***	***ns***	***ns***	***(Chian et al.,***

Agent	Model	Gender	Dosology	Start (days)	Onset change (%)	Survival change (%)	Reference
protein		***37)***	***infusion for 7-10 days***				***2009)***
MGF plasmid	***SOD1^{G93A}***	***nd***	***200 µl (1 µg/µl) plasmid, im***	***70***	***na***	***na, but increased muscle strength, motor unit and motor neuron number at 120 d***	***(Riddoch-Contreras et al., 2009)***
LIF	SOD1^{G93A}	m/f	25 µg/kg/d, ip	60	↑	ns	(Azari et al., 2003)
	SOD1$^{G93A\ G1L}$	m/f	10 µg/kg/d, sc	168	ns	ns	(Feeney et al.)
	SOD1$^{G93A\ G1L}$	m/f	25 ng/d, im	168	ns	ns	(Feeney et al.)
	SOD1$^{G93A\ G1L}$	m/f	3 µg/kg/d, is	Onset	ns	ns	(Feeney et al.)
Neurophilin ligands	SOD1^{G93A}	m/f	26.5–79 mg/kg/d, po	30	ns	ns	(Shefner et al., 2001)
p75^{NTR} antagonist	SOD1^{G93A}	m/f	1 mg/kg, 3 times a week, ip	70	ns	ns	(Turner et al., 2004a)
SUN N8075	***SOD1^{G93A}***	***nd (n=12)***	***30 mg/kg/d, sc***	***70***	***↑***	***↑ 11***	***(Shimazawa et al., 2010)***
TGF-β2	SOD1^{G93A}	nd	2 µg, 3 times a week, ip	84	↑	nd	(Day et al., 2005)
TRO19622	SOD1^{G93A}	m/f	3, 30 mg/kg/d, sc	60	↑	↑ 10, 8	(Bordet et al., 2007)
VEGF	SOD1^{G93A}	f	1 µg/kg, 1 times a week, ip	74	↑ 10	↑ 8	(Zheng et al., 2004)
Non-glutamatergic neurotransmission							
Acetyl-L-carnitine	SOD1^{G93A}	m/f	3.5 mmol/kg/d, diet	40	nd	ns	(Crochemore et al., 2005)
Cannabinoid	SOD1^{G93A}	m	10 mg/kg/d, ip	60	↑	↑ 5	(Raman et al., 2004)
	SOD1^{G93A}	m	20 mg/kg/d, ip	75	↑	↑ 5	(Raman et al., 2004)
	SOD1^{G93A}	m/f	1 mg/kg/d, ip	75	na	ns	(Kim et al., 2006)
WIN-55,212	SOD1^{G93A}	nd	5 mg/kg/d, ip	90	na	↑	(Shoemaker et al., 2007)
AM-1241	SOD1^{G93A}	nd	0.3,3 mg/kg/d, ip	90	na	↑	(Shoemaker et al., 2007)
Cannabinol	SOD1^{G93A}	m	5 mg/kg/d, sc	42	↑	ns	(Weydt et al., 2005)
Clenbuterol	SOD1^{G93A}	m/f	1.5 mg/kg/d, ip	56	↑	↑ 10 f[c]	(Teng et al., 2006)
Clozapine	SOD1^{G93A}	f	2.5, 7.5 mg/kg, 3 times a week, po	60	ns	ns	(Turner et al., 2003d)
5-Hydroxytryptophan	SOD1^{G93A}	m/f	50 mg/kg, 3 times a week, ip	60	↑ 15	↑ 11	(Turner et al., 2003a)
Morphine	SOD1$^{G93A\ G1L}$	nd	25 mg/kg/d, ip	50	↑ 40	↑ 30	(Chritin et al., 2006)
Nortriptyline	SOD1^{G93A}	m/f	10, 20 mg/kg/d, ip	42	↑ 7, 13	↑ 7, 6	(Wang et al.,

Agent	Model	Gender	Dosology	Start (days)	Onset change (%)	Survival change (%)	Reference
							2007)
Pramipexole	SOD1^{G93A}	m/f	3 mg/kg/d, water	45	nd	ns	(Danzeisen et al., 2006)
Promethazine	SOD1^{G93A}	m/f	10, 20 mg/kg/d, ip	42	↑ 8, 10	ns	(Wang et al., 2007)
SND919CL2X	SOD1^{G93A}	m/f	100 mg/kg/d, water	45	nd	↑ 6	(Danzeisen et al., 2006)
Tianeptine	SOD1$^{G93A\ G1L}$	nd	20 mg/kg/d, ip	50	↑ 20	↑ 18	(Chritin et al., 2006)
WIN55,212-2	SOD1^{G93A}	m/f	5 mg/kg/d, ip	90	nd	ns	(Bilsland et al., 2006)
Gene and antisense therapy							
GDNF plasmid	SOD1^{G93A}	nd	50 µg plasmid, fornightly, im	63	↑	ns	(Yamamoto et al., 2001)
AV-CT-1	SOD1^{G93A}	nd	1 × 10^8 units, im	5–6	↑ 21	↑ 8	(Bordet et al., 2001)
AV-GDNF	SOD1^{G93A}	nd	5 × 10^9 units, im	5–7	↑ 7	↑ 12	(Acsadi et al., 2002)
AAV-Bcl-2	SOD1^{G93A}	nd	~1 × 10^8 units, im	35	↑ 8	ns	(Azzouz et al., 2000)
AAV-GDNF	SOD1^{G93A}	nd	1 × 10^{11} units, im	63	↑ 13	↑ 14	(Wang et al., 2002b)
	SOD1^{G93A}	nd	1 × 10^{10} units, im	60	↑ 18	↑ 9	(Kaspar et al., 2003)
	SOD1^{G93A}	nd	1 × 10^{10} units, im	90	nd	↑ 6	(Kaspar et al., 2003)
AAV-Follistatin	SOD1^{G93A}	nd	1 × 10^{11} units, im	40	nd	ns	(Miller et al., 2006)
AAV-IGF-1	SOD1^{G93A}	nd	1 × 10^{10} units, im	60	↑ 34	↑ 30	(Kaspar et al., 2003)
	SOD1^{G93A}	nd	1 × 10^{10} units, im	90	nd	↑ 18	(Kaspar et al., 2003)
	SOD1^{G93A}	m/f	5 × 10^{10} units, is	60	↑ 20 m	↑ 10 m	(Lepore et al., 2007)
AAV4-IGF-1	***SOD1^{G93A}***	***m/f (n=30-35)***	***8 x 10^{10} units, icv***	***85***	***nd***	***↑ 10 m^{c} ↑ 10 f^{c}***	***(Dodge et al., 2010)***
AAV-shRNA	SOD1^{G93A}	nd	1 × 10^7 units, im	40	↑	nd	(Miller et al., 2006)
AAV6-shRNA	***SOD1^{G93A}***	***m/f (n= ≥20 age, sex and litter balanced)***	***Injection into, tongue hindlimb, forelimb, intercostal and facial muscles and within the thoracic cavity. Units injected not clearly defined.***	***P1-P5 (P15 for tongue)***	***nd***	***ns***	***(Towne et al., 2011)***
AAV6-shRNA	***SOD1^{G93A}***	***m/f (n=10 sex and litter balanced)***	***2 x 10^{11} viral genomes, iv***	***42***	***ns***	***ns***	***(Towne et al., 2008)***
AAV2-siRNA-GFP	***SOD1^{G93A}***	***nd (n=10)***	***Injection into right lower hind limb***	***45***	***nd***	***na***	***(Miller et al., 2005)***

Agent	Model	Gender	Dosology	Start (days)	Onset change (%)	Survival change (%)	Reference
AAV4-VEGF-165	***SOD1^{G93A}***	***m/f (n=30-35)***	***8 x 10^{10} units, icv***	***85***	***nd***	***↑ 8 m^{c} ↑ 17 f^{c}***	***(Dodge et al., 2010)***
pCMV-BDNF	***SOD1^{G93A}***	***m/f (n=10 littermate balanced)***	***300 µg plasmid, im***	***56***	***ns***	***ns***	***(Calvo et al., 2011)***
pCMVTTC	***SOD1^{G93A}***	***m/f (n=10 littermate balanced)***	***300 µg plasmid, im***	***56***	***↑22***	***↑12***	***(Calvo et al., 2011)***
	SOD1^{G93A}	***Balanced m and f, (n=20)***	***300µg plasmid, im***	***56***	***↑5***	***↑10***	***(Moreno-Igoa et al., 2010)***
EIAV-VEGF	SOD1^{G93A}	nd	~1 × 10^{8} units, im	21	↑ 30	↑ 30	(Azzouz et al., 2004a)
	SOD1^{G93A}	nd	~1 × 10^{8} units, im	90	nd	↑ 15	(Azzouz et al., 2004a)
EIAV-shRNA SOD1	SOD1^{G93A}	nd	~1 × 10^{8} units, im	7	↑ 115	**↑ 77**	(Ralph et al., 2005)
LV-shRNA SOD1	SOD1^{G93A}	nd	90 ng p24 antigen, is	40	↑ 20	nd	(Raoul et al., 2005)
LV-shRNA SOD1	SOD1^{G93A}	nd	1 × 10^{7} units, im	40	ns	nd	(Miller et al., 2006)
PNA GluR3	SOD1^{G93A}	m/f	2.5 mg/kg, 3 times a week, ip	50	↑ 9	↑ 9	(Rembach et al., 2004)
PNA p75^{NTR}	SOD1^{G93A}	f	2.5 mg/kg, 3 times a week, ip	60	↑ 10	↑ 8	(Turner et al., 2003b)
siRNA Fas	SOD1^{G93A}	nd	1 mg/kg/d, is	90	↑	↑ 14	(Locatelli et al., 2007)
Cell replacement							
Myoblast-GDNF	SOD1^{G93A}	nd	5 × 10^{4} cells, im	42	↑ 17	nd	(Mohajeri et al., 1999)
hMSCs	SOD1^{G93A}	nd	3 × 10^{6} cells, iv	56	↑ 11	↑ 12	(Zhao et al., 2007)
	SOD1^{G93A}	***f (n = 18)***	***5 x 10^{6} cells, icsf***	***56***	***ns***	***ns***	***(Zhang et al., 2009)***
	SOD1^{G93A}	***f (n = 21)***	***5 x 10^{6} cells, icsf at 56, 70 and 84 days***	***56***	***↑ 6***	***↑ 10***	***(Zhang et al., 2009)***
	SOD1$^{G93A\ G1L}$	***m/f (n=12-25)***	***1 x 10^{5} cells, is transplant***	***196***	***m↑ f ns***	***m ↑ f ns***	***(Vercelli et al., 2008)***
hMSCs (from an ALS patient)	***SOD1^{G93A}***	***nd (n = 27-29)***	***2 x 10^{5}, 1x10^{6} cells, ic***	***60***	***ns, ns***	***↑5, 7***	***(Kim et al., 2010)***
hNT neurons	SOD1^{G93A}	nd	1.5 × 10^{5} cells, is	49	↑	ns	(Garbuzova-Davis et al., 2002)
	SOD1^{G93A}	nd	1.5 × 10^{5} cells, is	56	↑	ns	(Willing et al., 2001)
	SOD1^{G93A}	nd	1.5 × 10^{5} cells, is	105–112	na	ns	(Garbuzova-Davis et al., 2001)
	SOD1^{G93A}	m	1.5 × 10^{5} cells, 3 times, is	61	nd	ns	(Garbuzova-Davis et al., 2006)

Agent	Model	Gender	Dosology	Start (days)	Onset change (%)	Survival change (%)	Reference
hNSCs	SOD1^{G93A}	m/f	**8 × 10^4 cells, is (combined with immunosuppression with 1µg/g each of FK506 plus rapamycin, ip from 55 days)**	56	↑ 17	↑ 9	(Yan et al., 2006)
mNSCs	SOD1^{G93A}	m/f	2 × 10^4 cells, is	70	↑	↑ 16	(Corti et al., 2007)
hNPs	***SOD1^{G93A}***	***m/f (n =16-124)***	***10µl cells, ic^e***	***75***	***nd***	***ns***	***(Park et al., 2009)***
hNPs expressing BDNF by AAV	***SOD1^{G93A}***	***m/f (n =18-124)***	***10µl cells, ic^e***	***75***	***nd***	***ns***	***(Park et al., 2009)***
hNPs expressing IGF-1 by AAV	***SOD1^{G93A}***	***m/f (n =22-124)***	***10µl cells, ic^e***	***75***	***nd***	***ns***	***(Park et al., 2009)***
hNPs expressing VEGF by AAV	***SOD1^{G93A}***	***m/f (n =29-124)***	***10µl cells, ic^e***	***75***	***nd***	***ns***	***(Park et al., 2009)***
hNPs expressing GDNF by AAV	***SOD1^{G93A}***	***m/f (n =46-124)***	***10µl cells, ic^e***	***75***	***nd***	***ns***	***(Park et al., 2009)***
hNPs expressing GDNF by LV	***SOD1^{G93A}***	***m/f (n =21-23)***	***10µl cells, ic^e***	***75***	***nd***	***↓8***	***(Park et al., 2009)***
hUCB cells	SOD1^{G93A}	nd	3.5 × 10^7 cells, iv	56	nd	↑ 17	(Ende et al., 2000)
	SOD1^{G93A}	nd	7.0 × 10^7 cells, iv	49	nd	↑ 31	(Chen and Ende, 2000)
	SOD1^{G93A}	nd	1.0 × 10^6 cells, iv	63	nd	ns	(Garbuzova-Davis et al., 2003)
	SOD1^{G93A}	nd	1 × 10^5 cells, is	45	ns	ns	(Habisch et al., 2007b)
OB-NPCs	SOD1^{G93A}	m	1 × 10^5 cells, is	70	ns	↑	(Martin and Liu, 2007)
BM cells	SOD1^{G93A}	m/f	3 × 10^7 cells, ip	28	nd	↑ 9	(Corti et al., 2004)
	SOD1^{G93A}	m/f	5 × 10^6 cells, iv	42	ns	ns	(Solomon et al., 2006)
	SOD1^{G93A}	nd	1 × 10^5 cells, is	45	ns	ns	(Habisch et al., 2007b)
	SOD1^{G93A}	***f (n =7-10)***	***6 x 10^7 cells from 84 day old eGFP mice, ibm***	***~84***	***na***	***↑ 10***	***(Ohnishi et al., 2009)***
	SOD1^{G93A}	***f (n =8-10)***	***6 x 10^7 cells from 84 day old SOD1^{G93A} m mice, ibm***	***~84***	***na***	***ns***	***(Ohnishi et al., 2009)***
Sertoli cells	SOD1^{G93A}	nd	1 × 10^5 cells, is	55–65	ns	ns	(Hemendinger et al., 2005)
Combinatorial							
AAV4-IGF-1 and AAV4-VEGF-165	***SOD1^{G93A}***	***m/f (n=30-35)***	***4 x 10^{10} units of each AAV, icv***	***85***	***nd***	***↑ 8 m^c ↑ 8 f^c***	***(Dodge et al., 2010)***
pCMV-BDNF-TTC	***SOD1^{G93A}***	***m/f (n=10 littermate***	***300 µg plasmid, im***	***56***	***29***	***15***	***(Calvo et al., 2011)***

Agent	Model	Gender	Dosology	Start (days)	Onset change (%)	Survival change (%)	Reference
		balanced)					
Creatine + celecoxib	SOD1^{G93A}	m/f	2%/0.012% diet	30	nd	↑ 29	(Klivenyi et al., 2004)
Creatine + rofecoxib	SOD1^{G93A}	m/f	2%/0.005% diet	30	nd	↑ 31	(Klivenyi et al., 2004)
	SOD1^{G93A}	nd	2%/0.005% diet	Onset	na	↑ 4	(Crow et al., 2005)
Creatine + riluzole	SOD1$^{G93A\ G1L}$	m/f	2% diet/100 µg/ml water	40	↑	nd	(Snow et al., 2003)
Folic acid + Vitamin B12	***SOD1^{G93A}***	***nd (n=9)***	***4/0.2mg/kg/d, po***	***42***	***↑8***	***↑10***	***(Zhang et al., 2008)***
Light+ Riboflavin	***SOD1^{G93A}***	***nd (n=11-12)***	***Light:140-mW output power, 1.4 cm2 spot size, 120s treatment, 12 J/cm2 energy density per treatment site/day (3 treatment sites across CNS and spinal cord)/ Riboflavin: 12mg/kg diet***	***51***	***nd***	***ns***	***(Moges et al., 2009)***
Lithium + Valproic acid	***SOD1^{G93A}***	***m/f (n=6 sex and littermate balanced)***	***60/30 mg/kg twice daily, ip***	***30***	***↑14***	***↑15***	***(Feng et al., 2008)***
Minocycline + creatine	SOD1^{G93A}	nd	2% diet/22 mg/kg/d, ip	21/28	↑ 30	↑ 25	(Zhang et al., 2003)
Minocycline + riluzole + nimodipine	SOD1^{G37R}	nd	80–100/30–40/30–40 mg/kg, diet	240–270	↑ 11	↑ 13	(Kriz et al., 2003)
Mn-porphyrin + creatine + rofecoxib	SOD1^{G93A}	nd	2.5 mg/kg/d, ip/2%/0.005% diet	Onset	na	↑ 24	(Crow et al., 2005)
Mn-porphyrin + PBA	SOD1^{G93A}	nd	2.5/400 mg/kg/d, ip	Onset	na	↑ 19	(Petri et al., 2006b)
Morphine + tianeptine	SOD1$^{G93A\ G1L}$	nd	25/20 mg/kg/d, ip	50	↑ 23	↑ 18	(Chritin et al., 2006)
Neu2000 + lithium	SOD1^{G93A}	nd	30/200 mg/kg/d, diet	56	↑ 23	↑ 21	(Shin et al., 2007)
Noscapine + pioglitazone	SOD1^{G93A}	f	100 mg/kg/d, ip/40 mg/kg/d, diet	70	↑	↑ 26	(Fanara et al., 2007)
Rasagiline + riluzole	SOD1$^{G93A\ G1L}$	nd	0.5, 2/30 mg/kg/d, po	60	nd	↑ 18, 20	(Waibel et al., 2004)
Trientine + ascorbate	SOD1$^{G93A\ G1L}$	nd	0.2% water/0.8% diet	45	↑ 8	↑ 10	(Nagano et al., 1999)
	SOD1^{G93A}	m	0.5% water/0.8% diet	50	ns	↑ 7	(Nagano et al., 2003)
Vitamin E/exercise **(running wheel)**	SOD1^{G93A}	m/f	200 U/kg diet	30/45	↑ 16	ns	(Gurney et al., 1996)
AAV-IGF-1/exercise **(running wheel)**	SOD1^{G93A}	m/f	$\sim 6 \times 10^{10}$ units, im	90/40	nd	↑ 70[c]	(Kaspar et al., 2005)
Other							

Agent	Model	Gender	Dosology	Start (days)	Onset change (%)	Survival change (%)	Reference
Human recombinant angiogenin	***SOD1^{G93A}***	***m/f sex matched (n=12-15)***	***1µg/d, ip***	***50, 90***	***nd***	***↑ 10, 9***	***(Kieran et al., 2008)***
Ammonium tetrathiomolybdate (copper chelator)	***SOD1^{G93A}***	***m/d (n=28-34)***	***5mg/kg/d, ip***	***28***	***↑20***	***↑25***	***(Tokuda et al., 2008)***
WT APC (enzymatically active)	***SOD1^{G93A}***	***m, (n=10-19)***	***40 µg/kg/d, ip***	***7 days after onset***	***nd***	***↑ 10***	***(Zhong et al., 2009)***
3K3A-APC (enzymatically active)	***SOD1^{G93A}***	***m, (n=11-19)***	***40 µg/kg/d, ip***	***7 days after onset***	***nd***	***↑ 13***	***(Zhong et al., 2009)***
5A-APC (enzymatically active)	***SOD1^{G93A}***	***m, (n=10-19)***	***100 µg/kg/d, ip***	***7 days after onset***	***nd***	***↑ 25***	***(Zhong et al., 2009)***
5360A-APC (enzymatically inactive)	***SOD1^{G93A}***	***m, (n=10-19)***	***100 µg/kg/d, ip***	***7 days after onset***	***nd***	***ns***	***(Zhong et al., 2009)***
Cu	SOD1^{G93A}	nd	400 ppm **in diet**	21	nd	ns	(Jonsson et al., 2006)
Dietary restriction	SOD1$^{G93A\ G1L}$	nd	30–40% diet **reduction**	42	ns	↓	(Pedersen and Mattson, 1999)
	SOD1^{G93A}	m/f	60% diet **reduction**	40	↓ 10	ns	(Hamadeh et al., 2005)
	SOD1^{G93A}	m/f	transient 60% diet **reduction from 40-55 days**	40–55	↓ 3 m	↓ 7 m	(Hamadeh and Tarnopolsky, 2006)
	SOD1^{G93A}	***m/f (n=22-31 not gender or litter balanced)***	***60% diet reduction***	***40***	***↓ 6***	***↓ 9***	***(Patel et al., 2010)***
High-energy diet	SOD1^{G86R}	nd	21% fat, 0.15% cholesterol diet	42	nd	↑ 20	(Dupuis et al., 2004)
Exercise	SOD1^{G93A}	m/f	Low, 390 m, 5 times a week	49	nd	↑ 8 m	(Kirkinezos et al., 2003)
	SOD1^{G93A}	m/f	Moderate, 720 m, 5 times a week	56	ns	↑ f	(Veldink et al., 2003)
	SOD1$^{G93A\ G1L}$	m/f	Moderate, 720 m, 5 times a week	56	↑ f	ns	(Veldink et al., 2003)
	SOD1^{G93A}	m/f	High, 405–990 m, 5 times a week	40	ns	↓ m	(Mahoney et al., 2004)
	SOD1^{G93A}	m/f	High, 1400 m, d	35	ns	ns	(Liebetanz et al., 2004)
Environmental enrichment	***SOD1^{G93A}***	***m (n=9-11) f (n=7-8)***	***Larger cage, enrichment changed twice weekly, access to extra exploratory area for one hour 3x/week from 30 days of age.***	***28***	***nd***	***f↓10 m, ns***	***(Stam et al., 2008)***
Hypoxia	SOD1^{G93A}	nd	10% O_2 for 21 days,	60, 100	nd	ns	(Van Den Bosch

Agent	Model	Gender	Dosology	Start (days)	Onset change (%)	Survival change (%)	Reference
			10% O_2 from 100 days till end stage				et al., 2004)
Ketogenic diet	$SOD1^{G93A}$	m	60% fat diet	50	↑	ns	(Zhao et al., 2006)
Lead-acetate	***$SOD1^{G93A}$***	***m (n =8)***	***200ppm, water***	***21-25***	***ns***	↑*10*	***(Barbeito et al., 2010)***
Ovarectomy	$SOD1^{G93A}$	f	na	40	ns	↓ 8	(Groeneveld et al., 2004b)
	$SOD1^{G93A}$	f	17β-estradiol, 1 mg/kg/d, water	50	ns	↑ 6a	(Groeneveld et al., 2004b)
	$SOD1^{G93A}$	***f (n=10)***	***na***	***50***	***ns***	***↓ 5***	***(Choi et al., 2008)***
	$SOD1^{G93A}$	***f (n=10)***	***0.18 mg of 17β-estradiol released over 60 days from sc implant starting at 60 days of age***	***50***	***ns***	***↑ 6a***	***(Choi et al., 2008)***
Soluble activin receptor type IIB	**$SOD1^{G93A}$, $SOD1^{G93Ab}$**	**m/f (n=18), (n=24-26)**	**10 mg/kg, ip, twice weekly**	**60, 90**	**11, na**	**ns, ns**	**(Morrison et al., 2009)**
Trichostatin A (TSA, a histone deacetylase inhibitor)	***$SOD1^{G93Ab}$***	***m (n =16-18) littermates***	***1mg/kg/d 5 days a week ip until 120 days***	***90***	***nd***	***↑ 7***	***(Yoo and Ko, 2011)***
$ZnSO_4$	$SOD1^{G93A}$	nd	375 mg/kg/d, water	50	ns	↓ 8	(Groeneveld et al., 2003)
	$SOD1^{G93A}$	m	6–8 mg/kg/d, water	50	nd	ns	(Ermilova et al., 2005)
Zn restriction	$SOD1^{G93A}$	m/f	<2 ppm diet	50	nd	↑ b	(Ermilova et al., 2005)

-Age of disease onset specified by authors using clinical signs, locomotor or grip strength deficit.

-Abbreviations: m, male; f, female; ibm, intra-bone marrow; icv, intracerebroventricular; ic, intracisternal; ig, intragastric; im, intramuscular; in, intranasal; ip, intraperitoneal; is, intraspinal; it, intrathecal; iv, intravenous; po, per os (oral); sc, subcutaneous; na, non-applicable; nd; not described, ns, not significant, ↑, increased; ↓, decreased; a, cf. ovariectomised mice; b, cf. Zn supplemented mice, AAV, adeno-associated virus; APC, Activated protein C; ADNF, activity-dependent neurotrophic factor; BMP-7, bone morphogenic protein-7; BM, bone marrow; CMV, cytomegalovirus ; CT-1, cardiotrophin 1; BDNF, bone derived neurotrophic factor; EGF, epidermal growth factor; EIAV, equine infectious anemia virus; FGF, fibroblast growth factor; GCSF, granulocyte colony stimulating factor; GDNF, glial cell-derived neurotrophic factor; GluR3, glutamate receptor subunit 3; GSK-3, glycogen synthase kinase-3; Hsp70, heat shock protein 70; IGF-1, insulin-like growth factor; LIF, leukemia inhibitory factor; L-NAME, nitro-l-arginine methyl ester; LPS, lipopolysaccharide; LV, lentivirus; MSC, mesenchymal stromal cell; NSC, neural stem cell; hNP, human neural progenitor cell; OB-NPC, olfactory bulb neural precursor cell; PBA, phenylbutyrate; PNA, peptide nucleic acid; $SOD1^{G93A}$, high copy $SOD1^{G93A}$ mice (25 predicted copies); $SOD1^{G93A\ G1L}$, low copy $SOD1^{G93A}$ mice (8 predicted transgene copies); siRNA, small interfering RNA; TAT-modified BCL-X_L, protein transduction domain derived from the human immunodeficiency virus TAT protein fused with an antiapoptotic modified Bcl-X_L protein; TCC, non-toxic C-terminal fragment of tetanus toxin ; TGF-β2, transforming growth factor-β2; UBC, umbilical blood cells; uPA, urokinase-type plasminogen activator; VEGF, vascular endothelial growth factor; VPA, valproate.

-[a] $SOD1^{G93A}$ × Mdr1a/b$^{-/-}$ mice.

-[b] B6.Cg-Tg(SOD1*G93A)1Gur/J strain or equivalent.

-[c] Median survival.

-[d] There were no differences in disease onset and survival between the two ginseng doses tested in this study and hence disease onset and survival data for both doses were combined when performing statistical comparisons to untreated controls.
-[e] The number of hNPs injected (ic) was not defined in this study.
-[f] Onset and survival not defined but no benefit on disease progression.

7.2 Appendix 2. Optimising survival studies in SOD1^{G93A} mice

7.2.1 The requirement to address animal husbandry and welfare issues when performing survival studies in SOD1^{G93A} mice.

When designing our metformin dose-response survival study (discussed in detail in **Chapter 4**) it was critically important to us to employ a study format that minimized error introduced by confounding variables including non-ALS deaths, low copy transgenics, littermate clustering and gender imbalance (in order of influence) in experiments involving SOD1^{G93A} mice (Scott et al., 2008). We therefore followed guidelines produced by Scott and colleagues at the ALSTDI that were designed to bring error resulting from these variables to a virtual zero (Scott et al., 2008). This allowed us to be confident that the results produced in our study were meaningful. Specifically, in order to control for the variability introduced by non-ALS deaths, we closely monitored the health of mice throughout the study (via twice weekly monitoring of weight and neurological score and then daily monitoring from 100 days onwards) and excluded relevant data from any mice observed to experience a non-ALS death. In order to control for transgene copy number losses, we checked for potential copy number variations in any mice displaying outlying disease progression or survival characteristics by Q-PCR (Alexander et al., 2004) and were prepared to exclude any mice which had lost copies of the transgene. To prevent the negative effects of litter clustering, we balanced all experimental groups for litter and starting weight and finally to control for the effect of gender, we considered results for male and female mice separately and ensured that all experimental groups began with near identical numbers of male and female mice. The minimum n-number for survival studies in SOD1^{G93A} mice on a mixed-hybrid background

(providing mice experiencing non-ALS deaths or loss of copy number are excluded and groups are balanced for litter, weight and gender) has been calculated by Scott and colleagues to be 12 males and 12 females per group (Scott et al., 2008). We ensured that we met these requirements by beginning the study with 14 males and 15 females per group.

Having never performed survival studies in $SOD1^{G93A}$ mice, we found guidelines produced by Scott and colleagues very useful in terms of overall study design to ensure meaningful results. However, we found it hard to find information about optimal husbandry conditions for $SOD1^{G93A}$ mice during these studies in the literature. We also encountered several unpredicted welfare issues for which we have now employed standard operating procedures (SOPs) in order to minimize animal suffering. We feel that standard operating procedures for husbandry and welfare in survival studies in $SOD1^{G93A}$ mice are critical in order to ensure that mice enrolled in survival studies are well cared for and furthermore that error is not introduced into results through environmental variations or non-ALS-related health issues. We have outlined below many of the husbandry and welfare issues encountered and the methods we employed to overcome them. Finally we have outlined a set of optimal husbandry conditions for survival studies in $SOD1^{G93A}$ mice that are now employed for all survival studies in our group.

7.2.2 Minimising fighting between male mice

Although several studies have indicated that singly housed mice so not suffer undue stress (Hunt and Hambly, 2006, Arndt et al., 2009) it has been shown that mice prefer the presence of cage mates (Van Loo et al., 2004, Jennings et al., 1998). Consequently we elect to avoid housing mice singly as far as possible in all our experiments. In our metformin survival

study, mice were arranged into cages of either 4 or 5 for males and 5 for females (there were 14 males and 15 females per group in this study). As we were treating mice via the drinking water and were performing litter mate balancing between groups, it was necessary to mix mice from different litters within cages. In our laboratory, we normally wait until mice are weaned (at 21 days of age) before taking an ear biopsy for the purposes of genotyping. Consequently, mice enrolled in our metformin survival study were genotyped post weaning and then re-housed into their experimental groups at 35 days of age when metformin treatment commenced and genotyping was completed. In their natural habitat, male mice live in social groups consisting of one dominant male, females with their progeny and a number of subordinate males. In these groups, the dominant male defends his territory which includes resources such as females, food and a nesting site. Although a number of subordinate males are often tolerated within the territorial boundaries of the dominant male, aggression is used when required to establish and maintain the social structure. Additionally, the dominant male is likely to react with aggression to any unfamiliar males entering the territory (Van Loo et al., 2003). As in the wild, male laboratory mice also develop a hierarchical social structure (Hayashi, 1993) and it is therefore not possible to mix male mice after they have reached puberty as this can lead to severe fighting (Jennings et al., 1998). Although we were aware of this fact, we thought that at 35 days of age, mice would not yet have reached puberty and therefore that aggressive behaviour could be avoided. We were also not concerned about mixing female mice as non-breeding females normally live harmoniously together (Jennings et al., 1998). As predicted, we did not have any problems mixing female mice at this stage, but unfortunately experienced considerable problems with fighting between male mice upon sorting them into their groups. The onset of puberty in male and female mice can vary greatly between strains (Silver, 1995) and we therefore concluded that in our $SOD1^{G93A}$ mice, the

onset of puberty in males may occur prior to 35 days of age. Although it is preferred to take ear biopsies from mice post weaning, it is also possible to biopsy mice from two weeks of age onwards, as their ears are usually sufficiently developed by this stage (Robinson et al., 2003). Consequently, we decided to take ear biopsies (for the purposes of genotyping and identification) from mice at two weeks of age in any future survival studies involving treatment of mice via the diet or drinking water, as this would allow them to be weaned directly into their experimental groups. This was successfully performed in our subsequent trehalose survival study (discussed in detail in **Chapter 5**) and was observed to considerably reduce fighting.

When faced with fighting in male mice in our metformin survival study, we employed several methods to reduce the severity of this fighting. These were as follows:

1. Cages of male and female mice were moved to opposite sides of the holding room, as exposure to female odours can promote aggression in male mice as a consequence of their tendency to compete for opportunities to breed (Hurst, 2005).
2. To further minimise exposure of male mice to female odours, gloves were changed between handling female and male mice and surfaces were cleaned between working with mice of different sexes.
3. The role of enrichment materials in promoting/reducing aggression in male mice is complex and highly dependent on the nature of the enrichment (Van Loo et al., 2002), however, it has been shown that provision of nesting material, which mice can actively arrange and shape, reduces aggression between male mice (Van Loo et al., 2002). We therefore provided nesting material in all cages (both male and female). The nesting material chosen was Enviro-Dri from Lillico, a highly absorbent paper

wool that requires less frequent changing than traditional paper wools. Less frequent changing of nesting material is advantageous as it has been shown that transferring existing nesting material from old cages to fresh cages when male mice are cleaned out, substantially reduces fighting (Van Loo et al., 2000). Consequently, we always transferred over some nesting material when cleaning out male cages.

4. In addition to providing nesting in all male cages, we provided two fun tunnels (Lilico) which mice could move, arrange and chew as they pleased. Our reasoning for including the fun tunnels was that it has been suggested that laboratory mice that are living in a cage without enrichment may be unable to respond to each other in a way that is socially normal for them. Subordinate mice are for example unable to escape from the most dominant male's sight, or to migrate out of his territory. This may cause the dominant male to respond with more extreme aggression than usual, in an attempt to achieve the desired effect (i.e. disappearance of the subordinate) (Van Loo et al., 2003). We felt that inclusion of fun tunnels would provide opportunity for subordinate males to hide as well as provide entertainment that may reduce boredom-induced fighting.
5. If fighting became so severe in individual cages that we felt that injuries sustained may severely affect the welfare of the mice or influence weight and neurological score data collected from them, we removed the dominant male from the affected cage. The removed male was then housed singly for the remainder of the study. This is a common practise when working with aggressive strains of laboratory mice (Van Loo et al., 2003) and worked well in this instance. However, we were keen to avoid having to separate males at this early stage in future studies as we wanted to keep cage conditions between experimental groups as uniform as possible. If individual

mice sustained such severe fighting injuries that their disease course could be affected, they were excluded from analyses from the timepoint at which the injury occurred.

7.2.3 Employing the ALSTDI neurological scoring system

7.2.3.1 Establishing the difference between a score of 0 and a score of 1

During our metformin survival study, we employed a neurological scoring system developed by the ALSTDI (Scott et al., 2008, Gill et al., 2009, Lincecum et al., 2010), to assess the onset and progression of neurological symptoms and survival in $SOD1^{G93A}$ mice. This scoring system was as follows:

0 Full extension of hind legs away from lateral midline when mouse is suspended by it tail and mouse can hold this for 2 seconds, suspended 2-3 times.

1 Collapse or partial collapse of leg extension towards lateral midline (weakness) or trembling of hind legs during tail suspension.

2 Toes curl under at least twice during walking of 12 inches or any part of foot is dragging along cage bottom

3 Rigid paralysis or minimal joint movement, foot not being used for forward motion.

4 Mouse cannot right itself within 30s of being placed on a side

Although we found criteria used to determine scores 2, 3 and 4, distinct and easy to determine without ambiguity, we initially found the distinction between scores 0 and 1 for individual hindlimbs more difficult to establish. Specifically, it was difficult to determine how widely

splayed a mouse's hindlimbs needed to be upon suspension of the mouse by its tail to warrant the description of 'full extension of hind legs away from lateral midline'. Consequently, neurological score curves for mice in our metformin survival study **(Figures 23 and 25)** fluctuated between 0 and 1 at early time-points (between approximately 41 and 76 days of age) rather than starting low and continuously rising. In order to overcome this problem we analysed the nature of the hindlimb splay upon suspension by the tail of a number of WT mice in the age range of 35 to 80 days ,when SOD1 mice would normally be scored either 0 or 1. Through analysis of these wild type mice and comparison to $SOD1^{G93A}$ mice at varying stages of pathology, we realized that even in healthy WT mice, there is variation in how widely splayed a mouse's hindlimbs will be upon suspension by the tail. However, the critical indicator of collapse to the midline in $SOD1^{G93A}$ mice is that the mouse no-longer holds its hindlimbs out straight and instead bends them at the ankle and the knee. This bend is initially subtle and becomes more pronounced as the disease progresses. **Figure 34** shows a photograph of a WT mouse being suspended by its tail and a $SOD1^{G93A}$ mouse next to it, also being suspended by its tail. In these photographs the WT mouse shows a classic healthy hindlimb splay where both hindlimbs are held straight and away from the lateral midline, whereas the $SOD1^{G93A}$ mouse shows a full collapse to the midline with both hindlimbs bent and tucked in towards the body. As a consequence of our observations in WT and $SOD1^{G93A}$ mice, we decided that if a mouse could hold a hindlimb out straight without tremor for 2 seconds when suspended 2-3 times by its tail, this hindlimb should be awarded a score of 0. Conversely, if a mouse's hindlimb was bent to any extent upon suspension of the mouse by its tail, a score of 1 was awarded for this hindlimb. Scores were assigned to each hindlimb individually and in some instances one hindlimb was given a score of 0 and the other a score of 1. After establishing the hindlimb bending criterion for hindlimb collapse to the midline,

we found that scores 0 and 1 could be assigned with confidence. This is evidenced in neurological score curves for our subsequent trehalose dose-response survival study **(Figures 29 and 31)** where neurological scores show a much smoother progression from low to high.

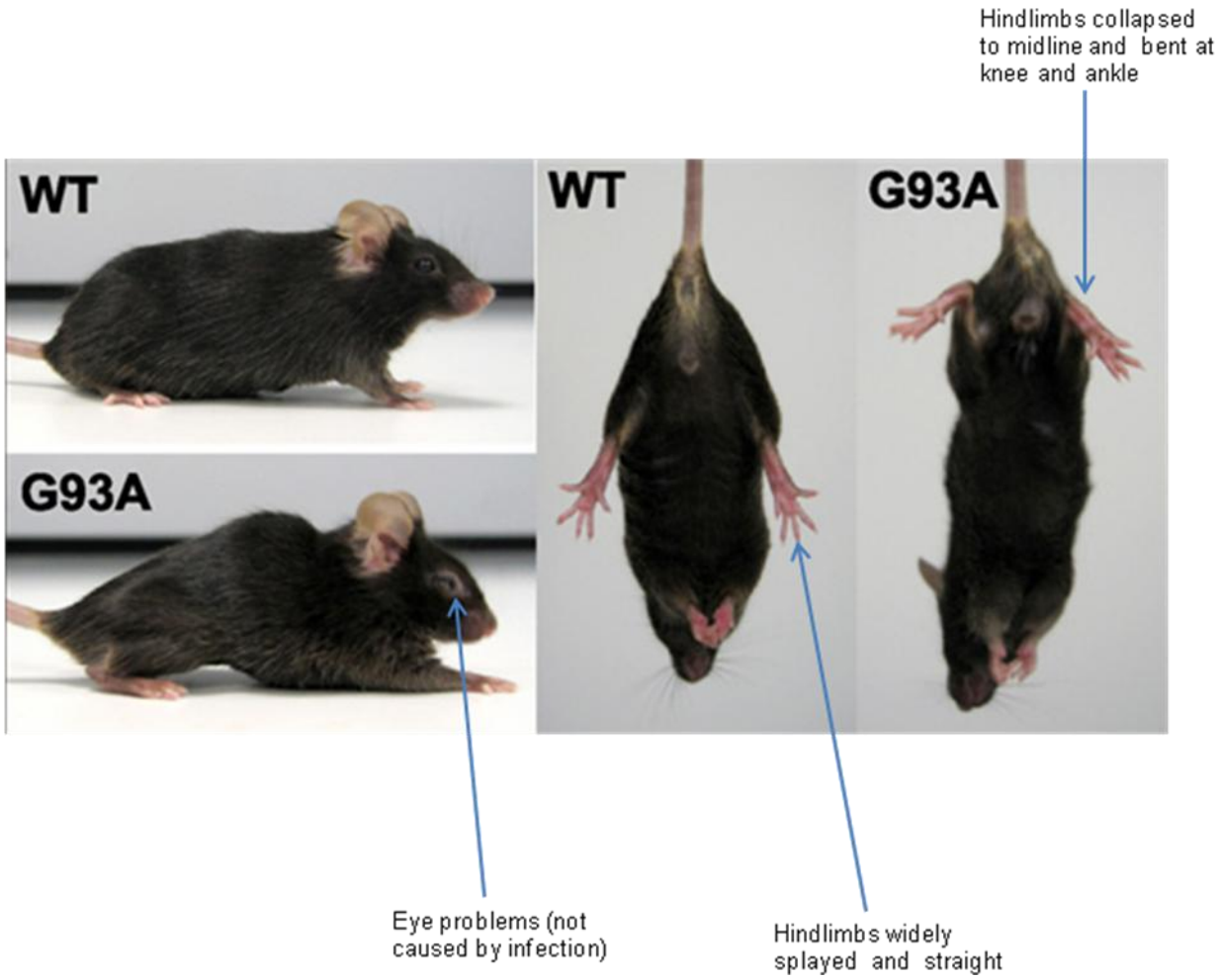


Figure 34: Characteristics of pathology in SOD1^{G93A} mice compared to WT mice (Figure adapted from Turner & Talbot, 2008).

The left panel shows a SOD1^{G93A} mouse at a symptomatic time point in its pathology. Comparison of this mouse to the WT mouse above it highlights the muscle wasting, atrophy and kyphosis that occurs as a result of motor neuron degeneration in SOD1^{G93A} mice. Additionally, this SOD1^{G93A} mouse shows abnormal white material around its right eye and an inability to open the eye fully. We observed similar eye problems to this in a number of SOD1^{G93A} mice approaching the humane end stage in our survival studies. We determined, through sending a swab of the white material around the eye for analysis, that these eye problems were not the result of eye infections. While WT mice are able to hold their hindlimbs out straight and away from the lateral midline when suspended by their tails (as evidenced by the WT mouse in the right panel), SOD1^{G93A} mice find it increasingly more difficult to do this as their muscles become weaker and paralysis progresses. This results in a progressively worsening bending and collapsing of hindlimbs to the lateral midline upon suspension by the tail (as is demonstrated by the SOD1^{G93A} mouse in the right panel of this figure, which shows a full collapse of the hindlimbs to the lateral midline).

7.2.3.2 Determining the existence of toe curling in SOD1^{G93A} mice non-invasively.

In order for the hindlimb of a SOD1^{G93A} mouse to be assigned a score of 2 in the ALSTDI neurological scoring system, the toes on the foot of this hindlimb must curl under at least twice during walking of 12 inches or part of the foot must be dragging along the cage bottom. During our metformin survival study, we found that as mice became more advanced in their pathology, they were less likely to voluntarily walk along the bottom of the low sided empty cage used for neurological scoring assessments (an empty cage without bedding was used for these assessments as the presence of bedding made it difficult to see the toes and feet of the mice as they walked). We felt that encouraging mice to walk by nudging them or tapping the cage was excessively invasive and may cause distress. Furthermore, we noticed that mice encouraged to walk by these measures, walked differently to those walking voluntarily. Consequently, we developed a system in which a cardboard tube (Fun tunnel, Lillico) was placed in front of the mouse and then slowly dragged away from the mouse across the cage bottom. Invariably the mouse would begin to crawl into the tunnel and then follow the tunnel as it was being moved across the cage. As the mouse was walking to follow the tunnel it was easy to observe whether its toes were curling under or whether its feet were dragging. Furthermore, when following the fun tunnel, mice walked in a straight line, which made it much easier to confirm that they had walked 12 inches. We therefore highly recommend this non-invasive method for observing the walking of SOD1^{G93A} mice when employing the ALSTDI neurological scoring system.

7.2.3.3 Determining the humane end stage of SOD1^{G93A} mice in conditions that are relevant to the home cage environment.

When we reached a stage in our metformin survival study at which it was necessary to begin testing the righting reflexes of the mice, we carefully considered the surface on which we should perform the righting reflex test i.e. table top, home cage, empty cage, cage containing the same bedding as home cage. Eventually we decided that a clean cage containing the same bedding on its base as the mouse's home cage would be the most appropriate. Our reasoning behind this was that there were usually other mice within the mouse's home cage, which interfered with the assessment of the mouse's righting reflex and therefore the home cage was not appropriate. However, we felt that it was important to check that a mouse could right itself within the conditions that it lived in, as if it could not, this would be a welfare issue. We therefore concluded that a separate cage containing the same bedding as the home cage would allow us to establish this without the interference of other mice. We did not include nesting or enrichment material in this extra cage as being slightly propped up by this nesting/enrichment material or pushing against it with the forelimbs could help mice right themselves quicker than in a cage without nesting material.

7.2.4 Changing bedding and enrichment conditions to accommodate advancing pathology in SOD1^{G93A} mice.

We began our metformin survival study with each cage containing gold chips bedding (a form of sawdust bedding) as well as a handful of nesting material (initially standard paper wool, then Enviro-Dri paper wool when fighting was observed in males) and two fun tunnels (all bedding and nesting material was purchased from Lillico). Although these cage conditions were appropriate for SOD1^{G93A} mice in pre-symptomatic and early symptomatic

stages in their pathology, we found that as mice began to show paralysis in their hindlimbs, they began to get these hindlimbs caught up in the nesting material. Furthermore, mice with reduced strength and mobility sometimes became stuck between the wall of the cage and a fun tunnel. We therefore made the decision that Enviro-Dri paper wool and fun tunnels should be removed from the cages when mice began to experience hindlimb paralysis and/or reduced mobility. Ideally we would have liked to have removed these items from all cages at the same time to keep cage conditions consistent between groups. However, considering the problems we had had with fighting in male mice, we were concerned about taking nesting and enrichment material away from cages in which male mice were still relatively healthy, as we felt that this may lead to increased fighting. Consequently, we removed nesting and enrichment material from all female cages from 110 days of age onwards and from any male cages in which a mouse was showing signs of reduced mobility or hindlimb paralysis from this point forward. Although this removal of bedding/enrichment material prevented mice becoming caught up or trapped, we became increasingly concerned that mice may become cold and/or distressed without any form of nesting material in their cages, particularly when they became thinner and less mobile and could therefore not hold their temperature as well. We therefore, with the help of staff at the RVC BSU, conducted a search for any types of bedding/enrichment material that mice would not get caught up in, but that would afford them some warmth and shelter. We were fortunate to find nestlets (Lillico, **Figure 35**), which are 5 x 5cm squares of pulped, virgin cotton fiber, which mice can pull apart/shred and shape to form nests if they desire. The material used to form the nestlets is soft, non-desiccative and breathable and we therefore felt that it would be ideal for $SOD1^{G93A}$ mice at varying stages in their pathology. In order to confirm that the nestlets would be suitable for $SOD1^{G93A}$ mice at late symptomatic time points, we provided nestlets in several test cages of late-

symptomatic SOD1^{G93A} mice that were not enrolled in the study. We found that mice did not become caught up in the nestlet material, even when it had been pulled out completely to form a large cotton wool-like nest and furthermore that they chose to spend most of their time within the nesting material. We therefore concluded that two nestlets should be provided to every cage from this time point forward. When observing the behaviour of the SOD1^{G93A} mice in the presence of the nestlets, we were pleased to observe that they afforded adaptation of the nesting material to the pathological time-point of the mice in the cage. Specifically, healthy mice could spend their time pulling apart and shaping the nestlets to form large nests that mice at later pathological time points could find it harder to navigate around. Whereas mice at later pathological time points would spend less time pulling apart the nestlets and instead lie on top of them and only pull them apart slightly, therefore creating bedding conditions which were easier for them to manoeuvre around. We therefore decided that nestlets should be provided from the start to the end of any future survival studies performed and that fun tunnels should be provided initially but removed at 100 days of age when mice were likely to begin to become less mobile and start dragging hindlimbs.



Figure 35: Lillico Nestlets

Nestlets are 5 x 5cm squares of pulped, virgin cotton fiber, which mice can pull apart/shred to form nests. We found these to be ideal nesting material for SOD1^{G93A} mice at all stages in their pathology as the less mobile the mice were, the less they would pull apart the nestlets and therefore the less of an obstacle the nestlets provided within the cage, whilst still providing a warm and dry surface to lay on. (Image taken from http://www.lillicobiotech.co.uk/bedding_nesting/bedding_2nd/nestlets/nestlets.php)

7.2.5 The correct time to introduce long sipper tubes and a mashed diet in survival studies in SOD1^{G93A} mice.

In mid- late symptomatic time points when SOD1^{G93A} experience hindlimb weakness and/or paralysis, it is not possible for them to stand on their hindlegs in order to reach the short sipper tubes that are normally used to cap their drinking water bottles. Consequently, we decided to follow the recommendation of the ALSTDI and purchase longer sipper tubes (Techniplast) which reached down far enough within the cages that mice could access them without having to stand on their hindlegs or bend their head too far upwards (we noticed that late-symptomatic SOD1^{G93A} mice had a smaller range of head motion and could therefore not bend their heads as far upwards as WT mice). An example of a long sipper tube is shown in **Figure 36.** We also decided to provide mice with food pellets soaked in water or drug solution (a mashed diet) in addition to their normal dry pellets as we felt that this would provide an additional easy source of hydration for the mice. We placed the mashed food pellets on the low sided lids of plastic petri dishes to avoid the bedding sticking to the pellets. After an initial period of caution following the introduction of the petri dish lids, mice became used to eating mash from them. We also ensured that we pushed the petri-dish lids into the corner of the cage to reduce the risk of mice becoming stuck between the cage wall and the lid. We initially decided to introduce a mashed diet and long sipper tubes at 100 days of age in our metformin survival study, when mice began to start showing signs of hindlimb weakness and paralysis. However, at this stage, all cages contained Enviro-Dri paper wool and many mice were still very mobile. Consequently we experienced problems with mice pushing this nesting material up against the long sipper tubes as they were in some cases initially distressed by the appearance the new fixture within the cages. In many cases this caused the cages to become flooded. At this stage we were already considering removing the

Enviro-Dri paper wool from the cages as symptomatic mice had begun to get their legs caught in it **(see section 7.2.4)** and the occurrence of leaks helped to confirm that this was the right decision. Once the paper wool was removed, the occurrence of leaks was greatly diminished. As an additional measure, we also reduced the depth of the golden chip bedding placed on the bases of the cages. This increased the distance between the bedding and the sipper tube just enough that the bedding did not come into contact with the sipper tube whilst still allowing mice to reach the sipper tube. We also established that placing a few food pellets in the water bottle holder of the cage lid could allow adjustment of the depth to which the sipper tube fell within the cage. This meant that the sipper tube could be raised up for healthier mice that may push their bedding against it and lowered for less mobile mice. After introducing nestlets into the cages **(see section 7.2.4)** we were pleased to see that the nests that mice made with nestlets were more contained and of a lower height than those made with paper wool. This meant that the occurrence of leaks with nestlets was far lower than with Enviro-Dri paper wool. This confirmed our decision that nestlets should be the nesting material of choice in future survival studies and that long sipper tubes and a mashed diet should still be introduced at 100 days of age, providing careful monitoring of the distance between the bedding and the sipper tube was carried out to prevent the occurrence of leaks.

Although provision of long sipper tubes and a mashed diet in our survival studies ensured that dehydration was a rare occurrence, we carefully monitored mice throughout these studies and gave any mice showing signs of excessive dehydration an intra peritoneal injection of sterile saline (100ml/kg/24 hrs which worked out as 300-400µl every two hours) and closely monitored their health thereafter.

Figure 36: Techniplast long sipper tube



7.2.6 Eye problems in SOD1^{G93A} mice at late symptomatic time points.

As mice began to approach the humane end stage (inability to right within 30s of being placed on a side) in our metformin survival study, we observed that some mice began to develop a sticky discharge around one or both of their eyes. This sometimes prevented them from opening the affected eye fully. We had not read about this phenomenon in the literature and consequently became concerned that these mice had contracted an eye infection. We therefore took swabs from the eyes of several affected mice and sent them away for pathological analyses. The results of these analyses revealed no signs of infection. We therefore concluded that the eye problems were likely have resulted from mice being less able to groom themselves efficiently in order to keep dust from bedding material etc. out of their eyes. This is particularly relevant for mice approaching end stage as they spend a larger proportion of time lying down with their heads in contact with the bedding. In order to understand these eye problems further, we contacted colleagues in the ALS field who also perform survival studies in SOD1^{G93A} mice. Interestingly, Dr Richard Mead, a member of Professor Pamela Shaw's team at the Academic Neurology Unit, University of Sheffield, informed us that they observe similar eye problems in their colony of SOD1^{G93A} at late symptomatic time points. They, like us have concluded that these eye problems are not caused by infection and that they may be derived from irritation of the eye through the inability to groom appropriately. In order to overcome these problems, Dr Mead and colleagues, have implemented an SOP involving the replacement of bedding in the cages of affected mice with a piece of absorbent tissue paper (to minimize dust) and the daily cleaning of the eyes of affected mice with sterile saline. They have also included a section in their home office project license detailing the occurrence of these eye problems and the methods that should be employed to treat them. Interestingly, **Figure 34**, which was adapted from a

publication by Turner and Talbot, also shows a SOD1^{G93A} mouse with a slightly closed eye surrounded by white discharge (Turner and Talbot, 2008) . This further indicates that eye problems are not an abnormal occurrence in SOD1^{G93A} mice.

In order to overcome the eye problems observed in our mice, we began to clean affected eyes with sterile saline and sterile tissues/cotton buds, twice daily. We also put Tears Naturale eye drops (Alcon) into the eyes of affected mice twice daily to soothe and lubricate the eyes. Furthermore, with the help of staff at the RVC BSU, we conducted a search for bedding materials that may produce less dust and therefore less eye irritation than the golden chips (Lillico) bedding used for our metformin survival study. Though this search we found ALPHA-dri bedding (Lillico) which is dust free, and formed from 5mm width squares of highly absorbent pure cellulose fibre **(Figure 37)**. We conducted a test with this bedding in non-experimental late-symptomatic SOD1^{G93A} mice and found it to be easy for mice to manoeuvre across and very good at keeping cages dry, clean and dust free. We therefore decided to use ALPHA-dri bedding throughout for all future SOD1^{G93A} survival studies. Although we still experienced eye problems in SOD1^{G93A} mice approaching end stage in our subsequent trehalose survival study in which ALPHA-dri bedding was used **(Chapter 5)**, these were less frequent. Additionally, we felt that the bedding was overall more comfortable for the mice as it kept their environment dryer, cleaner and easier to navigate.



Figure 37: Lillico ALPHA dri bedding

ALPHA-dri bedding is formed from 5mm width squares of highly absorbent pure cellulose fibre. It is dust free and we therefore hypothesised that it may minimise eye irritation in $SOD1^{G93A}$ mice. (Image taken from: http://www.lillicobiotech.co.uk/bedding_nesting/bedding_2nd/alpha_dri_plus/alpha_dri_plusl.php)

7.2.7 Separating SOD1^{G93A} mice at late symptomatic time points from healthier cage mates to prevent over grooming and hindlimb mutilation.

SOD1^{G93A} mice used in our metformin survival study and subsequent survival studies were bred on a mixed-hybrid genetic background. Consequently, there was a degree of variation in the disease course between individual mice within the same treatment groups. This meant that at any one time, one or more mice in a cage could be experiencing hindlimb paralysis and approaching the end stage, while others were still moving around the cage with relative ease. As mice began to show hindlimb paralysis, we noticed (particularly in females) that healthier cage mates would spend a lot of time grooming and lying next to or on top of those mice that were more advanced in their pathology. We began to become concerned that the actions of these healthier cage mates may be detrimental to those mice that were more advanced in their pathology. This was confirmed when we were distressed to find a mouse which appeared to have had several of the toes on one of its hindlimbs bitten off. Hind limb mutilation and autophagia has been shown to occur in laboratory rats after spinal cord injury (Zhang et al., 2001) and therefore we considered it possible that this mouse had bitten its own toes upon experiencing paralysis in this hindlimb. However, considering the relatively low mobility of this mouse, we found it surprising that the mouse would be able to reach its toes in order to bite them. Female mice can sometimes cannibalise their own newborn litters when under stress (Poley, 1974). We therefore considered it possible that a healthier cage mate may have become distressed by the injured mouse's hindlimb becoming paralysed and therefore bitten the toes off on this abnormal leg. When a second female mouse experienced a less severe bite injury on her hindlimb (one that she quickly recovered from once she was placed in a separate cage and the foot was cleaned with chlorhexidine (Hibiscrub)), we considered it essential that any further injuries were prevented. We therefore began to place any mice that

were dragging a hindlimb or receiving undue attention from a healthier cage mate in their own separate cage. Following this we did not experience any further problems with hindlimb mutilation. This suggested to us that the hindlimb injuries sustained were caused by other healthier mice rather than through autophagia. We therefore concluded that in any future survival studies, mice should be separated from their cage mates as soon as they began to show signs of hindlimb paralysis.

7.2.7 The importance of twice daily checks in survival studies in SOD1^{G93A} mice at late symptomatic time points.

Although mice in our metformin study were carefully checked over twice weekly when weighing and neurological scoring was being performed, we considered it critical to check mice daily once they began to show signs of hindlimb paralysis or loss of righting reflex. This was particularly important considering our observations of leaks as a result of long sipper tubes, eye problems and maltreatment of mice by their healthier cage mates. In our metformin survival study, the first occurrence of a mouse reaching the humane end stage was at 103 days of age. Following the death of this mouse we decided to check all mice daily for their righting reflex as we did not want to miss the correct end stage of any mice. As we had already begun putting mash in all cages everyday from 100 days of age, this was an easy transition to make. Once more mice began to approach the end stage of the inability to right themselves within 30s of being placed on a side, we began to realize that when mice were approaching this end stage, they could deteriorate very rapidly from one hour to the next. For example a mouse that was able to right itself in the morning may not be able to right itself in the evening. Consequently, in order to prevent mice from spending excessive time at end stage, we decided that it was necessary to perform a morning check and an afternoon check

for all mice. This was carried out for the remainder of the metformin survival study and is now standard protocol in our laboratory.

7.2.8 Optimising the humane end point used for SOD1^{G93A} mice in survival studies.

When planning our metformin dose response survival study, we decided to employ the most commonly used end point of the inability of mice to right within 30s of being placed on a side (Scott et al., 2008). Having not performed survival studies in SOD1^{G93A} mice before, we felt that it was best to begin with a format that had previously been shown to be successful and then to carry out detailed observations throughout this study to see whether the end point could be refined in any way to minimize the suffering of the mice. In our metformin survival study, we observed that in the majority of cases, mice that could not right themselves within 20s, continued to remain on their sides to reach the threshold of 30s. However, some mice still managed to right after 20s and were consequently kept for another day. When comparing the overall condition of these mice to those that had remained on their sides for 30s, we felt that there was little difference and therefore that waiting for these mice to reach the 30s threshold did not offer any experimental advantage and prolonged suffering. We therefore decided that for any future studies, the end point employed should be the inability of mice to right themselves within 20s of being placed on their side. We additionally noticed that the speed with which mice deteriorated from late symptomatic time points involving hindlimb dragging/paralysis to the end stage of the inability to right within 30s of being placed on a side was sometimes very rapid. Consequently we became worried that mice which took over 15 seconds to right in an evening check, may reach the end stage at some point throughout the night. Although there were not many mice which met this criterion, we made detailed observations any of mice taking 15s and above to right on the evening check and found that

in the majority of cases, these mice would be at end stage the next morning. We therefore made the decision that in all future studies, any mice that took over 15s to right in the evening check should be culled then and their survival recorded as the next day. This was employed successfully in our trehalose survivals study.

After completion of our metformin survival study, we carefully reviewed the data generated and observations made during the study in order to see whether an endpoint earlier than the loss of righting reflex could be used to generate the same information. However, we found that the pathological route via which mice reached the loss of righting reflex was very heterogeneous between individual mice. For example, some mice experienced bilateral hindlimb paralysis and some only unilateral, some mice lost more weight than others before reaching end sage and some mice spent many days dragging their hindlimbs but remained highly alert and mobile (via movement of their forelimbs) throughout, whereas others reached end stage immediately after the onset of hindlimb paralysis. It was therefore difficult to find an earlier unifying end point that could be identified in all mice. Furthermore, it is increasingly becoming clear that different pathological mechanisms are in play at different phases in the disease (Yang et al., 2011b). It is therefore possible that a particular drug may be of benefit at one phase in the disease but not at others. Consequently to exclude the end stage of the disease, represented by the inability of mice to right themselves, may result in the loss of important information about the effect of a particular drug on the length of time spent at the symptomatic phase of the disease prior to end stage. In light of this we decided to keep the end stage as the inability of mice to right themselves within 20s of being placed on their side for future studies.

7.2.9 Optimal husbandry for survival studies in SOD1^{G93A} mice

Considering all the issues discussed above, we have developed the following optimal husbandry conditions when employing survival studies in SOD1^{G93A} mice:

- If mice from different litters are to be combined within the same cages, mice should be genotyped prior to weaning and weaned directly into their experimental groups.
- Males should be housed in groups of three, as this has been shown to be the optimal group size to minimise fighting (Van Loo et al., 2001)
- Male and female mice should be weaned into cages as far as possible from each other to avoid the exposure of males to female odours.
- Gloves should be changed and work surfaces cleaned between the handling of male and female mice.
- All cages should contain ALPHA dri bedding, 2 nestlets and 2 fun tunnels. Fun tunnels should be removed at 100 days of age when mice may begin to show signs of hindlimb weakness and paralysis.
- Existing nesting material should be kept as far as possible when cleaning out male cages (new nestlets can be provided, as long as a handful of the old nestlet material is still included)
- Cages should be fitted with long sipper tubes and mash provided daily (on a petri dish lid pushed into the corner of the cage) from 100 days of age.
- The depth to which long sipper tubes descend into the cage, should be controlled so as to prevent contact with bedding/nesting material and therefore leaks.
- The general health of mice as well as their righting reflex should be checked twice daily (AM and PM) from 100 days of age or the earliest time-point at which a mouse appears to be approaching end stage.

- If mice are seen to experience eye problems, the affected eyes should be cleaned with sterile saline twice daily and Tears Naturale eye drops (Alcon) should be provided to lubricate the eyes.
- If mice are seen to become dehydrated, they should be given an intraperitoneal injection of sterile saline (100ml/kg/24 hrs which works out as 300-400μl every two hours) and closely monitored.
- Mice should be separated from their cage mates as soon as they show signs of hindlimb paralysis or undue attention from healthier cage mates.
- The humane end stage should be the inability to right within 20s of being placed on a side and any mice, taking longer than 15s to right in the evening check should be culled and one day added to their survival.
- All animal technicians and investigators should be aware of the optimal husbandry conditions to ensure that mice are always well cared for.

7.3 Appendix 3. Potential method for assessing the ability of orally administered trehalose to reach the CNS.

Trehalose levels in mouse tissues (Tanaka et al., 2004) and in *saccharomyces cervisiae* (Kienle et al., 1993, Lee and Goldberg, 1998) have previously been determined by measuring glucose concentrations in these samples before and after treatment with the enzyme trehalase. As trehalose is composed of two glucose molecules, halving the increase in glucose derived from trehalase treatment indicates the amount of trehalose present (providing all other metabolic processes that may change glucose concentration are disabled during the assay). We reasoned that providing appropriate controls were put in place, this would be an appropriate method for determining whether trehalose, when administered orally, can reach the CNS. We therefore planned the following method for implementing this assay:

- Dr Butters at the Oxford Glycobiology institute informed us that his laboratory frequently uses a Glucose (GO) Assay Kit (GAGO-20, Sigma) for measuring glucose levels in cells and tissue homogenates. In this kit, glucose is oxidised to gluconic acid and hydrogen peroxidase by glucose oxidase. The hydrogen peroxidase produced then reacts with o-dianisidine in the presence of peroxidase to form a coloured product. This coloured oxidised o-dianisidine then reacts with sulphuric acid to form a more stable pink-coloured product. The intensity of this pink product, measured at 540nm is proportional to the original glucose concentration.
- Trehalase purified from porcine kidney can also be purchased from Sigma (product number T8778). It has been shown to have a high level of purity, having ≤1%

contamination with enzymes such as α-glucosisase, invertase and amylase, which could bring about non-trehalose dependent increases in the glucose concentration in tissue homegenates if present at significantly high levels.

- The basic assay procedure that we would employ using the Sigma Glucose (GO) Assay Kit and trehalase enzyme described, would be as follows (we based this assay procedure on previously described assays using similar reagents (Lee and Goldberg, 1998, Kienle et al., 1993)):
    - Crush tissues of interest in liquid nitrogen using a pestle and mortar (note: while we would ideally want to measure trehalose levels in the spinal cord, we were aware of the possibility that it might be difficult to collect enough spinal cord tissue from each mouse to be within the limits of detection for changes in glucose concentration post trehalase treatment in our assay. Consequently, we decided that if sufficient tissue could not be obtained from spinal cords, then we would perform the assay on brain homogenates as this would still give us an indication of whether trehalose reached the CNS).
    - Resuspend crushed tissue in a suitable volume of water (no more than 0.5ml) in an eppendorf tube on ice.
    - Quickly take out and freeze at -80°C, a small aliquot of the tissue homogenate on which to perform a Bradford DC protein assay (Biorad).
    - Immediately transfer remaining tissue homogenate to a hot block at 95°C for 10 minutes in order to denature endogenous enzymes and prevent further glucose metabolism (keeping the water volume in which crushed tissue is resuspended below 0.5ml ensures that the heating process will be quick and

denaturation of enzymes that could change the glucose concentration will be rapid).

- Centrifuge homogenate for 15-20 minutes at 15000g then collect supernatant.
- Split the collected supernatant between two eppendorfs and add a suitable amount of trehalase (see below) to one tube whilst leaving the other untouched. Incubate both tubes at 37°C for 8 hours.
- Carry out Sigma Glucose (GO) Assay (as per the manufacturer's instructions) on both the untouched aliquot and the aliquot exposed to trehalase.
- Using the concentration of protein measured for the original tissue homogenate, determine the amount of glucose per µg of protein present in the tissue homogenate pre-and post incubation with trehalase. Halving this difference will indicate the amount of trehalose originally present in the tissue homogenate (per µg protein).

- Prior to performing this assay on tissue samples collected from trehalose-treated and control animals, we would first need to optimise the assay using the following steps:
  - Validate the accuracy and sensitivity of detection of the Sigma Glucose (GO) Assay kit on WT mice, ensuring that the amount of glucose measured in the tissue of interest is relatively consistent between mice.
  - Optimise the amount of trehalase enzyme required to break down any trehalose present in tissue homogenates. Do this by calculating the maximum possible amount of trehalose that could have reached the tissue of interest in treated mice by analysing the daily dose of trehalose per gram of tissue that a mouse would receive, assuming it drank 5.8 ml of trehalose solution per day and all ingested trehalose was absorbed into the bloodstream (note:

Bachmanov and colleagues have described the average water intake across 28 strains of mice to be 5.8+/-2 ml/mouse/day(Bachmanov et al., 2002)). Then incubate this maximum amount of trehalose with increasing amounts of trehalase enzyme for 8 hours at 37°C and perform a Sigma Glucose (GO) Assay on the product. This will allow determination of how much trehalase enzyme is required to completely digest the maximum possible amount of trehalose present. The incubation time of 8 hours was selected as this has previously been described to be suitable (Lee and Goldberg, 1998), however, different incubation times could be tested to further optimise trehalose digestion conditions.

- Once the Sigma Glucose (GO) Assay has been optimised for WT tissue and the amount of trehalase required has been determined, spike WT tissue homogenates with the maximum possible amount of trehalose that could reach this tissue. Measurement of the amount of trehalose in these samples using our assay system should then reveal the efficacy of the assay (as the true amount of trehalose in the samples is already known).
- Once the assay has been fully optimised on trehalose-spiked WT tissue homogenates, move on to performing the assay on tissues taken from WT and early symptomatic SOD1^{G93A} mice treated with either 0.5, 2 or 5% trehalose (the doses used in our trehalose survival study) via the drinking water for 2 weeks (treating for two weeks allows mice to become used to the taste of trehalose and therefore drink a normal amount). Comparison of the amount of trehalose in tissues of interest in trehalose-treated and control mice, should

allow determination of how much of the trehalose administered via the drinking water reached the tissue of interest in the mice.

ACEVEDO-AROZENA, A., KALMAR, B., ESSA, S., RICKETTS, T., JOYCE, P., KENT, R., ROWE, C., PARKER, A., GRAY, A., HAFEZPARAST, M., THORPE, J. R., GREENSMITH, L. & FISHER, E. M. C. 2011. A comprehensive assessment of the SOD1G93A low-copy transgenic mouse, which models human amyotrophic lateral sclerosis. *Disease Models & Mechanisms*.

ACSADI, G., ANGUELOV, R. A., YANG, H., TOTH, G., THOMAS, R., JANI, A., WANG, Y., IANAKOVA, E., MOHAMMAD, S., LEWIS, R. A. & SHY, M. E. 2002. Increased Survival and Function of SOD1 Mice After Glial Cell-Derived Neurotrophic Factor Gene Therapy. *Human Gene Therapy,* 13**,** 1047-1059.

AFIFI, A., ALEU, F., GOODGOLD, J. & MACKAY, B. 1966. Ultrastructure of atrophic muscle in amyotrophic lateral sclerosis. *Neurology,* 16**,** 475 - 481.

AL-SAIF, A., AL-MOHANNA, F. & BOHLEGA, S. 2011. A mutation in sigma-1 receptor causes juvenile amyotrophic lateral sclerosis. *Annals of Neurology,* 70**,** 913-919.

ALEXANDER, C., VOTRUBA, M., PESCH, U. E., THISELTON, D. L., MAYER, S., MOORE, A., RODRIGUEZ, M., KELLNER, U., LEO-KOTTLER, B., AUBURGER, G., BHATTACHARYA, S. S. & WISSINGER, B. 2000. OPA1, encoding a dynamin-related GTPase, is mutated in autosomal dominant optic atrophy linked to chromosome 3q28. *Nat Genet,* 26**,** 211-5.

ALEXANDER, G. M., ERWIN, K. L., BYERS, N., DEITCH, J. S., AUGELLI, B. J., BLANKENHORN, E. P. & HEIMAN-PATTERSON, T. D. 2004. Effect of transgene copy number on survival in the G93A SOD1 transgenic mouse model of ALS. *Brain research.Molecular brain research,* 130**,** 7-15.

ALEXIANU, M. E., KOZOVSKA, M. & APPEL, S. H. 2001. Immune reactivity in a mouse model of familial ALS correlates with disease progression. *Neurology,* 57**,** 1282-1289.

ALS-FORUM. 2011. *Fate Accompli—Cells With NG2 Become Oligodendrocytes, Drive ALS?* [Online]. The ALS Forum. Available: http://www.researchals.org/page/4746/6343/0/17/ [Accessed].

AMODIO, R., ESPOSITO, E., DE RUVO, C., BELLAVIA, V., AMODIO, E. & CARRUBA, G. 2006. Red Wine Extract Prevents Neuronal Apoptosis in Vitro and Reduces Mortality of Transgenic Mice. *Annals of the New York Academy of Sciences,* 1089**,** 88-97.

ANDERSON, P. & KEDERSHA, N. 2008. Stress granules: the Tao of RNA triage. *Trends in Biochemical Sciences,* 33**,** 141-150.

ANDREASSEN, O. A., DEDEOGLU, A., FRIEDLICH, A., FERRANTE, K. L., HUGHES, D., SZABO, C. & BEAL, M. F. 2001. Effects of an Inhibitor of Poly(ADP-Ribose) Polymerase, Desmethylselegiline, Trientine, and Lipoic Acid in Transgenic ALS Mice. *Experimental Neurology,* 168**,** 419-424.

ANDREASSEN, O. A., DEDEOGLU, A., KLIVENYI, P., BEAL, M. F. & BUSH, A. I. 2000. N-acetyl-L-cysteine improves survival and preserves motor performance in an animal model of familial amyotrophic lateral sclerosis. *Neuroreport,* 11**,** 2491-3.

ANDRIES, M., VAN DAMME, P., ROBBERECHT, W. & VAN DEN BOSCH, L. 2007. Ivermectin inhibits AMPA receptor-mediated excitotoxicity in cultured motor neurons and extends the life span of a transgenic mouse model of amyotrophic lateral sclerosis. *Neurobiology of Disease,* 25**,** 8-16.

ANGELOV, D. N., WAIBEL, S., GUNTINAS-LICHIUS, O., LENZEN, M., NEISS, W. F., TOMOV, T. L., YOLES, E., KIPNIS, J., SCHORI, H., REUTER, A., LUDOLPH, A. & SCHWARTZ, M. 2003. Therapeutic vaccine for acute and chronic motor neuron diseases: Implications for amyotrophic lateral sclerosis. *Proceedings of the National Academy of Sciences,* 100**,** 4790-4795.

ANNESER, J. M., GMEREK, A., GERKRATH, J., BORASIO, G. D. & HEUMANN, R. 2001. Immunosuppressant FK506 does not exert beneficial effects in symptomatic G93A superoxide dismutase-1 transgenic mice. *Neuroreport,* 12**,** 2663-5.

APPEL, S. H., BEERS, D. R. & HENKEL, J. S. 2010. T cell-microglial dialogue in Parkinson's disease and amyotrophic lateral sclerosis: are we listening? *Trends in Immunology,* 31**,** 7-17.

ARAI, T., HASEGAWA, M., AKIYAMA, H., IKEDA, K., NONAKA, T., MORI, H., MANN, D., TSUCHIYA, K., YOSHIDA, M., HASHIZUME, Y. & ODA, T. 2006a. TDP-43 is a component of ubiquitin-positive tau-negative inclusions in frontotemporal lobar degeneration and amyotrophic lateral sclerosis. *Biochemical and Biophysical Research Communications,* 351**,** 602-611.

ARAI, T., HASEGAWA, M., AKIYAMA, H., IKEDA, K., NONAKA, T., MORI, H., MANN, D., TSUCHIYA, K., YOSHIDA, M., HASHIZUME, Y. & ODA, T. 2006b. TDP-43 is a component of ubiquitin-positive tau-negative inclusions in frontotemporal lobar degeneration and amyotrophic lateral sclerosis. *Biochemical and Biophysical Research Communications,* 351**,** 602 - 611.

ARNDT, S. S., LAARAKKER, M. C., VAN LITH, H. A., VAN DER STAAY, F. J., GIELING, E., SALOMONS, A. R., VAN'T KLOOSTER, J. & OHL, F. 2009. Individual housing of mice -- Impact on behaviour and stress responses. *Physiology & Behavior,* 97**,** 385-393.

ARROYO, E. J. & SCHERER, S. S. 2000. On the molecular architecture of myelinated fibers. *Histochemistry and Cell Biology,* 113**,** 1-18.

ASH, P. E. A., ZHANG, Y.-J., ROBERTS, C. M., SALDI, T., HUTTER, H., BURATTI, E., PETRUCELLI, L. & LINK, C. D. 2010. Neurotoxic effects of TDP-43 overexpression in C. elegans. *Human Molecular Genetics,* 19**,** 3206-3218.

ATKIN, J. D., FARG, M. A., TURNER, B. J., TOMAS, D., LYSAGHT, J. A., NUNAN, J., REMBACH, A., NAGLEY, P., BEART, P. M., CHEEMA, S. S. & HORNE, M. K. 2006. Induction of the Unfolded Protein Response in Familial Amyotrophic Lateral Sclerosis and Association of Protein-disulfide Isomerase with Superoxide Dismutase 1. *Journal of Biological Chemistry,* 281**,** 30152-30165.

ATKIN, J. D., FARG, M. A., WALKER, A. K., MCLEAN, C., TOMAS, D. & HORNE, M. K. 2008. Endoplasmic reticulum stress and induction of the unfolded protein response in human sporadic amyotrophic lateral sclerosis. *Neurobiology of disease,* 30**,** 400-407.

AZARI, M. F., LOPES, E. C., STUBNA, C., TURNER, B. J., ZANG, D., NICOLA, N. A., KUREK, J. B. & CHEEMA, S. S. 2003. Behavioural and anatomical effects of systemically administered leukemia inhibitory factor in the SOD1G93A G1H mouse model of familial amyotrophic lateral sclerosis. *Brain Research,* 982**,** 92-97.

AZARI, M. F., PROFYRIS, C., LE GRANDE, M. R., LOPES, E. C., HIRST, J., PETRATOS, S. & CHEEMA, S. S. 2005. Effects of intraperitoneal injection of Rofecoxib in a mouse model of ALS. *European Journal of Neurology,* 12**,** 357-364.

AZZOUZ, M., HOTTINGER, A., PATERNA, J. C., ZURN, A. D., AEBISCHER, P. & BUELER, H. 2000. Increased motoneuron survival and improved neuromuscular function in transgenic ALS mice after intraspinal injection of an adeno-associated virus encoding Bcl-2. *Hum Mol Genet,* 9**,** 803-11.

AZZOUZ, M., RALPH, G., STORKEBAUM, E., WALMSLEY, L., MITROPHANOUS, K., KINGSMAN, S., CARMELIET, P. & MAZARAKIS, N. 2004a. VEGF delivery with retrogradely transported lentivector prolongs survival in a mouse ALS model. *Nature,* 429**,** 413 - 417.

AZZOUZ, M., RALPH, G. S., STORKEBAUM, E., WALMSLEY, L. E., MITROPHANOUS, K. A., KINGSMAN, S. M., CARMELIET, P. & MAZARAKIS, N. D. 2004b. VEGF delivery with retrogradely transported lentivector prolongs survival in a mouse ALS model. *Nature,* 429**,** 413-417.

BACHMANOV, A. A., REED, D. R., BEAUCHAMP, G. K. & TORDOFF, M. G. 2002. Food Intake, Water Intake, and Drinking Spout Side Preference of 28 Mouse Strains. *Behavior Genetics,* 32**,** 435-443.

BALOH, R. H. 2011. TDP-43: The relationship between protein aggregation and neurodegeneration in ALS and FTLD. *FEBS Journal***,** no-no.

BANERJEE, R., MOSLEY, R. L., REYNOLDS, A. D., DHAR, A., JACKSON-LEWIS, V., GORDON, P. H., PRZEDBORSKI, S. & GENDELMAN, H. E. 2008. Adaptive Immune Neuroprotection in G93A-SOD1 Amyotrophic Lateral Sclerosis Mice. *PLoS ONE,* 3**,** e2740.

BARBEITO, A. G., MARTINEZ-PALMA, L., VARGAS, M. R., PEHAR, M., MAÑAY, N., BECKMAN, J. S., BARBEITO, L. & CASSINA, P. 2010. Lead exposure stimulates VEGF expression in the spinal cord and extends survival in a mouse model of ALS. *Neurobiology of Disease,* 37**,** 574-580.

BARHA, C. K., LIEBLICH, S. E. & GALEA, L. A. M. 2009. Different Forms of Oestrogen Rapidly Upregulate Cell Proliferation in the Dentate Gyrus of Adult Female Rats. *Journal of Neuroendocrinology,* 21**,** 155-166.

BARNÉOUD, P. & CURET, O. 1999. Beneficial Effects of Lysine Acetylsalicylate, a Soluble Salt of Aspirin, on Motor Performance in a Transgenic Model of Amyotrophic Lateral Sclerosis. *Experimental Neurology,* 155**,** 243-251.

BARTH, S., GLICK, D. & MACLEOD, K. F. 2010. Autophagy: assays and artifacts. *The Journal of Pathology,* 221**,** 117-124.

BÄUMER, D., ANSORGE, O., ALMEIDA, M. & TALBOT, K. 2010. The role of RNA processing in the pathogenesis of motor neuron degeneration. *Expert Reviews in Molecular Medicine,* 12**,** null-null.

BEAL, M. F. & FERRANTE, R. J. 2004. Experimental therapeutics in transgenic mouse models of Huntington's disease. *Nat Rev Neurosci,* 5**,** 373-384.

BECKMAN, J. S., CARSON, M., SMITH, C. D. & KOPPENOL, W. H. 1993. ALS, SOD and peroxynitrite. *Nature,* 364**,** 584-584.

BEERS, D. R., HENKEL, J. S., ZHAO, W., WANG, J. & APPEL, S. H. 2008. CD4+ T cells support glial neuroprotection, slow disease progression, and modify glial morphology in an animal model of inherited ALS. *Proceedings of the National Academy of Sciences,* 105**,** 15558-15563.

BENMOHAMED, R., ARVANITES, A. C., KIM, J., FERRANTE, R. J., SILVERMAN, R. B., MORIMOTO, R. I. & KIRSCH, D. R. 2011. Identification of compounds protective against G93A-SOD1 toxicity for the treatment of amyotrophic lateral sclerosis. *Amyotroph Lateral Scler,* 12**,** 87-96.

BENSIMON, G., LACOMBLEZ, L. & MEININGER, V. 1994. A Controlled Trial of Riluzole in Amyotrophic Lateral Sclerosis. *New England Journal of Medicine,* 330**,** 585-591.

BÉRANGER, F., CROZET, C., GOLDSBOROUGH, A. & LEHMANN, S. 2008. Trehalose impairs aggregation of PrPSc molecules and protects prion-infected cells against oxidative damage. *Biochemical and Biophysical Research Communications,* 374**,** 44-48.

BILSLAND, L. G., DICK, J. R. T., PRYCE, G., PETROSINO, S., DI MARZO, V., BAKER, D. & GREENSMITH, L. 2006. Increasing cannabinoid levels by pharmacological and genetic manipulation delay disease progression in SOD1 mice. *FASEB J.,* 20**,** 1003-1005.

BILSLAND, L. G., NIRMALANANTHAN, N., YIP, J., GREENSMITH, L. & DUCHEN, M. R. 2008. Expression of mutant SOD1 in astrocytes induces functional deficits in motoneuron mitochondria. *Journal of Neurochemistry,* 107**,** 1271-1283.

BILSLAND, L. G., SAHAI, E., KELLY, G., GOLDING, M., GREENSMITH, L. & SCHIAVO, G. 2010. Deficits in axonal transport precede ALS symptoms in vivo. *Proceedings of the National Academy of Sciences,* 107**,** 20523-20528.

BODE, F. J., STEPHAN, M., SUHLING, H., PABST, R., STRAUB, R. H., RABER, K. A., BONIN, M., NGUYEN, H. P., RIESS, O., BAUER, A., SJOBERG, C., PETERSÉN, Å. & VON HÖRSTEN, S. 2008. Sex differences in a transgenic rat model of Huntington's disease: decreased 17β-estradiol levels correlate with reduced numbers of DARPP32+ neurons in males. *Human Molecular Genetics,* 17**,** 2595-2609.

BOILLEE, S., YAMANAKA, K., LOBSIGER, C. S., COPELAND, N. G., JENKINS, N. A., KASSIOTIS, G., KOLLIAS, G. & CLEVELAND, D. W. 2006. Onset and progression in inherited ALS determined by motor neurons and microglia. *Science (New York, N.Y.),* 312**,** 1389-1392.

BOLAND, B., KUMAR, A., LEE, S., PLATT, F. M., WEGIEL, J., YU, W. H. & NIXON, R. A. 2008. Autophagy Induction and Autophagosome Clearance in Neurons: Relationship to Autophagic Pathology in Alzheimer's Disease. *The Journal of Neuroscience,* 28**,** 6926-6937.

BORCHELT, D. R., LEE, M. K., SLUNT, H. S., GUARNIERI, M., XU, Z. S., WONG, P. C., BROWN, R. H., PRICE, D. L., SISODIA, S. S. & CLEVELAND, D. W. 1994. Superoxide dismutase 1 with mutations linked to familial amyotrophic lateral sclerosis possesses significant activity. *Proceedings of the National Academy of Sciences,* 91**,** 8292-8296.

BORDET, T., BUISSON, B., MICHAUD, M., DROUOT, C., GALÉA, P., DELAAGE, P., AKENTIEVA, N. P., EVERS, A. S., COVEY, D. F., OSTUNI, M. A., LACAPÈRE, J.-J., MASSAAD, C., SCHUMACHER, M., STEIDL, E.-M., MAUX, D., DELAAGE, M., HENDERSON, C. E. & PRUSS, R. M. 2007. Identification and Characterization of Cholest-4-en-3-one, Oxime (TRO19622), a Novel Drug Candidate for Amyotrophic Lateral Sclerosis. *Journal of Pharmacology and Experimental Therapeutics,* 322**,** 709-720.

BORDET, T., LESBORDES, J.-C., ROUHANI, S., CASTELNAU-PTAKHINE, L., SCHMALBRUCH, H., HAASE, G. & KAHN, A. 2001. Protective effects of cardiotrophin-1 adenoviral gene transfer on neuromuscular degeneration in transgenic ALS mice. *Human Molecular Genetics,* 10**,** 1925-1933.

BORTHWICK, G. M., JOHNSON, M. A., INCE, P. G., SHAW, P. J. & TURNBULL, D. M. 1999. Mitochondrial enzyme activity in amyotrophic lateral sclerosis: implications for the role of mitochondria in neuronal cell death. *Ann Neurol,* 46**,** 787-90.

BOSCO, D. A., LEMAY, N., KO, H. K., ZHOU, H., BURKE, C., KWIATKOWSKI, T. J., SAPP, P., MCKENNA-YASEK, D., BROWN, R. H. & HAYWARD, L. J. 2010a. Mutant FUS proteins that cause amyotrophic lateral sclerosis incorporate into stress granules. *Human Molecular Genetics,* 19**,** 4160-4175.

BOSCO, D. A., MORFINI, G., KARABACAK, N. M., SONG, Y., GROS-LOUIS, F., PASINELLI, P., GOOLSBY, H., FONTAINE, B. A., LEMAY, N., MCKENNA-YASEK, D., FROSCH, M. P., AGAR, J. N., JULIEN, J.-P., BRADY, S. T. & BROWN, R. H. 2010b. Wild-type and mutant SOD1 share an aberrant conformation and a common pathogenic pathway in ALS. *Nat Neurosci,* 13**,** 1396-1403.

BOSTON-HOWES, W., WILLIAMS, E. O., BOGUSH, A., SCOLERE, M., PASINELLI, P. & TROTTI, D. 2008. Nordihydroguaiaretic acid increases glutamate uptake in vitro and in vivo: Therapeutic implications for amyotrophic lateral sclerosis. *Experimental Neurology,* 213**,** 229-237.

BOZIK, M. E., MATHER, J. L., KRAMER, W. G., GRIBKOFF, V. K. & INGERSOLL, E. W. 2011. Safety, Tolerability, and Pharmacokinetics of KNS-760704 (Dexpramipexole) in Healthy Adult Subjects. *The Journal of Clinical Pharmacology,* 51**,** 1177-1185.

BRECKENRIDGE, D. G., STOJANOVIC, M., MARCELLUS, R. C. & SHORE, G. C. 2003. Caspase cleavage product of BAP31 induces mitochondrial fission through endoplasmic reticulum calcium signals, enhancing cytochrome c release to the cytosol. *The Journal of Cell Biology,* 160**,** 1115-1127.

BROOKS, S. V. & FAULKNER, J. A. 1988. Contractile properties of skeletal muscles from young, adult and aged mice. *The Journal of physiology,* 404**,** 71-82.

BROWN, W. F. & MILNER-BROWN, H. S. 1976. Some electrical properties of motor units and their effects on the methods of estimating motor unit numbers. *J Neurol Neurosurg Psychiatry,* 39**,** 249-57.

BROWN, W. F., STRONG, M. J. & SNOW, R. 1988. Methods for estimating numbers of motor units in biceps-brachialis muscles and losses of motor units with aging. *Muscle & Nerve,* 11**,** 423-432.

BROWNE, S. E., YANG, L., DIMAURO, J.-P., FULLER, S. W., LICATA, S. C. & BEAL, M. F. 2006. Bioenergetic abnormalities in discrete cerebral motor pathways presage spinal cord pathology in the G93A SOD1 mouse model of ALS. *Neurobiology of Disease,* 22**,** 599-610.

BRUCE, K. M., NARAYAN, K., KONG, H. C., LARMOUR, I., LOPES, E. C., TURNER, B. J., BERTRAM, J. F. & CHEEMA, S. S. 2004. Chemotherapy Delays Progression of Motor Neuron Disease in the SOD1 G93A Transgenic Mouse. *Chemotherapy,* 50**,** 138-142.

BRUIJN, L. I. 1997. ALS-linked SOD1 mutant G85R mediates damage to astrocytes and promotes rapidly progressive disease with SOD1-containing inclusions. *Neuron,* 18**,** 327-338.

BRUIJN, L. I., BECHER, M. W., LEE, M. K., ANDERSON, K. L., JENKINS, N. A., COPELAND, N. G., SISODIA, S. S., ROTHSTEIN, J. D., BORCHELT, D. R., PRICE, D. L. & CLEVELAND, D. W. 1997. ALS-Linked SOD1 Mutant G85R Mediates Damage to Astrocytes and Promotes Rapidly Progressive Disease with SOD1-Containing Inclusions. *Neuron,* 18**,** 327-338.

BRUIJN, L. I., HOUSEWEART, M. K., KATO, S., ANDERSON, K. L., ANDERSON, S. D., OHAMA, E., REAUME, A. G., SCOTT, R. W. & CLEVELAND, D. W. 1998. Aggregation and motor neuron toxicity of an ALS-linked SOD1 mutant independent from wild-type SOD1. *Science (New York, N.Y.),* 281**,** 1851-1854.

BRUNMAIR, B., STANIEK, K., GRAS, F., SCHARF, N., ALTHAYM, A., CLARA, R., RODEN, M., GNAIGER, E., NOHL, H., WALDHÄUSL, W. & FÜRNSINN, C. 2004. Thiazolidinediones, Like Metformin, Inhibit Respiratory Complex I. *Diabetes,* 53**,** 1052-1059.

CALVO, A., MORENO-IGOA, M., MANCUSO, R., MANZANO, R., OLIVAN, S., MUNOZ, M., PENAS, C., ZARAGOZA, P., NAVARRO, X. & OSTA, R. 2011. Lack of a synergistic effect of a non-viral ALS gene therapy based on BDNF and a TTC fusion molecule. *Orphanet Journal of Rare Diseases,* 6**,** 10.

CANTÓ, C. & AUWERX, J. 2009. PGC-1[alpha], SIRT1 and AMPK, an energy sensing network that controls energy expenditure. *Current Opinion in Lipidology,* 20**,** 98-105 10.1097/MOL.0b013e328328d0a4.

CANTON, T., BÖHME, G. A., BOIREAU, A., BORDIER, F., MIGNANI, S., JIMONET, P., JAHN, G., ALAVIJEH, M., STYGALL, J., ROBERTS, S., BREALEY, C., VUILHORGNE, M., DEBONO, M.-W., LE GUERN, S., LAVILLE, M., BRIET, D., ROUX, M., STUTZMANN, J.-M. & PRATT, J. 2001. RPR 119990, a Novel α-Amino-3-hydroxy-5-methyl-4-isoxazolepropionic Acid Antagonist: Synthesis, Pharmacological Properties, and Activity in an Animal Model of Amyotrophic Lateral Sclerosis. *Journal of Pharmacology and Experimental Therapeutics,* 299**,** 314-322.

CEREDA, C., BAIOCCHI, C., BONGIOANNI, P., COVA, E., GUARESCHI, S., METELLI, M. R., ROSSI, B., SBALSI, I., CUCCIA, M. C. & CERONI, M. 2008. TNF and sTNFR1/2 plasma levels in ALS patients. *Journal of neuroimmunology,* 194**,** 123-131.

CHANG-HONG, R., WADA, M., KOYAMA, S., KIMURA, H., ARAWAKA, S., KAWANAMI, T., KURITA, K., KADOYA, T., AOKI, M., ITOYAMA, Y. & KATO, T. 2005. Neuroprotective effect of oxidized galectin-1 in a transgenic mouse model of amyotrophic lateral sclerosis. *Experimental Neurology,* 194**,** 203-211.

CHARCOT, J. M. & JOFFORY, A. 1869. Deux cas d'atrophie musculaire progressive avec lesions de la substance grise et des faisceaux antero-lateraux de la moelle epiniere. *Arch. Physiol. Neurol. Pathol.***,** 744-754.

CHEN, Q. & HADDAD, G. G. 2004. Role of trehalose phosphate synthase and trehalose during hypoxia: from flies to mammals. *Journal of Experimental Biology,* 207**,** 3125-3129.

CHEN, R. & ENDE, N. 2000. The potential for the use of mononuclear cells from human umbilical cord blood in the treatment of amyotrophic lateral sclerosis in SOD1 mice. *J Med,* 31**,** 21-30.

CHEN, X.-J., LEVEDAKOU, E. N., MILLEN, K. J., WOLLMANN, R. L., SOLIVEN, B. & POPKO, B. 2007. Proprioceptive Sensory Neuropathy in Mice with a Mutation in the Cytoplasmic Dynein Heavy Chain 1 Gene. *The Journal of Neuroscience,* 27**,** 14515-14524.

CHEN, Y.-Z., BENNETT, C. L., HUYNH, H. M., BLAIR, I. P., PULS, I., IROBI, J., DIERICK, I., ABEL, A., KENNERSON, M. L., RABIN, B. A., NICHOLSON, G. A., AUER-GRUMBACH, M., WAGNER, K., DE JONGHE, P., GRIFFIN, J. W., FISCHBECK, K. H., TIMMERMAN, V., CORNBLATH, D. R. & CHANCE, P. F. 2004a. DNA/RNA Helicase Gene Mutations in a Form of Juvenile Amyotrophic Lateral Sclerosis (ALS4). *The American Journal of Human Genetics,* 74**,** 1128-1135.

CHEN, Y., BENNETT, C., HUYNH, H., BLAIR, I., PULS, I., IROBI, J., DIERICK, I., ABEL, A., KENNERSON, M. & RABIN, B. 2004b. DNA/RNA helicase gene mutations in a form of juvenile amyotrophic lateral sclerosis (ALS4). *Am J Hum Genet,* 74**,** 1128 - 1135.

CHEN, Y., YANG, M., DENG, J., CHEN, X., YE, Y., ZHU, L., LIU, J., YE, H., SHEN, Y., LI, Y., RAO, E., FUSHIMI, K., ZHOU, X., BIGIO, E., MESULAM, M., XU, Q. & WU, J. 2011. Expression of human FUS protein in <i>Drosophila</i> leads to progressive neurodegeneration. *Protein & Cell,* 2**,** 477-486.

CHEN, Y., ZHOU, K., WANG, R., LIU, Y., KWAK, Y.-D., MA, T., THOMPSON, R. C., ZHAO, Y., SMITH, L., GASPARINI, L., LUO, Z., XU, H. & LIAO, F.-F. 2009. Antidiabetic drug metformin (GlucophageR) increases biogenesis of Alzheimer's amyloid peptides via up-regulating BACE1 transcription. *Proceedings of the National Academy of Sciences,* 106**,** 3907-3912.

CHENGYUN, Z., INGER, N., BENGT, F. & JAN-INGE, H. 2004. Vascular endothelial growth factor prolongs survival in a transgenic mouse model of ALS. *Annals of Neurology,* 56**,** 564-567.

CHERONI, C., MARINO, M., TORTAROLO, M., VEGLIANESE, P., DE BIASI, S., FONTANA, E., ZUCCARELLO, L. V., MAYNARD, C. J., DANTUMA, N. P. & BENDOTTI, C. 2009. Functional alterations of the ubiquitin-proteasome system in motor neurons of a mouse model of familial amyotrophic lateral sclerosis†. *Human Molecular Genetics,* 18**,** 82-96.

CHEUNG, Z. H. & IP, N. Y. 2011. Autophagy deregulation in neurodegenerative diseases – recent advances and future perspectives. *Journal of Neurochemistry,* 118**,** 317-325.

CHIAN, R.-J., LI, J., AY, I., CELIA, S. A., KASHI, B. B., TAMRAZIAN, E., MATTHEWS, J. C., BRONSON, R. T., ROSSOMANDO, A., PEPINSKY, R. B., FISHMAN, P. S., BROWN JR, R. H. & FRANCIS, J. W. 2009. IGF-1:Tetanus toxin fragment C fusion protein improves delivery of IGF-1 to spinal cord but fails to prolong survival of ALS mice. *Brain Research,* 1287**,** 1-19.

CHIBA, T., HASHIMOTO, Y., TAJIMA, H., YAMADA, M., KATO, R., NIIKURA, T., TERASHITA, K., SCHULMAN, H., AISO, S., KITA, Y., MATSUOKA, M. & NISHIMOTO, I. 2004. Neuroprotective effect of activity-dependent neurotrophic factor against toxicity from familial amyotrophic lateral sclerosis-linked mutant SOD1 in vitro and in vivo. *Journal of Neuroscience Research,* 78**,** 542-552.

CHIBA, T., YAMADA, M., SASABE, J., TERASHITA, K., AISO, S., MATSUOKA, M. & NISHIMOTO, I. 2006. Colivelin prolongs survival of an ALS model mouse. *Biochemical and Biophysical Research Communications,* 343**,** 793-798.

CHIU, A. Y., ZHAI, P., DAL CANTO, M. C., PETERS, T. M., KWON, Y. W., PRATTIS, S. M. & GURNEY, M. E. 1995. Age-Dependent Penetrance of Disease in a Transgenic Mouse Model of Familial Amyotrophic Lateral Sclerosis. *Molecular and Cellular Neuroscience,* 6**,** 349-362.

CHIU, I. M., CHEN, A., ZHENG, Y., KOSARAS, B., TSIFTSOGLOU, S. A., VARTANIAN, T. K., BROWN, R. H. & CARROLL, M. C. 2008. T lymphocytes potentiate endogenous neuroprotective inflammation in a mouse model of ALS. *Proceedings of the National Academy of Sciences,* 105**,** 17913-17918.

CHO, D.-H., NAKAMURA, T. & LIPTON, S. 2010. Mitochondrial dynamics in cell death and neurodegeneration. *Cellular and Molecular Life Sciences,* 67**,** 3435-3447.

CHO, Y. & KIEFFER, T. 2011. New aspects of an old drug: metformin as a glucagon-like peptide 1 (GLP-1) enhancer and sensitiser. *Diabetologia,* 54**,** 219-222.

CHOI, C.-I., LEE, Y.-D., GWAG, B. J., CHO, S. I., KIM, S.-S. & SUH-KIM, H. 2008. Effects of estrogen on lifespan and motor functions in female hSOD1 G93A transgenic mice. *Journal of the neurological sciences,* 268**,** 40-47.

CHOI, J.-K., KÜSTERMANN, E., DEDEOGLU, A. & JENKINS, B. G. 2009. Magnetic resonance spectroscopy of regional brain metabolite markers in FALS mice and the effects of dietary creatine supplementation. *European Journal of Neuroscience,* 30**,** 2143-2150.

CHOW, C. Y., LANDERS, J. E., BERGREN, S. K., SAPP, P. C., GRANT, A. E., JONES, J. M., EVERETT, L., LENK, G. M., MCKENNA-YASEK, D. M., WEISMAN, L. S., FIGLEWICZ, D., BROWN, R. H. & MEISLER, M. H. 2009. Deleterious variants of FIG4, a phosphoinositide phosphatase, in patients with ALS. *Am J Hum Genet,* 84**,** 85-8.

CHRITIN, M., SAVASTA, M. & BESSON, G. 2006. Benefit of tianeptine and morphine in a transgenic model of familial amyotrophic lateral sclerosis. *Amyotrophic Lateral Sclerosis,* 7**,** 32-37.

CLEMENT, A. M., NGUYEN, M. D., ROBERTS, E. A., GARCIA, M. L., BOILLEE, S., RULE, M., MCMAHON, A. P., DOUCETTE, W., SIWEK, D., FERRANTE, R. J., BROWN, R. H., JR., JULIEN, J. P., GOLDSTEIN, L. S. & CLEVELAND, D. W. 2003. Wild-type nonneuronal cells extend survival of SOD1 mutant motor neurons in ALS mice. *Science (New York, N.Y.),* 302**,** 113-117.

CLINICALTRIALS.GOV. 2010a. *Safety, Tolerability, and Activity Study of ISIS SOD1Rx to Treat Familial Amyotrophic Lateral Sclerosis (ALS) Caused by SOD1 Gene Mutations (SOD-1) (No. NCT01041222)* [Online]. Available: http://www.clinicaltrials.gov/ct2/show/NCT01041222?term=NCT01041222&rank=1 [Accessed].

CLINICALTRIALS.GOV. 2010b. *Safety and Efficacy of TRO19622 as add-on Therapy to Riluzole Versus Placebo in Treatment of Patients Suffering From Amyotrophic Lateral Sclerosis (ALS) (MITOTARGET) (No. NCT00868166)* [Online]. Available: http://www.clinicaltrials.gov/ct2/show/NCT00868166?term=NCT00868166&rank=1 [Accessed].

CLINICALTRIALS.GOV. 2011a. *Clinical Trial Ceftriaxone in Subjects With ALS (no. NCT00349622)* [Online]. ClinicalTrials.gov. Available: http://www.clinicaltrials.gov/ct2/show/NCT00349622?term=ceftriaxone+and+als&rank=1 [Accessed].

CLINICALTRIALS.GOV. 2011b. *Phase II/III Randomized, Placebo-controlled Trial of Arimoclomol in SOD1 Positive Familial Amyotrophic Lateral Sclerosis (no. NCT00706147)* [Online]. Available: http://www.clinicaltrials.gov/ct2/show/NCT00706147?term=nct00706147&rank=1 [Accessed].

CLINICALTRIALS.GOV. 2011c. *A Safety and Tolerability Study of Intracerebroventricular Administration of sNN0029 to Patients With Amyotrophic Lateral Sclerosis (No. NCT00800501)* [Online]. Available: http://www.clinicaltrials.gov/ct2/show/NCT00800501?term=NCT00800501&rank=1 [Accessed].

CLINICALTRIALS.GOV. 2011d. *A Study of CK-2017357 in Patients With Amyotrophic Lateral Sclerosis (ALS) (No. NCT01089010)* [Online]. Available: http://www.clinicaltrials.gov/ct2/show/NCT01089010?term=NCT01089010&rank=1 [Accessed].

CORTI, S., LOCATELLI, F., DONADONI, C., GUGLIERI, M., PAPADIMITRIOU, D., STRAZZER, S., DEL BO, R. & COMI, G. P. 2004. Wild-type bone marrow cells ameliorate the phenotype of SOD1-G93A ALS mice and contribute to CNS, heart and skeletal muscle tissues. *Brain,* 127**,** 2518-2532.

CORTI, S., LOCATELLI, F., PAPADIMITRIOU, D., DEL BO, R., NIZZARDO, M., NARDINI, M., DONADONI, C., SALANI, S., FORTUNATO, F., STRAZZER, S., BRESOLIN, N. & COMI, G. P. 2007. Neural stem cells LewisX + CXCR4 + modify disease progression in an amyotrophic lateral sclerosis model. *Brain,* 130**,** 1289-1305.

COVA, E., BONGIOANNI, P., CEREDA, C., METELLI, M. R., SALVANESCHI, L., BERNUZZI, S., GUARESCHI, S., ROSSI, B. & CERONI, M. 2010. Time course of oxidant markers and antioxidant defenses in subgroups of amyotrophic lateral sclerosis patients. *Neurochemistry International,* 56**,** 687-693.

COX, L. E., FERRAIUOLO, L., GOODALL, E. F., HEATH, P. R., HIGGINBOTTOM, A., MORTIBOYS, H., HOLLINGER, H. C., HARTLEY, J. A., BROCKINGTON, A., BURNESS, C. E., MORRISON, K. E., WHARTON, S. B., GRIERSON, A. J., INCE, P. G., KIRBY, J. & SHAW, P. J. 2010. Mutations in <italic>CHMP2B</italic> in Lower Motor Neuron Predominant Amyotrophic Lateral Sclerosis (ALS). *PLoS ONE,* 5**,** e9872.

COZZOLINO, M., FERRI, A. & CARRI, M. 2008a. Amyotrophic lateral sclerosis: from current developments in the laboratory to clinical implications. *Antioxid Redox Signal,* 10**,** 405 - 443.

COZZOLINO, M., FERRI, A. & CARRI, M. T. 2008b. Amyotrophic lateral sclerosis: from current developments in the laboratory to clinical implications. *Antioxidants & redox signaling,* 10**,** 405-443.

COZZOLINO, M., PESARESI, M. G., AMORI, I., CROSIO, C., FERRI, A., NENCINI, M. & CARRÌ, M. T. 2009. Oligomerization of Mutant SOD1 in Mitochondria of Motoneuronal Cells Drives Mitochondrial Damage and Cell Toxicity. *Antioxidants & Redox Signaling,* 11**,** 1547-1558.

CRABTREE, B., THIYAGARAJAN, N., PRIOR, S. H., WILSON, P., IYER, S., FERNS, T., SHAPIRO, R., BREW, K., SUBRAMANIAN, V. & ACHARYA, K. R. 2007. Characterization of Human Angiogenin Variants Implicated in Amyotrophic Lateral Sclerosis†. *Biochemistry,* 46**,** 11810-11818.

CROCHEMORE, C., PEÑA-ALTAMIRA, E., VIRGILI, M., MONTI, B. & CONTESTABILE, A. 2005. Disease-related regressive alterations of forebrain cholinergic system in SOD1 mutant transgenic mice. *Neurochemistry International,* 46**,** 357-368.

CRONIN, S., HARDIMAN, O. & TRAYNOR, B. 2007. Ethnic variation in the incidence of ALS: A systematic review. *Neurology,* 68**,** 1002 - 1007.

CROW, J. P., CALINGASAN, N. Y., CHEN, J., HILL, J. L. & BEAL, M. F. 2005. Manganese porphyrin given at symptom onset markedly extends survival of ALS mice. *Annals of Neurology,* 58**,** 258-265.

CRUGNOLA, V., LAMPERTI, C., LUCCHINI, V., RONCHI, D., PEVERELLI, L., PRELLE, A., SCIACCO, M., BORDONI, A., FASSONE, E., FORTUNATO, F., CORTI, S., SILANI, V., BRESOLIN, N., DI MAURO, S., COMI, G. P. & MOGGIO, M. 2010. Mitochondrial Respiratory Chain Dysfunction in Muscle From Patients With Amyotrophic Lateral Sclerosis. *Arch Neurol,* 67**,** 849-854.

CUDKOWICZ, M. E., SHEFNER, J. M., SIMPSON, E., GRASSO, D., YU, H., ZHANG, H., SHUI, A., SCHOENFELD, D., BROWN, R. H., WIELAND, S. & BARBER, J. R. 2008. Arimoclomol at dosages up to 300 mg/day is well tolerated and safe in amyotrophic lateral sclerosis. *Muscle & Nerve,* 38**,** 837-844.

CULOTTA, V. C., JOH, H. D., LIN, S. J., SLEKAR, K. H. & STRAIN, J. 1995. A physiological role for Saccharomyces cerevisiae copper/zinc superoxide dismutase in copper buffering. *J Biol Chem,* 270**,** 29991-7.

DA CRUZ, S. & CLEVELAND, D. W. 2011. Understanding the role of TDP-43 and FUS/TLS in ALS and beyond. *Curr Opin Neurobiol*.

DADON-NACHUM, M., MELAMED, E. & OFFEN, D. 2011. The "Dying-Back" Phenomenon of Motor Neurons in ALS. *Journal of Molecular Neuroscience,* 43**,** 470-477.

DAL CANTO, M. C. & GURNEY, M. E. 1995. Neuropathological changes in two lines of mice carrying a transgene for mutant human Cu,Zn SOD, and in mice overexpressing wild type human SOD: a model of familial amyotrophic lateral sclerosis (FALS). *Brain Research,* 676**,** 25-40.

DAMIANO, M., STARKOV, A. A., PETRI, S., KIPIANI, K., KIAEI, M., MATTIAZZI, M., FLINT BEAL, M. & MANFREDI, G. 2006. Neural mitochondrial Ca2+ capacity impairment precedes the onset of motor symptoms in G93A Cu/Zn-superoxide dismutase mutant mice. *Journal of Neurochemistry,* 96**,** 1349-1361.

DANDONA, P., ALJADA, A., GHANIM, H., MOHANTY, P., TRIPATHY, C., HOFMEYER, D. & CHAUDHURI, A. 2004. Increased Plasma Concentration of Macrophage Migration Inhibitory Factor (MIF) and MIF mRNA in Mononuclear Cells in the Obese and the Suppressive Action of Metformin. *J Clin Endocrinol Metab,* 89**,** 5043-5047.

DANZEISEN, R., SCHWALENSTOECKER, B., GILLARDON, F., BUERGER, E., KRZYKALLA, V., KLINDER, K., SCHILD, L., HENGERER, B., LUDOLPH, A. C., DORNER-CIOSSEK, C. & KUSSMAUL, L. 2006. Targeted Antioxidative and Neuroprotective Properties of the Dopamine Agonist Pramipexole and Its Nondopaminergic Enantiomer SND919CL2x [(+)2-Amino-4,5,6,7-tetrahydro-6-lpropylamino-benzathiazole Dihydrochloride]. *Journal of Pharmacology and Experimental Therapeutics,* 316**,** 189-199.

DAUBE, J. R. 1995. Estimating the number of motor units in a muscle. *J Clin Neurophysiol,* 12**,** 585-94.

DAVIES, J. E., SARKAR, S. & RUBINSZTEIN, D. C. 2006. Trehalose reduces aggregate formation and delays pathology in a transgenic mouse model of oculopharyngeal muscular dystrophy. *Hum. Mol. Genet.,* 15**,** 23-31.

DAY, W. A., KOISHI, K., NUKUDA, H. & MCLENNAN, I. S. 2005. Transforming growth factor-beta 2 causes an acute improvement in the motor performance of transgenic ALS mice. *Neurobiol Dis,* 19**,** 323-30.

DE CARVALHO, M. & SWASH, M. 2011. Amyotrophic lateral sclerosis: an update. *Curr Opin Neurol,* 24**,** 497-503.

DE VOS, K. J., CHAPMAN, A. L., TENNANT, M. E., MANSER, C., TUDOR, E. L., LAU, K.-F., BROWNLEES, J., ACKERLEY, S., SHAW, P. J., MCLOUGHLIN, D. M., SHAW, C. E., LEIGH, P. N., MILLER, C. C. J. & GRIERSON, A. J. 2007. Familial amyotrophic lateral sclerosis-linked SOD1 mutants perturb fast axonal transport to reduce axonal mitochondria content. *Human Molecular Genetics,* 16**,** 2720-2728.

DEJESUS-HERNANDEZ, M., MACKENZIE, IAN R., BOEVE, BRADLEY F., BOXER, ADAM L., BAKER, M., RUTHERFORD, NICOLA J., NICHOLSON, ALEXANDRA M., FINCH, NICOLE A., FLYNN, H., ADAMSON, J., KOURI, N., WOJTAS, A., SENGDY, P., HSIUNG, G.-YUEK R., KARYDAS, A., SEELEY, WILLIAM W., JOSEPHS, KEITH A., COPPOLA, G., GESCHWIND, DANIEL H., WSZOLEK, ZBIGNIEW K., FELDMAN, H., KNOPMAN, DAVID S., PETERSEN, RONALD C., MILLER, BRUCE L., DICKSON, DENNIS W., BOYLAN, KEVIN B., GRAFF-RADFORD, NEILL R. & RADEMAKERS, R. 2011. Expanded GGGGCC Hexanucleotide Repeat in Noncoding Region of C9ORF72 Causes Chromosome 9p-Linked FTD and ALS. *Neuron,* 72**,** 245-256.

DENG, H.-X., CHEN, W., HONG, S.-T., BOYCOTT, K. M., GORRIE, G. H., SIDDIQUE, N., YANG, Y., FECTO, F., SHI, Y., ZHAI, H., JIANG, H., HIRANO, M., RAMPERSAUD, E., JANSEN, G. H., DONKERVOORT, S., BIGIO, E. H., BROOKS, B. R., AJROUD, K., SUFIT, R. L., HAINES, J. L., MUGNAINI, E., PERICAK-VANCE, M. A. & SIDDIQUE, T. 2011. Mutations in UBQLN2 cause dominant X-linked juvenile and adult-onset ALS and ALS/dementia. *Nature,* 477**,** 211-215.

DENG, H.-X., ZHAI, H., BIGIO, E. H., YAN, J., FECTO, F., AJROUD, K., MISHRA, M., AJROUD-DRISS, S., HELLER, S., SUFIT, R., SIDDIQUE, N., MUGNAINI, E. & SIDDIQUE, T. 2010. FUS-immunoreactive inclusions are a common feature in sporadic and non-SOD1 familial amyotrophic lateral sclerosis. *Annals of Neurology,* 67**,** 739-748.

DESALERMOS, A., MUHAMMED, M., GLAVIS-BLOOM, J. & MYLONAKIS, E. 2011. Using C. elegans for antimicrobial drug discovery. *Expert Opin Drug Discov,* 6**,** 645-652.

DESPORT, J., PREUX, P., MAGY, L., BOIRIE, Y., VALLAT, J., BEAUFRERE, B. & COURATIER, P. 2001. Factors correlated with hypermetabolism in patients with amyotrophic lateral sclerosis. *Am J Clin Nutr,* 74**,** 328 - 334.

DESPORT, J. C., TORNY, F., LACOSTE, M., PREUX, P. M. & COURATIER, P. 2005. Hypermetabolism in ALS: Correlations with Clinical and Paraclinical Parameters. *Neurodegenerative Diseases,* 2**,** 202-207.

DEWIL, M., DELA CRUZ, V. F., VAN DEN BOSCH, L. & ROBBERECHT, W. 2007. Inhibition of p38 mitogen activated protein kinase activation and mutant SOD1G93A-induced motor neuron death. *Neurobiology of Disease,* 26**,** 332-341.

DIAZ, F. & MORAES, C. T. 2008. Mitochondrial biogenesis and turnover. *Cell calcium,* 44**,** 24-35.

DOBLE, A. 1996. The pharmacology and mechanism of action of riluzole. *Neurology,* 47**,** S233-41.

DOBROWOLNY, G., AUCELLO, M., RIZZUTO, E., BECCAFICO, S., MAMMUCARI, C., BONCONPAGNI, S., BELIA, S., WANNENES, F., NICOLETTI, C., DEL PRETE, Z., ROSENTHAL, N., MOLINARO, M., PROTASI, F., FANÒ, G., SANDRI, M. & MUSARÒ, A. 2008. Skeletal Muscle Is a Primary Target of SOD1G93A-Mediated Toxicity. *Cell Metabolism,* 8**,** 425-436.

DODGE, J. C., TRELEAVEN, C. M., FIDLER, J. A., HESTER, M., HAIDET, A., HANDY, C., RAO, M., EAGLE, A., MATTHEWS, J. C., TAKSIR, T. V., CHENG, S. H., SHIHABUDDIN, L. S. & KASPAR, B. K. 2010. AAV4-mediated Expression of IGF-1 and VEGF Within Cellular Components of the Ventricular System Improves Survival Outcome in Familial ALS Mice. *Mol Ther,* 18**,** 2075-2084.

DOHERTY, T. J. & BROWN, W. F. 1993. The estimated numbers and relative sizes of thenar motor units as selected by multiple point stimulation in young and older adults. *Muscle Nerve,* 16**,** 355-66.

DRACHMAN, D. B., FRANK, K., DYKES-HOBERG, M., TEISMANN, P., ALMER, G., PRZEDBORSKI, S. & ROTHSTEIN, J. D. 2002. Cyclooxygenase 2 inhibition protects motor neurons and prolongs survival in a transgenic mouse model of ALS. *Annals of Neurology,* 52**,** 771-778.

DRAGATSIS, I., GOLDOWITZ, D., DEL MAR, N., DENG, Y. P., MEADE, C. A., LIU, L., SUN, Z., DIETRICH, P., YUE, J. & REINER, A. 2009. CAG repeat lengths ≥ 335 attenuate the phenotype in the R6/2 Huntington's disease transgenic mouse. *Neurobiology of Disease,* 33**,** 315-330.

DREIBELBIS, J. E., BROWN, R. H., PASTUSZAK, K. A., SMITH, E. R., KAPLAN, P. L. & CUDKOWICZ, M. E. 2002. Disease course unaltered by a single intracisternal injection of BMP-7 in ALS mice. *Muscle & Nerve,* 25**,** 122-123.

DUFFY, L. M., CHAPMAN, A. L., SHAW, P. J. & GRIERSON, A. J. 2011. Review: The role of mitochondria in the pathogenesis of amyotrophic lateral sclerosis. *Neuropathology and Applied Neurobiology,* 37**,** 336-352.

DUGAN, L. L., TURETSKY, D. M., DU, C., LOBNER, D., WHEELER, M., ALMLI, C. R., SHEN, C. K.-F., LUH, T.-Y., CHOI, D. W. & LIN, T.-S. 1997. Carboxyfullerenes as neuroprotective agents. *Proceedings of the National Academy of Sciences,* 94**,** 9434-9439.

DUPUIS, L., CORCIA, P., FERGANI, A., GONZALEZ DE AGUILAR, J.-L., BONNEFONT-ROUSSELOT, D., BITTAR, R., SEILHEAN, D., HAUW, J.-J., LACOMBLEZ, L., LOEFFLER, J.-P. & MEININGER, V. 2008. Dyslipidemia is a protective factor in amyotrophic lateral sclerosis. *Neurology,* 70**,** 1004-1009.

DUPUIS, L., DI SCALA, F., RENE, F., DE TAPIA, M., OUDART, H., PRADAT, P.-F., MEININGER, V. & LOEFFLER, J.-P. 2003. Up-regulation of mitochondrial uncoupling protein 3 reveals an early muscular metabolic defect in amyotrophic lateral sclerosis. *The FASEB Journal*.

DUPUIS, L., GONZALEZ DE AGUILAR, J. L., ECHANIZ-LAGUNA, A., ESCHBACH, J., RENE, F., OUDART, H., HALTER, B., HUZE, C., SCHAEFFER, L., BOUILLAUD, F. & LOEFFLER, J. P. 2009. Muscle mitochondrial uncoupling dismantles neuromuscular junction and triggers distal degeneration of motor neurons. *PLoS ONE,* 4**,** e5390.

DUPUIS, L., OUDART, H., RENÃ©, F. D. R., DE AGUILAR, J.-L. G. & LOEFFLER, J.-P. 2004. Evidence for defective energy homeostasis in amyotrophic lateral sclerosis: Benefit of a high-energy diet in a transgenic mouse model. *Proceedings of the National Academy of Sciences of the United States of America,* 101**,** 11159-11164.

DUPUIS, L., PRADAT, P.-F., LUDOLPH, A. C. & LOEFFLER, J.-P. 2011. Energy metabolism in amyotrophic lateral sclerosis. *The Lancet Neurology,* 10**,** 75-82.

ECHANIZ-LAGUNA, A., ZOLL, J., PONSOT, E., N'GUESSAN, B., TRANCHANT, C., LOEFFLER, J.-P. & LAMPERT, E. 2006. Muscular mitochondrial function in amyotrophic lateral sclerosis is progressively altered as the disease develops: A temporal study in man. *Experimental Neurology,* 198**,** 25-30.

EDOR, K., JEFFREY, N. A., YU, H., DAVID, M. T., SANDRA, M., DENISE, A. F. & HEATHER, D. D. 2008. Proteasomes remain intact, but show early focal alteration in their composition in a mouse model of amyotrophic lateral sclerosis. *Journal of Neurochemistry,* 105**,** 2353-2366.

EL-KADI, A. M., BROS-FACER, V., DENG, W., PHILPOTT, A., STODDART, E., BANKS, G., JACKSON, G. S., FISHER, E. M. C., DUCHEN, M. R., GREENSMITH, L., MOORE, A. L. & HAFEZPARAST, M. 2010. The Legs at odd angles (Loa) Mutation in Cytoplasmic Dynein Ameliorates Mitochondrial Function in SOD1G93A Mouse Model for Motor Neuron Disease. *Journal of Biological Chemistry,* 285**,** 18627-18639.

ELDEN, A. C., KIM, H.-J., HART, M. P., CHEN-PLOTKIN, A. S., JOHNSON, B. S., FANG, X., ARMAKOLA, M., GESER, F., GREENE, R., LU, M. M., PADMANABHAN, A., CLAY-FALCONE, D., MCCLUSKEY, L., ELMAN, L., JUHR, D., GRUBER, P. J., RUB, U., AUBURGER, G., TROJANOWSKI, J. Q., LEE, V. M. Y., VAN DEERLIN, V. M., BONINI, N. M. & GITLER, A. D. 2010. Ataxin-2 intermediate-length polyglutamine expansions are associated with increased risk for ALS. *Nature,* 466**,** 1069-1075.

ENDE, N., WEINSTEIN, F., CHEN, R. & ENDE, M. 2000. Human umbilical cord blood effect on sod mice (amyotrophic lateral sclerosis). *Life Sciences,* 67**,** 53-59.

ENGELHARDT, J. I., TAJTI, J. & APPEL, S. H. 1993. Lymphocytic Infiltrates in the Spinal Cord in Amyotrophic Lateral Sclerosis. *Arch Neurol,* 50**,** 30-36.

ERMILOVA, I. P., ERMILOV, V. B., LEVY, M., HO, E., PEREIRA, C. & BECKMAN, J. S. 2005. Protection by dietary zinc in ALS mutant G93A SOD transgenic mice. *Neuroscience Letters,* 379**,** 42-46.

ESPOSITO, E., CAPASSO, M., DI TOMASSO, N., CORONA, C., PELLEGRINI, F., UNCINI, A., VITAGLIONE, P., FOGLIANO, V., PIANTELLI, M. & SENSI, S. L. 2007. Antioxidant strategies based on tomato-enriched food or pyruvate do not affect disease onset and survival in an animal model of amyotrophic lateral sclerosis. *Brain Research,* 1168**,** 90-96.

ESPOSITO, E., ROSSI, C., AMODIO, R., DI CASTELNUOVO, A., BENDOTTI, C., ROTONDO, T., ALGERI, S. & ROTILIO, D. 2000. Lyophilized red wine administration prolongs survival in an animal model of amyotrophic lateral sclerosis. *Ann Neurol,* 48**,** 686-7.

EZZI, S. A., LARIVIÈRE, R., URUSHITANI, M. & JULIEN, J.-P. 2010. Neuronal over-expression of chromogranin A accelerates disease onset in a mouse model of ALS. *Journal of Neurochemistry,* 115**,** 1102-1111.

FACCHINETTI, F., SASAKI, M., CUTTING, F. B., MACDONALD, J. E., REIF, D., BEAL, M. F., HUANG, P. L., DAWSON, T. M., GURNEY, M. E., DAWSON, V. L. & ZHAI, P. 1999. Lack of involvement of neuronal nitric oxide synthase in the pathogenesis of a transgenic mouse model of familial amyotrophic lateral sclerosis. *Neuroscience,* 90**,** 1483-1492.

FANARA, P., BANERJEE, J., HUECK, R. V., HARPER, M. R., AWADA, M., TURNER, H., HUSTED, K. H., BRANDT, R. & HELLERSTEIN, M. K. 2007. Stabilization of Hyperdynamic Microtubules Is Neuroprotective in Amyotrophic Lateral Sclerosis. *Journal of Biological Chemistry,* 282**,** 23465-23472.

FEENEY, S. J., AUSTIN, L., BENNETT, T. M., KUREK, J. B., JEAN-FRANCOIS, M. J. B., MULDOON, C. & BYRNE, E. The effect of leukaemia inhibitory factor on SOD1 G93A murine amyotrophic lateral sclerosis. *Cytokine,* 23**,** 108-118.

FENG, H. L., LENG, Y., MA, C. H., ZHANG, J., REN, M. & CHUANG, D. M. 2008. Combined lithium and valproate treatment delays disease onset, reduces neurological deficits and prolongs survival in an amyotrophic lateral sclerosis mouse model. *Neuroscience,* 155**,** 567-572.

FERRANTE, R., KLEIN, A., DEDEOGLU, A. & FLINT BEAL, M. 2001. Therapeutic efficacy of EGb761 (<i>Gingko biloba</i> extract) in a transgenic mouse model of amyotrophic lateral sclerosis. *Journal of Molecular Neuroscience,* 17**,** 89-96.

FERRI, A., COZZOLINO, M., CROSIO, C., NENCINI, M., CASCIATI, A., GRALLA, E. B., ROTILIO, G., VALENTINE, J. S. & CARRÌ, M. T. 2006. Familial ALS-superoxide dismutases associate with

mitochondria and shift their redox potentials. *Proceedings of the National Academy of Sciences,* 103**,** 13860-13865.

FISCHER, L. R., CULVER, D. G., TENNANT, P., DAVIS, A. A., WANG, M., CASTELLANO-SANCHEZ, A., KHAN, J., POLAK, M. A. & GLASS, J. D. 2004. Amyotrophic lateral sclerosis is a distal axonopathy: evidence in mice and man. *Experimental Neurology,* 185**,** 232-240.

FLOOD, D. G., REAUME, A. G., GRUNER, J. A., HOFFMAN, E. K., HIRSCH, J. D., LIN, Y. G., DORFMAN, K. S. & SCOTT, R. W. 1999. Hindlimb motor neurons require Cu/Zn superoxide dismutase for maintenance of neuromuscular junctions. *Am J Pathol,* 155**,** 663-72.

FLOWERS, J. M., POWELL, J. F., LEIGH, P. N., ANDERSEN, P. & SHAW, C. E. 2001. Intron 7 retention and exon 9 skipping EAAT2 mRNA variants are not associated with amyotrophic lateral sclerosis. *Ann Neurol,* 49**,** 643-9.

FORNAI, F., LONGONE, P., CAFARO, L., KASTSIUCHENKA, O., FERRUCCI, M., MANCA, M. L., LAZZERI, G., SPALLONI, A., BELLIO, N., LENZI, P., MODUGNO, N., SICILIANO, G., ISIDORO, C., MURRI, L., RUGGIERI, S. & PAPARELLI, A. 2008. Lithium delays progression of amyotrophic lateral sclerosis. *Proceedings of the National Academy of Sciences,* 105**,** 2052-2057.

FUNALOT, B., DESPORT, J. C., STURTZ, F., CAMU, W. & COURATIER, P. 2009. High metabolic level in patients with familial amyotrophic lateral sclerosis. *Amyotroph Lateral Scler,* 10**,** 113-7.

GANEL, R., HO, T., MARAGAKIS, N. J., JACKSON, M., STEINER, J. P. & ROTHSTEIN, J. D. 2006. Selective up-regulation of the glial Na+-dependent glutamate transporter GLT1 by a neuroimmunophilin ligand results in neuroprotection. *Neurobiology of Disease,* 21**,** 556-567.

GANESALINGAM, J., AN, J., SHAW, C. E., SHAW, G., LACOMIS, D. & BOWSER, R. 2011. Combination of neurofilament heavy chain and complement C3 as CSF biomarkers for ALS. *Journal of Neurochemistry,* 117**,** 528-537.

GARBUZOVA-DAVIS, S., WILLING, A. E., MILLIKEN, M., SAPORTA, S., SOWERBY, B., CAHILL, D. W. & SANBERG, P. R. 2001. Intraspinal implantation of hNT neurons into SOD1 mice with apparent motor deficit. *Amyotrophic Lateral Sclerosis,* 2**,** 175-180.

GARBUZOVA-DAVIS, S., WILLING, A. E., MILLIKEN, M., SAPORTA, S., ZIGOVA, T., CAHILL, D. W. & SANBERG, P. R. 2002. Positive Effect of Transplantation of hNT Neurons (NTera 2/D1 Cell-Line) in a Model of Familial Amyotrophic Lateral Sclerosis. *Experimental Neurology,* 174**,** 169-180.

GARBUZOVA-DAVIS, S., WILLING, A. E., SAPORTA, S., JUSTEN, E. B., MISIUTA, I. E., DELLIS, J. & SANBERG, P. R. 2006. Multiple transplants of hNT cells into the spinal cord of SOD1 mouse model of familial amyotrophic lateral sclerosis. *Amyotroph Lateral Scler,* 7**,** 221-6.

GARBUZOVA-DAVIS, S., WILLING, A. E., ZIGOVA, T., SAPORTA, S., JUSTEN, E. B., LANE, J. C., HUDSON, J. E., CHEN, N., DAVIS, C. D. & SANBERG, P. R. 2003. Intravenous administration of human umbilical cord blood cells in a mouse model of amyotrophic lateral sclerosis: distribution, migration, and differentiation. *J Hematother Stem Cell Res,* 12**,** 255-70.

GAROFALO, O., KENNEDY, P. G., SWASH, M., MARTIN, J. E., LUTHERT, P., ANDERTON, B. H. & LEIGH, P. N. 1991. Ubiquitin and heat shock protein expression in amyotrophic lateral sclerosis. *Neuropathol Appl Neurobiol,* 17**,** 39-45.

GEISLER, S., HOLMSTROM, K. M., SKUJAT, D., FIESEL, F. C., ROTHFUSS, O. C., KAHLE, P. J. & SPRINGER, W. 2010. PINK1/Parkin-mediated mitophagy is dependent on VDAC1 and p62/SQSTM1. *Nat Cell Biol,* 12**,** 119-131.

GHADGE, G. D., SLUSHER, B. S., BODNER, A., CANTO, M. D., WOZNIAK, K., THOMAS, A. G., ROJAS, C., TSUKAMOTO, T., MAJER, P., MILLER, R. J., MONTI, A. L. & ROOS, R. P. 2003. Glutamate carboxypeptidase II inhibition protects motor neurons from death in familial amyotrophic lateral sclerosis models. *Proceedings of the National Academy of Sciences,* 100**,** 9554-9559.

GHODDOUSSI, F., GALLOWAY, M. P., JAMBEKAR, A., BAME, M., NEEDLEMAN, R. & BRUSILOW, W. S. A. 2010. Methionine sulfoximine, an inhibitor of glutamine synthetase, lowers brain

glutamine and glutamate in a mouse model of ALS. *Journal of the Neurological Sciences,* 290**,** 41-47.

GIFONDORWA, D. J., ROBINSON, M. B., HAYES, C. D., TAYLOR, A. R., PREVETTE, D. M., OPPENHEIM, R. W., CARESS, J. & MILLIGAN, C. E. 2007. Exogenous Delivery of Heat Shock Protein 70 Increases Lifespan in a Mouse Model of Amyotrophic Lateral Sclerosis. *The Journal of Neuroscience,* 27**,** 13173-13180.

GILL, A., KIDD, J., VIEIRA, F., THOMPSON, K. & PERRIN, S. 2009. No Benefit from Chronic Lithium Dosing in a Sibling-Matched, Gender Balanced, Investigator-Blinded Trial Using a Standard Mouse Model of Familial ALS. *PLoS ONE,* 4**,** e6489.

GITCHO, M. A., BALOH, R. H., CHAKRAVERTY, S., MAYO, K., NORTON, J. B., LEVITCH, D., HATANPAA, K. J., WHITE, C. L., BIGIO, E. H., CASELLI, R., BAKER, M., AL-LOZI, M. T., MORRIS, J. C., PESTRONK, A., RADEMAKERS, R., GOATE, A. M. & CAIRNS, N. J. 2008. TDP-43 A315T mutation in familial motor neuron disease. *Annals of Neurology,* 63**,** 535-538.

GLAS, M., POPP, B., ANGELE, B., KOEDEL, U., CHAHLI, C., SCHMALIX, W. A., ANNESER, J. M., PFISTER, H. W. & LORENZL, S. 2007. A role for the urokinase-type plasminogen activator system in amyotrophic lateral sclerosis. *Experimental Neurology,* 207**,** 350-356.

GOLDBERG, A. L. 2003. Protein degradation and protection against misfolded or damaged proteins. *Nature,* 426**,** 895-899.

GOLDSTEINS, G., KEKSA-GOLDSTEINE, V., AHTONIEMI, T., JARONEN, M., ARENS, E., ÅKERMAN, K., CHAN, P. H. & KOISTINAHO, J. 2008. Deleterious Role of Superoxide Dismutase in the Mitochondrial Intermembrane Space. *Journal of Biological Chemistry,* 283**,** 8446-8452.

GOMES, C., ESCREVENTE, C. & COSTA, J. 2010. Mutant superoxide dismutase 1 overexpression in NSC-34 cells: Effect of trehalose on aggregation, TDP-43 localization and levels of co-expressed glycoproteins. *Neuroscience letters,* 475**,** 145-149.

GORDON, P. H., CHENG, B., KATZ, I. B., PINTO, M., HAYS, A. P., MITSUMOTO, H. & ROWLAND, L. P. 2006. The natural history of primary lateral sclerosis. *Neurology,* 66**,** 647-653.

GOULD, T. W., BUSS, R. R., VINSANT, S., PREVETTE, D., SUN, W., KNUDSON, C. M., MILLIGAN, C. E. & OPPENHEIM, R. W. 2006. Complete Dissociation of Motor Neuron Death from Motor Dysfunction by Bax Deletion in a Mouse Model of ALS. *J. Neurosci.,* 26**,** 8774-8786.

GRAIER, W. F., FRIEDEN, M. & MALLI, R. 2007. Mitochondria and Ca(2+) signaling: old guests, new functions. *Pflugers Arch,* 455**,** 375-96.

GREENWAY, M., ANDERSEN, P., RUSS, C., ENNIS, S., CASHMAN, S., DONAGHY, C., PATTERSON, V., SWINGLER, R., KIERAN, D. & PREHN, J. 2006. ANG mutations segregate with familial and 'sporadic' amyotrophic lateral sclerosis. *Nat Genet,* 38**,** 411 - 413.

GRIGNASCHI, G., ZENNARO, E., TORTAROLO, M., CALVARESI, N. & BENDOTTI, C. 2007. Erythropoietin does not preserve motor neurons in a mouse model of familial ALS. *Amyotrophic Lateral Sclerosis,* 8**,** 31-35.

GROENEVELD, G., VAN MUISWINKEL, F., DE LEEUW VAN WEENEN, J., BLAUW, H., VELDINK, J., WOKKE, J., VAN DEN BERG, L. & BÄR, P. 2004a. CGP 3466B has no effect on disease course of (G93A) mSOD1 transgenic mice. *Amyotrophic Lateral Sclerosis,* 5**,** 220-225.

GROENEVELD, G. J., DE LEEUW VAN WEENEN, J., VAN MUISWINKEL, F. L., VELDMAN, H., VELDINK, J. H., WOKKE, J. H. J., BÄR, P. R. & VAN DEN BERG, L. H. 2003. Zinc amplifies mSOD1-mediated toxicity in a transgenic mouse model of amyotrophic lateral sclerosis. *Neuroscience Letters,* 352**,** 175-178.

GROENEVELD, G. J., VAN MUISWINKEL, F. L., STURKENBOOM, J. M., WOKKE, J. H. J., BÄR, P. R. & VAN DEN BERG, L. H. 2004b. Ovariectomy and 17[beta]-estradiol modulate disease progression of a mouse model of ALS. *Brain research,* 1021**,** 128-131.

GROS-LOUIS, F., SOUCY, G., LARIVIÈRE, R. & JULIEN, J.-P. 2010. Intracerebroventricular infusion of monoclonal antibody or its derived Fab fragment against misfolded forms of SOD1 mutant delays mortality in a mouse model of ALS. *Journal of Neurochemistry,* 113**,** 1188-1199.

GRUNFELD, J. F., BARHUM, Y., BLONDHEIM, N., RABEY, J.-M., MELAMED, E. & OFFEN, D. 2007. Erythropoietin delays disease onset in an amyotrophic lateral sclerosis model. *Experimental Neurology,* 204**,** 260-263.

GUO, F., MA, J., MCCAULEY, E., BANNERMAN, P. & PLEASURE, D. 2009. Early Postnatal Proteolipid Promoter-Expressing Progenitors Produce Multilineage Cells In Vivo. *The Journal of Neuroscience,* 29**,** 7256-7270.

GURNEY, M. E. 1994. Motor neuron degeneration in mice that express a human Cu,Zn superoxide dismutase mutation. *Science,* 264**,** 1772-1775.

GURNEY, M. E. 1997. The use of transgenic mouse models of amyotrophic lateral sclerosis in preclinical drug studies. *Journal of the Neurological Sciences,* 152**,** s67-s73.

GURNEY, M. E., CUTTING, F. B., ZHAI, P., DOBLE, A., TAYLOR, C. P., ANDRUS, P. K. & HALL, E. D. 1996. Benefit of vitamin E, riluzole, and gababapentin in a transgenic model of familial amyotrophic lateral sclerosis. *Annals of Neurology,* 39**,** 147-157.

GURNEY, M. E., FLECK, T. J., HIMES, C. S. & HALL, E. D. 1998. Riluzole preserves motor function in a transgenic model of familial amyotrophic lateral sclerosis. *Neurology,* 50**,** 62-6.

GURNEY, M. E., PU, H., CHIU, A. Y., DAL CANTO, M. C., POLCHOW, C. Y., ALEXANDER, D. D., CALIENDO, J., HENTATI, A., KWON, Y. W. & DENG, H. X. 1994. Motor neuron degeneration in mice that express a human Cu,Zn superoxide dismutase mutation. *Science (New York, N.Y.),* 264**,** 1772-1775.

HABISCH, H.-J., SCHWALENSTÖCKER, B., DANZEISEN, R., NEUHAUS, O., HARTUNG, H.-P. & LUDOLPH, A. 2007a. Limited effects of glatiramer acetate in the high-copy number hSOD1-G93A mouse model of ALS. *Experimental Neurology,* 206**,** 288-295.

HABISCH, H. J., JANOWSKI, M., BINDER, D., KUZMA-KOZAKIEWICZ, M., WIDMANN, A., HABICH, A., SCHWALENSTÖCKER, B., HERMANN, A., BRENNER, R., LUKOMSKA, B., DOMANSKA-JANIK, K., LUDOLPH, A. C. & STORCH, A. 2007b. Intrathecal application of neuroectodermally converted stem cells into a mouse model of ALS: limited intraparenchymal migration and survival narrows therapeutic effects. *Journal of Neural Transmission,* 114**,** 1395-1406.

HADANO, S., HAND, C., OSUGA, H., YANAGISAWA, Y., OTOMO, A., DEVON, R., MIYAMOTO, N., SHOWGUCHI-MIYATA, J., OKADA, Y. & SINGARAJA, R. 2001. A gene encoding a putative GTPase regulator is mutated in familial amyotrophic lateral sclerosis 2. *Nat Genet,* 29**,** 166 - 173.

HAENGGELI, C., JULIEN, J.-P., LEE MOSLEY, R., PEREZ, N., DHAR, A., GENDELMAN, H. E. & ROTHSTEIN, J. D. 2007. Therapeutic immunization with a glatiramer acetate derivative does not alter survival in G93A and G37R SOD1 mouse models of familial ALS. *Neurobiology of Disease,* 26**,** 146-152.

HAFEZPARAST, M., KLOCKE, R., RUHRBERG, C., MARQUARDT, A., AHMAD-ANNUAR, A., BOWEN, S., LALLI, G., WITHERDEN, A. S., HUMMERICH, H., NICHOLSON, S., MORGAN, P. J., OOZAGEER, R., PRIESTLEY, J. V., AVERILL, S., KING, V. R., BALL, S., PETERS, J., TODA, T., YAMAMOTO, A., HIRAOKA, Y., AUGUSTIN, M., KORTHAUS, D., WATTLER, S., WABNITZ, P., DICKNEITE, C., LAMPEL, S., BOEHME, F., PERAUS, G., POPP, A., RUDELIUS, M., SCHLEGEL, J., FUCHS, H., DE ANGELIS, M. H., SCHIAVO, G., SHIMA, D. T., RUSS, A. P., STUMM, G., MARTIN, J. E. & FISHER, E. M. C. 2003. Mutations in Dynein Link Motor Neuron Degeneration to Defects in Retrograde Transport. *Science,* 300**,** 808-812.

HALL, E., OOSTVEEN, J. & GURNEY, M. 1998. Relationship of microglial and astrocytic activation to disease onset and progression in a transgenic model of familial ALS. *Glia,* 23**,** 249 - 256.

HAMADEH, M. J., RODRIGUEZ, M. C., KACZOR, J. J. & TARNOPOLSKY, M. A. 2005. Caloric restriction transiently improves motor performance but hastens clinical onset of disease in the Cu/Zn-superoxide dismutase mutant G93A mouse. *Muscle & Nerve,* 31**,** 214-220.

HAMADEH, M. J. & TARNOPOLSKY, M. A. 2006. Transient caloric restriction in early adulthood hastens disease endpoint in male, but not female, Cu/Zn-SOD mutant G93A mice. *Muscle & Nerve,* 34**,** 709-719.

HAMBY, M. & SOFRONIEW, M. 2010. Reactive astrocytes as therapeutic targets for CNS disorders. *Neurotherapeutics,* 7**,** 494-506.

HAND, C. K., KHORIS, J., SALACHAS, F., GROS-LOUIS, F., LOPES, A. A. S., MAYEUX-PORTAS, V., BROWN JR, R. H., MEININGER, V., CAMU, W. & ROULEAU, G. A. 2002. A Novel Locus for Familial Amyotrophic Lateral Sclerosis, on Chromosome 18q. *The American Journal of Human Genetics,* 70**,** 251-256.

HANISCH, U.-K. & KETTENMANN, H. 2007. Microglia: active sensor and versatile effector cells in the normal and pathologic brain. *Nat Neurosci,* 10**,** 1387-1394.

HARDIMAN, O. 2011. Management of respiratory symptoms in ALS. *Journal of Neurology,* 258**,** 359-365.

HARRAZ, M. M., MARDEN, J. J., ZHOU, W., ZHANG, Y., WILLIAMS, A., SHAROV, V. S., NELSON, K., LUO, M., PAULSON, H., SCHÖNEICH, C. & ENGELHARDT, J. F. 2008. SOD1 mutations disrupt redox-sensitive Rac regulation of NADPH oxidase in a familial ALS model. *The Journal of Clinical Investigation,* 118**,** 659-670.

HAWLEY, S. A., GADALLA, A. E., OLSEN, G. S. & HARDIE, D. G. 2002. The Antidiabetic Drug Metformin Activates the AMP-Activated Protein Kinase Cascade via an Adenine Nucleotide-Independent Mechanism. *Diabetes,* 51**,** 2420-2425.

HAYASHI, S. 1993. Development and diversity of social structure in male mice. *Journal of Ethology,* 11**,** 77-82.

HEGEDUS, J., PUTMAN, C. T. & GORDON, T. 2007. Time course of preferential motor unit loss in the SOD1 G93A mouse model of amyotrophic lateral sclerosis. *Neurobiology of disease,* 28**,** 154-164.

HEGEDUS, J., PUTMAN, C. T., TYREMAN, N. & GORDON, T. 2008. Preferential motor unit loss in the SOD1 G93A transgenic mouse model of amyotrophic lateral sclerosis. *The Journal of physiology,* 586**,** 3337-3351.

HEMENDINGER, R., WANG, J., MALIK, S., PERSINSKI, R., COPELAND, J., EMERICH, D., GORES, P., HALBERSTADT, C. & ROSENFELD, J. 2005. Sertoli cells improve survival of motor neurons in SOD1 transgenic mice, a model of amyotrophic lateral sclerosis. *Experimental Neurology,* 196**,** 235-243.

HENKEL, J., BEERS, D., ZHAO, W. & APPEL, S. 2009. Microglia in ALS: The Good, The Bad, and The Resting. *Journal of Neuroimmune Pharmacology,* 4**,** 389-398.

HENRIQUES, A., PITZER, C. & SCHNEIDER, A. 2010. Neurotrophic growth factors for the treatment of amyotrophic lateral sclerosis: where do we stand ? *Frontiers in Neuroscience,* 4.

HENSLEY, K., ABDEL-MOATY, H., HUNTER, J., MHATRE, M., MOU, S., NGUYEN, K., POTAPOVA, T., PYE, Q. N., QI, M., RICE, H., STEWART, C., STROUKOFF, K. & WEST, M. 2006. Primary glia expressing the G93A-SOD1 mutation present a neuroinflammatory phenotype and provide a cellular system for studies of glial inflammation. *Journal of neuroinflammation,* 3**,** 2.

HENSLEY, K., FLOYD, R. A., GORDON, B., MOU, S., PYE, Q. N., STEWART, C., WEST, M. & WILLIAMSON, K. 2002. Temporal patterns of cytokine and apoptosis-related gene expression in spinal cords of the G93A-SOD1 mouse model of amyotrophic lateral sclerosis. *Journal of Neurochemistry,* 82**,** 365-374.

HERSCH, S. M. & ROSAS, H. D. 2011. Biomarkers to Enable the Development of Neuroprotective Therapies for Huntington's Disease.

HIDEO TOHGI, T., KINYA, Y., TAKAHIKO, M., ERI, I. & CHIAKI, I. 1999. Remarkable increase in cerebrospinal fluid 3-nitrotyrosine in patients with sporadic amyotrophic lateral sclerosis. *Annals of Neurology,* 46**,** 129 - 131.

HIGGINS, C. M., JUNG, C. & XU, Z. 2003. ALS-associated mutant SOD1G93A causes mitochondrial vacuolation by expansion of the intermembrane space and by involvement of SOD1 aggregation and peroxisomes. *BMC neuroscience,* 4**,** 16.

HIRANO, A., DONNENFELD, H., SASAKI, S. & NAKANO, I. 1984a. Fine structural observations of neurofilamentous changes in amyotrophic lateral sclerosis. *J Neuropathol Exp Neurol,* 43**,** 461 - 470.

HIRANO, A., DONNENFELD, H., SASAKI, S. & NAKANO, I. 1984b. Fine structural observations of neurofilamentous changes in amyotrophic lateral sclerosis. *J Neuropathol Exp Neurol,* 43**,** 461-70.

HIRANO, A., NAKANO, I., KURLAND, L. T., MULDER, D. W., HOLLEY, P. W. & SACCOMANNO, G. 1984c. Fine structural study of neurofibrillary changes in a family with amyotrophic lateral sclerosis. *J Neuropathol Exp Neurol,* 43**,** 471-80.

HOFFMAN, E. K., WILCOX, H. M., SCOTT, R. W. & SIMAN, R. 1996. Proteasome inhibition enhances the stability of mouse Cu/Zn superoxide dismutase with mutations linked to familial amyotrophic lateral sclerosis. *J Neurol Sci,* 139**,** 15-20.

HOLZBAUR, E. L. F. 2004. Motor neurons rely on motor proteins. *Trends in Cell Biology,* 14**,** 233-240.

HOLZBAUR, E. L. F., HOWLAND, D. S., WEBER, N., WALLACE, K., SHE, Y., KWAK, S., TCHISTIAKOVA, L. A., MURPHY, E., HINSON, J., KARIM, R., TAN, X. Y., KELLEY, P., MCGILL, K. C., WILLIAMS, G., HOBBS, C., DOHERTY, P., ZALESKA, M. M., PANGALOS, M. N. & WALSH, F. S. 2006. Myostatin inhibition slows muscle atrophy in rodent models of amyotrophic lateral sclerosis. *Neurobiology of Disease,* 23**,** 697-707.

HOSLER, B. A., SIDDIQUE, T., SAPP, P. C., SAILOR, W., HUANG, M. C., HOSSAIN, A., DAUBE, J. R., NANCE, M., FAN, C., KAPLAN, J., HUNG, W.-Y., MCKENNA-YASEK, D., HAINES, J. L., PERICAK-VANCE, M. A., HORVITZ, H. R. & BROWN, R. H. 2000. Linkage of Familial Amyotrophic Lateral Sclerosis With Frontotemporal Dementia to Chromosome 9q21-q22. *JAMA: The Journal of the American Medical Association,* 284**,** 1664-1669.

HOTTINGER, A. F., FINE, E. G., GURNEY, M. E., ZURN, A. D. & AEBISCHER, P. 1997. The Copper Chelator d-Penicillamine Delays Onset of Disease and Extends Survival in a Transgenic Mouse Model of Familial Amyotrophic Lateral Sclerosis. *European Journal of Neuroscience,* 9**,** 1548-1551.

HOWLAND, D. S., LIU, J., SHE, Y., GOAD, B., MARAGAKIS, N. J., KIM, B., ERICKSON, J., KULIK, J., DEVITO, L., PSALTIS, G., DEGENNARO, L. J., CLEVELAND, D. W. & ROTHSTEIN, J. D. 2002. Focal loss of the glutamate transporter EAAT2 in a transgenic rat model of SOD1 mutant-mediated amyotrophic lateral sclerosis (ALS). *Proceedings of the National Academy of Sciences,* 99**,** 1604-1609.

HUANG, C., ZHOU, H., TONG, J., CHEN, H., LIU, Y.-J., WANG, D., WEI, X. & XIA, X.-G. 2011. FUS Transgenic Rats Develop the Phenotypes of Amyotrophic Lateral Sclerosis and Frontotemporal Lobar Degeneration. *PLoS Genet,* 7**,** e1002011.

HUNT, C. & HAMBLY, C. 2006. Faecal corticosterone concentrations indicate that separately housed male mice are not more stressed than group housed males. *Physiology & Behavior,* 87**,** 519-526.

HURST, J. 2005. Making sense of scents: reducing aggression and uncontrolled variation in laboratory mice. *NC3Rs #2 Mouse scents and optimal husbandry* [Online].

HWANG, D. H., LEE, H. J., PARK, I. H., SEOK, J. I., KIM, B. G., JOO, I. S. & KIM, S. U. 2009. Intrathecal transplantation of human neural stem cells overexpressing VEGF provide behavioral

improvement, disease onset delay and survival extension in transgenic ALS mice. *Gene Ther,* 16**,** 1234-1244.

IGNACIO, S., MOORE, D. H., SMITH, A. P. & LEE, N. M. 2005. Effect of Neuroprotective Drugs on Gene Expression in G93A/SOD1 Mice. *Annals of the New York Academy of Sciences,* 1053**,** 121-136.

ILIEVA, H., POLYMENIDOU, M. & CLEVELAND, D. W. 2009. Non–cell autonomous toxicity in neurodegenerative disorders: ALS and beyond. *The Journal of cell biology,* 187**,** 761-772.

ILIEVA, H. S., YAMANAKA, K., MALKMUS, S., KAKINOHANA, O., YAKSH, T., MARSALA, M. & CLEVELAND, D. W. 2008. Mutant dynein (Loa) triggers proprioceptive axon loss that extends survival only in the SOD1 ALS model with highest motor neuron death. *Proceedings of the National Academy of Sciences,* 105**,** 12599-12604.

INCE, P., HIGHLEY, J., KIRBY, J., WHARTON, S., TAKAHASHI, H., STRONG, M. & SHAW, P. 2011. Molecular pathology and genetic advances in amyotrophic lateral sclerosis: an emerging molecular pathway and the significance of glial pathology. *Acta Neuropathologica,* 122**,** 657-671.

ISODA, K., YOUNG, J. L., ZIRLIK, A., MACFARLANE, L. A., TSUBOI, N., GERDES, N., SCHONBECK, U. & LIBBY, P. 2006. Metformin Inhibits Proinflammatory Responses and Nuclear Factor-{kappa}B in Human Vascular Wall Cells. *Arterioscler Thromb Vasc Biol,* 26**,** 611-617.

ISRAELSON, A., ARBEL, N., DA CRUZ, S., ILIEVA, H., YAMANAKA, K., SHOSHAN-BARMATZ, V. & CLEVELAND, D. W. 2010. Misfolded Mutant SOD1 Directly Inhibits VDAC1 Conductance in a Mouse Model of Inherited ALS. *Neuron,* 67**,** 575-587.

IZMITLI, A., SCHEBOR, C., MCGOVERN, M. P., REDDY, A. S., ABBOTT, N. L. & DE PABLO, J. J. 2011. Effect of trehalose on the interaction of Alzheimer's A[beta]-peptide and anionic lipid monolayers. *Biochimica et Biophysica Acta (BBA) - Biomembranes,* 1808**,** 26-33.

JAARSMA, D. 2006. Swelling and vacuolisation of mitochondria in transgenic SOD1-ALS mice: A consequence of supranormal SOD1 expression? *Mitochondrion,* 6**,** 48-49.

JAARSMA, D., GUCHELAAR, H.-J., HAASDIJK, E., DE JONG, J. M. B. V. & HOLSTEGE, J. C. 1998. The antioxidant N-acetylcysteine does not delay disease onset and death in a transgenic mouse model of amyotrophic lateral sclerosis. *Annals of Neurology,* 44**,** 293-293.

JAARSMA, D., ROGNONI, F., VAN DUIJN, W., VERSPAGET, H., HAASDIJK, E. & HOLSTEGE, J. 2001. CuZn superoxide dismutase (SOD1) accumulates in vacuolated mitochondria in transgenic mice expressing amyotrophic lateral sclerosis-linked SOD1 mutations. *Acta Neuropathologica,* 102**,** 293-305.

JÄGER, S., HANDSCHIN, C., ST.-PIERRE, J. & SPIEGELMAN, B. M. 2007. AMP-activated protein kinase (AMPK) action in skeletal muscle via direct phosphorylation of PGC-1α. *Proceedings of the National Academy of Sciences,* 104**,** 12017-12022.

JAWAID, A., SALAMONE, A. R., STRUTT, A. M., MURTHY, S. B., WHEATON, M., MCDOWELL, E. J., SIMPSON, E., APPEL, S. H., YORK, M. K. & SCHULZ, P. E. 2010. ALS disease onset may occur later in patients with pre-morbid diabetes mellitus. *European Journal of Neurology,* 17**,** 733-739.

JENNINGS, M., BATCHELOR, G. R., BRAIN, P. F., DICK, A., ELLIOTT, H., FRANCIS, R. J., HUBRECHT, R. C., HURST, J. L., MORTON, D. B., PETERS, A. G., RAYMOND, R., SALES, G. D., SHERWIN, C. M. & WEST, C. 1998. Refining rodent husbandry: the mouse: Report of the Rodent Refinement Working Party. *Lab Anim,* 32**,** 233-259.

JEONG, S. Y., RATHORE, K. I., SCHULZ, K., PONKA, P., AROSIO, P. & DAVID, S. 2009. Dysregulation of Iron Homeostasis in the CNS Contributes to Disease Progression in a Mouse Model of Amyotrophic Lateral Sclerosis. *The Journal of Neuroscience,* 29**,** 610-619.

JIANG, F., DESILVA, S. & TURNBULL, J. 2000. Beneficial effect of ginseng root in SOD-1 (G93A) transgenic mice. *Journal of the Neurological Sciences,* 180**,** 52-54.

JIANG, F., LI, W. P., KWIECIEN, J. & TURNBULL, J. 2006. A study of the purine derivative AIT-082 in G93A SOD1 transgenic mice. *Int J Immunopathol Pharmacol,* 19**,** 489-98.

JOHNSON, J. O., MANDRIOLI, J., BENATAR, M., ABRAMZON, Y., VAN DEERLIN, V. M., TROJANOWSKI, J. Q., GIBBS, J. R., BRUNETTI, M., GRONKA, S., WUU, J., DING, J., MCCLUSKEY, L., MARTINEZ-LAGE, M., FALCONE, D., HERNANDEZ, D. G., AREPALLI, S., CHONG, S., SCHYMICK, J. C., ROTHSTEIN, J., LANDI, F., WANG, Y. D., CALVO, A., MORA, G., SABATELLI, M., MONSURRO, M. R., BATTISTINI, S., SALVI, F., SPATARO, R., SOLA, P., BORGHERO, G., GALASSI, G., SCHOLZ, S. W., TAYLOR, J. P., RESTAGNO, G., CHIO, A. & TRAYNOR, B. J. 2010. Exome sequencing reveals VCP mutations as a cause of familial ALS. *Neuron,* 68**,** 857-64.

JOHNSTON, J. A., DALTON, M. J., GURNEY, M. E. & KOPITO, R. R. 2000. Formation of high molecular weight complexes of mutant Cu, Zn-superoxide dismutase in a mouse model for familial amyotrophic lateral sclerosis. *Proceedings of the National Academy of Sciences of the United States of America,* 97**,** 12571-12576.

JONSSON, P. A., GRAFFMO, K. S., ANDERSEN, P. M., BRÄNNSTRÖM, T., LINDBERG, M., OLIVEBERG, M. & MARKLUND, S. L. 2006. Disulphide-reduced superoxide dismutase-1 in CNS of transgenic amyotrophic lateral sclerosis models. *Brain,* 129**,** 451-464.

JOO, I.-S., HWANG, D.-H., SEOK, J.-I., SHIN, S.-K. & KIM, S.-U. 2007. Oral Administration of Memantine Prolongs Survival in a Transgenic Mouse Model of Amyotrophic Lateral Sclerosis. *J Clin Neurol,* 3**,** 181-186.

JU, J.-S., MILLER, S. E., JACKSON, E., CADWELL, K., PIWNICA-WORMS, D. & WEIHL, C. C. 2009. Quantitation of selective autophagic protein aggregate degradation in vitro and in vivo using luciferase reporters. *Autophagy,* 5**,** 511-519.

JU, S., TARDIFF, D. F., HAN, H., DIVYA, K., ZHONG, Q., MAQUAT, L. E., BOSCO, D. A., HAYWARD, L. J., BROWN, R. H., JR., LINDQUIST, S., RINGE, D. & PETSKO, G. A. 2011. A Yeast Model of FUS/TLS-Dependent Cytotoxicity. *PLoS Biol,* 9**,** e1001052.

JUNG, C., HIGGINS, C. M. & XU, Z. 2002. Mitochondrial electron transport chain complex dysfunction in a transgenic mouse model for amyotrophic lateral sclerosis. *Journal of Neurochemistry,* 83**,** 535-545.

JUNG, C., RONG, Y., DOCTROW, S., BAUDRY, M., MALFROY, B. & XU, Z. 2001. Synthetic superoxide dismutase/catalase mimetics reduce oxidative stress and prolong survival in a mouse amyotrophic lateral sclerosis model. *Neuroscience Letters,* 304**,** 157-160.

KABASHI, E., AGAR, J. N., TAYLOR, D. M., MINOTTI, S. & DURHAM, H. D. 2004. Focal dysfunction of the proteasome: a pathogenic factor in a mouse model of amyotrophic lateral sclerosis. *Journal of Neurochemistry,* 89**,** 1325-1335.

KABASHI, E., LIN, L., TRADEWELL, M. L., DION, P. A., BERCIER, V., BOURGOUIN, P., ROCHEFORT, D., BEL HADJ, S., DURHAM, H. D., VELDE, C. V., ROULEAU, G. A. & DRAPEAU, P. 2010. Gain and loss of function of ALS-related mutations of TARDBP (TDP-43) cause motor deficits in vivo. *Human Molecular Genetics,* 19**,** 671-683.

KABASHI, E., VALDMANIS, P., DION, P., SPIEGELMAN, D., MCCONKEY, B., VELDE, C., BOUCHARD, J., LACOMBLEZ, L., POCHIGAEVA, K. & SALACHAS, F. 2008a. TARDBP mutations in individuals with sporadic and familial amyotrophic lateral sclerosis. *Nat Genet,* 40**,** 572 - 574.

KABASHI, E., VALDMANIS, P. N., DION, P., SPIEGELMAN, D., MCCONKEY, B. J., VELDE, C. V., BOUCHARD, J.-P., LACOMBLEZ, L., POCHIGAEVA, K., SALACHAS, F., PRADAT, P.-F., CAMU, W., MEININGER, V., DUPRE, N. & ROULEAU, G. A. 2008b. TARDBP mutations in individuals with sporadic and familial amyotrophic lateral sclerosis. *Nat Genet,* 40**,** 572-574.

KABUTA, T., SUZUKI, Y. & WADA, K. 2006. Degradation of Amyotrophic Lateral Sclerosis-linked Mutant Cu,Zn-Superoxide Dismutase Proteins by Macroautophagy and the Proteasome. *Journal of Biological Chemistry,* 281**,** 30524-30533.

KALMAR, B., NOVOSELOV, S., GRAY, A., CHEETHAM, M. E., MARGULIS, B. & GREENSMITH, L. 2008. Late stage treatment with arimoclomol delays disease progression and prevents protein aggregation in the SOD1G93A mouse model of ALS. *Journal of Neurochemistry,* 107**,** 339-350.

KANEB, H. M., SHARP, P. S., RAHMANI-KONDORI, N. & WELLS, D. J. 2011. Metformin treatment has no beneficial effect in a dose-response survival study in the SOD1G93A mouse model of ALS and is harmful in female mice. *PLoS ONE***,** In Press.

KANG, S. H., FUKAYA, M., YANG, J. K., ROTHSTEIN, J. D. & BERGLES, D. E. 2010. NG2+ CNS Glial Progenitors Remain Committed to the Oligodendrocyte Lineage in Postnatal Life and following Neurodegeneration. *Neuron,* 68**,** 668-681.

KARLSSON, J., FONG, K. S. K., HANSSON, M. J., ELMÀR, E., CSISZAR, K. & KEEP, M. F. 2004. Life span extension and reduced neuronal death after weekly intraventricular cyclosporin injections in the G93A transgenic mouse model of amyotrophic lateral sclerosis. *Journal of Neurosurgery,* 101**,** 128-137.

KASPAR, B., LLADO, J., SHERKAT, N., ROTHSTEIN, J. & GAGE, F. 2003. Retrograde viral delivery of IGF-1 prolongs survival in a mouse ALS model. *Science,* 301**,** 839-842.

KASPAR, B. K., FROST, L. M., CHRISTIAN, L., UMAPATHI, P. & GAGE, F. H. 2005. Synergy of insulin-like growth factor-1 and exercise in amyotrophic lateral sclerosis. *Annals of Neurology,* 57**,** 649-655.

KAUSHIK, J. K. & BHAT, R. 2003. Why Is Trehalose an Exceptional Protein Stabilizer? *Journal of Biological Chemistry,* 278**,** 26458-26465.

KAWAMATA, T., AKIYAMA, H., YAMADA, T. & MCGEER, P. L. 1992. Immunologic reactions in amyotrophic lateral sclerosis brain and spinal cord tissue. *The American journal of pathology,* 140**,** 691-707.

KEEP, M., ELMÉR, E., FONG, K. S. K. & CSISZAR, K. 2001. Intrathecal cyclosporin prolongs survival of late-stage ALS mice. *Brain Research,* 894**,** 327-331.

KELLER, A. F., GRAVEL, M. & KRIZ, J. 2011. Treatment with minocycline after disease onset alters astrocyte reactivity and increases microgliosis in SOD1 mutant mice. *Experimental Neurology,* 228**,** 69-79.

KERMAN, A., LIU, H.-N., CROUL, S., BILBAO, J., ROGAEVA, E., ZINMAN, L., ROBERTSON, J. & CHAKRABARTTY, A. 2010. Amyotrophic lateral sclerosis is a non-amyloid disease in which extensive misfolding of SOD1 is unique to the familial form. *Acta Neuropathologica,* 119**,** 335-344.

KHARE, S. D., CAPLOW, M. & DOKHOLYAN, N. V. 2004. The rate and equilibrium constants for a multistep reaction sequence for the aggregation of superoxide dismutase in amyotrophic lateral sclerosis. *Proceedings of the National Academy of Sciences of the United States of America,* 101**,** 15094-15099.

KIAEI, M., KIPIANI, K., CHEN, J., CALINGASAN, N. Y. & BEAL, M. F. 2005a. Peroxisome proliferator-activated receptor-gamma agonist extends survival in transgenic mouse model of amyotrophic lateral sclerosis. *Experimental Neurology,* 191**,** 331-336.

KIAEI, M., KIPIANI, K., PETRI, S., CHEN, J., CALINGASAN, N. Y. & BEAL, M. F. 2005b. Celastrol Blocks Neuronal Cell Death and Extends Life in Transgenic Mouse Model of Amyotrophic Lateral Sclerosis. *Neurodegenerative Diseases,* 2**,** 246-254.

KIAEI, M., KIPIANI, K., PETRI, S., CHOI, D.-K., CHEN, J., CALINGASAN, N. Y. & BEAL, M. F. 2005c. Integrative role of cPLA2 with COX-2 and the effect of non-steriodal anti-inflammatory drugs in a transgenic mouse model of amyotrophic lateral sclerosis. *Journal of Neurochemistry,* 93**,** 403-411.

KIAEI, M., PETRI, S., KIPIANI, K., GARDIAN, G., CHOI, D.-K., CHEN, J., CALINGASAN, N. Y., SCHAFER, P., MULLER, G. W., STEWART, C., HENSLEY, K. & BEAL, M. F. 2006. Thalidomide and

Lenalidomide Extend Survival in a Transgenic Mouse Model of Amyotrophic Lateral Sclerosis. *The Journal of Neuroscience,* 26**,** 2467-2473.

KIENLE, I., BURGERT, M. & HOLZER, H. 1993. Assay of trehalose with acid trehalase purified from Saccharomyces cerevisiae. *Yeast,* 9**,** 607-11.

KIERAN, D., KALMAR, B., DICK, J. R., RIDDOCH-CONTRERAS, J., BURNSTOCK, G. & GREENSMITH, L. 2004. Treatment with arimoclomol, a coinducer of heat shock proteins, delays disease progression in ALS mice. *Nat Med,* 10**,** 402-5.

KIERAN, D., SEBASTIA, J., GREENWAY, M. J., KING, M. A., CONNAUGHTON, D., CONCANNON, C. G., FENNER, B., HARDIMAN, O. & PREHN, J. H. M. 2008. Control of Motoneuron Survival by Angiogenin. *The Journal of Neuroscience,* 28**,** 14056-14061.

KIERNAN, M. C., VUCIC, S., CHEAH, B. C., TURNER, M. R., EISEN, A., HARDIMAN, O., BURRELL, J. R. & ZOING, M. C. 2011. Amyotrophic lateral sclerosis. *The Lancet,* 377**,** 942-955.

KIGERL, K. A., GENSEL, J. C., ANKENY, D. P., ALEXANDER, J. K., DONNELLY, D. J. & POPOVICH, P. G. 2009. Identification of Two Distinct Macrophage Subsets with Divergent Effects Causing either Neurotoxicity or Regeneration in the Injured Mouse Spinal Cord. *The Journal of Neuroscience,* 29**,** 13435-13444.

KIKUCHI, H., ALMER, G., YAMASHITA, S., GUÉGAN, C., NAGAI, M., XU, Z., SOSUNOV, A. A., MCKHANN, G. M. & PRZEDBORSKI, S. 2006. Spinal cord endoplasmic reticulum stress associated with a microsomal accumulation of mutant superoxide dismutase-1 in an ALS model. *Proceedings of the National Academy of Sciences,* 103**,** 6025-6030.

KIM, H., KIM, H. Y., CHOI, M. R., HWANG, S., NAM, K.-H., KIM, H.-C., HAN, J. S., KIM, K. S., YOON, H. S. & KIM, S. H. 2010. Dose-dependent efficacy of ALS-human mesenchymal stem cells transplantation into cisterna magna in SOD1-G93A ALS mice. *Neuroscience Letters,* 468**,** 190-194.

KIM, K., MOORE, D. H., MAKRIYANNIS, A. & ABOOD, M. E. 2006. AM1241, a cannabinoid CB2 receptor selective compound, delays disease progression in a mouse model of amyotrophic lateral sclerosis. *European Journal of Pharmacology,* 542**,** 100-105.

KIM, W.-K., LIU, X., SANDNER, J., PASMANTIER, M., ANDREWS, J., ROWLAND, L. P. & MITSUMOTO, H. 2009. Study of 962 patients indicates progressive muscular atrophy is a form of ALS. *Neurology,* 73**,** 1686-1692.

KIRA, Y., NISHIKAWA, M., OCHI, A., SATO, E. & INOUE, M. 2006. l-Carnitine suppresses the onset of neuromuscular degeneration and increases the life span of mice with familial amyotrophic lateral sclerosis. *Brain Research,* 1070**,** 206-214.

KIRKINEZOS, I. G., HERNANDEZ, D., BRADLEY, W. G. & MORAES, C. T. 2003. Regular exercise is beneficial to a mouse model of amyotrophic lateral sclerosis. *Annals of Neurology,* 53**,** 804-807.

KIRKINEZOS, I. G., HERNANDEZ, D., BRADLEY, W. G. & MORAES, C. T. 2004. An ALS mouse model with a permeable blood–brain barrier benefits from systemic cyclosporine A treatment. *Journal of Neurochemistry,* 88**,** 821-826.

KLIVENYI, P., FERRANTE, R. J., MATTHEWS, R. T., BOGDANOV, M. B., KLEIN, A. M., ANDREASSEN, O. A., MUELLER, G., WERMER, M., KADDURAH-DAOUK, R. & BEAL, M. F. 1999. Neuroprotective effects of creatine in a transgenic animal model of amyotrophic lateral sclerosis. *Nature medicine,* 5**,** 347-350.

KLIVENYI, P., KIAEI, M., GARDIAN, G., CALINGASAN, N. Y. & BEAL, M. F. 2004. Additive neuroprotective effects of creatine and cyclooxygenase 2 inhibitors in a transgenic mouse model of amyotrophic lateral sclerosis. *Journal of Neurochemistry,* 88**,** 576-582.

KNOTT, A. B., PERKINS, G., SCHWARZENBACHER, R. & BOSSY-WETZEL, E. 2008. Mitochondrial fragmentation in neurodegeneration. *Nat Rev Neurosci,* 9**,** 505-518.

KOH, S.-H., KIM, Y., KIM, H. Y., HWANG, S., LEE, C. H. & KIM, S. H. 2007a. Inhibition of glycogen synthase kinase-3 suppresses the onset of symptoms and disease progression of G93A-SOD1 mouse model of ALS. *Experimental Neurology,* 205**,** 336-346.

KOH, S.-H., KIM, Y., KIM, H. Y., WON CHO, G., KIM, K. S. & KIM, S. H. 2007b. Recombinant human erythropoietin suppresses symptom onset and progression of G93A-SOD1 mouse model of ALS by preventing motor neuron death and inflammation. *European Journal of Neuroscience,* 25**,** 1923-1930.

KOH, S.-H., LEE, S. M., KIM, H. Y., LEE, K.-Y., LEE, Y. J., KIM, H.-T., KIM, J., KIM, M.-H., HWANG, M. S., SONG, C., YANG, K.-W., LEE, K. W., KIM, S. H. & KIM, O.-H. 2006. The effect of epigallocatechin gallate on suppressing disease progression of ALS model mice. *Neuroscience Letters,* 395**,** 103-107.

KÖRNER, S., KOLLEWE, K., FAHLBUSCH, M., ZAPF, A., DENGLER, R., KRAMPFL, K. & PETRI, S. 2011. Onset and spreading patterns of upper and lower motor neuron symptoms in amyotrophic lateral sclerosis. *Muscle & Nerve,* 43**,** 636-642.

KOTULSKA, K., LEPECHEUR, M., MARCOL, W., LEWIN-KOWALIK, J., LARYSZ-BRYSZ, M., PALY, E., MATUSZEK, I. & LONDON, J. 2006. Overexpression of copper/zinc-superoxide dismutase in transgenic mice markedly impairs regeneration and increases development of neuropathic pain after sciatic nerve injury. *Journal of Neuroscience Research,* 84**,** 1091-1097.

KRIZ, J., GOWING, G. & JULIEN, J.-P. 2003. Efficient three-drug cocktail for disease induced by mutant superoxide dismutase. *Annals of Neurology,* 53**,** 429-436.

KRIZ, J., NGUYEN, M. D. & JULIEN, J.-P. 2002. Minocycline Slows Disease Progression in a Mouse Model of Amyotrophic Lateral Sclerosis. *Neurobiology of Disease,* 10**,** 268-278.

KRUMAN, I. I., PEDERSEN, W. A., SPRINGER, J. E. & MATTSON, M. P. 1999. ALS-Linked Cu/Zn-SOD Mutation Increases Vulnerability of Motor Neurons to Excitotoxicity by a Mechanism Involving Increased Oxidative Stress and Perturbed Calcium Homeostasis. *Experimental Neurology,* 160**,** 28-39.

KUHLE, J., LINDBERG, R. L. P., REGENITER, A., MEHLING, M., STECK, A. J., KAPPOS, L. & CZAPLINSKI, A. 2009. Increased levels of inflammatory chemokines in amyotrophic lateral sclerosis. *European Journal of Neurology,* 16**,** 771-774.

KUKIDOME, D., NISHIKAWA, T., SONODA, K., IMOTO, K., FUJISAWA, K., YANO, M., MOTOSHIMA, H., TAGUCHI, T., MATSUMURA, T. & ARAKI, E. 2006. Activation of AMP-Activated Protein Kinase Reduces Hyperglycemia-Induced Mitochondrial Reactive Oxygen Species Production and Promotes Mitochondrial Biogenesis in Human Umbilical Vein Endothelial Cells. *Diabetes,* 55**,** 120-127.

KUSHNER, P. D., STEPHENSON, D. T. & WRIGHT, S. 1991. Reactive astrogliosis is widespread in the subcortical white matter of amyotrophic lateral sclerosis brain. *J Neuropathol Exp Neurol,* 50**,** 263-77.

KWIATKOWSKI, T. J., BOSCO, D. A., LECLERC, A. L., TAMRAZIAN, E., VANDERBURG, C. R., RUSS, C., DAVIS, A., GILCHRIST, J., KASARSKIS, E. J., MUNSAT, T., VALDMANIS, P., ROULEAU, G. A., HOSLER, B. A., CORTELLI, P., DE JONG, P. J., YOSHINAGA, Y., HAINES, J. L., PERICAK-VANCE, M. A., YAN, J., TICOZZI, N., SIDDIQUE, T., MCKENNA-YASEK, D., SAPP, P. C., HORVITZ, H. R., LANDERS, J. E. & BROWN, R. H. 2009. Mutations in the FUS/TLS Gene on Chromosome 16 Cause Familial Amyotrophic Lateral Sclerosis. *Science,* 323**,** 1205-1208.

LACOMBLEZ, L., BENSIMON, G., LEIGH, P. N., GUILLET, P. & MEININGER, V. 1996. Dose-ranging study of riluzole in amyotrophic lateral sclerosis. Amyotrophic Lateral Sclerosis/Riluzole Study Group II. *Lancet,* 347**,** 1425-31.

LACOMBLEZ, L., DOPPLER, V., BEUCLER, I., COSTES, G., SALACHAS, F., RAISONNIER, A., LE FORESTIER, N., PRADAT, P.-F., BRUCKERT, E. & MEININGER, V. 2002. APOE: A potential marker of disease progression in ALS. *Neurology,* 58**,** 1112-1114.

LAMONTE, B. H., WALLACE, K. E., HOLLOWAY, B. A., SHELLY, S. S., ASCAÑO, J., TOKITO, M., VAN WINKLE, T., HOWLAND, D. S. & HOLZBAUR, E. L. F. 2002. Disruption of Dynein/Dynactin Inhibits Axonal Transport in Motor Neurons Causing Late-Onset Progressive Degeneration. *Neuron,* 34**,** 715-727.

LANSON, N. A., MALTARE, A., KING, H., SMITH, R., KIM, J. H., TAYLOR, J. P., LLOYD, T. E. & PANDEY, U. B. 2011. A Drosophila model of FUS-related neurodegeneration reveals genetic interaction between FUS and TDP-43. *Human Molecular Genetics,* 20**,** 2510-2523.

LARSSON, N. G., WANG, J., WILHELMSSON, H., OLDFORS, A., RUSTIN, P., LEWANDOSKI, M., BARSH, G. S. & CLAYTON, D. A. 1998. Mitochondrial transcription factor A is necessary for mtDNA maintenance and embryogenesis in mice. *Nat Genet,* 18**,** 231-6.

LEE, A. & MORLEY, J. E. 1998. Metformin decreases food consumption and induces weight loss in subjects with obesity with type II non-insulin-dependent diabetes. *Obes Res,* 6**,** 47-53.

LEE, D. H. & GOLDBERG, A. L. 1998. Proteasome Inhibitors Cause Induction of Heat Shock Proteins and Trehalose, Which Together Confer Thermotolerance in Saccharomyces cerevisiae. *Mol. Cell. Biol.,* 18**,** 30-38.

LEE, J., RYU, H. & KOWALL, N. W. 2009. Motor neuronal protection by l-arginine prolongs survival of mutant SOD1 (G93A) ALS mice. *Biochemical and Biophysical Research Communications,* 384**,** 524-529.

LEIGH, P. N., WHITWELL, H., GAROFALO, O., BULLER, J., SWASH, M., MARTIN, J. E., GALLO, J.-M., WELLER, R. O. & ANDERTON, B. H. 1991. UBIQUITIN-IMMUNOREACTIVE INTRANEURONAL INCLUSIONS IN AMYOTROPHIC LATERAL SCLEROSIS: MORPHOLOGY, DISTRIBUTION, AND SPECIFICITY. *Brain,* 114**,** 775-788.

LEPORE, A. C., HAENGGELI, C., GASMI, M., BISHOP, K. M., BARTUS, R. T., MARAGAKIS, N. J. & ROTHSTEIN, J. D. 2007. Intraparenchymal spinal cord delivery of adeno-associated virus IGF-1 is protective in the SOD1G93A model of ALS. *Brain Research,* 1185**,** 256-265.

LI, L., ZHANG, X. & LE, W. 2008. Altered macroautophagy in the spinal cord of SOD1 mutant mice. *Autophagy,* 4**,** 290-293.

LI, M., ONA, V. O., GUÉGAN, C., CHEN, M., JACKSON-LEWIS, V., ANDREWS, L. J., OLSZEWSKI, A. J., STIEG, P. E., LEE, J.-P., PRZEDBORSKI, S. & FRIEDLANDER, R. M. 2000. Functional Role of Caspase-1 and Caspase-3 in an ALS Transgenic Mouse Model. *Science,* 288**,** 335-339.

LI, Y., RAY, P., RAO, E. J., SHI, C., GUO, W., CHEN, X., WOODRUFF, E. A., FUSHIMI, K. & WU, J. Y. 2010. A Drosophila model for TDP-43 proteinopathy. *Proceedings of the National Academy of Sciences,* 107**,** 3169-3174.

LIACHKO, N. F., GUTHRIE, C. R. & KRAEMER, B. C. 2010. Phosphorylation Promotes Neurotoxicity in a Caenorhabditis elegans Model of TDP-43 Proteinopathy. *The Journal of Neuroscience,* 30**,** 16208-16219.

LIEBETANZ, D., HAGEMANN, K., VON LEWINSKI, F., KAHLER, E. & PAULUS, W. 2004. Extensive exercise is not harmful in amyotrophic lateral sclerosis. *European Journal of Neuroscience,* 20**,** 3115-3120.

LIGON, L. A., LAMONTE, B. H., WALLACE, K. E., WEBER, N., KALB, R. G. & HOLZBAUR, E. L. 2005. Mutant superoxide dismutase disrupts cytoplasmic dynein in motor neurons. *Neuroreport,* 16**,** 533-6.

LIN, C.-L. G., BRISTOL, L. A., JIN, L., DYKES-HOBERG, M., CRAWFORD, T., CLAWSON, L. & ROTHSTEIN, J. D. 1998. Aberrant RNA Processing in a Neurodegenerative Disease: the Cause for Absent EAAT2, a Glutamate Transporter, in Amyotrophic Lateral Sclerosis. *Neuron,* 20**,** 589-602.

LIN, H. Z., YANG, S. Q., CHUCKAREE, C., KUHAJDA, F., RONNET, G. & DIEHL, A. M. 2000. Metformin reverses fatty liver disease in obese, leptin-deficient mice. *Nat Med,* 6**,** 998-1003.

LIN, J., WU, H., TARR, P. T., ZHANG, C. Y., WU, Z., BOSS, O., MICHAEL, L. F., PUIGSERVER, P., ISOTANI, E., OLSON, E. N., LOWELL, B. B., BASSEL-DUBY, R. & SPIEGELMAN, B. M. 2002. Transcriptional

co-activator PGC-1 alpha drives the formation of slow-twitch muscle fibres. *Nature,* 418**,** 797-801.

LINCECUM, J. M., VIEIRA, F. G., WANG, M. Z., THOMPSON, K., DE ZUTTER, G. S., KIDD, J., MORENO, A., SANCHEZ, R., CARRION, I. J., LEVINE, B. A., AL-NAKHALA, B. M., SULLIVAN, S. M., GILL, A. & PERRIN, S. 2010. From transcriptome analysis to therapeutic anti-CD40L treatment in the SOD1 model of amyotrophic lateral sclerosis. *Nat Genet,* 42**,** 392-399.

LINDBERG, M. J., BYSTRÖM, R., BOKNÄS, N., ANDERSEN, P. M. & OLIVEBERG, M. 2005. Systematically perturbed folding patterns of amyotrophic lateral sclerosis (ALS)-associated SOD1 mutants. *Proceedings of the National Academy of Sciences of the United States of America,* 102**,** 9754-9759.

LIU, F.-F., JI, L., DONG, X.-Y. & SUN, Y. 2009. Molecular Insight into the Inhibition Effect of Trehalose on the Nucleation and Elongation of Amyloid β-Peptide Oligomers. *The Journal of Physical Chemistry B,* 113**,** 11320-11329.

LIU, R., LI, B., FLANAGAN, S. W., OBERLEY, L. W., GOZAL, D. & QIU, M. 2002. Increased mitochondrial antioxidative activity or decreased oxygen free radical propagation prevent mutant SOD1-mediated motor neuron cell death and increase amyotrophic lateral sclerosis-like transgenic mouse survival. *Journal of Neurochemistry,* 80**,** 488-500.

LOBSIGER, C. S., BOILLEE, S., MCALONIS-DOWNES, M., KHAN, A. M., FELTRI, M. L., YAMANAKA, K. & CLEVELAND, D. W. 2009. Schwann cells expressing dismutase active mutant SOD1 unexpectedly slow disease progression in ALS mice. *Proceedings of the National Academy of Sciences,* 106**,** 4465-4470.

LOCATELLI, F., CORTI, S., PAPADIMITRIOU, D., FORTUNATO, F., DEL BO, R., DONADONI, C., NIZZARDO, M., NARDINI, M., SALANI, S., GHEZZI, S., STRAZZER, S., BRESOLIN, N. & COMI, G. P. 2007. Fas small interfering RNA reduces motoneuron death in amyotrophic lateral sclerosis mice. *Annals of Neurology,* 62**,** 81-92.

LOGROSCINO, G., TRAYNOR, B. J., HARDIMAN, O., CHIÒ, A., MITCHELL, D., SWINGLER, R. J., MILLUL, A., BENN, E., BEGHI, E. & EURALS, F. 2010. Incidence of amyotrophic lateral sclerosis in Europe. *Journal of Neurology, Neurosurgery & Psychiatry,* 81**,** 385-390.

LOMEN-HOERTH, C., ANDERSON, T. & MILLER, B. 2002. The overlap of amyotrophic lateral sclerosis and frontotemporal dementia. *Neurology,* 59**,** 1077-1079.

LORENZL, S., NARR, S., ANGELE, B., KRELL, H. W., GREGORIO, J., KIAEI, M., PFISTER, H.-W. & BEAL, M. F. 2006. The matrix metalloproteinases inhibitor Ro 26-2853 extends survival in transgenic ALS mice. *Experimental Neurology,* 200**,** 166-171.

LUDOLPH, A. C., BENDOTTI, C., BLAUGRUND, E., CHIO, A., GREENSMITH, L., LOEFFLER, J. P., MEAD, R., NIESSEN, H. G., PETRI, S., PRADAT, P. F., ROBBERECHT, W., RUEGG, M., SCHWALENSTOCKER, B., STILLER, D., VAN DEN BERG, L., VIEIRA, F. & VON HORSTEN, S. 2010. Guidelines for preclinical animal research in ALS/MND: A consensus meeting. *Amyotroph Lateral Scler,* 11**,** 38-45.

LUDOLPH, A. C. & JESSE, S. 2009. Review: Evidence-based drug treatment in amyotrophic lateral sclerosis and upcoming clinical trials. *Therapeutic Advances in Neurological Disorders,* 2**,** 319-326.

LUNDBERG, J. O., WEITZBERG, E. & GLADWIN, M. T. 2008. The nitrate-nitrite-nitric oxide pathway in physiology and therapeutics. *Nat Rev Drug Discov,* 7**,** 156-167.

LUTY, A. A., KWOK, J. B. J., DOBSON-STONE, C., LOY, C. T., COUPLAND, K. G., KARLSTRÖM, H., SOBOW, T., TCHORZEWSKA, J., MARUSZAK, A., BARCIKOWSKA, M., PANEGYRES, P. K., ZEKANOWSKI, C., BROOKS, W. S., WILLIAMS, K. L., BLAIR, I. P., MATHER, K. A., SACHDEV, P. S., HALLIDAY, G. M. & SCHOFIELD, P. R. 2010. Sigma nonopioid intracellular receptor 1 mutations cause frontotemporal lobar degeneration–motor neuron disease. *Annals of Neurology,* 68**,** 639-649.

MA, T. C., BUESCHER, J. L., OATIS, B., FUNK, J. A., NASH, A. J., CARRIER, R. L. & HOYT, K. R. 2007. Metformin therapy in a transgenic mouse model of Huntington's disease. *Neuroscience letters,* 411**,** 98-103.

MACDONALD, M. E., AMBROSE, C. M., DUYAO, M. P., MYERS, R. H., LIN, C., SRINIDHI, L., BARNES, G., TAYLOR, S. A., JAMES, M., GROOT, N., MACFARLANE, H., JENKINS, B., ANDERSON, M. A., WEXLER, N. S., GUSELLA, J. F., BATES, G. P., BAXENDALE, S., HUMMERICH, H., KIRBY, S., NORTH, M., YOUNGMAN, S., MOTT, R., ZEHETNER, G., SEDLACEK, Z., POUSTKA, A., FRISCHAUF, A.-M., LEHRACH, H., BUCKLER, A. J., CHURCH, D., DOUCETTE-STAMM, L., O'DONOVAN, M. C., RIBA-RAMIREZ, L., SHAH, M., STANTON, V. P., STROBEL, S. A., DRATHS, K. M., WALES, J. L., DERVAN, P., HOUSMAN, D. E., ALTHERR, M., SHIANG, R., THOMPSON, L., FIELDER, T., WASMUTH, J. J., TAGLE, D., VALDES, J., ELMER, L., ALLARD, M., CASTILLA, L., SWAROOP, M., BLANCHARD, K., COLLINS, F. S., SNELL, R., HOLLOWAY, T., GILLESPIE, K., DATSON, N., SHAW, D. & HARPER, P. S. 1993. A novel gene containing a trinucleotide repeat that is expanded and unstable on Huntington's disease chromosomes. *Cell,* 72**,** 971-983.

MACKENZIE, I., NEUMANN, M., BIGIO, E., CAIRNS, N., ALAFUZOFF, I., KRIL, J., KOVACS, G., GHETTI, B., HALLIDAY, G., HOLM, I., INCE, P., KAMPHORST, W., REVESZ, T., ROZEMULLER, A., KUMAR-SINGH, S., AKIYAMA, H., BABORIE, A., SPINA, S., DICKSON, D., TROJANOWSKI, J. & MANN, D. 2010a. Nomenclature and nosology for neuropathologic subtypes of frontotemporal lobar degeneration: an update. *Acta Neuropathologica,* 119**,** 1-4.

MACKENZIE, I. R. & FELDMAN, H. H. 2005. Ubiquitin immunohistochemistry suggests classic motor neuron disease, motor neuron disease with dementia, and frontotemporal dementia of the motor neuron disease type represent a clinicopathologic spectrum. *J Neuropathol Exp Neurol,* 64**,** 730-9.

MACKENZIE, I. R. A., BIGIO, E. H., INCE, P. G., GESER, F., NEUMANN, M., CAIRNS, N. J., KWONG, L. K., FORMAN, M. S., RAVITS, J., STEWART, H., EISEN, A., MCCLUSKY, L., KRETZSCHMAR, H. A., MONORANU, C. M., HIGHLEY, J. R., KIRBY, J., SIDDIQUE, T., SHAW, P. J., LEE, V. M. Y. & TROJANOWSKI, J. Q. 2007. Pathological TDP-43 distinguishes sporadic amyotrophic lateral sclerosis from amyotrophic lateral sclerosis with SOD1 mutations. *Annals of Neurology,* 61**,** 427-434.

MACKENZIE, I. R. A., RADEMAKERS, R. & NEUMANN, M. 2010b. TDP-43 and FUS in amyotrophic lateral sclerosis and frontotemporal dementia. *The Lancet Neurology,* 9**,** 995-1007.

MAGRANÉ, J., HERVIAS, I., HENNING, M. S., DAMIANO, M., KAWAMATA, H. & MANFREDI, G. 2009. Mutant SOD1 in neuronal mitochondria causes toxicity and mitochondrial dynamics abnormalities. *Human Molecular Genetics,* 18**,** 4552-4564.

MAHONEY, D. J., RODRIGUEZ, C., DEVRIES, M., YASUDA, N. & TARNOPOLSKY, M. A. 2004. Effects of high-intensity endurance exercise training in the G93A mouse model of amyotrophic lateral sclerosis. *Muscle & Nerve,* 29**,** 656-662.

MANSFIELD, R., GALEA, R., BRINCAT, M., HOLE, D. & MASON, H. 2003. Metformin has direct effects on human ovarian steroidogenesis. *Fertility and Sterility,* 79**,** 956-962.

MARAGAKIS, N. J., JACKSON, M., GANEL, R. & ROTHSTEIN, J. D. 2003. Topiramate protects against motor neuron degeneration in organotypic spinal cord cultures but not in G93A SOD1 transgenic mice. *Neuroscience Letters,* 338**,** 107-110.

MARIKOVSKY, M., ZIV, V., NEVO, N., HARRIS-CERRUTI, C. & MAHLER, O. 2003. Cu/Zn Superoxide Dismutase Plays Important Role in Immune Response. *The Journal of Immunology,* 170**,** 2993-3001.

MARKERT, C. D., KIM, E., GIFONDORWA, D. J., CHILDERS, M. K. & MILLIGAN, C. E. 2010. A Single-Dose Resveratrol Treatment in a Mouse Model of Amyotrophic Lateral Sclerosis. *Journal of Medicinal Food,* 13**,** 1081-1085.

MARTIN, L. J. & LIU, Z. 2007. Adult olfactory bulb neural precursor cell grafts provide temporary protection from motor neuron degeneration, improve motor function, and extend survival in amyotrophic lateral sclerosis mice. *J Neuropathol Exp Neurol,* 66**,** 1002-18.

MARTINEZ, J. A., FRANCIS, G. J., LIU, W. Q., PRADZINSKY, N., FINE, J., WILSON, M., HANSON, L. R., FREY II, W. H., ZOCHODNE, D., GORDON, T. & TOTH, C. 2008. Intranasal delivery of insulin and a nitric oxide synthase inhibitor in an experimental model of amyotrophic lateral sclerosis. *Neuroscience,* 157**,** 908-925.

MARUYAMA, H., MORINO, H., ITO, H., IZUMI, Y., KATO, H., WATANABE, Y., KINOSHITA, Y., KAMADA, M., NODERA, H., SUZUKI, H., KOMURE, O., MATSUURA, S., KOBATAKE, K., MORIMOTO, N., ABE, K., SUZUKI, N., AOKI, M., KAWATA, A., HIRAI, T., KATO, T., OGASAWARA, K., HIRANO, A., TAKUMI, T., KUSAKA, H., HAGIWARA, K., KAJI, R. & KAWAKAMI, H. 2010. Mutations of optineurin in amyotrophic lateral sclerosis. *Nature,* 465**,** 223-226.

MATTHEWS, J. N., ALTMAN, D. G., CAMPBELL, M. J. & ROYSTON, P. 1990. Analysis of serial measurements in medical research. *BMJ,* 300**,** 230-5.

MATTHEWS, R. T., YANG, L., BROWNE, S., BAIK, M. & BEAL, M. F. 1998. Coenzyme Q10 administration increases brain mitochondrial concentrations and exerts neuroprotective effects. *Proceedings of the National Academy of Sciences,* 95**,** 8892-8897.

MATTIAZZI, M., D'AURELIO, M., GAJEWSKI, C. D., MARTUSHOVA, K., KIAEI, M., BEAL, M. F. & MANFREDI, G. 2002. Mutated human SOD1 causes dysfunction of oxidative phosphorylation in mitochondria of transgenic mice. *The Journal of biological chemistry,* 277**,** 29626-29633.

MATTSON, M., CUTLER, R. & CAMANDOLA, S. 2007. Energy intake and amyotrophic lateral sclerosis. *NeuroMolecular Medicine,* 9**,** 17-20.

MCHANWELL, S. & BISCOE, T. J. 1981. The Localization of Motoneurons Supplying the Hindlimb Muscles of the Mouse. *Philosophical Transactions of the Royal Society of London. B, Biological Sciences,* 293**,** 477-508.

MCKHANN, G. M., ALBERT, M. S., GROSSMAN, M., MILLER, B., DICKSON, D. & TROJANOWSKI, J. Q. 2001. Clinical and Pathological Diagnosis of Frontotemporal Dementia: Report of the Work Group on Frontotemporal Dementia and Pick's Disease. *Arch Neurol,* 58**,** 1803-1809.

MEAD, R. J., BENNETT, E. J., KENNERLEY, A. J., SHARP, P., SUNYACH, C., KASHER, P., BERWICK, J., PETTMANN, B., BATTAGLIA, G., AZZOUZ, M., GRIERSON, A. & SHAW, P. J. 2011. Optimised and Rapid Pre-clinical Screening in the SOD1^{G93A} Transgenic Mouse Model of Amyotrophic Lateral Sclerosis (ALS). *PLoS ONE,* 6**,** e23244.

MEISSNER, F., MOLAWI, K. & ZYCHLINSKY, A. 2010. Mutant superoxide dismutase 1-induced IL-1β accelerates ALS pathogenesis. *Proceedings of the National Academy of Sciences,* 107**,** 13046-13050.

MENALLED, L., EL-KHODOR, B. F., PATRY, M., SUÁREZ-FARIÑAS, M., ORENSTEIN, S. J., ZAHASKY, B., LEAHY, C., WHEELER, V., YANG, X. W., MACDONALD, M., MORTON, A. J., BATES, G., LEEDS, J., PARK, L., HOWLAND, D., SIGNER, E., TOBIN, A. & BRUNNER, D. 2009. Systematic behavioral evaluation of Huntington's disease transgenic and knock-in mouse models. *Neurobiology of Disease,* 35**,** 319-336.

MENALLED, L. B., PATRY, M., RAGLAND, N., LOWDEN, P. A. S., GOODMAN, J., MINNICH, J., ZAHASKY, B., PARK, L., LEEDS, J., HOWLAND, D., SIGNER, E., TOBIN, A. J. & BRUNNER, D. 2010. Comprehensive Behavioral Testing in the R6/2 Mouse Model of Huntington's Disease Shows No Benefit from CoQ10 or Minocycline. *PLoS ONE,* 5**,** e9793.

METCALF, D. J., GARCIA-ARENCIBIA, M., HOCHFELD, W. E. & RUBINSZTEIN, D. C. 2010. Autophagy and misfolded proteins in neurodegeneration. *Exp Neurol*.

METCALF, D. J., GARCÍA-ARENCIBIA, M., HOCHFELD, W. E. & RUBINSZTEIN, D. C. Autophagy and misfolded proteins in neurodegeneration. *Experimental Neurology,* Nov 21. [Epub ahead of print].

MEYER, T., FROMM, A., MÜNCH, C., SCHWALENSTÖCKER, B., FRAY, A. E., INCE, P. G., STAMM, S., GRÖN, G., LUDOLPH, A. C. & SHAW, P. J. 1999. The RNA of the glutamate transporter EAAT2 is variably spliced in amyotrophic lateral sclerosis and normal individuals. *Journal of the Neurological Sciences,* 170**,** 45-50.

MIGHELI, A., AUTILIO-GAMBETTI, L., GAMBETTI, P., MOCELLINI, C., VIGLIANI, M. C. & SCHIFFER, D. 1990. Ubiquitinated filamentous inclusions in spinal cord of patients with motor neuron disease. *Neurosci Lett,* 114**,** 5-10.

MIGUEL, L., FRÉBOURG, T., CAMPION, D. & LECOURTOIS, M. 2011. Both cytoplasmic and nuclear accumulations of the protein are neurotoxic in Drosophila models of TDP-43 proteinopathies. *Neurobiology of Disease,* 41**,** 398-406.

MILLECAMPS, S., SALACHAS, F., CAZENEUVE, C., GORDON, P., BRICKA, B., CAMUZAT, A., GUILLOT-NOËL, L., RUSSAOUEN, O., BRUNETEAU, G., PRADAT, P.-F., LE FORESTIER, N., VANDENBERGHE, N., DANEL-BRUNAUD, V., GUY, N., THAUVIN-ROBINET, C., LACOMBLEZ, L., COURATIER, P., HANNEQUIN, D., SEILHEAN, D., LE BER, I., CORCIA, P., CAMU, W., BRICE, A., ROULEAU, G., LEGUERN, E. & MEININGER, V. 2010. SOD1, ANG, VAPB, TARDBP, and FUS mutations in familial amyotrophic lateral sclerosis: genotype–phenotype correlations. *Journal of Medical Genetics,* 47**,** 554-560.

MILLER, R. G., MITCHELL, J. D., LYON, M. & MOORE, D. H. 2007. Riluzole for amyotrophic lateral sclerosis (ALS)/motor neuron disease (MND). *Cochrane Database Syst Rev***,** CD001447.

MILLER, R. G., MOORE, D. H., FORSHEW, D. A., KATZ, J. S., BAROHN, R. J., VALAN, M., BROMBERG, M. B., GOSLIN, K. L., GRAVES, M. C., MCCLUSKEY, L. F., MCVEY, A. L., MOZAFFAR, T., FLORENCE, J. M., PESTRONK, A., ROSS, M., SIMPSON, E. P. & APPEL, S. H. 2011. Phase II screening trial of lithium carbonate in amyotrophic lateral sclerosis. *Neurology*.

MILLER, T. M., KASPAR, B. K., KOPS, G. J., YAMANAKA, K., CHRISTIAN, L. J., GAGE, F. H. & CLEVELAND, D. W. 2005. Virus-delivered small RNA silencing sustains strength in amyotrophic lateral sclerosis. *Annals of Neurology,* 57**,** 773-776.

MILLER, T. M., KIM, S. H., YAMANAKA, K., HESTER, M., UMAPATHI, P., ARNSON, H., RIZO, L., MENDELL, J. R., GAGE, F. H., CLEVELAND, D. W. & KASPAR, B. K. 2006. Gene transfer demonstrates that muscle is not a primary target for non-cell-autonomous toxicity in familial amyotrophic lateral sclerosis. *Proceedings of the National Academy of Sciences,* 103**,** 19546-19551.

MILLIPORE. 2011. *Radioimmunoassay (RIA) (Millipore learning center)* [Online]. Available: http://www.millipore.com/immunodetection/id3/radioimmunoassay [Accessed].

MITCHELL, J., PAUL, P., CHEN, H.-J., MORRIS, A., PAYLING, M., FALCHI, M., HABGOOD, J., PANOUTSOU, S., WINKLER, S., TISATO, V., HAJITOU, A., SMITH, B., VANCE, C., SHAW, C., MAZARAKIS, N. D. & DE BELLEROCHE, J. 2010. Familial amyotrophic lateral sclerosis is associated with a mutation in D-amino acid oxidase. *Proceedings of the National Academy of Sciences,* 107**,** 7556-7561.

MITRI, J. & HAMDY, O. 2009. Diabetes medications and body weight. *Expert Opinion on Drug Safety,* 8**,** 573-584.

MOGES, H., VASCONCELOS, O. M., CAMPBELL, W. W., BORKE, R. C., MCCOY, J. A., KACZMARCZYK, L., FENG, J. & ANDERS, J. J. 2009. Light therapy and supplementary riboflavin in the SOD1 transgenic mouse model of familial amyotrophic lateral sclerosis (FALS). *Lasers in Surgery and Medicine,* 41**,** 52-59.

MOHAJERI, M. H., FIGLEWICZ, D. A. & BOHN, M. C. 1999. Intramuscular Grafts of Myoblasts Genetically Modified to Secrete Glial Cell Line-Derived Neurotrophic Factor Prevent Motoneuron Loss and Disease Progression in a Mouse Model of Familial Amyotrophic Lateral Sclerosis. *Human Gene Therapy,* 10**,** 1853-1866.

MORENO-IGOA, M., CALVO, A., PENAS, C., MANZANO, R., OLIVÁN, S., MUÑOZ, M., MANCUSO, R., ZARAGOZA, P., AGUILERA, J., NAVARRO, X. & OSTA PINZOLAS, R. 2010. Fragment C of tetanus toxin, more than a carrier. Novel perspectives in non-viral ALS gene therapy. *Journal of Molecular Medicine,* 88**,** 297-308.

MORIMOTO, N., NAGAI, M., OHTA, Y., MIYAZAKI, K., KURATA, T., MORIMOTO, M., MURAKAMI, T., TAKEHISA, Y., IKEDA, Y., KAMIYA, T. & ABE, K. 2007. Increased autophagy in transgenic mice with a G93A mutant SOD1 gene. *Brain Research,* 1167**,** 112-117.

MORRISON, B. M., LACHEY, J. L., WARSING, L. C., TING, B. L., PULLEN, A. E., UNDERWOOD, K. W., KUMAR, R., SAKO, D., GRINBERG, A., WONG, V., COLANTUONI, E., SEEHRA, J. S. & WAGNER, K. R. 2009. A soluble activin type IIB receptor improves function in a mouse model of amyotrophic lateral sclerosis. *Experimental Neurology,* 217**,** 258-268.

MÜNCH, C., O'BRIEN, J. & BERTOLOTTI, A. 2011. Prion-like propagation of mutant superoxide dismutase-1 misfolding in neuronal cells. *Proceedings of the National Academy of Sciences,* 108**,** 3548-3553.

MUNOZ, D. G., NEUMANN, M., KUSAKA, H., YOKOTA, O., ISHIHARA, K., TERADA, S., KURODA, S. & MACKENZIE, I. R. 2009. FUS pathology in basophilic inclusion body disease. *Acta Neuropathol,* 118**,** 617-27.

MURAKAMI, T., NAGANO, I., HAYASHI, T., MANABE, Y., SHOJI, M., SETOGUCHI, Y. & ABE, K. 2001. Impaired retrograde axonal transport of adenovirus-mediated E. coli LacZ gene in the mice carrying mutant SOD1 gene. *Neurosci Lett,* 308**,** 149 - 152.

MURPHY, J. M., HENRY, R. G., LANGMORE, S., KRAMER, J. H., MILLER, B. L. & LOMEN-HOERTH, C. 2007. Continuum of Frontal Lobe Impairment in Amyotrophic Lateral Sclerosis. *Arch Neurol,* 64**,** 530-534.

NAGANO, I., ILIEVA, H., SHIOTE, M., MURAKAMI, T., YOKOYAMA, M., SHOJI, M. & ABE, K. 2005. Therapeutic benefit of intrathecal injection of insulin-like growth factor-1 in a mouse model of Amyotrophic Lateral Sclerosis. *Journal of the Neurological Sciences,* 235**,** 61-68.

NAGANO, S., FUJII, Y., YAMAMOTO, T., TANIYAMA, M., FUKADA, K., YANAGIHARA, T. & SAKODA, S. 2003. The efficacy of trientine or ascorbate alone compared to that of the combined treatment with these two agents in familial amyotrophic lateral sclerosis model mice. *Experimental Neurology,* 179**,** 176-180.

NAGANO, S., OGAWA, Y., YANAGIHARA, T. & SAKODA, S. 1999. Benefit of a combined treatment with trientine and ascorbate in familial amyotrophic lateral sclerosis model mice. *Neuroscience Letters,* 265**,** 159-162.

NAGY, D., KATO, T. & KUSHNER, P. D. 1994. Reactive astrocytes are widespread in the cortical gray matter of amyotrophic lateral sclerosis. *J Neurosci Res,* 38**,** 336-47.

NARKAR, V. A., DOWNES, M., YU, R. T., EMBLER, E., WANG, Y. X., BANAYO, E., MIHAYLOVA, M. M., NELSON, M. C., ZOU, Y., JUGUILON, H., KANG, H., SHAW, R. J. & EVANS, R. M. 2008. AMPK and PPARdelta agonists are exercise mimetics. *Cell,* 134**,** 405-415.

NATH, N., KHAN, M., PAINTLIA, M. K., HODA, M. N. & GIRI, S. 2009. Metformin Attenuated the Autoimmune Disease of the Central Nervous System in Animal Models of Multiple Sclerosis. *The Journal of Immunology,* 182**,** 8005-8014.

NEUMANN, M., RADEMAKERS, R., ROEBER, S., BAKER, M., KRETZSCHMAR, H. A. & MACKENZIE, I. R. 2009. A new subtype of frontotemporal lobar degeneration with FUS pathology. *Brain,* 132**,** 2922-31.

NEUMANN, M., SAMPATHU, D., KWONG, L., TRUAX, A., MICSENYI, M., CHOU, T., BRUCE, J., SCHUCK, T., GROSSMAN, M. & CLARK, C. 2006a. Ubiquitinated TDP-43 in frontotemporal lobar degeneration and amyotrophic lateral sclerosis. *Science,* 314**,** 130 - 133.

NEUMANN, M., SAMPATHU, D. M., KWONG, L. K., TRUAX, A. C., MICSENYI, M. C., CHOU, T. T., BRUCE, J., SCHUCK, T., GROSSMAN, M., CLARK, C. M., MCCLUSKEY, L. F., MILLER, B. L.,

MASLIAH, E., MACKENZIE, I. R., FELDMAN, H., FEIDEN, W., KRETZSCHMAR, H. A., TROJANOWSKI, J. Q. & LEE, V. M.-Y. 2006b. Ubiquitinated TDP-43 in Frontotemporal Lobar Degeneration and Amyotrophic Lateral Sclerosis. *Science,* 314**,** 130-133.

NEYMOTIN, A., CALINGASAN, N. Y., WILLE, E., NASERI, N., PETRI, S., DAMIANO, M., LIBY, K. T., RISINGSONG, R., SPORN, M., BEAL, M. F. & KIAEI, M. 2011. Neuroprotective effect of Nrf2/ARE activators, CDDO ethylamide and CDDO trifluoroethylamide, in a mouse model of amyotrophic lateral sclerosis. *Free Radical Biology and Medicine,* 51**,** 88-96.

NEYMOTIN, A., PETRI, S., CALINGASAN, N. Y., WILLE, E., SCHAFER, P., STEWART, C., HENSLEY, K., BEAL, M. F. & KIAEI, M. 2009. Lenalidomide (Revlimid®) administration at symptom onset is neuroprotective in a mouse model of amyotrophic lateral sclerosis. *Experimental Neurology,* 220**,** 191-197.

NGUYEN, M. D., D'AIGLE, T., GOWING, G., JULIEN, J.-P. & RIVEST, S. 2004. Exacerbation of Motor Neuron Disease by Chronic Stimulation of Innate Immunity in a Mouse Model of Amyotrophic Lateral Sclerosis. *The Journal of Neuroscience,* 24**,** 1340-1349.

NISHIMURA, A., AL-CHALABI, A. & ZATZ, M. 2005. A common founder for amyotrophic lateral sclerosis type 8 (ALS8) in the Brazilian population. *Human Genetics,* 118**,** 499-500.

NISHIMURA, A. L., MITNE-NETO, M., SILVA, H. C. A., RICHIERI-COSTA, A., MIDDLETON, S., CASCIO, D., KOK, F., OLIVEIRA, J. R. M., GILLINGWATER, T., WEBB, J., SKEHEL, P. & ZATZ, M. 2004. A Mutation in the Vesicle-Trafficking Protein VAPB Causes Late-Onset Spinal Muscular Atrophy and Amyotrophic Lateral Sclerosis. *The American Journal of Human Genetics,* 75**,** 822-831.

NISHITOH, H., KADOWAKI, H., NAGAI, A., MARUYAMA, T., YOKOTA, T., FUKUTOMI, H., NOGUCHI, T., MATSUZAWA, A., TAKEDA, K. & ICHIJO, H. 2008. ALS-linked mutant SOD1 induces ER stress- and ASK1-dependent motor neuron death by targeting Derlin-1. *Genes & Development,* 22**,** 1451-1464.

NONHOFF, U., RALSER, M., WELZEL, F., PICCINI, I., BALZEREIT, D., YASPO, M.-L., LEHRACH, H. & KROBITSCH, S. 2007. Ataxin-2 Interacts with the DEAD/H-Box RNA Helicase DDX6 and Interferes with P-Bodies and Stress Granules. *Molecular Biology of the Cell,* 18**,** 1385-1396.

OHNISHI, S., ITO, H., SUZUKI, Y., ADACHI, Y., WATE, R., ZHANG, J., NAKANO, S., KUSAKA, H. & IKEHARA, S. 2009. Intra-bone marrow-bone marrow transplantation slows disease progression and prolongs survival in G93A mutant SOD1 transgenic mice, an animal model mouse for amyotrophic lateral sclerosis. *Brain Research,* 1296**,** 216-224.

OHTA, Y., KAMIYA, T., NAGAI, M., NAGATA, T., MORIMOTO, N., MIYAZAKI, K., MURAKAMI, T., KURATA, T., TAKEHISA, Y., IKEDA, Y., ASOH, S., OHTA, S. & ABE, K. 2008. Therapeutic benefits of intrathecal protein therapy in a mouse model of amyotrophic lateral sclerosis. *Journal of Neuroscience Research,* 86**,** 3028-3037.

OHTA, Y., NAGAI, M., NAGATA, T., MURAKAMI, T., NAGANO, I., NARAI, H., KURATA, T., SHIOTE, M., SHOJI, M. & ABE, K. 2006. Intrathecal injection of epidermal growth factor and fibroblast growth factor 2 promotes proliferation of neural precursor cells in the spinal cords of mice with mutant human SOD1 gene. *Journal of Neuroscience Research,* 84**,** 980-992.

OKADO-MATSUMOTO, A. & FRIDOVICH, I. 2002. Amyotrophic lateral sclerosis: A proposed mechanism. *Proceedings of the National Academy of Sciences,* 99**,** 9010-9014.

OOSTHUYSE, B., MOONS, L., STORKEBAUM, E., BECK, H., NUYENS, D., BRUSSELMANS, K., VAN DORPE, J., HELLINGS, P., GORSELINK, M., HEYMANS, S., THEILMEIER, G., DEWERCHIN, M., LAUDENBACH, V., VERMYLEN, P., RAAT, H., ACKER, T., VLEMINCKX, V., VAN DEN BOSCH, L., CASHMAN, N., FUJISAWA, H., DROST, M. R., SCIOT, R., BRUYNINCKX, F., HICKLIN, D. J., INCE, C., GRESSENS, P., LUPU, F., PLATE, K. H., ROBBERECHT, W., HERBERT, J. M., COLLEN, D. & CARMELIET, P. 2001. Deletion of the hypoxia-response element in the vascular endothelial growth factor promoter causes motor neuron degeneration. *Nat Genet,* 28**,** 131-8.

ORLACCHIO, A., BABALINI, C., BORRECA, A., PATRONO, C., MASSA, R., BASARAN, S., MUNHOZ, R. P., ROGAEVA, E. A., ST GEORGE-HYSLOP, P. H., BERNARDI, G. & KAWARAI, T. 2010. SPATACSIN mutations cause autosomal recessive juvenile amyotrophic lateral sclerosis. *Brain,* 133**,** 591-598.

OUSLIMANI, N., PEYNET, J., BONNEFONT-ROUSSELOT, D., THÉROND, P., LEGRAND, A. & BEAUDEUX, J.-L. 2005. Metformin decreases intracellular production of reactive oxygen species in aortic endothelial cells. *Metabolism,* 54**,** 829-834.

PAMPHLETT, R., TODD, E., VINK, R., MCQUILTY, R. & CHEEMA, S. S. 2003. Magnesium supplementation does not delay disease onset or increase survival in a mouse model of familial ALS. *Journal of the Neurological Sciences,* 216**,** 95-98.

PAPADIMITRIOU, D., LE VERCHE, V., JACQUIER, A., IKIZ, B., PRZEDBORSKI, S. & RE, D. B. 2010. Inflammation in ALS and SMA: Sorting out the good from the evil. *Neurobiology of disease,* 37**,** 493-502.

PARK, J.-H., HONG, Y.-H., KIM, H.-J., KIM, S.-M., KIM, M.-J., PARK, K.-S., SUNG, J.-J. & LEE, K.-W. 2007. Pyruvate slows disease progression in a G93A SOD1 mutant transgenic mouse model. *Neuroscience Letters,* 413**,** 265-269.

PARK, S., KIM, H. T., YUN, S., KIM, I. S., LEE, J., LEE, I. S. & PARK, K. I. 2009. Growth factor-expressing human neural progenitor cell grafts protect motor neurons but do not ameliorate motor performance and survival in ALS mice. *Exp Mol Med,* 41**,** 487-500.

PASINELLI, P., HOUSEWEART, M., BROWN, R. & CLEVELAND, D. 2000. Caspase-1 and -3 are sequentially activated in motor neuron death in Cu, Zn superoxide dismutase-mediated familial amyotrophic lateral sclerosis. *Proc Natl Acad Sci USA,* 97**,** 13901 - 13906.

PASQUALI, L., BUSCETI, C. L., FULCERI, F., PAPARELLI, A. & FORNAI, F. 2010. Intracellular pathways underlying the effects of lithium. *Behav Pharmacol,* 21**,** 473-92.

PATEL, B. P., SAFDAR, A., RAHA, S., TARNOPOLSKY, M. A. & HAMADEH, M. J. 2010. Caloric Restriction Shortens Lifespan through an Increase in Lipid Peroxidation, Inflammation and Apoptosis in the G93A Mouse, an Animal Model of ALS. *PLoS ONE,* 5**,** e9386.

PEDERSEN, W. A. & MATTSON, M. P. 1999. No benefit of dietary restriction on disease onset or progression in amyotrophic lateral sclerosis Cu/Zn-superoxide dismutase mutant mice. *Brain Research,* 833**,** 117-120.

PEDRINI, S., SAU, D., GUARESCHI, S., BOGUSH, M., BROWN, R. H., NANICHE, N., KIA, A., TROTTI, D. & PASINELLI, P. 2010. ALS-linked mutant SOD1 damages mitochondria by promoting conformational changes in Bcl-2. *Human Molecular Genetics,* 19**,** 2974-2986.

PETRI, S., CALINGASAN, N. Y., ALSAIED, O. A., WILLE, E., KIAEI, M., FRIEDMAN, J. E., BARANOVA, O., CHAVEZ, J. C. & BEAL, M. F. 2007. The lipophilic metal chelators DP-109 and DP-460 are neuroprotective in a transgenic mouse model of amyotrophic lateral sclerosis. *Journal of Neurochemistry,* 102**,** 991-1000.

PETRI, S., KIAEI, M., DAMIANO, M., HILLER, A., WILLE, E., MANFREDI, G., CALINGASAN, N. Y., SZETO, H. H. & BEAL, M. F. 2006a. Cell-permeable peptide antioxidants as a novel therapeutic approach in a mouse model of amyotrophic lateral sclerosis. *Journal of Neurochemistry,* 98**,** 1141-1148.

PETRI, S., KIAEI, M., KIPIANI, K., CHEN, J., CALINGASAN, N. Y., CROW, J. P. & BEAL, M. F. 2006b. Additive neuroprotective effects of a histone deacetylase inhibitor and a catalytic antioxidant in a transgenic mouse model of amyotrophic lateral sclerosis. *Neurobiology of Disease,* 22**,** 40-49.

PHILIPS, T. & ROBBERECHT, W. 2011. Neuroinflammation in amyotrophic lateral sclerosis: role of glial activation in motor neuron disease. *The Lancet Neurology,* 10**,** 253-263.

PITZER, C., KRÜGER, C., PLAAS, C., KIRSCH, F., DITTGEN, T., MÜLLER, R., LAAGE, R., KASTNER, S., SUESS, S., SPOELGEN, R., HENRIQUES, A., EHRENREICH, H., SCHÄBITZ, W.-R., BACH, A. &

SCHNEIDER, A. 2008. Granulocyte-colony stimulating factor improves outcome in a mouse model of amyotrophic lateral sclerosis. *Brain,* 131**,** 3335-3347.

PIZZASEGOLA, C., CARON, I., DALENO, C., RONCHI, A., MINOIA, C., CARRI, M. T. & BENDOTTI, C. 2009. Treatment with lithium carbonate does not improve disease progression in two different strains of SOD1 mutant mice. *Amyotroph Lateral Scler,* 10**,** 221-8.

PODUSLO, J. F., WHELAN, S. L., CURRAN, G. L. & WENGENACK, T. M. 2000. Therapeutic benefit of polyamine-modified catalase as a scavenger of hydrogen peroxide and nitric oxide in familial amyotrophic lateral sclerosis transgenics. *Ann Neurol,* 48**,** 943-7.

POLEY, W. 1974. Emotionality related to maternal cannibalism in BALB and C57BL mice. *Learning & Behavior,* 2**,** 241-244.

POLLARI, E., SAVCHENKO, E., JARONEN, M., KANNINEN, K., MALM, T., WOJCIECHOWSKI, S., AHTONIEMI, T., GOLDSTEINS, G., GINIATULLINA, R., GINIATULLIN, R., KOISTINAHO, J. & MAGGA, J. 2011. Granulocyte colony stimulating factor attenuates inflammation in a mouse model of amyotrophic lateral sclerosis. *Journal of Neuroinflammation,* 8**,** 74.

POMPL, P. N., HO, L., BIANCHI, M., MCMANUS, T., QIN, W. & PASINETTI, G. M. 2003. A therapeutic role for cyclooxygenase-2 inhibitors in a transgenic mouse model of amyotrophic lateral sclerosis. *The FASEB Journal*.

PULS, I., JONNAKUTY, C., LAMONTE, B. H., HOLZBAUR, E. L. F., TOKITO, M., MANN, E., FLOETER, M. K., BIDUS, K., DRAYNA, D., OH, S. J., BROWN, R. H., LUDLOW, C. L. & FISCHBECK, K. H. 2003. Mutant dynactin in motor neuron disease. *Nat Genet,* 33**,** 455-456.

PUN, S., SANTOS, A. F., SAXENA, S., XU, L. & CARONI, P. 2006. Selective vulnerability and pruning of phasic motoneuron axons in motoneuron disease alleviated by CNTF. *Nat Neurosci,* 9**,** 408-419.

RAKHIT, R. & CHAKRABARTTY, A. 2006. Structure, folding, and misfolding of Cu,Zn superoxide dismutase in amyotrophic lateral sclerosis. *Biochimica et Biophysica Acta (BBA) - Molecular Basis of Disease,* 1762**,** 1025-1037.

RAKHIT, R., ROBERTSON, J., VELDE, C. V., HORNE, P., RUTH, D. M., GRIFFIN, J., CLEVELAND, D. W., CASHMAN, N. R. & CHAKRABARTTY, A. 2007. An immunological epitope selective for pathological monomer-misfolded SOD1 in ALS. *Nat Med,* 13**,** 754-759.

RALPH, G., RADCLIFFE, P., DAY, D., CARTHY, J., LEROUX, M., LEE, D., WONG, L., BILSLAND, L., GREENSMITH, L., KINGSMAN, S., MITROPHANOUS, K., MAZARAKIS, N. & AZZOUZ, M. 2005. Silencing mutant SOD1 using RNAi protects against neurodegeneration and extends survival in an ALS model. *Nat Med,* 11**,** 429 - 433.

RAMAN, C., MCALLISTER, S. D., RIZVI, G., PATEL, S. G., MOORE, D. H. & ABOOD, M. E. 2004. Amyotrophic lateral sclerosis: delayed disease progression in mice by treatment with a cannabinoid. *Amyotrophic Lateral Sclerosis,* 5**,** 33-39.

RAOUL, C., ABBAS-TERKI, T., BENSADOUN, J.-C., GUILLOT, S., HAASE, G., SZULC, J., HENDERSON, C. E. & AEBISCHER, P. 2005. Lentiviral-mediated silencing of SOD1 through RNA interference retards disease onset and progression in a mouse model of ALS. *Nat Med,* 11**,** 423-428.

RASHIDIPOUR, O. & CHAN, K. M. 2008. Motor unit number estimation in neuromuscular disease. *Can J Neurol Sci,* 35**,** 153-9.

RATOVITSKI, T., CORSON, L. B., STRAIN, J., WONG, P., CLEVELAND, D. W., CULOTTA, V. C. & BORCHELT, D. R. 1999. Variation in the Biochemical/Biophysical Properties of Mutant Superoxide Dismutase 1 Enzymes and the Rate of Disease Progression in Familial Amyotrophic Lateral Sclerosis Kindreds. *Human Molecular Genetics,* 8**,** 1451-1460.

RAVIKUMAR, B., SARKAR, S., DAVIES, J. E., FUTTER, M., GARCIA-ARENCIBIA, M., GREEN-THOMPSON, Z. W., JIMENEZ-SANCHEZ, M., KOROLCHUK, V. I., LICHTENBERG, M., LUO, S., MASSEY, D. C. O., MENZIES, F. M., MOREAU, K., NARAYANAN, U., RENNA, M., SIDDIQI, F. H., UNDERWOOD,

B. R., WINSLOW, A. R. & RUBINSZTEIN, D. C. 2010. Regulation of Mammalian Autophagy in Physiology and Pathophysiology. *Physiological Reviews,* 90**,** 1383-1435.

RAVITS, J., PAUL, P. & JORG, C. 2007. Focality of upper and lower motor neuron degeneration at the clinical onset of ALS. *Neurology,* 68**,** 1571-1575.

REAGAN-SHAW, S., NIHAL, M. & AHMAD, N. 2008. Dose translation from animal to human studies revisited. *The FASEB Journal,* 22**,** 659-661.

REAUME, A. G., ELLIOTT, J. L., HOFFMAN, E. K., KOWALL, N. W., FERRANTE, R. J., SIWEK, D. F., WILCOX, H. M., FLOOD, D. G., BEAL, M. F., BROWN, R. H., JR., SCOTT, R. W. & SNIDER, W. D. 1996. Motor neurons in Cu/Zn superoxide dismutase-deficient mice develop normally but exhibit enhanced cell death after axonal injury. *Nature genetics,* 13**,** 43-47.

REINHOLZ, M. M., MERKLE, C. M. & PODUSLO, J. F. 1999. Therapeutic Benefits of Putrescine-Modified Catalase in a Transgenic Mouse Model of Familial Amyotrophic Lateral Sclerosis. *Experimental Neurology,* 159**,** 204-216.

REMBACH, A., TURNER, B. J., BRUCE, S., CHEAH, I. K., SCOTT, R. L., LOPES, E. C., ZAGAMI, C. J., BEART, P. M., CHEUNG, N. S., LANGFORD, S. J. & CHEEMA, S. S. 2004. Antisense peptide nucleic acid targeting GluR3 delays disease onset and progression in the SOD1 G93A mouse model of familial ALS. *Journal of Neuroscience Research,* 77**,** 573-582.

RENTON, A. E., MAJOUNIE, E., WAITE, A., SIMON-SANCHEZ, J., ROLLINSON, S., GIBBS, J. R., SCHYMICK, J. C., LAAKSOVIRTA, H., VAN SWIETEN, J. C., MYLLYKANGAS, L., KALIMO, H., PAETAU, A., ABRAMZON, Y., REMES, A. M., KAGANOVICH, A., SCHOLZ, S. W., DUCKWORTH, J., DING, J., HARMER, D. W., HERNANDEZ, D. G., JOHNSON, J. O., MOK, K., RYTEN, M., TRABZUNI, D., GUERREIRO, R. J., ORRELL, R. W., NEAL, J., MURRAY, A., PEARSON, J., JANSEN, I. E., SONDERVAN, D., SEELAAR, H., BLAKE, D., YOUNG, K., HALLIWELL, N., CALLISTER, J. B., TOULSON, G., RICHARDSON, A., GERHARD, A., SNOWDEN, J., MANN, D., NEARY, D., NALLS, M. A., PEURALINNA, T., JANSSON, L., ISOVIITA, V. M., KAIVORINNE, A. L., HOLTTA-VUORI, M., IKONEN, E., SULKAVA, R., BENATAR, M., WUU, J., CHIO, A., RESTAGNO, G., BORGHERO, G., SABATELLI, M., HECKERMAN, D., ROGAEVA, E., ZINMAN, L., ROTHSTEIN, J. D., SENDTNER, M., DREPPER, C., EICHLER, E. E., ALKAN, C., ABDULLAEV, Z., PACK, S. D., DUTRA, A., PAK, E., HARDY, J., SINGLETON, A., WILLIAMS, N. M., HEUTINK, P., PICKERING-BROWN, S., MORRIS, H. R., TIENARI, P. J. & TRAYNOR, B. J. 2011. A Hexanucleotide Repeat Expansion in C9ORF72 Is the Cause of Chromosome 9p21-Linked ALS-FTD. *Neuron*.

RICE, S., PELLATT, L., RAMANATHAN, K., WHITEHEAD, S. A. & MASON, H. D. 2009. Metformin Inhibits Aromatase via an Extracellular Signal-Regulated Kinase-Mediated Pathway. *Endocrinology,* 150**,** 4794-4801.

RICHARDS, A. B., KRAKOWKA, S., DEXTER, L. B., SCHMID, H., WOLTERBEEK, A. P. M., WAALKENS-BERENDSEN, D. H., SHIGOYUKI, A. & KURIMOTO, M. 2002. Trehalose: a review of properties, history of use and human tolerance, and results of multiple safety studies. *Food and Chemical Toxicology,* 40**,** 871-898.

RIDDOCH-CONTRERAS, J., YANG, S.-Y., DICK, J. R. T., GOLDSPINK, G., ORRELL, R. W. & GREENSMITH, L. 2009. Mechano-growth factor, an IGF-I splice variant, rescues motoneurons and improves muscle function in SOD1G93A mice. *Experimental Neurology,* 215**,** 281-289.

ROBINSON, V., ANDERSON, D., CARVER, J. F. A., FRANCIS, R. J., HUBRECHT, R., JENKINS, E., MATHERS, K. E., RAYMOND, R., ROSEWELL, I., WALLACE, J. & WELLS, D. J. 2003. Refinement and reduction in production of genetically modified mice. *Lab Anim,* 37 Suppl 1**,** S1-S49.

RODGERS, J. T., LERIN, C., GERHART-HINES, Z. & PUIGSERVER, P. 2008. Metabolic adaptations through the PGC-1[alpha] and SIRT1 pathways. *FEBS Letters,* 582**,** 46-53.

RODRÍGUEZ-NAVARRO, J. A., RODRÍGUEZ, L., CASAREJOS, M. J., SOLANO, R. M., GÓMEZ, A., PERUCHO, J., CUERVO, A. M., GARCÍA DE YÉBENES, J. & MENA, M. A. 2010. Trehalose

ameliorates dopaminergic and tau pathology in parkin deleted/tau overexpressing mice through autophagy activation. *Neurobiology of disease,* 39**,** 423-438.

ROSEN, D., SIDDIQUE, T., PATTERSON, D., FIGLEWICZ, D., SAPP, P., HENTATI, A., DONALDSON, D., GOTO, J., O'REGAN, J. & DENG, H. 1993a. Mutations in Cu/Zn superoxide dismutase gene are associated with familial amyotrophic lateral sclerosis. *Nature,* 362**,** 59 - 62.

ROTHSTEIN, J., VAN KAMMEN, M., LEVEY, A., MARTIN, L. & KUNCL, R. 1995. Selective loss of glial glutamate transporter GLT-1 in amyotrophic lateral sclerosis. *Ann Neurol,* 38**,** 73 - 84.

ROTHSTEIN, J. D., PATEL, S., REGAN, M. R., HAENGGELI, C., HUANG, Y. H., BERGLES, D. E., JIN, L., DYKES HOBERG, M., VIDENSKY, S., CHUNG, D. S., TOAN, S. V., BRUIJN, L. I., SU, Z.-Z., GUPTA, P. & FISHER, P. B. 2005. [beta]-Lactam antibiotics offer neuroprotection by increasing glutamate transporter expression. *Nature,* 433**,** 73-77.

ROUAUX, C., PANTELEEVA, I., RENÉ, F., GONZALEZ DE AGUILAR, J.-L., ECHANIZ-LAGUNA, A., DUPUIS, L., MENGER, Y., BOUTILLIER, A.-L. & LOEFFLER, J.-P. 2007. Sodium Valproate Exerts Neuroprotective Effects In Vivo through CREB-Binding Protein-Dependent Mechanisms But Does Not Improve Survival in an Amyotrophic Lateral Sclerosis Mouse Model. *The Journal of Neuroscience,* 27**,** 5535-5545.

ROULEAU, G. A., CLARK, A. W., ROOKE, K., PRAMATAROVA, A., KRIZUS, A., SUCHOWERSKY, O., JULIEN, J. P. & FIGLEWICZ, D. 1996. SOD1 mutation is associated with accumulation of neurofilaments in amyotrophic lateral sclerosis. *Ann Neurol,* 39**,** 128-31.

ROWLAND, L. P. & SHNEIDER, N. A. 2001. Amyotrophic Lateral Sclerosis. *New England Journal of Medicine,* 344**,** 1688-1700.

RYU, H., SMITH, K., CAMELO, S. I., CARRERAS, I., LEE, J., IGLESIAS, A. H., DANGOND, F., CORMIER, K. A., CUDKOWICZ, M. E., H. BROWN, R. & FERRANTE, R. J. 2005. Sodium phenylbutyrate prolongs survival and regulates expression of anti-apoptotic genes in transgenic amyotrophic lateral sclerosis mice. *Journal of Neurochemistry,* 93**,** 1087-1098.

SAENZ, A., FERNANDEZ-ESTEBAN, I., MATAIX, A., AUSEJO, M., ROQUE, M. & MOHER, D. 2005. Metformin monotherapy for type 2 diabetes mellitus. *Cochrane database of systematic reviews (Online),* (3)**,** CD002966.

SAG, D., CARLING, D., STOUT, R. D. & SUTTLES, J. 2008. Adenosine 5'-Monophosphate-Activated Protein Kinase Promotes Macrophage Polarization to an Anti-Inflammatory Functional Phenotype. *The Journal of Immunology,* 181**,** 8633-8641.

SAPP, P. C., HOSLER, B. A., MCKENNA-YASEK, D., CHIN, W., GANN, A., GENISE, H., GORENSTEIN, J., HUANG, M., SAILER, W., SCHEFFLER, M., VALESKY, M., HAINES, J. L., PERICAK-VANCE, M., SIDDIQUE, T., HORVITZ, H. R. & BROWN JR, R. H. 2003. Identification of Two Novel Loci for Dominantly Inherited Familial Amyotrophic Lateral Sclerosis. *The American Journal of Human Genetics,* 73**,** 397-403.

SARKAR, S., DAVIES, J. E., HUANG, Z., TUNNACLIFFE, A. & RUBINSZTEIN, D. C. 2007. Trehalose, a Novel mTOR-independent Autophagy Enhancer, Accelerates the Clearance of Mutant Huntingtin and Î±-Synuclein. *Journal of Biological Chemistry,* 282**,** 5641-5652.

SARKAR, S., FLOTO, R. A., BERGER, Z., IMARISIO, S., CORDENIER, A., PASCO, M., COOK, L. J. & RUBINSZTEIN, D. C. 2005. Lithium induces autophagy by inhibiting inositol monophosphatase. *The Journal of Cell Biology,* 170**,** 1101-1111.

SARKAR, S. & RUBINSZTEIN, D. C. 2008. Small molecule enhancers of autophagy for neurodegenerative diseases. *Molecular BioSystems,* 4**,** 895-901.

SASAKI, S. 2011. Autophagy in spinal cord motor neurons in sporadic amyotrophic lateral sclerosis. *J Neuropathol Exp Neurol,* 70**,** 349-59.

SASAKI, S. & IWATA, M. 1996. Dendritic synapses of anterior horn neurons in amyotrophic lateral sclerosis: an ultrastructural study. *Acta Neuropathol,* 91**,** 278-83.

SASAKI, S. & IWATA, M. 2007. Mitochondrial alterations in the spinal cord of patients with sporadic amyotrophic lateral sclerosis. *J Neuropathol Exp Neurol,* 66**,** 10-6.

SAU, D., RUSMINI, P., CRIPPA, V., ONESTO, E., BOLZONI, E., RATTI, A. & POLETTI, A. 2011. Dysregulation of axonal transport and motorneuron diseases. *Biology of the Cell,* 103**,** 87-107.

SAXENA, S., CABUY, E. & CARONI, P. 2009. A role for motoneuron subtype-selective ER stress in disease manifestations of FALS mice. *Nat Neurosci,* 12**,** 627-636.

SCHIFFER, D., CORDERA, S., CAVALLA, P. & MIGHELI, A. 1996. Reactive astrogliosis of the spinal cord in amyotrophic lateral sclerosis. *J Neurol Sci,* 139 Suppl**,** 27-33.

SCHNEEBERGER, C., SPEISER, P., KURY, F. & ZEILLINGER, R. 1995. Quantitative detection of reverse transcriptase-PCR products by means of a novel and sensitive DNA stain. *PCR Methods Appl,* 4**,** 234-8.

SCHRODER, M. & KAUFMAN, R. J. 2005. The mammalian unfolded protein response. *Annu Rev Biochem,* 74**,** 739-89.

SCHUTZ, B., REIMANN, J., DUMITRESCU-OZIMEK, L., KAPPES-HORN, K., LANDRETH, G. E., SCHURMANN, B., ZIMMER, A. & HENEKA, M. T. 2005. The Oral Antidiabetic Pioglitazone Protects from Neurodegeneration and Amyotrophic Lateral Sclerosis-Like Symptoms in Superoxide Dismutase-G93A Transgenic Mice. *J. Neurosci.,* 25**,** 7805-7812.

SCOTT, S., KRANZ, J. E., COLE, J., LINCECUM, J. M., THOMPSON, K., KELLY, N., BOSTROM, A., THEODOSS, J., AL-NAKHALA, B. M., VIEIRA, F. G., RAMASUBBU, J. & HEYWOOD, J. A. 2008. Design, power, and interpretation of studies in the standard murine model of ALS. *Amyotrophic lateral sclerosis : official publication of the World Federation of Neurology Research Group on Motor Neuron Diseases,* 9**,** 4-15.

SEKIYA, M., ICHIYANAGI, T., IKESHIRO, Y. & YOKOZAWA, T. 2009. The Chinese Prescription Wen-Pi-Tang Extract Delays Disease Onset in Amyotrophic Lateral Sclerosis Model Mice While Attenuating the Activation of Glial Cells in the Spinal Cord. *Biological & Pharmaceutical Bulletin,* 32**,** 382-388.

SEO, J.-S., BAEK, I.-S., LEEM, Y.-H., KIM, T.-K., CHO, Y., LEE, S. M., PARK, Y. H. & HAN, P.-L. 2011. SK-PC-B70M alleviates neurologic symptoms in G93A-SOD1 amyotrophic lateral sclerosis mice. *Brain Research,* 1368**,** 299-307.

SHAN, X., CHIANG, P.-M., PRICE, D. L. & WONG, P. C. 2010. Altered distributions of Gemini of coiled bodies and mitochondria in motor neurons of TDP-43 transgenic mice. *Proceedings of the National Academy of Sciences,* 107**,** 16325-16330.

SHARP, P. S., AKBAR, M. T., BOURI, S., SENDA, A., JOSHI, K., CHEN, H.-J., LATCHMAN, D. S., WELLS, D. J. & DE BELLEROCHE, J. 2008. Protective effects of heat shock protein 27 in a model of ALS occur in the early stages of disease progression. *Neurobiology of disease,* 30**,** 42-55.

SHARP, P. S., DICK, J. R. & GREENSMITH, L. 2005. The effect of peripheral nerve injury on disease progression in the SOD1(G93A) mouse model of amyotrophic lateral sclerosis. *Neuroscience,* 130**,** 897-910.

SHAW, B. F., LELIE, H. L., DURAZO, A., NERSISSIAN, A. M., XU, G., CHAN, P. K., GRALLA, E. B., TIWARI, A., HAYWARD, L. J., BORCHELT, D. R., VALENTINE, J. S. & WHITELEGGE, J. P. 2008. Detergent-insoluble Aggregates Associated with Amyotrophic Lateral Sclerosis in Transgenic Mice Contain Primarily Full-length, Unmodified Superoxide Dismutase-1. *Journal of Biological Chemistry,* 283**,** 8340-8350.

SHEFNER, J. M., BROWN, R. H., COLE, D., CHATURVEDI, P., SCHOENFELD, D., PASTUSZAK, K., MATTHEWS, R., UPTON–RICE, M. & CUDKOWICZ, M. E. 2001. Effect of neurophilin ligands on motor units in mice with SOD1 ALS mutations. *Neurology,* 57**,** 1857-1861.

SHEFNER, J. M., CUDKOWICZ, M. E. & BROWN, R. H. 2002. Comparison of incremental with multipoint MUNE methods in transgenic ALS mice. *Muscle & Nerve,* 25**,** 39-42.

SHEFNER, J. M., REAUME, A. G., FLOOD, D. G., SCOTT, R. W., KOWALL, N. W., FERRANTE, R. J., SIWEK, D. F., UPTON–RICE, M. & BROWN, R. H. 1999. Mice lacking cytosolic copper/zinc superoxide dismutase display a distinctive motor axonopathy. *Neurology,* 53**,** 1239.

SHI, P., WEI, Y., ZHANG, J., GAL, J. & ZHU, H. 2010. Mitochondrial dysfunction is a converging point of multiple pathological pathways in amyotrophic lateral sclerosis. *J Alzheimers Dis,* 20 Suppl 2**,** S311-24.

SHIMAZAWA, M., TANAKA, H., ITO, Y., MORIMOTO, N., TSURUMA, K., KADOKURA, M., TAMURA, S., INOUE, T., YAMADA, M., TAKAHASHI, H., WARITA, H., AOKI, M. & HARA, H. 2010. An Inducer of VGF Protects Cells against ER Stress-Induced Cell Death and Prolongs Survival in the Mutant SOD1 Animal Models of Familial ALS. *PLoS ONE,* 5**,** e15307.

SHIMOJO, Y., KOSAKA, K., NODA, Y., SHIMIZU, T. & SHIRASAWA, T. 2010. Effect of rosmarinic acid in motor dysfunction and life span in a mouse model of familial amyotrophic lateral sclerosis. *Journal of Neuroscience Research,* 88**,** 896-904.

SHIN, J. H., CHO, S. I., LIM, H. R., LEE, J. K., LEE, Y. A., NOH, J. S., JOO, I. S., KIM, K.-W. & GWAG, B. J. 2007. Concurrent Administration of Neu2000 and Lithium Produces Marked Improvement of Motor Neuron Survival, Motor Function, and Mortality in a Mouse Model of Amyotrophic Lateral Sclerosis. *Molecular Pharmacology,* 71**,** 965-975.

SHINDER, G. A., LACOURSE, M.-C., MINOTTI, S. & DURHAM, H. D. 2001. Mutant Cu/Zn-Superoxide Dismutase Proteins Have Altered Solubility and Interact with Heat Shock/Stress Proteins in Models of Amyotrophic Lateral Sclerosis. *Journal of Biological Chemistry,* 276**,** 12791-12796.

SHOEMAKER, J. L., SEELY, K. A., REED, R. L., CROW, J. P. & PRATHER, P. L. 2007. The CB2 cannabinoid agonist AM-1241 prolongs survival in a transgenic mouse model of amyotrophic lateral sclerosis when initiated at symptom onset. *Journal of Neurochemistry,* 101**,** 87-98.

SHOSHAN-BARMATZ, V., DE PINTO, V., ZWECKSTETTER, M., RAVIV, Z., KEINAN, N. & ARBEL, N. 2010. VDAC, a multi-functional mitochondrial protein regulating cell life and death. *Molecular Aspects of Medicine,* 31**,** 227-285.

SICILIANO, G., D'AVINO, C., DEL CORONA, A., BARSACCHI, R., KUSMIC, C., ROCCHI, A., PASTORINI, E. & MURRI, L. 2002. Impaired oxidative metabolism and lipid peroxidation in exercising muscle from ALS patients. *Amyotroph Lateral Scler Other Motor Neuron Disord,* 3**,** 57-62.

SILVER, L. M. 1995. *Mouse Genetics: Concepts and Applications*

Oxford University Press.

SINADINOS, C. & MUDHER, A. 2011. Keeping it Together. Axonal Transport to the Synapse and the Effects of Molecular Chaperones in Health and Disease

Folding for the Synapse. *In:* WYTTENBACH, A. & O'CONNOR, V. (eds.). Springer US.

SINGER, M. A. & LINDQUIST, S. 1998. Multiple Effects of Trehalose on Protein Folding In Vitro and In Vivo. *Molecular Cell,* 1**,** 639-648.

SINGH, S., SWARNKAR, S., GOSWAMI, P. & NATH, C. 2011. Astrocytes and Microglia: Responses to Neuropathological Conditions. *Int J Neurosci*.

SMITH, R. A., MILLER, T. M., YAMANAKA, K., MONIA, B. P., CONDON, T. P., HUNG, G., LOBSIGER, C. S., WARD, C. M., MCALONIS-DOWNES, M., WEI, H., WANCEWICZ, E. V., BENNETT, C. F. & CLEVELAND, D. W. 2006. Antisense oligonucleotide therapy for neurodegenerative disease. *The Journal of Clinical Investigation,* 116**,** 2290-2296.

SNOW, R. J., TURNBULL, J., DA SILVA, S., JIANG, F. & TARNOPOLSKY, M. A. 2003. Creatine supplementation and riluzole treatment provide similar beneficial effects in copper, zinc superoxide dismutase (G93A) transgenic mice. *Neuroscience,* 119**,** 661-667.

SOFRONIEW, M. & VINTERS, H. 2010. Astrocytes: biology and pathology. *Acta Neuropathologica,* 119**,** 7-35.

SOFRONIEW, M. V. 2009. Molecular dissection of reactive astrogliosis and glial scar formation. *Trends in neurosciences,* 32**,** 638-647.

SOLOMON, J. N., LEWIS, C.-A. B., AJAMI, B., CORBEL, S. Y., ROSSI, F. M. V. & KRIEGER, C. 2006. Origin and distribution of bone marrow-derived cells in the central nervous system in a mouse model of amyotrophic lateral sclerosis. *Glia,* 53**,** 744-753.

SREEDHARAN, J., BLAIR, I., TRIPATHI, V., HU, X., VANCE, C., ROGELJ, B., ACKERLEY, S., DURNALL, J., WILLIAMS, K. & BURATTI, E. 2008. TDP-43 mutations in familial and sporadic amyotrophic lateral sclerosis. *Science,* 319**,** 1668 - 1672.

SRIVIDHYA, S., RAVICHANDRAN, M. K. & ANURADHA, C. V. 2002. Metformin attenuates blood lipid peroxidation and potentiates antioxidant defense in high fructose-fed rats. *J Biochem Mol Biol Biophys,* 6**,** 379-85.

ST-PIERRE, J., DRORI, S., ULDRY, M., SILVAGGI, J. M., RHEE, J., JÄGER, S., HANDSCHIN, C., ZHENG, K., LIN, J., YANG, W., SIMON, D. K., BACHOO, R. & SPIEGELMAN, B. M. 2006. Suppression of Reactive Oxygen Species and Neurodegeneration by the PGC-1 Transcriptional Coactivators. *Cell,* 127**,** 397-408.

STADELMANN, C. 2011. Multiple sclerosis as a neurodegenerative disease: pathology, mechanisms and therapeutic implications. *Curr Opin Neurol*.

STAM, N. C., NITHIANANTHARAJAH, J., HOWARD, M. L., ATKIN, J. D., CHEEMA, S. S. & HANNAN, A. J. 2008. Sex-specific behavioural effects of environmental enrichment in a transgenic mouse model of amyotrophic lateral sclerosis. *European Journal of Neuroscience,* 28**,** 717-723.

STORKEBAUM, E., LAMBRECHTS, D., DEWERCHIN, M., MORENO-MURCIANO, M.-P., APPELMANS, S., OH, H., VAN DAMME, P., RUTTEN, B., MAN, W. Y., DE MOL, M., WYNS, S., MANKA, D., VERMEULEN, K., VAN DEN BOSCH, L., MERTENS, N., SCHMITZ, C., ROBBERECHT, W., CONWAY, E. M., COLLEN, D., MOONS, L. & CARMELIET, P. 2005. Treatment of motoneuron degeneration by intracerebroventricular delivery of VEGF in a rat model of ALS. *Nat Neurosci,* 8**,** 85-92.

STUMVOLL, M., NURJHAN, N., PERRIELLO, G., DAILEY, G. & GERICH, J. E. 1995. Metabolic Effects of Metformin in Non-Insulin-Dependent Diabetes Mellitus. *New England Journal of Medicine,* 333**,** 550-554.

SUGAI, F., YAMAMOTO, Y., MIYAGUCHI, K., ZHOU, Z., SUMI, H., HAMASAKI, T., GOTO, M. & SAKODA, S. 2004. Benefit of valproic acid in suppressing disease progression of ALS model mice. *European Journal of Neuroscience,* 20**,** 3179-3183.

SUN, Z., DIAZ, Z., FANG, X., HART, M. P., CHESI, A., SHORTER, J. & GITLER, A. D. 2011. Molecular Determinants and Genetic Modifiers of Aggregation and Toxicity for the ALS Disease Protein FUS/TLS. *PLoS Biol,* 9**,** e1000614.

SUWA, M., EGASHIRA, T., NAKANO, H., SASAKI, H. & KUMAGAI, S. 2006. Metformin increases the PGC-1alpha protein and oxidative enzyme activities possibly via AMPK phosphorylation in skeletal muscle in vivo. *Journal of applied physiology (Bethesda, Md.: 1985),* 101**,** 1685-1692.

TAFT, R. A., DAVISSON, M. & WILES, M. V. 2006. Know thy mouse. *Trends in Genetics,* 22**,** 649-653.

TAKEUCHI, S., FUJIWARA, N., IDO, A., OONO, M., TAKEUCHI, Y., TATENO, M., SUZUKI, K., TAKAHASHI, R., TOOYAMA, I., TANIGUCHI, N., JULIEN, J. P. & URUSHITANI, M. 2010. Induction of protective immunity by vaccination with wild-type apo superoxide dismutase 1 in mutant SOD1 transgenic mice. *J Neuropathol Exp Neurol,* 69**,** 1044-56.

TANAKA, K., OKADA, Y., KANNO, T., OTOMO, A., YANAGISAWA, Y., SHOUGUCHI-MIYATA, J., SUGA, E., KOHIKI, E., ONOE, K., OSUGA, H., AOKI, M., HADANO, S., ITOYAMA, Y. & IKEDA, J.-E. 2008. A dopamine receptor antagonist L-745,870 suppresses microglia activation in spinal cord and mitigates the progression in ALS model mice. *Experimental Neurology,* 211**,** 378-386.

TANAKA, M., MACHIDA, Y., NIU, S., IKEDA, T., JANA, N. R., DOI, H., KUROSAWA, M., NEKOOKI, M. & NUKINA, N. 2004. Trehalose alleviates polyglutamine-mediated pathology in a mouse model of Huntington disease. *Nat Med,* 10**,** 148-154.

TATENO, M., SADAKATA, H., TANAKA, M., ITOHARA, S., SHIN, R. M., MIURA, M., MASUDA, M., AOSAKI, T., URUSHITANI, M., MISAWA, H. & TAKAHASHI, R. 2004. Calcium-permeable AMPA receptors promote misfolding of mutant SOD1 protein and development of amyotrophic lateral sclerosis in a transgenic mouse model. *Hum Mol Genet,* 13**,** 2183-96.

TAUPENOT, L., HARPER, K. L. & O'CONNOR, D. T. 2003. The Chromogranin–Secretogranin Family. *New England Journal of Medicine,* 348**,** 1134-1149.

TENG, Y. D., CHOI, H., HUANG, W., ONARIO, R. C., FRONTERA, W. R., SNYDER, E. Y. & SABHARWAL, S. 2006. Therapeutic effects of clenbuterol in a murine model of amyotrophic lateral sclerosis. *Neuroscience Letters,* 397**,** 155-158.

TIEMESSEN, M. M., JAGGER, A. L., EVANS, H. G., VAN HERWIJNEN, M. J. C., JOHN, S. & TAAMS, L. S. 2007. CD4+CD25+Foxp3+ regulatory T cells induce alternative activation of human monocytes/macrophages. *Proceedings of the National Academy of Sciences,* 104**,** 19446-19451.

TOKUDA, E., ONO, S.-I., ISHIGE, K., WATANABE, S., OKAWA, E., ITO, Y. & SUZUKI, T. 2008. Ammonium tetrathiomolybdate delays onset, prolongs survival, and slows progression of disease in a mouse model for amyotrophic lateral sclerosis. *Experimental Neurology,* 213**,** 122-128.

Glutamate AMPA receptors change in motor neurons of SOD1G93A transgenic mice and their inhibition by a noncompetitive antagonist ameliorates the progression of amytrophic lateral sclerosis-like disease, Year. Directed by TORTAROLO, M., GRIGNASCHI, G., CALVARESI, N., ZENNARO, E., SPALTRO, G., COLOVIC, M., FRACASSO, C., GUISO, G., ELGER, B., SCHNEIDER, H., SEILHEIMER, B., CACCIA, S. & BENDOTTI, C.: Wiley Subscription Services, Inc., A Wiley Company.

TORTAROLO, M., GRIGNASCHI, G., CALVARESI, N., ZENNARO, E., SPALTRO, G., COLOVIC, M., FRACASSO, C., GUISO, G., ELGER, B., SCHNEIDER, H., SEILHEIMER, B., CACCIA, S. & BENDOTTI, C. 2006b. Glutamate AMPA receptors change in motor neurons of SOD1G93A transgenic mice and their inhibition by a noncompetitive antagonist ameliorates the progression of amytrophic lateral sclerosis-like disease. *Journal of Neuroscience Research,* 83**,** 134-146.

TOWNE, C., RAOUL, C., SCHNEIDER, B. L. & AEBISCHER, P. 2008. Systemic AAV6 delivery mediating RNA interference against SOD1: neuromuscular transduction does not alter disease progression in fALS mice. *Molecular therapy : the journal of the American Society of Gene Therapy,* 16**,** 1018-1025.

TOWNE, C., SETOLA, V., SCHNEIDER, B. L. & AEBISCHER, P. 2011. Neuroprotection by Gene Therapy Targeting Mutant SOD1 in Individual Pools of Motor Neurons Does not Translate Into Therapeutic Benefit in fALS Mice. *Mol Ther,* 19**,** 274-283.

TRADEWELL, M. L., COOPER, L. A., MINOTTI, S. & DURHAM, H. D. 2011. Calcium dysregulation, mitochondrial pathology and protein aggregation in a culture model of amyotrophic lateral sclerosis: Mechanistic relationship and differential sensitivity to intervention. *Neurobiology of Disease,* 42**,** 265-275.

TRAYNOR, B. J., BRUIJN, L., CONWIT, R., BEAL, F., O'NEILL, G., FAGAN, S. C. & CUDKOWICZ, M. E. 2006. Neuroprotective agents for clinical trials in ALS: A systematic assessment. *Neurology,* 67**,** 20-27.

TRICAUD, N., PERRIN-TRICAUD, C., BRUSÉS, J. L. & RUTISHAUSER, U. 2005. Adherens Junctions in Myelinating Schwann Cells Stabilize Schmidt-Lanterman Incisures via Recruitment of p120 Catenin to E-Cadherin. *The Journal of Neuroscience,* 25**,** 3259-3269.

TRIEU, V. N., LIU, R., LIU, X.-P. & UCKUN, F. M. 2000. A Specific Inhibitor of Janus Kinase-3 Increases Survival in a Transgenic Mouse Model of Amyotrophic Lateral Sclerosis. *Biochemical and Biophysical Research Communications,* 267**,** 22-25.

TRIEU, V. N. & UCKUN, F. M. 1999. Genistein Is Neuroprotective in Murine Models of Familial Amyotrophic Lateral Sclerosis and Stroke. *Biochemical and Biophysical Research Communications,* 258**,** 685-688.

TUDOR, E. L., GALTREY, C. M., PERKINTON, M. S., LAU, K. F., DE VOS, K. J., MITCHELL, J. C., ACKERLEY, S., HORTOBÁGYI, T., VÁMOS, E., LEIGH, P. N., KLASEN, C., MCLOUGHLIN, D. M., SHAW, C. E. & MILLER, C. C. J. 2010. Amyotrophic lateral sclerosis mutant vesicle-associated membrane protein-associated protein-B transgenic mice develop TAR-DNA-binding protein-43 pathology. *Neuroscience,* 167**,** 774-785.

TÚNEZ, I., COLLADO, J. A., MEDINA, F. J., PEÑA, J., MUÑOZ, M. D. C., JIMENA, I., FRANCO, F., RUEDA, I., FEIJÓO, M., MUNTANÉ, J. & MONTILLA, P. 2006. 17 [beta]-Estradiol may affect vulnerability of striatum in a 3-nitropropionic acid-induced experimental model of Huntington's disease in ovariectomized rats. *Neurochemistry International,* 48**,** 367-373.

TURNER, B., LOPES, E. & CHEEMA, S. 2003a. The serotonin precursor 5-hydroxytryptophan delays neuromuscular disease in murine familial amyotrophic lateral sclerosis. *Amyotrophic Lateral Sclerosis,* 4**,** 171-176.

TURNER, B. J., CHEAH, I. K., MACFARLANE, K. J., LOPES, E. C., PETRATOS, S., LANGFORD, S. J. & CHEEMA, S. S. 2003b. Antisense peptide nucleic acid-mediated knockdown of the p75 neurotrophin receptor delays motor neuron disease in mutant SOD1 transgenic mice. *Journal of Neurochemistry,* 87**,** 752-763.

TURNER, B. J., LOPES, E. C. & CHEEMA, S. S. 2003c. Neuromuscular accumulation of mutant superoxide dismutase 1 aggregates in a transgenic mouse model of familial amyotrophic lateral sclerosis. *Neuroscience letters,* 350**,** 132-136.

TURNER, B. J., MURRAY, S. S., PICCENNA, L. G., LOPES, E. C., KILPATRICK, T. J. & CHEEMA, S. S. 2004a. Effect of p75 neurotrophin receptor antagonist on disease progression in transgenic amyotrophic lateral sclerosis mice. *Journal of Neuroscience Research,* 78**,** 193-199.

TURNER, B. J., REMBACH, A., SPARK, R., LOPES, E. C. & CHEEMA, S. S. 2003d. Opposing effects of low and high-dose clozapine on survival of transgenic amyotrophic lateral sclerosis mice. *Journal of Neuroscience Research,* 74**,** 605-613.

TURNER, B. J. & TALBOT, K. 2008. Transgenics, toxicity and therapeutics in rodent models of mutant SOD1-mediated familial ALS. *Progress in neurobiology,* 85**,** 94-134.

TURNER, M. R., CAGNIN, A., TURKHEIMER, F. E., MILLER, C. C. J., SHAW, C. E., BROOKS, D. J., LEIGH, P. N. & BANATI, R. B. 2004b. Evidence of widespread cerebral microglial activation in amyotrophic lateral sclerosis: an [11C](R)-PK11195 positron emission tomography study. *Neurobiology of Disease,* 15**,** 601-609.

UPTON-RICE, M. N., CUDKOWICZ, M. E., MATHEW, R. K., REIF, D. & BROWN, R. H. 1999a. Administration of nitric oxide synthase inhibitors does not alter disease course of amyotrophic lateral sclerosis SOD1 mutant transgenic mice. *Annals of Neurology,* 45**,** 413-414.

UPTON-RICE, M. N., CUDKOWICZ, M. E., WARREN, L., MATHEW, R. K., REN, J. M., FINKLESTEIN, S. P. & BROWN, R. H. 1999b. Basic fibroblast growth factor does not prolong survival in a transgenic model of familial amyotrophic lateral sclerosis. *Annals of Neurology,* 46**,** 934-934.

URUSHITANI, M., EZZI, S. A. & JULIEN, J.-P. 2007. Therapeutic effects of immunization with mutant superoxide dismutase in mice models of amyotrophic lateral sclerosis. *Proceedings of the National Academy of Sciences,* 104**,** 2495-2500.

URUSHITANI, M., KURISU, J., TSUKITA, K. & TAKAHASHI, R. 2002. Proteasomal inhibition by misfolded mutant superoxide dismutase 1 induces selective motor neuron death in familial amyotrophic lateral sclerosis. *Journal of Neurochemistry,* 83**,** 1030-1042.

URUSHITANI, M., SIK, A., SAKURAI, T., NUKINA, N., TAKAHASHI, R. & JULIEN, J.-P. 2006. Chromogranin-mediated secretion of mutant superoxide dismutase proteins linked to amyotrophic lateral sclerosis. *Nat Neurosci,* 9**,** 108-118.

VAN DAMME, P., BOGAERT, E., DEWIL, M., HERSMUS, N., KIRALY, D., SCHEVENEELS, W., BOCKX, I., BRAEKEN, D., VERPOORTEN, N., VERHOEVEN, K., TIMMERMAN, V., HERIJGERS, P., CALLEWAERT, G., CARMELIET, P., VAN DEN BOSCH, L. & ROBBERECHT, W. 2007. Astrocytes regulate GluR2 expression in motor neurons and their vulnerability to excitotoxicity. *Proceedings of the National Academy of Sciences,* 104**,** 14825-14830.

VAN DAMME, P., LEYSSEN, M., CALLEWAERT, G., ROBBERECHT, W. & VAN DEN BOSCH, L. 2003. The AMPA receptor antagonist NBQX prolongs survival in a transgenic mouse model of amyotrophic lateral sclerosis. *Neuroscience Letters,* 343**,** 81-84.

VAN DEN BOSCH, L., STORKEBAUM, E., VLEMINCKX, V., MOONS, L., VANOPDENBOSCH, L., SCHEVENEELS, W., CARMELIET, P. & ROBBERECHT, W. 2004. Effects of vascular endothelial growth factor (VEGF) on motor neuron degeneration. *Neurobiology of Disease,* 17**,** 21-28.

VAN DEN BOSCH, L., TILKIN, P., LEMMENS, G. & ROBBERECHT, W. 2002. Minocycline delays disease onset and mortality in a transgenic model of ALS. *Neuroreport,* 13**,** 1067-1070.

VAN DEN BOSCH, L., VAN DAMME, P., BOGAERT, E. & ROBBERECHT, W. 2006. The role of excitotoxicity in the pathogenesis of amyotrophic lateral sclerosis. *Biochimica et Biophysica Acta (BBA) - Molecular Basis of Disease,* 1762**,** 1068-1082.

VAN ELBURG, R. M., UIL, J. J., KOKKE, F. T. M., MULDER, A. M., VAN DE BROEK, W. G. M., MULDER, C. J. J. & HEYMANS, H. S. A. 1995. Repeatability of the Sugar-Absorption Test, Using Lactulose and Mannitol, for Measuring Intestinal Permeability for Sugars. *Journal of Pediatric Gastroenterology and Nutrition,* 20**,** 184-188.

VAN LOO, P. L. P., KRUITWAGEN, C. L. J. J., KOOLHAAS, J. M., VAN DE WEERD, H. A., VAN ZUTPHEN, L. F. M. & BAUMANS, V. 2002. Influence of cage enrichment on aggressive behaviour and physiological parameters in male mice. 76**,** 65-81.

VAN LOO, P. L. P., KRUITWAGEN, C. L. J. J., VAN ZUTPHEN, B. F. M., KOOLHAAS, J. M. & BAUMANS, V. 2000. Modulation of aggression in male mice: influence of cage cleaning regime and scent marks. *Animal Welfare*

VAN LOO, P. L. P., MOL, J. A., KOOLHAAS, J. M., VAN ZUTPHEN, B. F. M. & BAUMANS, V. 2001. Modulation of aggression in male mice: influence of group size and cage size. *Physiology & Behavior,* 72**,** 675-683.

VAN LOO, P. L. P., VAN DE WEERD, H. A., VAN ZUTPHEN, L. F. M. & BAUMANS, V. 2004. Preference for social contact versus environmental enrichment in male laboratory mice. *Lab Anim,* 38**,** 178-188.

VAN LOO, P. L. P., VAN ZUTPHEN, L. F. M. & BAUMANS, V. 2003. Male management: coping with aggression problems in male laboratory mice. *Lab Anim,* 37**,** 300-313.

VANCE, C., ROGELJ, B., HORTOBÁGYI, T., DE VOS, K. J., NISHIMURA, A. L., SREEDHARAN, J., HU, X., SMITH, B., RUDDY, D., WRIGHT, P., GANESALINGAM, J., WILLIAMS, K. L., TRIPATHI, V., AL-SARAJ, S., AL-CHALABI, A., LEIGH, P. N., BLAIR, I. P., NICHOLSON, G., DE BELLEROCHE, J., GALLO, J.-M., MILLER, C. C. & SHAW, C. E. 2009. Mutations in FUS, an RNA Processing Protein, Cause Familial Amyotrophic Lateral Sclerosis Type 6. *Science,* 323**,** 1208-1211.

VANDE VELDE, C., MCDONALD, K. K., BOUKHEDIMI, Y., MCALONIS-DOWNES, M., LOBSIGER, C. S., BEL HADJ, S., ZANDONA, A., JULIEN, J.-P., SHAH, S. B. & CLEVELAND, D. W. 2011. Misfolded SOD1 Associated with Motor Neuron Mitochondria Alters Mitochondrial Shape and Distribution Prior to Clinical Onset. *PLoS ONE,* 6**,** e22031.

VANDE VELDE, C., MILLER, T. M., CASHMAN, N. R. & CLEVELAND, D. W. 2008. Selective association of misfolded ALS-linked mutant SOD1 with the cytoplasmic face of mitochondria. *Proceedings of the National Academy of Sciences,* 105**,** 4022-4027.

VARGAS, M. R., PEHAR, M., CASSINA, P., BECKMAN, J. S. & BARBEITO, L. 2006. Increased glutathione biosynthesis by Nrf2 activation in astrocytes prevents p75NTR-dependent motor neuron apoptosis. *Journal of Neurochemistry,* 97**,** 687-696.

VELDINK, J. H., BÄR, P. R., JOOSTEN, E. A. J., OTTEN, M., WOKKE, J. H. J. & VAN DEN BERG, L. H. 2003. Sexual differences in onset of disease and response to exercise in a transgenic model of ALS. *Neuromuscular Disorders,* 13**,** 737-743.

VERCELLI, A., MEREUTA, O. M., GARBOSSA, D., MURACA, G., MARESCHI, K., RUSTICHELLI, D., FERRERO, I., MAZZINI, L., MADON, E. & FAGIOLI, F. 2008. Human mesenchymal stem cell transplantation extends survival, improves motor performance and decreases neuroinflammation in mouse model of amyotrophic lateral sclerosis. *Neurobiology of Disease,* 31**,** 395-405.

VLEMINCKX, V., VAN DAMME, P., GOFFIN, K., DELYE, H., VAN DEN BOSCH, L. & ROBBERECHT, W. 2002. Upregulation of HSP27 in a transgenic model of ALS. *J Neuropathol Exp Neurol,* 61**,** 968-74.

WAIBEL, S., REUTER, A., MALESSA, S., BLAUGRUND, E. & LUDOLPH, A. C. 2004. Rasagiline alone and in combination with riluzole prolongs survival in an ALS mouse model. *Journal of Neurology,* 251**,** 1080-1084.

WALKER, S. L., ARIGA, J., MATHIAS, J. R., COOTHANKANDASWAMY, V., XIE, X., DISTEL, M., KÖSTER, R. W., PARSONS, M. J., BHALLA, K. N., SAXENA, M. T. & MUMM, J. S. 2012. Automated Reporter Quantification <italic>In Vivo</italic>: High-Throughput Screening Method for Reporter-Based Assays in Zebrafish. *PLoS ONE,* 7**,** e29916.

WANG, H., GHOSH, A., BAIGUDE, H., YANG, C.-S., QIU, L., XIA, X., ZHOU, H., RANA, T. M. & XU, Z. 2008a. Therapeutic Gene Silencing Delivered by a Chemically Modified Small Interfering RNA against Mutant SOD1 Slows Amyotrophic Lateral Sclerosis Progression. *Journal of Biological Chemistry,* 283**,** 15845-15852.

WANG, H., GUAN, Y., WANG, X., SMITH, K., CORMIER, K., ZHU, S., STAVROVSKAYA, I. G., HUO, C., FERRANTE, R. J., KRISTAL, B. S. & FRIEDLANDER, R. M. 2007. Nortriptyline delays disease onset in models of chronic neurodegeneration. *European Journal of Neuroscience,* 26**,** 633-641.

WANG, J., XU, G. & BORCHELT, D. R. 2002a. High Molecular Weight Complexes of Mutant Superoxide Dismutase 1: Age-Dependent and Tissue-Specific Accumulation. *Neurobiology of Disease,* 9**,** 139-148.

WANG, J., XU, G., SLUNT, H. H., GONZALES, V., COONFIELD, M., FROMHOLT, D., COPELAND, N. G., JENKINS, N. A. & BORCHELT, D. R. 2005. Coincident thresholds of mutant protein for paralytic disease and protein aggregation caused by restrictively expressed superoxide dismutase cDNA. *Neurobiology of Disease,* 20**,** 943-952.

WANG, L.-J., LU, Y.-Y., MURAMATSU, S.-I., IKEGUCHI, K., FUJIMOTO, K.-I., OKADA, T., MIZUKAMI, H., MATSUSHITA, T., HANAZONO, Y., KUME, A., NAGATSU, T., OZAWA, K. & NAKANO, I. 2002b. Neuroprotective Effects of Glial Cell Line-Derived Neurotrophic Factor Mediated by an Adeno-Associated Virus Vector in a Transgenic Animal Model of Amyotrophic Lateral Sclerosis. *The Journal of Neuroscience,* 22**,** 6920-6928.

WANG, L., POPKO, B. & ROOS, R. P. 2011. The unfolded protein response in familial amyotrophic lateral sclerosis. *Human molecular genetics,* 20**,** 1008-1015.

WANG, Q., JOHNSON, J. L., AGAR, N. Y. R. & AGAR, J. N. 2008b. Protein Aggregation and Protein Instability Govern Familial Amyotrophic Lateral Sclerosis Patient Survival. *PLoS Biol,* 6**,** e170.

WANG, R. & ZHANG, D. 2005. Memantine prolongs survival in an amyotrophic lateral sclerosis mouse model. *European Journal of Neuroscience,* 22**,** 2376-2380.

WANG, X., CULOTTA, V. C. & KLEE, C. B. 1996. Superoxide dismutase protects calcineurin from inactivation. *Nature,* 383**,** 434-437.

WANNET, W. J. B., HERMANS, J. H. M., VAN DER DRIFT, C. & OP DEN CAMP, H. J. M. 2000. HPLC Detection of Soluble Carbohydrates Involved in Mannitol and Trehalose Metabolism in the Edible Mushroom Agaricus bisporus. *Journal of Agricultural and Food Chemistry,* 48**,** 287-291.

WATSON, C., PAXINOS, G. & KAYALIOGLU, G. 2008. *The Spinal Cord: A Christopher and Dana Reeve Foundation Text and Atlas*

WEI, J.-P. J., SRINIVASAN, C., HAN, H., VALENTINE, J. S. & GRALLA, E. B. 2001. Evidence for a Novel Role of Copper-Zinc Superoxide Dismutase in Zinc Metabolism. *Journal of Biological Chemistry,* 276**,** 44798-44803.

WEISHAUPT, J. H., BARTELS, C., PÖLKING, E., DIETRICH, J., ROHDE, G., POEGGELER, B., MERTENS, N., SPERLING, S., BOHN, M., HÜTHER, G., SCHNEIDER, A., BACH, A., SIRÉN, A.-L., HARDELAND, R., BÄHR, M., NAVE, K.-A. & EHRENREICH, H. 2006. Reduced oxidative damage in ALS by high-dose enteral melatonin treatment. *Journal of Pineal Research,* 41**,** 313-323.

WEST, M., MHATRE, M., CEBALLOS, A., FLOYD, R. A., GRAMMAS, P., GABBITA, S. P., HAMDHEYDARI, L., MAI, T., MOU, S., PYE, Q. N., STEWART, C., WEST, S., WILLIAMSON, K. S., ZEMLAN, F. & HENSLEY, K. 2004. The arachidonic acid 5-lipoxygenase inhibitor nordihydroguaiaretic acid inhibits tumor necrosis factor α activation of microglia and extends survival of G93A-SOD1 transgenic mice. *Journal of Neurochemistry,* 91**,** 133-143.

WEYDT, P., HONG, S., WITTING, A., MÖLLER, T., STELLA, N. & KLIOT, M. 2005. Cannabinol delays symptom onset in SOD1 (G93A) transgenic mice without affecting survival. *Amyotrophic Lateral Sclerosis,* 6**,** 182-184.

WEYDT, P., HONG, S. Y., KLIOT, M. & MÃ¶LLER, T. 2003. Assessing disease onset and progression in the SOD1 mouse model of ALS. *NeuroReport,* 14**,** 1051-1054.

WEYDT, P., YUEN, E. C., RANSOM, B. R. & MÖLLER, T. 2004. Increased cytotoxic potential of microglia from ALS-transgenic mice. *Glia,* 48**,** 179-182.

WIEDEMANN, F. R., MANFREDI, G., MAWRIN, C., BEAL, M. F. & SCHON, E. A. 2002. Mitochondrial DNA and respiratory chain function in spinal cords of ALS patients. *Journal of Neurochemistry,* 80**,** 616-625.

WIJESEKERA, L. & LEIGH, P. N. 2009. Amyotrophic lateral sclerosis. *Orphanet Journal of Rare Diseases,* 4**,** 3.

WILLIAMSON, T. L. & CLEVELAND, D. W. 1999. Slowing of axonal transport is a very early event in the toxicity of ALS-linked SOD1 mutants to motor neurons. *Nat Neurosci,* 2**,** 50-56.

WILLING, A. E., GARBUZOVA-DAVIS, S., SAPORTA, S., MILLIKEN, M., CAHILL, D. W. & SANBERG, P. R. 2001. hNT neurons delay onset of motor deficits in a model of amyotrophic lateral sclerosis. *Brain Research Bulletin,* 56**,** 525-530.

WILS, H., KLEINBERGER, G., JANSSENS, J., PERESON, S., JORIS, G., CUIJT, I., SMITS, V., CEUTERICK-DE GROOTE, C., VAN BROECKHOVEN, C. & KUMAR-SINGH, S. 2010. TDP-43 transgenic mice develop spastic paralysis and neuronal inclusions characteristic of ALS and frontotemporal lobar degeneration. *Proceedings of the National Academy of Sciences,* 107**,** 3858-3863.

WINTERBOURN, C. C., PESKIN, A. V. & PARSONS-MAIR, H. N. 2002. Thiol Oxidase Activity of Copper,Zinc Superoxide Dismutase. *Journal of Biological Chemistry,* 277**,** 1906-1911.

WOJCIECHOWSKA, M. & KRZYZOSIAK, W. J. 2011. Cellular toxicity of expanded RNA repeats: focus on RNA foci. *Human Molecular Genetics,* 20**,** 3811-3821.

WONG, N. K., HE, B. P. & STRONG, M. J. 2000. Characterization of neuronal intermediate filament protein expression in cervical spinal motor neurons in sporadic amyotrophic lateral sclerosis (ALS). *J Neuropathol Exp Neurol,* 59**,** 972-82.

WONG, P. C., PARDO, C. A., BORCHELT, D. R., LEE, M. K., COPELAND, N. G., JENKINS, N. A., SISODIA, S. S., CLEVELAND, D. W. & PRICE, D. L. 1995. An adverse property of a familial ALS-linked SOD1

mutation causes motor neuron disease characterized by vacuolar degeneration of mitochondria. *Neuron,* 14**,** 1105-1116.

WU, A. S., KIAEI, M., AGUIRRE, N., CROW, J. P., CALINGASAN, N. Y., BROWNE, S. E. & BEAL, M. F. 2003. Iron porphyrin treatment extends survival in a transgenic animal model of amyotrophic lateral sclerosis. *Journal of Neurochemistry,* 85**,** 142-150.

XIAO, Q., ZHAO, W., BEERS, D. R., YEN, A. A., XIE, W., HENKEL, J. S. & APPEL, S. H. 2007. Mutant SOD1G93A microglia are more neurotoxic relative to wild-type microglia. *Journal of Neurochemistry,* 102**,** 2008-2019.

XU, Y.-F., GENDRON, T. F., ZHANG, Y.-J., LIN, W.-L., D'ALTON, S., SHENG, H., CASEY, M. C., TONG, J., KNIGHT, J., YU, X., RADEMAKERS, R., BOYLAN, K., HUTTON, M., MCGOWAN, E., DICKSON, D. W., LEWIS, J. & PETRUCELLI, L. 2010. Wild-Type Human TDP-43 Expression Causes TDP-43 Phosphorylation, Mitochondrial Aggregation, Motor Deficits, and Early Mortality in Transgenic Mice. *The Journal of Neuroscience,* 30**,** 10851-10859.

XU, Z., CHEN, S., LI, X., LUO, G., LI, L. & LE, W. 2006. Neuroprotective Effects of (-)-Epigallocatechin-3-gallate in a Transgenic Mouse Model of Amyotrophic Lateral Sclerosis. *Neurochemical Research,* 31**,** 1263-1269.

YAMAMOTO, M., KOBAYASHI, Y., LI, M., NIWA, H., MITSUMA, N., ITO, Y., MURAMATSU, T. & SOBUE, G. 2001. In Vivo Gene Electroporation of Glial Cell Line-Derived Neurotrophic Factor (GDNF) into Skeletal Muscle of SOD1 Mutant Mice. *Neurochemical Research,* 26**,** 1201-1207.

YAMANAKA, K., CHUN, S. J., BOILLEE, S., FUJIMORI-TONOU, N., YAMASHITA, H., GUTMANN, D. H., TAKAHASHI, R., MISAWA, H. & CLEVELAND, D. W. 2008. Astrocytes as determinants of disease progression in inherited amyotrophic lateral sclerosis. *Nature neuroscience,* 11**,** 251-253.

YAN, J., XU, L., WELSH, A. M., CHEN, D., HAZEL, T., JOHE, K. & KOLIATSOS, V. E. 2006. Combined Immunosuppressive Agents or CD4 Antibodies Prolong Survival of Human Neural Stem Cell Grafts and Improve Disease Outcomes in Amyotrophic Lateral Sclerosis Transgenic Mice. *STEM CELLS,* 24**,** 1976-1985.

YANG, E. J., JIANG, J. H., LEE, S. M., YANG, S. C., HWANG, H. S., LEE, M. S. & CHOI, S.-M. 2010. Bee venom attenuates neuroinflammatory events and extends survival in amyotrophic lateral sclerosis models. *Journal of Neuroinflammation,* 7**,** 69.

YANG, E. J., KIM, S. H., YANG, S. C., LEE, S. M. & CHOI, S.-M. 2011a. Melittin restores proteasome function in an animal model of ALS. *Journal of Neuroinflammation,* 8**,** 69.

YANG, W. W., SIDMAN, R. L., TAKSIR, T. V., TRELEAVEN, C. M., FIDLER, J. A., CHENG, S. H., DODGE, J. C. & SHIHABUDDIN, L. S. 2011b. Relationship between neuropathology and disease progression in the SOD1G93A ALS mouse. *Experimental Neurology,* 227**,** 287-295.

YANG, Y., GOZEN, O., WATKINS, A., LORENZINI, I., LEPORE, A., GAO, Y., VIDENSKY, S., BRENNAN, J., POULSEN, D., WON PARK, J., LI JEON, N., ROBINSON, M. B. & ROTHSTEIN, J. D. 2009. Presynaptic Regulation of Astroglial Excitatory Neurotransmitter Transporter GLT1. *Neuron,* 61**,** 880-894.

YANG, Y., HENTATI, A., DENG, H., DABBAGH, O., SASAKI, T., HIRANO, M., HUNG, W., OUAHCHI, K., YAN, J. & AZIM, A. 2001. The gene encoding alsin, a protein with three guanine-nucleotide exchange factor domains, is mutated in a form of recessive amyotrophic lateral sclerosis. *Nat Genet,* 29**,** 160 - 165.

YANG, Z. & KLIONSKY, D. J. 2010. Mammalian autophagy: core molecular machinery and signaling regulation. *Current Opinion in Cell Biology,* 22**,** 124-131.

YI, M., WEAVER, D. & HAJNÓCZKY, G. 2004. Control of mitochondrial motility and distribution by the calcium signal. *The Journal of Cell Biology,* 167**,** 661-672.

YIM, M. B., CHOCK, P. B. & STADTMAN, E. R. 1990. Copper, zinc superoxide dismutase catalyzes hydroxyl radical production from hydrogen peroxide. *Proceedings of the National Academy of Sciences,* 87**,** 5006-5010.

YOKOSEKI, A., SHIGA, A., TAN, C., TAGAWA, A., KANEKO, H., KOYAMA, A., EGUCHI, H., TSUJINO, A., IKEUCHI, T. & KAKITA, A. 2008. TDP-43 mutation in familial amyotrophic lateral sclerosis. *Ann Neurol,* 63**,** 538 - 542.

YOO, Y.-E. & KO, C.-P. 2011. Treatment with trichostatin A initiated after disease onset delays disease progression and increases survival in a mouse model of amyotrophic lateral sclerosis. *Experimental Neurology,* 231**,** 147-159.

YOSHIHARA, T., ISHIGAKI, S., YAMAMOTO, M., LIANG, Y., JUN, NIWA, I., TAKEUCHI, H., DOYU, M. & SOBUE, G. 2002. Differential expression of inflammation- and apoptosis-related genes in spinal cords of a mutant SOD1 transgenic mouse model of familial amyotrophic lateral sclerosis. *Journal of Neurochemistry,* 80**,** 158-167.

YOSHIYAMA, Y., YAMADA, T., ASANUMA, K. & ASAHI, T. 1994. Apoptosis related antigen, Le(Y) and nick-end labeling are positive in spinal motor neurons in amyotrophic lateral sclerosis. *Acta Neuropathol,* 88**,** 207-11.

YUE, Z. 2007. Regulation of Neuronal Autophagy in Axon: Implication of Autophagy in Axonal Function and Dysfunction/Degeneration. *Autophagy,* 3**,** 139-141.

ZANG, D. W. & CHEEMA, S. S. 2002. Degeneration of corticospinal and bulbospinal systems in the superoxide dismutase 1G93A G1H transgenic mouse model of familial amyotrophic lateral sclerosis. *Neuroscience Letters,* 332**,** 99-102.

ZHANG, C., ZHOU, C., TENG, J.-J., ZHAO, R.-L. & SONG, Y.-Q. 2009. Multiple administrations of human marrow stromal cells through cerebrospinal fluid prolong survival in a transgenic mouse model of amyotrophic lateral sclerosis. *Cytotherapy,* 11**,** 299-306.

ZHANG, F., STRÖM, A.-L., FUKADA, K., LEE, S., HAYWARD, L. J. & ZHU, H. 2007a. Interaction between Familial Amyotrophic Lateral Sclerosis (ALS)-linked SOD1 Mutants and the Dynein Complex. *Journal of Biological Chemistry,* 282**,** 16691-16699.

ZHANG, W., NARAYANAN, M. & FRIEDLANDER, R. M. 2003. Additive neuroprotective effects of minocycline with creatine in a mouse model of ALS. *Annals of Neurology,* 53**,** 267-270.

ZHANG, X., CHEN, S., LI, L., WANG, Q. & LE, W. 2008. Folic acid protects motor neurons against the increased homocysteine, inflammation and apoptosis in SOD1G93A transgenic mice. *Neuropharmacology,* 54**,** 1112-1119.

ZHANG, X., LI, L., CHEN, S., YANG, D., WANG, Y., WANG, Z. & LE, W. 2011. Rapamycin treatment augments motor neuron degeneration in SOD1(G93A) mouse model of amyotrophic lateral sclerosis. *Autophagy,* 7**,** 412-25.

ZHANG, Y.-J., XU, Y.-F., DICKEY, C. A., BURATTI, E., BARALLE, F., BAILEY, R., PICKERING-BROWN, S., DICKSON, D. & PETRUCELLI, L. 2007b. Progranulin Mediates Caspase-Dependent Cleavage of TAR DNA Binding Protein-43. *The Journal of Neuroscience,* 27**,** 10530-10534.

ZHANG, Y. P., ONIFER, S. M., BURKE, D. A. & SHIELDS, C. B. 2001. A topical mixture for preventing, abolishing, and treating autophagia and self-mutilation in laboratory rats. *Contemp Top Lab Anim Sci,* 40**,** 35-6.

ZHAO, C.-P., ZHANG, C., ZHOU, S.-N., XIE, Y.-M., WANG, Y.-H., HUANG, H., SHANG, Y.-C., LI, W.-Y., ZHOU, C., YU, M.-J. & FENG, S.-W. 2007. Human mesenchymal stromal cells ameliorate the phenotype of SOD1-G93A ALS mice. *Cytotherapy,* 9**,** 414-426.

ZHAO, W., BEERS, D. R., HENKEL, J. S., ZHANG, W., URUSHITANI, M., JULIEN, J.-P. & APPEL, S. H. 2010. Extracellular mutant SOD1 induces microglial-mediated motoneuron injury. *Glia,* 58**,** 231-243.

ZHAO, W., VARGHESE, M., YEMUL, S., PAN, Y., CHENG, A., MARANO, P., HASSAN, S., VEMPATI, P., CHEN, F., QIAN, X. & PASINETTI, G. 2011. Peroxisome proliferator activator receptor gamma

coactivator-1alpha (PGC-1alpha) improves motor performance and survival in a mouse model of amyotrophic lateral sclerosis. *Molecular Neurodegeneration,* 6**,** 51.

ZHAO, W., XIE, W., LE, W., BEERS, D. R., HE, Y., HENKEL, J. S., SIMPSON, E. P., YEN, A. A., XIAO, Q. & APPEL, S. H. 2004. Activated microglia initiate motor neuron injury by a nitric oxide and glutamate-mediated mechanism. *J Neuropathol Exp Neurol,* 63**,** 964-77.

ZHAO, Z., LANGE, D., VOUSTIANIOUK, A., MACGROGAN, D., HO, L., SUH, J., HUMALA, N., THIYAGARAJAN, M., WANG, J. & PASINETTI, G. 2006. A ketogenic diet as a potential novel therapeutic intervention in amyotrophic lateral sclerosis. *BMC Neuroscience,* 7**,** 29.

ZHENG, C., NENNESMO, I., FADEEL, B. & HENTER, J.-I. 2004. Vascular endothelial growth factor prolongs survival in a transgenic mouse model of ALS. *Annals of Neurology,* 56**,** 564-567.

ZHONG, Z., ILIEVA, H., HALLAGAN, L., BELL, R., SINGH, I., PAQUETTE, N., THIYAGARAJAN, M., DEANE, R., FERNANDEZ, J. A., LANE, S., ZLOKOVIC, A. B., LIU, T., GRIFFIN, J. H., CHOW, N., CASTELLINO, F. J., STOJANOVIC, K., CLEVELAND, D. W. & ZLOKOVIC, B. V. 2009. Activated protein C therapy slows ALS-like disease in mice by transcriptionally inhibiting SOD1 in motor neurons and microglia cells. *The Journal of Clinical Investigation,* 119**,** 3437-3449.

ZHOU, G., MYERS, R., LI, Y., CHEN, Y., SHEN, X., FENYK-MELODY, J., WU, M., VENTRE, J., DOEBBER, T., FUJII, N., MUSI, N., HIRSHMAN, M. F., GOODYEAR, L. J. & MOLLER, D. E. 2001. Role of AMP-activated protein kinase in mechanism of metformin action. *The Journal of Clinical Investigation,* 108**,** 1167-1174.

ZHOU, H., HUANG, C., CHEN, H., WANG, D., LANDEL, C. P., XIA, P. Y., BOWSER, R., LIU, Y.-J. & XIA, X. G. 2010. Transgenic Rat Model of Neurodegeneration Caused by Mutation in the <italic>TDP</italic> Gene. *PLoS Genet,* 6**,** e1000887.

ZHU, S., STAVROVSKAYA, I. G., DROZDA, M., KIM, B. Y. S., ONA, V., LI, M., SARANG, S., LIU, A. S., HARTLEY, D. M., WU, D. C., GULLANS, S., FERRANTE, R. J., PRZEDBORSKI, S., KRISTAL, B. S. & FRIEDLANDER, R. M. 2002. Minocycline inhibits cytochrome c release and delays progression of amyotrophic lateral sclerosis in mice. *Nature,* 417**,** 74-78.

ZINMAN, L. & CUDKOWICZ, M. 2011. Emerging targets and treatments in amyotrophic lateral sclerosis. *The Lancet Neurology,* 10**,** 481-490.

ZUCHNER, S., MERSIYANOVA, I. V., MUGLIA, M., BISSAR-TADMOURI, N., ROCHELLE, J., DADALI, E. L., ZAPPIA, M., NELIS, E., PATITUCCI, A., SENDEREK, J., PARMAN, Y., EVGRAFOV, O., JONGHE, P. D., TAKAHASHI, Y., TSUJI, S., PERICAK-VANCE, M. A., QUATTRONE, A., BATTALOGLU, E., POLYAKOV, A. V., TIMMERMAN, V., SCHRODER, J. M. & VANCE, J. M. 2004. Mutations in the mitochondrial GTPase mitofusin 2 cause Charcot-Marie-Tooth neuropathy type 2A. *Nat Genet,* 36**,** 449-51.